MONITORING AND MODELING OF PAVEMENT RESPONSE AND PERFORMANCE
TASK B: NEW YORK
Pooled Fund Project TPF-5 (121)
Volume 3: I90

by
Shad M. Sargand, Issam S. Khoury,
and Drew Hatton

for the
Ohio Department of Transportation
Research Section
the
New York State Department of Transportation
and the
United States Department of Transportation
Federal Highway Administration

State Job Number 134287

May 2012

Ohio Research Institute for
Transportation and the Environment

1. Report No. FHWA/OH-2012/08C	2. Government Accession No.	3. Recipient's Catalog No.
4. Title and Subtitle MONITORING AND MODELING OF PAVEMENT RESPONSE AND PERFORMANCE TASK B: NEW YORK Volume 3: I90		**5. Report Date** May 2012 **6. Performing Organization Code**
7. Author(s) Shad Sargand, Issam Khoury, and Drew Hatton		**8. Performing Organization Report No.**
9. Performing Organization Name and Address Ohio Research Institute for Transportation and the Environment (ORITE) 141 Stocker Center Ohio University Athens OH 45701-2979		**10. Work Unit No. (TRAIS)** **11. Contract or Grant No**. Pooled Fund Project TPF-5(121) State Job No. 134287 Agreement No. 21182
12. Sponsoring Agency Name and Address Ohio Department of Transportation Innovation, Research, and Implementation Section 1980 West Broad St. Columbus OH 43223		**13. Type of Report and Period Covered** Technical Report 14. Sponsoring Agency Code

15. Supplementary Notes
Prepared in cooperation with the Ohio Department of Transportation (ODOT), the New York State Department of Transportation (NYSDOT) and the U.S. Department of Transportation, Federal Highway Administration

16. Abstract

This research presents the evaluation and comparison of two Portland-cement concrete (PCC) pavement test sections with cement-treated permeable bases (CTPB) and dense-graded aggregate bases (DGAB) on the Interstate 90 Thruway in New York. Two instrumented test sections were constructed to assess rigid pavement performance with CTPB compared to DGAB. The first test section had a DGAB layer only, while the second section had a CTPB layer above the DGAB layer. Continual environmental data were collected and dynamic testing was conducted to evaluate the load response of each test section.

The results from the environmental monitoring show that the CTPB section had higher strains and began to experience higher edge deflections after a year of service. The moisture probes indicated the CTPB did not affect subgrade moisture content. Dynamic truck load tests indicated the CTPB section had higher mid-slab strains and greater transverse joint deflections. The higher strains and deflections in the environmental and dynamic tests were attributed to the rigid CTPB layer, which caused a loss of support at the slab edges. This study found there were no benefits from the CTPB, and that the rigid base layer had a negative impact on early-age pavement performance.

17. Key Words	18. Distribution Statement No Restrictions. This document is available to the public through the National Technical Information Service, Springfield, Virginia 22161		
19. Security Classif. (of this report) Unclassified	**20. Security Classif. (of this page)** Unclassified	**21. No. of Pages** 182	**22. Price**

SI* (MODERN METRIC) CONVERSION FACTORS

APPROXIMATE CONVERSIONS TO SI UNITS

Symbol	When You Know	Multiply By	To Find	Symbol
LENGTH				
in	inches	25.4	millimeters	mm
ft	feet	0.305	meters	m
yd	yards	0.914	meters	m
mi	miles	1.61	kilometers	km
AREA				
in^2	square inches	645.2	square millimeters	mm^2
ft^2	square feet	0.093	square meters	m^2
yd^2	square yards	0.836	square meters	m^2
ac	acres	0.405	hectares	ha
mi^2	square miles	2.59	square kilometers	km^2
VOLUME				
fl oz	fluid ounces	29.57	milliliters	mL
gal	gallons	3.785	liters	L
ft^3	cubic feet	0.028	cubic meters	m^3
yd^3	cubic yards	0.765	cubic meters	m^3
NOTE: Volumes greater than 1000 L shall be shown in m^3.				
MASS				
oz	ounces	28.35	grams	g
lb	pounds	0.454	kilograms	kg
T	short tons (2000 lb)	0.907	megagrams (or "metric ton")	Mg (or "t")
TEMPERATURE (exact)				
°F	Fahrenheit temperature	5(°F-32)/9 or (°F-32)/1.8	Celsius temperature	°C
ILLUMINATION				
fc	foot-candles	10.76	lux	lx
fl	foot-Lamberts	3.426	candela/m^2	cd/m^2
FORCE and PRESSURE or STRESS				
lbf	poundforce	4.45	newtons	N
lbf/in^2 or psi	poundforce per square inch	6.89	kilopascals	kPa

APPROXIMATE CONVERSIONS FROM SI UNITS

Symbol	When You Know	Multiply By	To Find	Symbol
LENGTH				
mm	millimeters	0.039	inches	in
m	meters	3.28	feet	ft
m	meters	1.09	yards	yd
km	kilometers	0.621	miles	mi
AREA				
mm^2	square millimeters	0.0016	square inches	in^2
m^2	square meters	10.764	square feet	ft^2
m^2	square meters	1.195	square yards	yd^2
ha	hectares	2.47	acres	ac
km^2	square kilometers	0.386	square miles	mi^2
VOLUME				
mL	milliliters	0.034	fluid ounces	fl oz
L	liters	0.264	gallons	gal
m^3	cubic meters	35.314	cubic feet	ft^3
m^3	cubic meters	1.307	cubic yards	yd^3
MASS				
g	grams	0.035	ounces	oz
kg	kilograms	2.202	pounds	lb
Mg (or "t")	megagrams (or "metric ton")	1.103	short tons (2000 lb)	T
TEMPERATURE (exact)				
°C	Celsius temperature	1.8°C + 32	Fahrenheit temperature	°F
ILLUMINATION				
lx	lux	0.0929	foot-candles	fc
cd/m^2	candela/m^2	0.2919	foot-Lamberts	fl
FORCE and PRESSURE or STRESS				
N	newtons	0.225	poundforce	lbf
kPa	kilopascals	0.145	poundforce per square inch	lbf/in^2 or psi

* SI is the symbol for the International Symbol of Units. Appropriate rounding should be made to comply with Section 4 of ASTM E380.

(Revised March 2003)

MONITORING AND MODELING OF PAVEMENT RESPONSE AND PERFORMANCE TASK B: NEW YORK Volume 3: I90

Draft Final Report

Prepared in Cooperation with the
Ohio Department of Transportation,
the
The New York State Department of Transportation,
and the
U.S. Department of Transportation,
Federal Highway Administration

Prepared by

Shad M. Sargand
Issam Khoury
Drew Hatton

Ohio Research Institute for Transportation and the Environment
Russ College of Engineering and Technology
Ohio University
Athens, Ohio 45701-2979

May 2012

TABLE OF CONTENTS

LIST OF TABLES

LIST OF FIGURES

ACKNOWLEDGEMENTS

On large field-oriented projects such as this, many tasks are involved and many people contribute to the successful completion of those tasks. On this project, NYSDOT personnel were needed to collect certain types of data and to secure the field sites for testing. Julián Bendaña and Wes Yang from the central office, who coordinated all activities, and the various FWD operators, who performed the FWD testing. From the Region Offices were several people who supported the research by allowing the researchers access to the road, by providing, loading, and driving dump trucks for controlled vehicle testing, and by providing traffic control.

Several people at ORITE were also necessary to complete this work, including Sam Khoury who coordinated all of the instrumentation, scheduled and trained students for the field activities and maintained contact with NYSDOT to keep everything going smoothly. Mike Krumlauf assisted with the instrumentation, and with designing and fabricating various devices used in the lab and field. Many students worked on the project team, and some wrote theses on topics associated with the project.

Chapter 1 Introduction

Rigid pavements in the New York state are commonly constructed with a cement-treated permeable base (CTPB) layer over a dense-graded aggregate base (DGAB) layer. The CTPB drainage layer is intended to help remove water from the pavement structure to prevent distress and to serve as a platform for construction. However, this is a costly construction step, and the benefits of CTPB are questionable. The option for using only a DGAB layer would reduce construction time and costs, and may lead to an overall improved pavement performance. These two base layer options need to be investigated to identify their benefits and shortfalls for rigid pavement performance. Therefore, the Ohio Research Institute for Transportation and the Environment (ORITE), in conjunction with the New York State Department of Transportation (NYSDOT) have constructed and monitored two instrumented test sections on a fully reconstructed interstate highway. The first test section was constructed over a DGAB layer, and the second was constructed over CTPB with a DGAB layer beneath. Each section was instrumented with electronic sensors for measuring both environmental and dynamic load responses. The results from these two test sections herein presented were used to examine the performance of pavements constructed on CTPB and DGAB layers after 18 months of service.

1.1 Project Overview

The New State York Thruway Authority (NYSTA) has undertaken a 15-mile (24 km) reconstruction project on Interstate 90 (I-90) in upstate New York at Weedsport, near Syracuse. The project was a full-depth reconstruction of the pavement structure, and included new Portland cement concrete (PCC) pavement, base and sub-base. The two test sections were constructed at the end of construction phase A (Figure 1, reproduced from NYSTA, www.thruway.ny.gov).

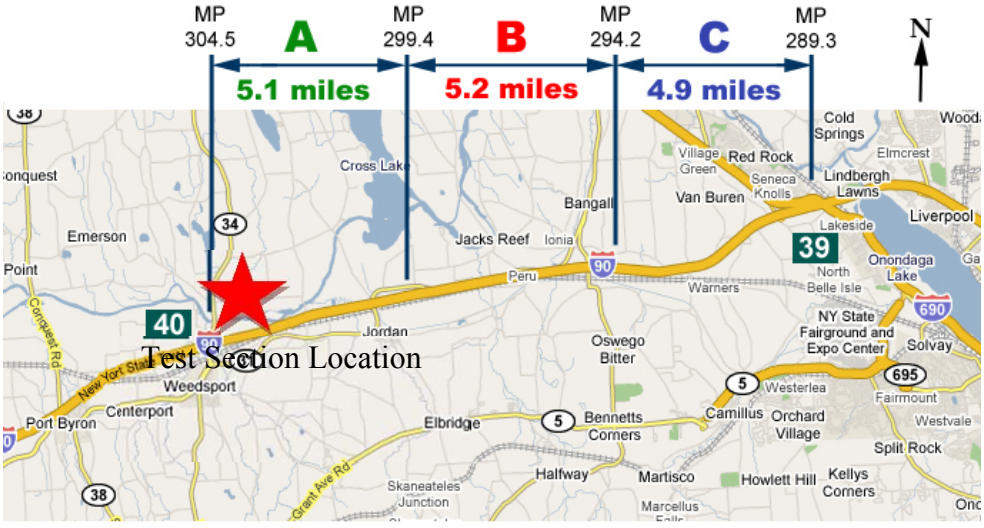

Figure 1 Construction schedule of I-90 thruway rehabilitation (NYSTA) (5.1 mi = 8.2 km, 5.2 mi = 8.4 km, 4.9 mi = 7.9 km).

1.2 Design Criteria

The reconstruction of the I-90 Thruway was based upon the NYSDOT Highway Design Manual (HDM). The roadway is a principle arterial interstate in an urban region, with an AADT of 34,320 vehicles and experienced less than 1% growth between 2006 and 2009 (NYSDOT, 2011). The CTPB and DGAB thicknesses were based on the standard design used in the HDM, with an expected design life of 50 years (NYSDOT HDM, 2002).

1.3 Objectives and Outline

The main objective of this study was to compare the responses of rigid pavements with CTPB and DGAB layers and to determine their impact on pavement performance. To accomplish this objective, environmental monitoring and dynamic testing were conducted on the two test pavements during the first 18 months of service. This base material study will help NYSDOT improve pavement design practices and calibrate the New York Mechanistic-Empirical Pavement Design Guide (MEPDG) catalog.

This study is presented in four parts, beginning with a literature review of base materials for rigid pavements in Chapter 2. In this section, common base materials are discussed, followed by sources of stresses in rigid pavements, and finally a discussion of case studies that have examined the usage of different base materials. In Chapter 3, the research methodology is presented, including instrumentation, construction techniques, data reduction, and testing methods. Next, Chapter 4 presents the results of laboratory testing, environmental monitoring, and dynamic testing; followed by a discussion of each topic. Chapter 5 summarizes the research and draws conclusions. Finally, additional tables, figures, and data are included in the appendices.

Chapter 2 Methodology

This chapter describes the methods and materials used throughout this project. Sensors and instrumentation layout are described, followed by a brief description of each type of sensor and the data acquisition units used. Afterwards, the procedure for placing concrete in the instrumented test sections is described. Finally, the dynamic testing procedures are discussed.

2.1.1 Test Section Layout

The test sections were instrumented prior to paving with 46 sensors, summarized in Table 1. The sensor layout designed by the ORITE researchers is a typical instrumentation plan used by ORITE. The first slab has 14 strain gauges and 10 thermocouples, the second slab contains five LVDTs and two pressure cells, and the third slab contains four strain gauges and eight and seven TDR probes in sections 1 and 2, respectively. Instrumentation plans and profiles are shown in Figure 2 and Figure 3.

Table 1 Summary of sensors

Label	Sensor Name	Manufacturer	Model	No. per Section	Measurement
KMA / KMB	Strain gauge	Tokyo Sokki Kenkyujo Co.	KM-100A / KM-100B	18	Slab Strain
VW	Vibrating Wire Tie Bar Strain gauge	Geokon	4911A-6X	4	Tie bar Strain
LVDT	Liner Variable Displacement Transducer	Honeywell	DW7S	5	Deflection
PC	Earth Pressure Cell	Geokon	3500	2	Dynamic Pressure
TDR	Time Domain Reflectometer	Campbell Scientific	TDR100	7 (8 @ Sect. 1)	Soil Moisture
TC	Thermocouple			10	Temperature

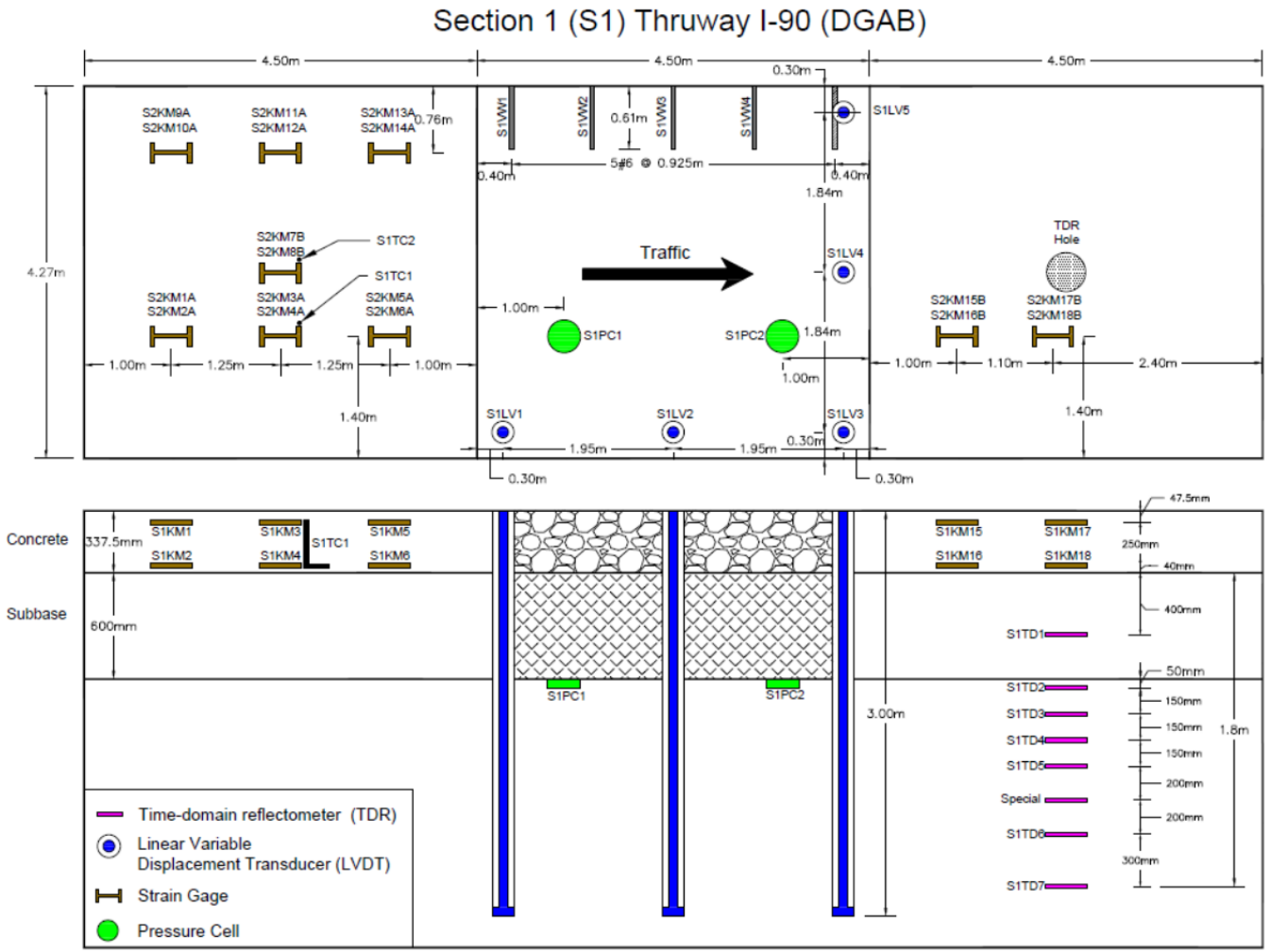

Figure 2 Section 1 instrumentation plan and profile (1m = 3.28 ft)

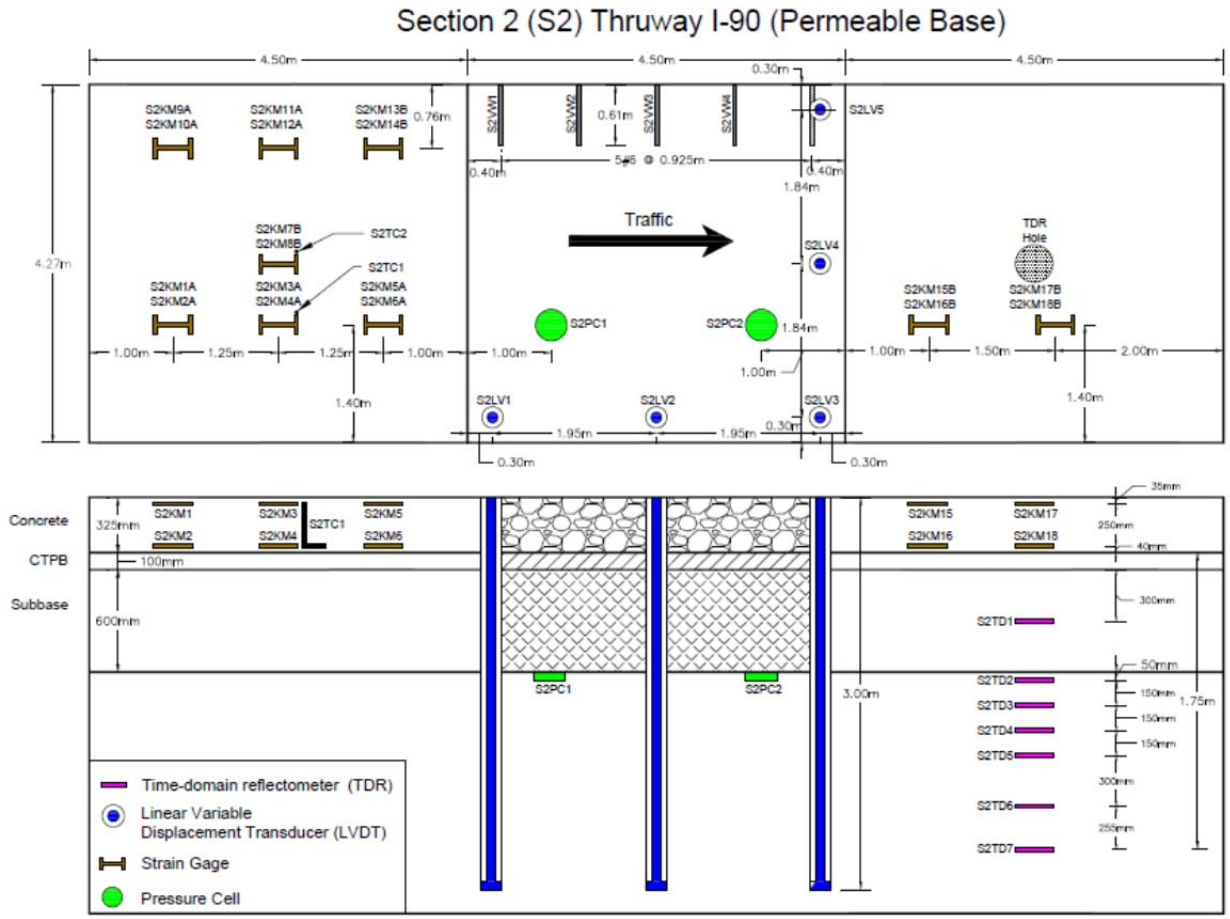

Figure 3 Section 2 instrumentation plan and profile (1m = 3.28 ft)

2.1.2 Data Acquisition

Each test section had its own set of data acquisition units stored in secure roadside boxes. Yokogawa MW100 data acquisition units were used to record LVDT, KM strain gauge, and thermocouple data. This system has multiple channels for recording strain, temperature, and voltage, which can be configured to record at specific time intervals. Campbell Scientific CR10 and CR 1000 units recorded tie-bar strain data and weather station data, respectively. Instrumentation boxes housing the data acquisition units were located 12.5 m (41.0 ft) from the shoulder. Sensor wiring was first run through underground conduit to a temporary pull box, and later to the instrumentation box. The data acquisition systems collect LVDT, strain gauge, vibrating wire tie bar and thermocouple data every 30 minutes, and store the information on memory until it is recovered during field visits.

2.1.3 KM Strain gauges

KM strain gauges measured strain at various locations in the slabs due to both environmental and dynamic loading effects. The KM strain gauges were installed in the longitudinal direction in pairs, top and bottom, at nine locations per site. gauges KM 1 through 6 and 15 through 18 are located along the right wheel-path, with 15 through 18 being redundant sensors placed on the third slab. Strain gauges KM 9 through 14 are positioned along the left wheel-path, and KM 7 and 8 are in the center of the first slab. At each location, a metal chair was positioned to support the gauges during concrete placement (Figure 4). Each chair held two gauges at elevations of 290 mm (11.4 in) and 40 mm (1.57 in) above the base. The gauges were bound to the chair at both ends with binding wire, and the chairs were nailed to the DGAB or glued to the CTPB to prevent movement during paving.

Figure 4 Paired KM strain gauges and supporting metal chair

There were two different elastic moduli for the KM strain gauges. The KM-A gauges have a stiffer elastic modulus (100 N/mm^2 or 14.5 ksi) compared to the KM-B gauges (40 N/mm^2 or 5.80 ksi), making the latter more sensitive to initial-curing strains. However, once the concrete elastic modulus exceeded the gauges moduli, there was no difference in the strain output between the two types. The modulus of the KM strain gauges is indicated in Figure 2 and Figure

3 by the suffix “A” or “B.” The KM-B gauges were placed at the slab center since this location typically experiences the highest environmental strains.

2.1.4 Vibrating Wire Tie Bar Strain gauges

At the longitudinal joint, load transfer and joint opening are affected by cyclic temperature changes. To monitor these effects, four tie bars were replaced with Geocon vibrating wire strain gauge tie bars (Figure 5). These sensors measure strain along the tie bar axis and temperature. The mechanized paver used on this project automatically inserts dowel and tie bars; however, for the instrumented test sections, both dowels and tie bars were positioned using baskets. The instrumented tie bars were bound to the basket with bailing wire. The strain gauge was located in the middle of the tie bar, and was carefully positioned at the longitudinal joint.

Figure 5 Geocon vibrating wire strain gauge tie bars placed at longitudinal joint

2.1.5 LVDTs

Honeywell LVDTs measure relative slab deflections under environmental and dynamic loads. Each test section was instrumented with five LVDTs, located 300 mm (11.8 in) from the slab edge along the shoulder and transverse joint (Figure 2 and Figure 3). Metal rods were driven 3 m (9.84 ft) below the pavement surface and grouted in place. The rods were encased in 5.1 cm (2 in) diameter polyvinyl chloride (PVC) pipe. The LVDTs were positioned over the metal rods inside a 7.6 cm (3 in) diameter PVC pipe, which holds the LVDT in place. The 7.6 cm (3 in) PVC tube was connected to the 5.1 cm (2 in) tube with a flexible rubber coupler, which allowed the LVDT and 7.6 cm (3 in) tube to deform with the pavement (Figure 6).

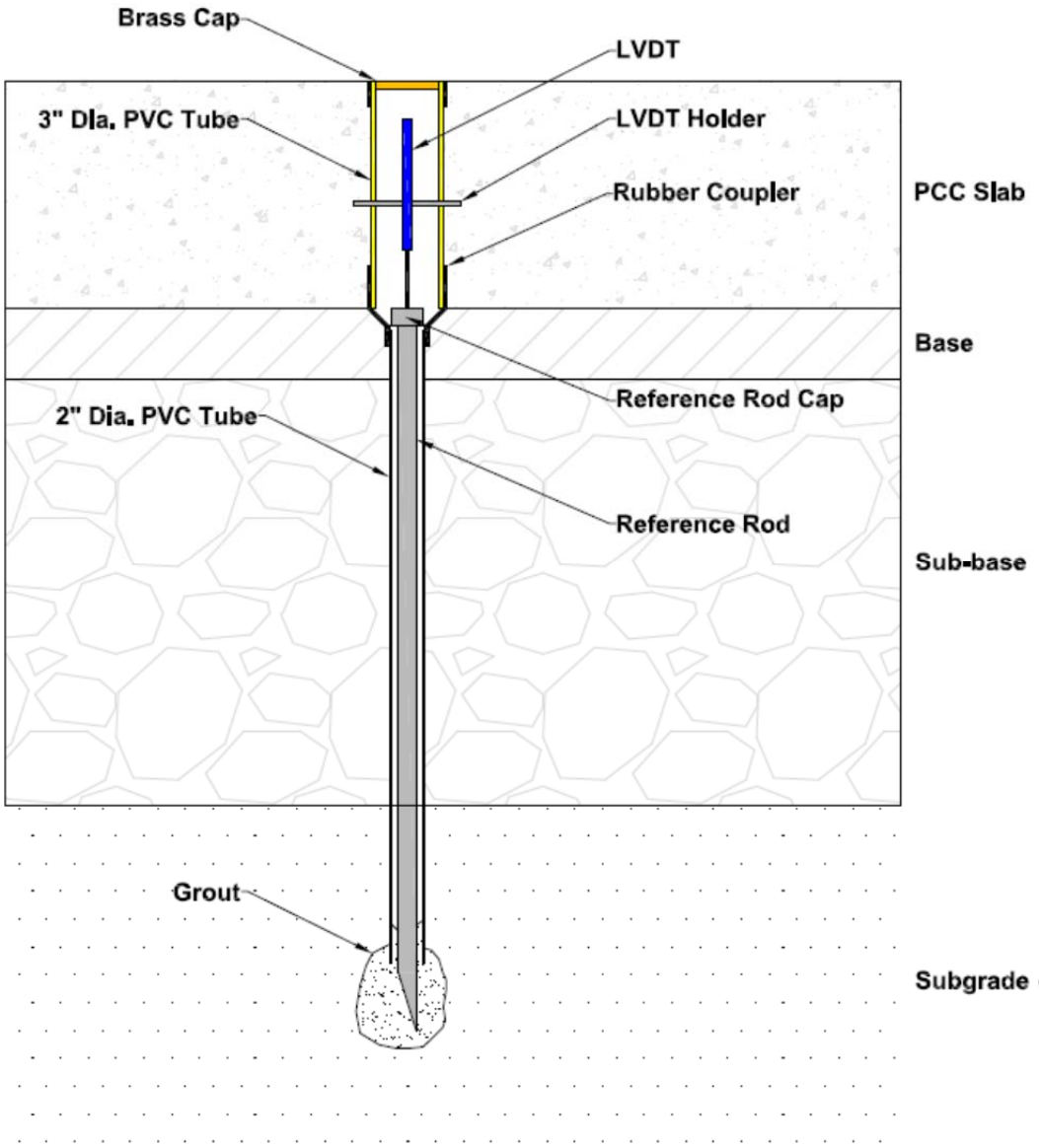

Figure 6 LVDT instrumentation diagram (1" = 2.54 cm)

2.1.6 Earth Pressure Cells

Each section was instrumented with two Geokon earth pressure cells, positioned directly beneath the DGAB layer along the right wheel path (Figure 7). The sensors are located 1-m away from the transverse joint on both sides of the slab (Figure 2 and Figure 3). At each sensor location, the DGAB sub-base material was excavated down the top of the subgrade. Sand was placed above and below the pressure cell to help evenly distribute pressure to the gauge and prevent stress concentrations from larger aggregates in the sub-base. The sub-base was then carefully re-compacted over the sensor, and in Section 2, the CTPB was replaced with new mix.

Figure 7 Earth pressure cell beneath the DGAB layer

2.1.7 TDR Soil Moisture Probes

Time-domain reflectometers (TDRs) measure the moisture profile of the sub-base and subgrade layers in each section (Figure 8). The first TDR probe was located at mid-depth of the DGAB layer, while the others were positioned a various depths in the subgrade, down to 1.75 m (5.74 ft) below the slab (Figure 2 and Figure 3). During instrumentation, soil layers were excavated and stored sequentially, then replaced and re-compacted to replicate the original site conditions.

Figure 8 Campbell Scientific TDR100 moisture probe

2.1.8 Thermocouples

The thermocouple sensors were used to collect temperature data from within the PCC slab. The L-shape gauges are configured with four evenly spaced temperature sensors along the length. An additional single sensor was included for an extra data point. Table 2 lists the sensors elevations relative to the top of the base at each location. These sensors were attached to the chains supporting strain gauges 3 and 4 (TC1) and strain gauges 7 and 8 (TC2) (Figure 2 and Figure 3), and positioned such that the top and bottom sensors were at the same elevation as the strain gauges in corresponding locations.

Table 2 Thermocouple positions above top of base

	Section 1 TC1		Section 1 TC2		Section 2 TC1		Section 2 TC2	
Sensor	(cm)	(in)	(cm)	(in)	(cm)	(in)	(cm)	(in)
1	29.5	11.6	29.5	11.6	29.5	11.6	29.3	11.5
2	25.7	10.1	25.7	10.1	25.7	10.1	25.5	10.0
3	21.9	8.6	21.9	8.6	21.9	8.6	21.7	8.5
4	18.0	7.1	18.0	7.1	18.0	7.1	17.8	7.0
5	3.2	1.3	3.8	1.5	3.0	1.2	3.5	1.4

2.1.9 Weather Station

We installed the Campbell Scientific weather station, shown in Figure 9, in December 2009 after the test sections were built. This equipment monitored and recorded hourly wind speed and direction, ambient air temperature, solar radiation and precipitation accumulation. The data collected from the weather station was used in the long-term environmental analysis to depict seasonal conditions for the selected periods.

Figure 9 Weather station at mile marker 300 along I-90

2.1.10 Construction Process

Temporary metal boxes were placed around the KM strain gauges and LVDTs to protect them during paving, as shown in Figure 10. These boxes provided rigidity against the flow of wet concrete and protected the sensors from damage or displacement by the paver. The boxes were built such that the four side panels could slide past one another when pulled vertically. The legs of the boxes extended into the base to provide stability during construction. Prior to paving, the boxes were filled with concrete by hand and vibrated to consolidate the material around the sensors. Wet concrete was also placed around the box to prevent lateral displacement and ensure full concrete coverage around the box. Immediately after the paver passed each sensor location, the sides of the boxes were pulled vertically from the concrete, and the concrete was vibrated to consolidate any additional air voids.

Figure 10 Sensors are enclosed in metal boxes during paving to prevent damage

Unfortunately, the paver did make contact with two metal boxes housing LVDTs 2 and 3 in Section 2 (Figure 11). After closer inspection, it was determined that the sensors were unharmed and functional. The PVC encasements around the LVDTs were realigned and the concrete around the gauges was reconsolidated. As a result, the contractor gradually increased the pavement depth from 325 mm (12.79 in) at Section 2 to 337.5 mm (13.29 in) at Section 1 to prevent further complications.

Figure 11 LVDT 2 in Section 2 after paver struck metal box

2.2 Dynamic Testing

This section describes the procedures followed and data reduction used for the falling-weight deflectometer (FWD) and truck load tests performed on the test sections. Included in the data reduction for the FWD tests are common parameters found from the FWD data.

2.2.1 Falling Weight Deflectometer

A common non-destructive test (NDT) procedure for pavements is the falling-weight deflectometer (FWD) test. This NDT can be done either during base construction or on completed highways to determine structural capacity, mechanistic pavement properties, and performance properties. The test drops a weight from a specific height onto a spring buffer system, delivering a dynamic pulse through a round metal plate, which simulates a wheel passing at highway speeds (Sargand, 2002). Several load levels were delivered in succession at each test location, the magnitude of which depends on the material being tested. The base was tested with loads of 26.7 kN (6.0 kip), 40 kN (9.0 kip), and 53.4 kN (12.0 kip), and the PCC pavement was tested with loads of 40 kN (9.0 kip), 53.4 kN (12.0 kip), and 71.2 kN (16.0 kip). Geophones measured the surface deflections at distances of 0 to 72 in (182.9 cm) from the load plate center. Figure 12 shows the geophone configurations used to test PCC pavement on this project. On rigid pavement, the test is commonly performed at mid-panel and at transverse joints. Mid-panel tests determine structural stiffness and mechanical properties of the pavement layers, while tests at the transverse joints determine the joint load transfer efficiency and slab edge support conditions.

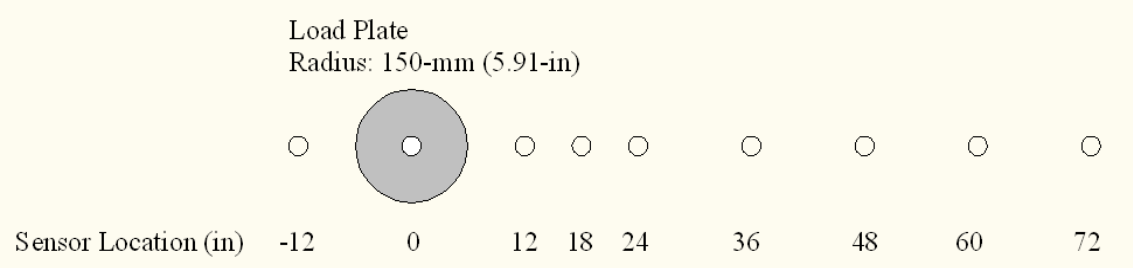

Figure 12 FWD geophone sensor configuration (12 in =30.48 cm)

2.2.2 Truck Load Testing

The dynamic load response to vehicle loads at various speeds was measured at each test section. Two different single-axle, dual rear tire, fully loaded trucks were used to apply dynamic loads; the light truck is shown in Figure 13. The same vehicles used during the spring 2010 test were used again during the fall 2010 test. In November 2011, tests were performed with both a single-axle and dual-axle truck. The geometry for each vehicle is shown in Figure 14 and Table 3. We measured the axle weights and tire pressures of each truck during the spring and fall tests prior to testing, as shown in Table 4.

Figure 13 Light truck load during truck test

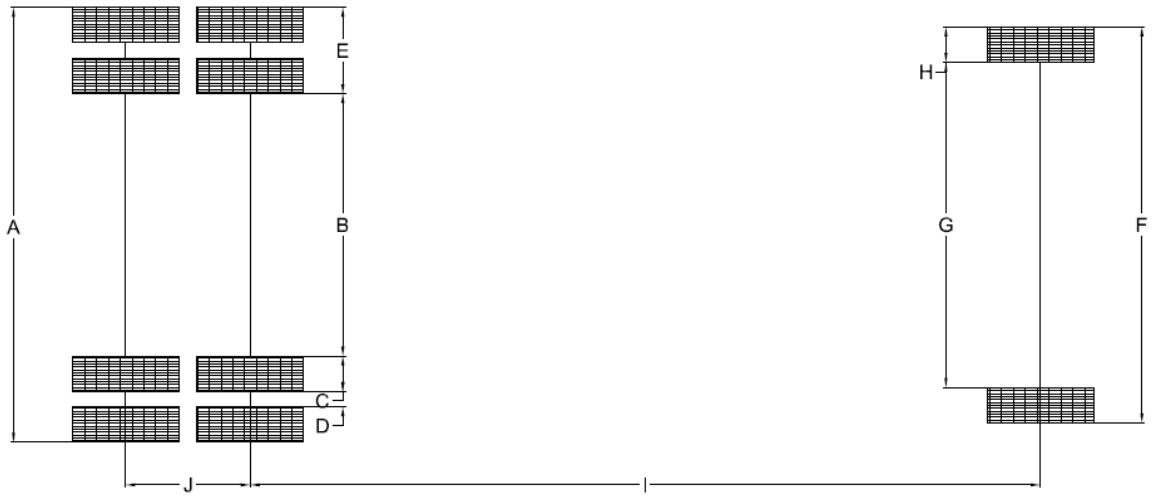

Figure 14 Truck geometry

Table 3 Truck Dimensions

Dimensions (cm)				
	Spring & Fall 2010		Fall 2011	
	Single Axle (Light)	Single Axle (Heavy)	Tandem Axle	Single Axle
A	233	224	234	224
B	141	128	130	128
C	19	20.3	20	20.3
D	8.25	11.4	16.5	11.4
E	46	52	57	52
F	213	224	234	224
G	175	183	183	183
H	19	20.3	25.4	20.3
I	424	447	418	447
J	-	-	52.5	-
Dimensions (in)				
A	91.7	88.2	92.1	88.2
B	55.5	50.4	51.2	50.4
C	7.5	8.0	7.9	8.0
D	3.2	4.5	6.5	4.5
E	18.1	20.5	22.4	20.5
F	83.9	88.2	92.1	88.2
G	68.9	72.0	72.0	72.0
H	7.5	8.0	10.0	8.0
I	166.9	176.0	164.6	176.0
J	-	-	20.7	-

Table 4 Truck test axle weights and tire pressures

Test date	Axle Config-uration	Side	Axle Number 1 (kN)	1 (kip)	2 (kN)	2 (kip)	3 (kN)	3 (kip)	Tire Pressure Front (kPa)	Front (psi)	Rear (kPa)	Rear (psi)
Spring 2010	Single (Light)	Driver	12.90	2.90	34.25	7.70	-	-	620.5	90.0	620.5	90.0
		Passenger	12.68	2.85	36.00	8.09						
		Total	25.58	5.75	70.28	15.80						
	Single (Heavy)	Driver	21.13	4.75	44.70	10.05	-	-	758.4	110.0	758.4	110.0
		Passenger	21.57	4.85	44.04	9.90						
		Total	42.70	9.60	88.74	19.95						
Fall 2010	Single (Light)	Driver	14.01	3.15	40.48	9.10	-	-	620.5	90.0	620.5	90.0
		Passenger	14.46	3.25	40.92	9.20						
		Total	28.47	6.40	81.40	18.30						
	Single (Heavy)	Driver	20.02	4.50	41.15	9.25	-	-	758.4	110.0	758.4	110.0
		Passenger	20.68	4.65	46.04	10.35						
		Total	40.70	9.15	87.19	19.60						
Fall 2011	Single	Driver	20.33	4.57	31.14	7.00	-	-	758.4	110.0	723.9	105.0
		Passenger	19.79	4.45	28.02	6.30						
		Total	40.12	9.02	59.16	13.30						
	Tandem	Driver	33.81	7.60	33.58	7.55	32.03	7.20	758.4	110.0	758.4	110.0
		Passenger	33.14	7.45	28.25	6.35	29.36	6.60				
		Total	66.95	15.05	61.83	13.90	61.39	13.80				

Each vehicle made three passes at speeds of 8 km/h (5 mph), 40 km/h (25 mph), 55 km/h (34 mph), and 70 km/h (43 mph) during the spring 2010 test, 8 km/h (5 mph), 40 km/h (25 mph), and 70 km/h (43 mph) during the fall 2010 test, and 8 km/h (5 mph), 40 km/h (25 mph), and 90 km/h (56 mph) during the fall 2011 test. Different speeds were used to examine the affect speed has on pavement deflection and strain response. While maintaining a constant speed, each vehicle was driven through the test sections with the right rear tires centered over the strain gauges along the right wheel-path. We spread damp sand across the wheel-path at the beginning and end of each test section to measure the location of the rear wheels. Figure 15 shows tire imprint captured in the damp sand during a typical test; the painted line in this figure represents the right wheel-path.

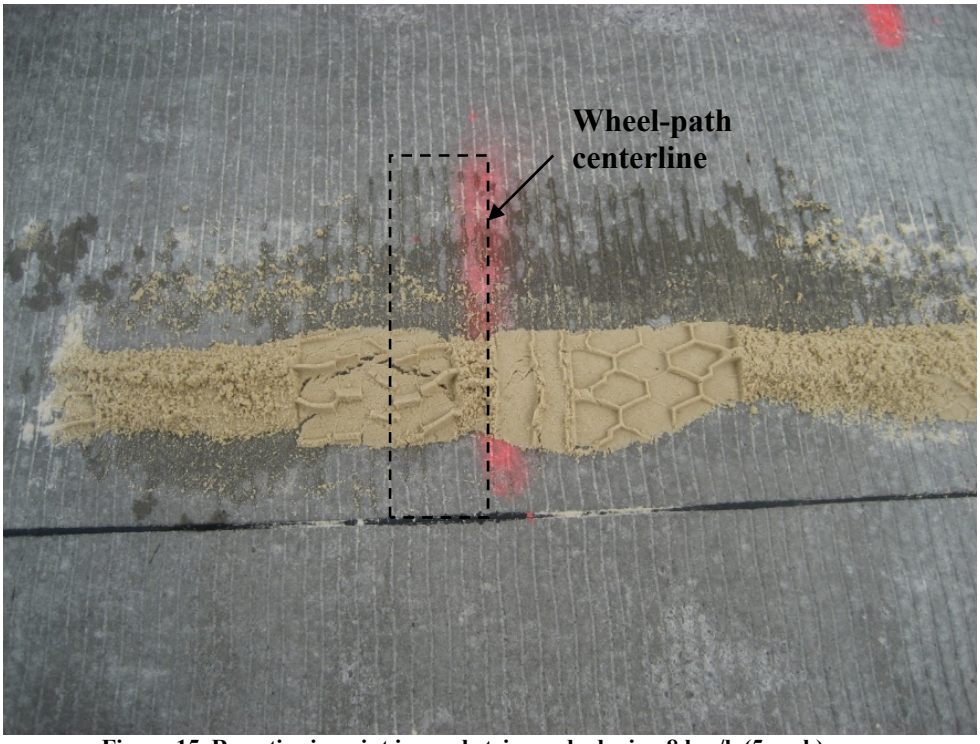

Figure 15 Rear tire imprint in sand strip made during 8 km/h (5 mph) pass

Chapter 3 Results and Discussion

In this section, laboratory test results from the subgrade, DGAB, CTPB and PCC concrete are presented. Next, the environmental monitoring results for initial curing and long-term pavement response is presented and discussed. This discussion includes temperature gradients, strains, and deflections at each test section. Then the FWD results for base and early-age PCC pavement testing are presented and discussed in terms of deflections at mid-slab and transverse joints. Finally, the dynamic truck tests for spring 2010 and fall 2010 are presented with discussion, including strain and deflection responses from both test sections during morning and afternoon tests.

3.1 Laboratory Testing

In order to characterize the material properties found at each test section, subgrade, DGAB, CTPB and PCC test specimen were collected. ORITE researchers and graduate research assistants recovered subgrade material during TDR and LVDT instrumentation from various depths at each section. We then combined this material in the laboratory to obtain a composite sample for the entire site. The DGAB sample was collected from the contractor's material stockpile in September 2010. CTPB specimen were cast in cylinders on-site and transported to Ohio University for testing. FHWA technicians cast concrete beams and cylinders during construction, which were then cured and tested on-site.

3.1.1 Subgrade Properties

In the lab, we processed and tested the subgrade soil samples for classification. The sample was and dried and broken down to separate collated material. Next, the soil was wet-washed to determine the quantity passing the No. 200 sieve. A sieve analysis was then conducted on the remaining dried sample, shown in Table 5. Finally, the Atterberg limits were determined to classify the soil, as summarized in Table 6.

Table 5 Subgrade sieve analysis

Sieve No.	Diameter		Retained			Passed		
	(mm)	(mil)	(g)	(oz)	(%)	(g)	(oz)	(%)
4	4.75	187	63	2.2	9.30%	616.5	21.7	90.70%
10	2	79	55	1.9	8.10%	561.5	19.8	82.60%
20	0.84	33	47	1.7	6.90%	514.5	18.1	75.70%
40	0.425	16.7	37	1.3	5.40%	477.5	16.8	70.30%
60	0.25	9.8	38	1.3	5.60%	439.5	15.5	64.70%
100	0.15	5.9	39.5	1.4	5.80%	400	14.1	58.90%
200	0.075	2.95	46	1.6	6.80%	354	12.5	52.10%
pan	-	-	354	12.5	52.10%	-	-	-

Table 6 Atterberg limits

Property	Value
Liquid Limit (LL)	24.6%
Plastic Limit (PL)	13.4%
Plasticity Index (Ip)	11.2%
Group Index (GI)	2.53

Using the AASHTO and Unified Soil Classification (USC) systems, the soil was classified respectively as A-6 and CL. Under the USC, the soil was further characterized by the group name sandy lean clay.

3.1.2 DGAB Properties

The DGAB was placed in two layers with different gradations, classified as NYSDOT Type 3 and Type 4. Both materials were crushed reclaimed concrete pavement (RCP); however, Type 3 was a finer material used as the upper DGAB layer. The grain-size distribution of both materials is shown in Figure 16. ORITE researchers and graduate research assistants performed the resilient modulus tests on both material types. Deviator stress was varied for different confining stresses to test each sample at different stress levels. The resilient modulus at a confining stress of 20 kPa (2.9 psi) and a deviator stress of 59 kPa (8.6 psi), chosen as the expected pavement stress state, resulted in a resilient modulus of 142.0 MPa (20.60 ksi) and 134.7 MPa (19.54 ksi) for Type 3 and Type 4, respectively.

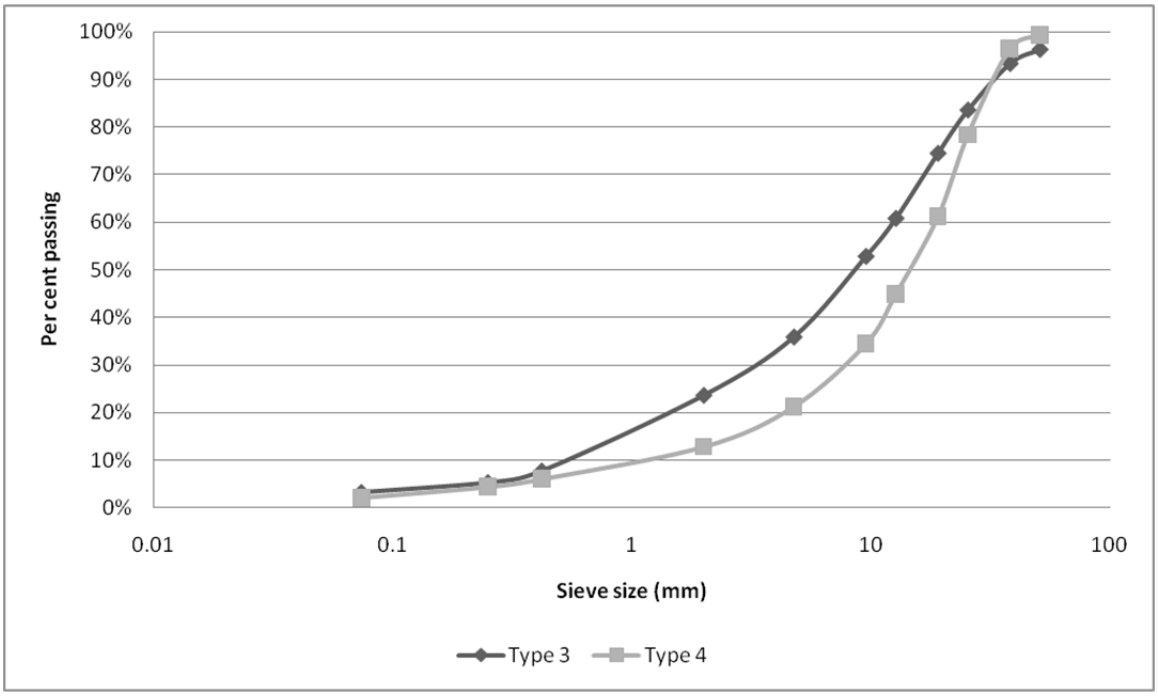

Figure 16 Grain-size distribution for NYSDOT Type 3 and Type 4 DGAB (1 mm = 39.4 mil; 25.4 mm = 1 in)

3.1.3 CTPB Properties

The CTPB mix, shown in Table 7, was also tested for mechanical properties. Test cylinders were cast in September 2009, and additional cylinders were cast for further testing in September 2010. The contractor verified that the mix design and material sources had not changed over that period, making the samples collected at both times representative of the project.

Table 7 CTPB mix design

Material	kg/m^3	pcf
Cement	143	8.93
Fine Aggregate	193	12.05
Coarse Aggregate (#1)	736	45.95
Coarse Aggregate (#2)	673	42.01
Water (max.)	53	3.31
Water/cement Ratio (max)	0.37	

The static modulus of elasticity and Poisson's ratio were found according to the American Society for Testing and Materials (ASTM) C469/C469M using a ring-compressometer, since strain gauges would be difficult to adhere to the material's irregular surface. Dial gauges on the ring-compressometer measure strain in both transverse and longitudinal directions. During loading, strains measurements were taken at a strain of 50με and at 40% of ultimate compressive strength (ASTM C469/C469M, 2010). Using these two data points, the static elastic modulus and Poisson's ratio were calculated. Figure 17 shows the test setup for the static modulus and Poisson's ratio test. After the static modulus test, the ring compressometer device was removed and the specimen was loaded to capacity to determine the ultimate compressive strength of the CTPB sample.

Figure 17 Static modulus and Poisson's ratio test setup for CTPB specimen

Split-cylinder tensile tests were also performed to determine the tensile strength of the CTPB. For this test, a 15.2 cm (6 in) diameter cylinder was cut into two 15.2 cm (6 in) long specimens. Each specimen was loaded along its length with two wood shims positioned horizontally along the specimen length to distribute the compressive force during the test (Figure 18). The specimen was loaded until failure, which occurred along the vertical plane as tensile stresses formed perpendicular to the load direction, shown in Figure 19.

Figure 18 Split-cylinder tensile test setup on CTPB sample

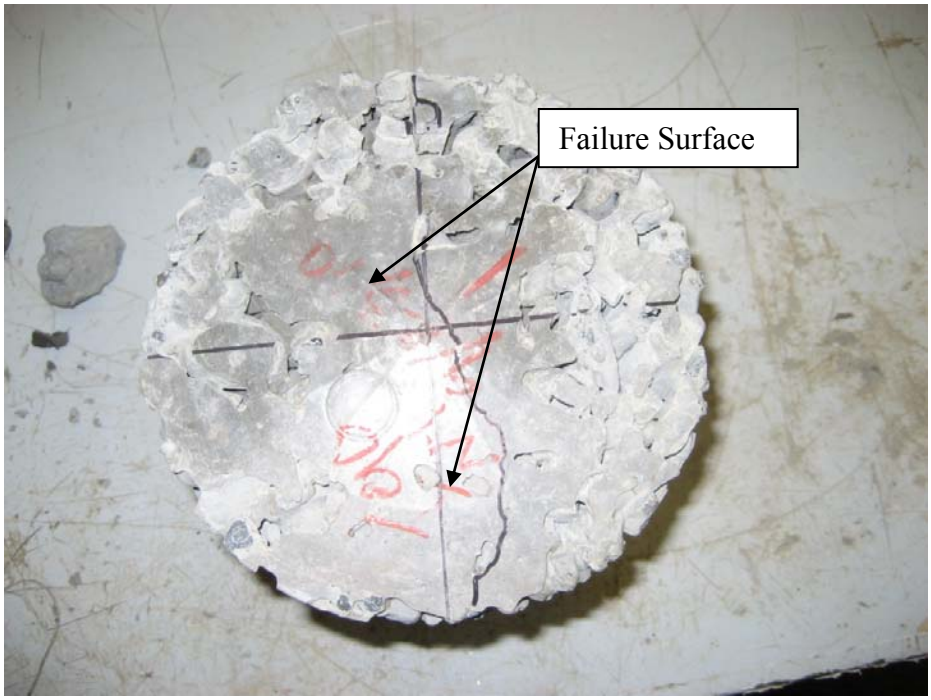

Figure 19 Failure of specimen during split-cylinder tensile test

The split tensile strength was found by using Equation 1. Results for the CTPB compressive strength, elastic modulus, and tensile strength are summarized in Table 8. The range of results indicates the material properties were quite variable. The variability of the CTPB was related to concrete coverage and specimen unit weight. The samples with higher strengths were observed to have more cement coverage and greater unit weights.

Equation 1

$$f'_{ct} = \frac{2 * P}{\pi * d * L}$$

where $f'_{ct} = Split - tensile\ strength$
$P = compressive\ load\ at\ failure\ of\ specimen$
$d = diameter\ of\ specimen$
$L = length\ of\ specimen$

Table 8 CTPB Mechanical Properties

Age (day)	Sample No.	Compressive Strength		Tensile Strength		Elastic Modulus		Poisson's Ratio	Unit Weight	
		(kPa)	(psi)	(kPa)	(psi)	(MPa)	(ksi)		(kN/m^3)	(pcf)
14	1	3,375	490	-	-	9,299	1,349	0.167	18.03	0.1148
	2	7,501	1,088	-	-	13,975	2,027	0.303	19.13	0.1218
28	1	5,506	799	-	-	15,883	2,304	0.012	19.34	0.1231
	2	-	-	1,169	170	-	-	-	19.42	0.1236
Average		5,461	792	1,169	170	13,052	1,893	0.161	18.83	0.1199
Std. Dev.		2,063	299	-	-	3,388	491	0.146	0.64	0.0041

3.1.4 Concrete Properties

The specified mix design for the concrete pavement was NYSDOT Class C Modified, as summarized in Table 9. During paving, test cylinders and beams were cast by FHWA technicians. The specimen were cured on-site and tested in the mobile FHWA testing laboratory. Tests conducted on the samples at various curing ages are summarized in Table 10.

Table 9 Concrete Mix Design

Material	Quantity/m^3	Quantity/ft^3
Cement	287 kg	17.9 lb
Fly Ash	72 kg	4.5 lb
Fine Aggregate	703 kg	43.9 lb
Coarse Aggregate	1083 kg	67.6 lb
Water Reducing Agent	1172 mL	112.2 fl oz
Air Entraining Agent	96.7 mL	9.26 fl oz
Water	148 kg	9.2 lb
Slump	5.1 ± 1.25cm	2.0 ± 0.5 in
Air Content	6.5 ± 1.5%	
Water/cement Ratio (max.)	0.44	

Table 10 Concrete Test Results

Age (days)	Compressive Strength		Modulus of Rupture		Compressive Strength		Modulus of Rupture		Elastic Modulus		Poisson's Ratio
	(MPa)	(ksi)	(MPa)	(ksi)	(MPa)	(ksi)	(MPa)	(ksi)	(MPa)	(ksi)	
7	24.57	3.56	2.87	0.42	24.44	3.54	3.06	0.44	-	-	-
14	31.20	4.53	3.85	0.56	29.77	4.32	3.74	0.54	22431.70	3253.44	0.252
28	37.44	5.43	4.22	0.61	37.30	5.41	4.27	0.62	23843.50	3458.21	0.240

3.2 Field Forensic Observations

During construction operations, the contractor reported bonding between the CTPB and PCC slab shortly after construction. When paving was halted at the end of each day, a portion of unfinished pavement was left, which was cut and removed at the beginning of the next day. When the pavement was removed, the CTPB was adhered to the PCC slab, and was removed with the slab. During a data collection trip, we visited the material refuse area where used material was stored on site prior to recycling. As reported by the contractor, the CTPB was bonded to the PCC slabs (Figure 20). This verifies the claim that the PCC mortar penetrates the porous CTPB structure and forms a bond as the concrete slab cures.

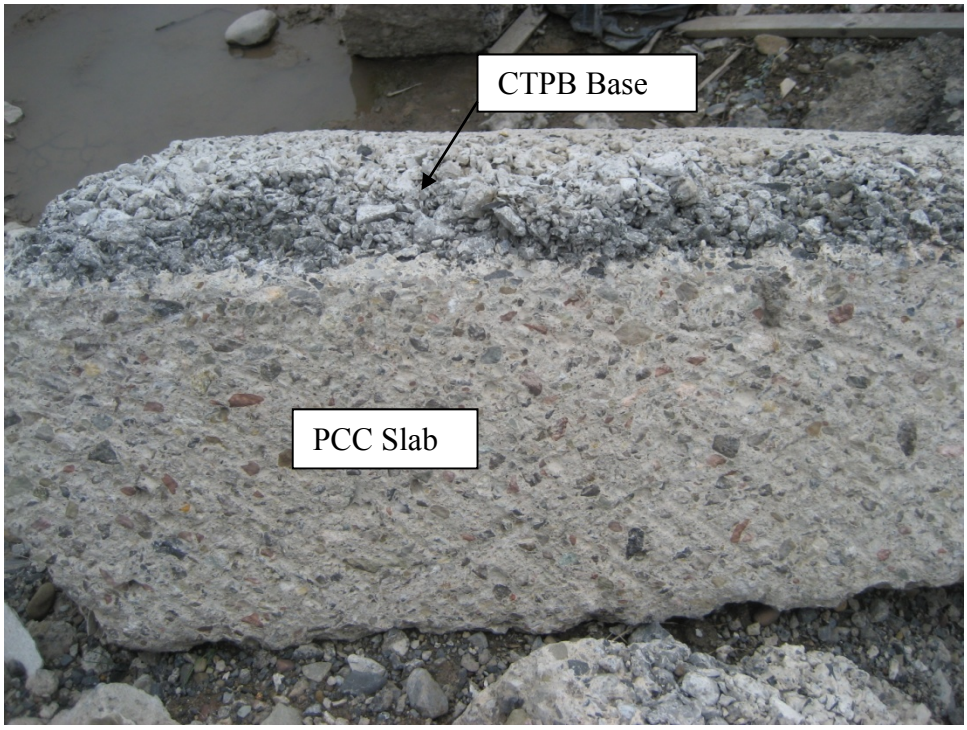

Figure 20 Bonded CTPB and PCC slab in refuse pile at construction site

3.3 Environmental Monitoring

Environmental data has been continually collected since test section construction on October 8 2009. LVDTs recorded slab deflections, KM strain gauges monitored longitudinal strain in the slab, vibrating-wire (VW) strain gauges recorded axial strain within the tie bars, and thermocouples measured slab temperatures. Additionally, weather station data has been collected since December 2009 and soil moisture readings have been periodically collected during site visits using the TDR probes. This section presents the findings from initial curing and long-term environmental monitoring, including strain gauge, LVDT and soil moisture data.

3.3.1 Pavement Curing Strains

According to Mindess, Young, and Darwin (2003), the concrete setting process begins with the initial set, a time when the mortar begins to stiffen, which is typically two to four hours after placement. The final set occurs approximately five to eight hours after placement, and indicates the time in which concrete can carry load without deformation. ASTM specifies two tests, ASTM C 191 and ASTM C 266, for determining the initial and final set times using needle penetration devices (Mindess, Young, & Darwin, 2003); however, determining the set times are out of the scope of this project and shall not be discussed herein.

The test sections were paved on October 8 2009, beginning with Section 2, which was placed between 7:25 and 8:30 AM, followed by Section 1, which was placed between 10:25 and 11:25 AM. The initial curing strains began when the sensor readings stabilized and began to increase in strain. The initial set time was estimated in Section 2 and Section 1 to be at 9:30 AM and 12:30 PM, respectively. The curing total and load related strain development in sections 1 and 2 at the mid-slab wheel-path locations are shown in Figure 21 and Figure 22, respectively. Strains

at mid-slab center are not shown here due to discontinuous data; however, the sensors at mid-slab have a lower modulus and are more sensitive to initial curing strains.

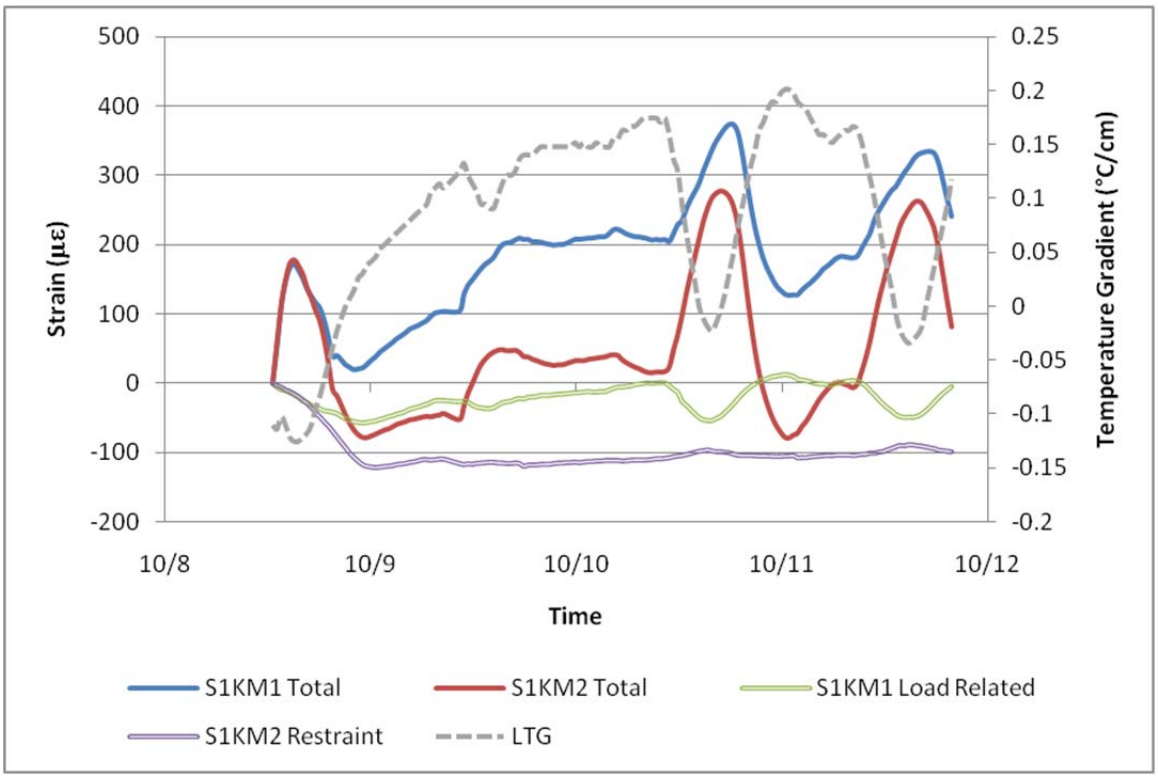

Figure 21 Curing total strains and restraining strains in Section 1 (1C°/cm = 4.6°F/in)

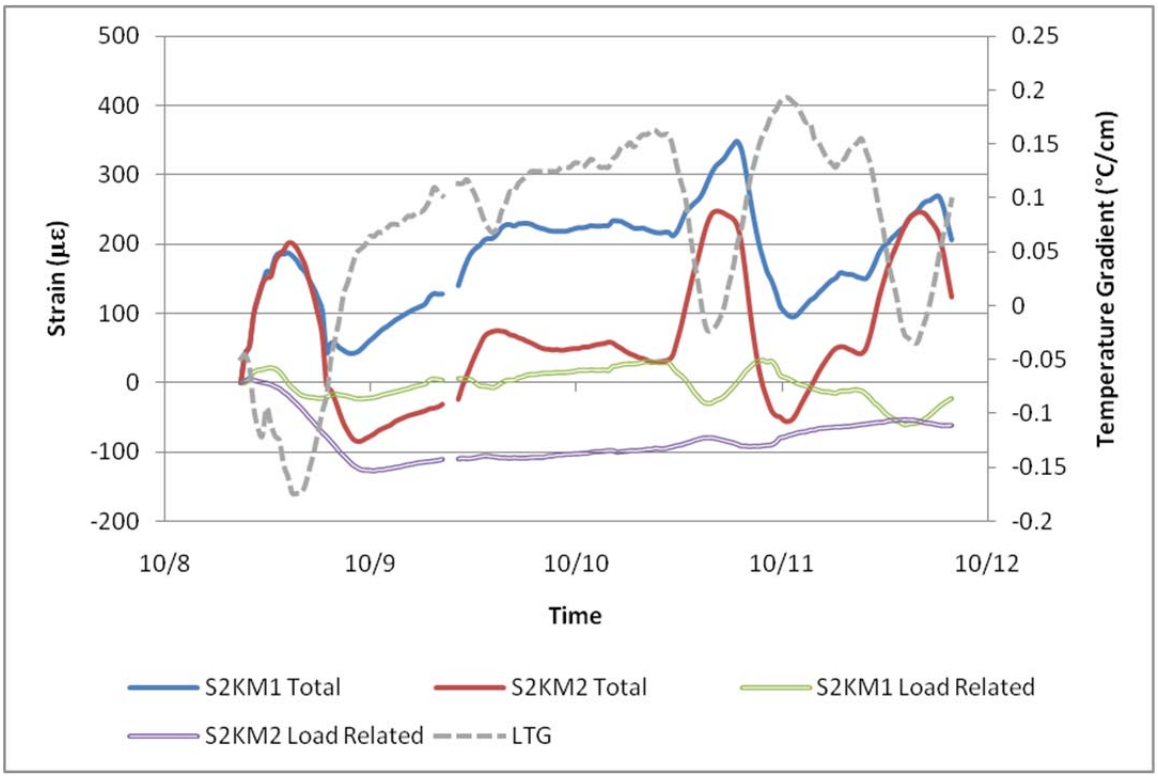

Figure 22 Curing total strains and restraining strains in Section 2 (1C°/cm = 4.6°F/in)

The total strains in both sections initially behave in a similar trend, both peaking at almost 200 με in the first 12 hours after placement. As the concrete continues to cure, the tensile strains in Section 1 were greater than in Section 2. However, the load-related strains at the slab bottom in Section 2 peak at a higher compressive strain than Section 1, followed by a linear increase in tensile strains. The load-related strains at the slab bottom in Section 1 remain constant after reaching their peak compressive value of approximately 100 με. The load-related strains at the slab surface in both sections are similar; however, Section 2 does show slightly larger peak values for this location.

3.3.2 Discussion of Curing Strains

The load-related curing strains indicated a bond forming at the slab/base interface in Section 2. From Figure 22, the bottom load-related strains, S2KM4, increase linearly after reaching peak compressive strains on October 9. The positive increase in strains indicates the shear transfer at the slab/base interface is inducing tensile strains as the slab cures. Therefore, the bonding was restraining the slab as drying shrinkage occurred. In Section 1, the bottom load-related strains, S1KM4, also reached peak compressive strains on October 9; however, the subsequent trend remained nearly constant throughout this period. This indicates load-related strains at the slab bottom in Section 1 were constant over time, and were not influenced by base layer restraint.

3.3.3 Long-term Pavement Response

Environmental data has been continually recorded since construction. The daily change in load-related strain was determined to compare the diurnal strain fluctuations experienced by the

concrete pavements. The difference between the maximum and minimum peaks in strain was found over a 24-hour period, and the daily change in strain was averaged over a six to eight day observation period. Peak strains and deflections typically coincide with peak temperature gradients; therefore, the average maximum and minimum daily temperature gradients were also computed. The linear temperature gradients (LTGs) in Section 2 were always slightly larger in magnitude than Section 1.

Changes in load-related strain indicate the amount of strain each section experiences on a daily basis. This value does not represent the actual stress in the pavement, which is relative to the zero-stress condition at final set. The final set time can only be estimated with the given information, and therefore, is not in the scope of this project. However, the daily changes in strain are representative of the amount of stress the pavements undergo daily, and shall be used to evaluate the base materials.

The time periods selected, as summarized in Table 11 and Table 12 were typical responses and were representative of the pavement behavior during each season. The periods were selected such that the minimum and maximum number of days was six and eight, respectively. The seasonal data was selected in terms of the meteorological seasons, which defines winter as December through February, spring as March through May, and so on. This definition is based average temperatures in the Northern hemisphere and not equinoxes and solstices as we traditionally define seasons (Hopkins, 2005).

The daily maximum and minimum deflection readings at each sensor were used to determine the daily change in deflection. The daily change in deflection was averaged over each observed period to examine the mean deflection at each sensor. The average daily change in deflections are referred to as "deflections" herein, and are shown in Figure 23 and Figure 24 for Section 1 and Section 2, respectively, at each sensor location.

The average daily changes in load-related strain are herein referred to as "strains." The strains in the top of the slab are shown in Figure 25 and Figure 26 and the strains in the bottom of the slab are shown in Figure 27 and Figure 28 for Sections 1 and 2, respectively. The strain gauge layout is redundant in configuration on the first and third test slabs, and sensors in similar locations produced similar results; therefore, only strain gauges KM 1 through KM 14 are shown. Additional strain and deflection data is presented in the appendices.

During the July 13 – 20 2010 period, no temperature data and limited strain gauge data was collected for Section 1. The strain values presented are based on the temperature data observed in Section 2; however, the temperatures in both sections were typically similar so the strains calculated should be representative.

Table 11 Summary of seasonal response data time periods and conditions (Metric units)

Season	Fall 2009		Winter 2009/10		Spring 2010			Summer 2010		Fall 2010	
Dates	Nov 5-11	Nov 12-17	Dec 19-25	Jan 11-17	Apr 8-14	Apr 24-May 1	May 13-20	June 5-12	July 13-20	Sept 30-Oct 6	Oct 14-21
Average Air Temperature (°C)	NA	NA	-5.3	-1.5	9.5	12.0	14.3	16.5	24.4	12.1	9.2
Average Solar Radiation (kW)	NA	NA	0.050	0.052	0.244	0.209	0.242	0.212	0.247	0.092	0.098
Total Precipitation (mm)	NA	NA	15.0	5.8	6.4	8.1	18.0	71.6	1.5	90.7	36.8
Section 1 Average Max. LTG +/- (°C/cm)	0.113	0.1222	0.046	0.112	0.29943	0.276	0.315	0.203	NA	0.095	0.122
	-0.116	-0.142	-0.104	-0.055	-0.1335	-0.093	-0.099	-0.131	NA	-0.113	-0.135
Section 2 Average Max. LTG +/- (°C/cm)	0.122	0.1403	0.0565	0.1141	0.31858	0.296	0.348	0.221	NA	0.111	0.146
	-0.124	-0.155	-0.113	-0.069	-0.1701	-0.113	-0.120	-0.158	NA	-0.117	-0.142
Section 1 Max LTG +/- (°C/cm)	0.221	0.177	0.117	0.208	0.381	0.442	0.453	0.365	NA	0.186	0.232
	-0.156	-0.188	-0.146	-0.110	-0.196	-0.177	-0.179	-0.177	NA	-0.150	-0.162
Section 2 Max LTG +/- (°C/cm)	0.233	0.200	0.113	0.210	0.392	0.466	0.480	0.386	NA	0.216	0.269
	-0.177	-0.200	-0.145	-0.122	-0.223	-0.199	-0.201	-0.195	NA	-0.155	-0.166

Table 11 continued.

Season	Fall 2010	Winter 2010/11			Spring 2011			Summer 2011			Fall 2011		
Dates	Nov 7-16	Dec 29-Jan 6	Jan 15-22	Feb 20-27	Mar 17-24	Apr 9-16	May 9-16	June 1-7	July 9-16	Aug 9-16	Sept 16-23	Oct 9-16	Nov 1-7
Average Air Temperature (°C)	5.0	0.0	-6.9	-5.4	3.8	10.0	15.2	18.5	22.5	20.3	14.7	14.8	8.1
Average Solar Radiation (kW)	0.086	0.050	0.055	0.111	0.147	0.160	0.209	0.278	0.309	0.177	0.157	0.094	0.108
Total Precipitation (mm)	16.0	1.5	9.9	45.7	0.0	0.0	11.4	NA	NA	NA	NA	NA	NA
Section 1 Average Max. LTG +/- (°C/cm)	0.165	0.103	0.062	0.153	0.210	0.239	0.358	0.327	0.380	0.230	0.225	0.177	0.191
	-0.133	-0.091	-0.140	-0.138	-0.099	-0.090	-0.116	-0.140	-0.158	-0.126	-0.157	-0.127	-0.135
Section 2 Average Max. LTG +/- (°C/cm)	0.194	0.117	0.079	0.166	0.227	0.258	0.331	0.355	0.409	0.261	0.257	0.202	0.217
	-0.137	-0.097	-0.145	-0.141	-0.117	-0.106	-0.132	-0.167	-0.176	-0.133	-0.164	-0.132	-0.148
Section 1 Max LTG +/- (°C/cm)	0.234	0.208	0.152	0.273	0.407	0.434	0.450	0.456	0.425	0.363	0.319	0.336	0.236
	-0.187	-0.187	-0.227	-0.256	-0.186	-0.177	-0.177	-0.227	-0.208	-0.173	-0.221	-0.148	-0.225
Section 2 Max LTG +/- (°C/cm)	0.275	0.226	0.178	0.317	0.434	0.470	0.482	0.497	0.459	0.400	0.359	0.369	0.269
	-0.189	-0.184	-0.235	-0.252	-0.197	-0.191	-0.197	-0.245	-0.224	-0.185	-0.228	-0.153	-0.239

Table 12 Summary of seasonal response data time periods and conditions (English units)

Season	Fall 2009		Winter 2009/10		Spring 2010			Summer 2010		Fall 2010	
Dates	Nov 5-11	Nov 12-17	Dec 19-25	Jan 11-17	Apr 8-14	Apr 24-May 1	May 13-20	June 5-12	July 13-20	Sept 30-Oct 6	Oct 14-21
Average Air Temperature (°F)	NA	NA	22.5	29.3	49.1	53.6	57.7	61.7	75.9	53.8	48.6
Average Solar Radiation (hp)	NA	NA	0.067	0.070	0.327	0.280	0.324	0.284	0.331	0.123	0.131
Total Precipitation (in)	NA	NA	0.59	0.23	0.25	0.32	0.71	2.82	0.06	3.57	1.45
Section 1 Average Max. LTG +/- (°F/in)	0.520	0.562	0.212	0.515	1.377	1.270	1.449	0.934	NA	0.437	0.561
	-0.534	-0.653	-0.478	-0.253	-0.614	-0.428	-0.455	-0.603	NA	-0.520	-0.621
Section 2 Average Max. LTG +/- (°F/in)	0.561	0.645	0.260	0.525	1.465	1.362	1.601	1.017	NA	0.511	0.672
	-0.570	-0.713	-0.520	-0.317	-0.782	-0.520	-0.552	-0.727	NA	-0.538	-0.653
Section 1 Max LTG +/- (°F/in)	1.017	0.814	0.538	0.957	1.753	2.033	2.084	1.679	NA	0.856	1.067
	-0.718	-0.865	-0.672	-0.506	-0.902	-0.814	-0.823	-0.814	NA	-0.690	-0.745
Section 2 Max LTG +/- (°F/in)	1.072	0.920	0.520	0.966	1.803	2.144	2.208	1.776	NA	0.994	1.237
	-0.814	-0.920	-0.667	-0.561	-1.026	-0.915	-0.925	-0.897	NA	-0.713	-0.764

Table 12 continued.

Season	Fall 2010	Winter 2010/11			Spring 2011			Summer 2011			Fall 2011		
Dates	Nov 7-16	Dec 29-Jan 6	Jan 15-22	Feb 20-27	Mar 17-24	Apr 9-16	May 9-16	June 1-7	July 9-16	Aug 9-16	Sept 16-23	Oct 9-16	Nov 1-7
Average Air Temperature (°F)	41.0	32.0	19.6	22.3	38.8	50.0	59.4	65.3	72.5	68.5	58.5	58.6	46.6
Average Solar Radiation (hp)	0.115	0.067	0.074	0.149	0.197	0.214	0.280	0.373	0.414	0.237	0.210	0.126	0.145
Total Precipitation (in)	0.63	0.06	0.39	1.80	0.00	0.00	0.45	NA	NA	NA	NA	NA	NA
Section 1 Average Max. LTG +/- (°F/in)	0.759	0.474	0.285	0.704	0.966	1.099	1.647	1.504	1.748	1.058	1.035	0.814	0.879
	-0.612	-0.419	-0.644	-0.635	-0.455	-0.414	-0.534	-0.644	-0.727	-0.580	-0.722	-0.584	-0.621
Section 2 Average Max. LTG +/- (°F/in)	0.892	0.538	0.363	0.764	1.044	1.187	1.523	1.633	1.881	1.201	1.182	0.929	0.998
	-0.630	-0.446	-0.667	-0.649	-0.538	-0.488	-0.607	-0.768	-0.810	-0.612	-0.754	-0.607	-0.681
Section 1 Max LTG +/- (°F/in)	1.076	0.957	0.699	1.256	1.872	1.996	2.070	2.098	1.955	1.670	1.467	1.546	1.086
	-0.860	-0.860	-1.044	-1.178	-0.856	-0.814	-0.814	-1.044	-0.957	-0.796	-1.017	-0.681	-1.035
Section 2 Max LTG +/- (°F/in)	1.265	1.040	0.819	1.458	1.996	2.162	2.217	2.286	2.111	1.840	1.651	1.697	1.237
	-0.869	-0.846	-1.081	-1.159	-0.906	-0.879	-0.906	-1.127	-1.030	-0.851	-1.049	-0.704	-1.099

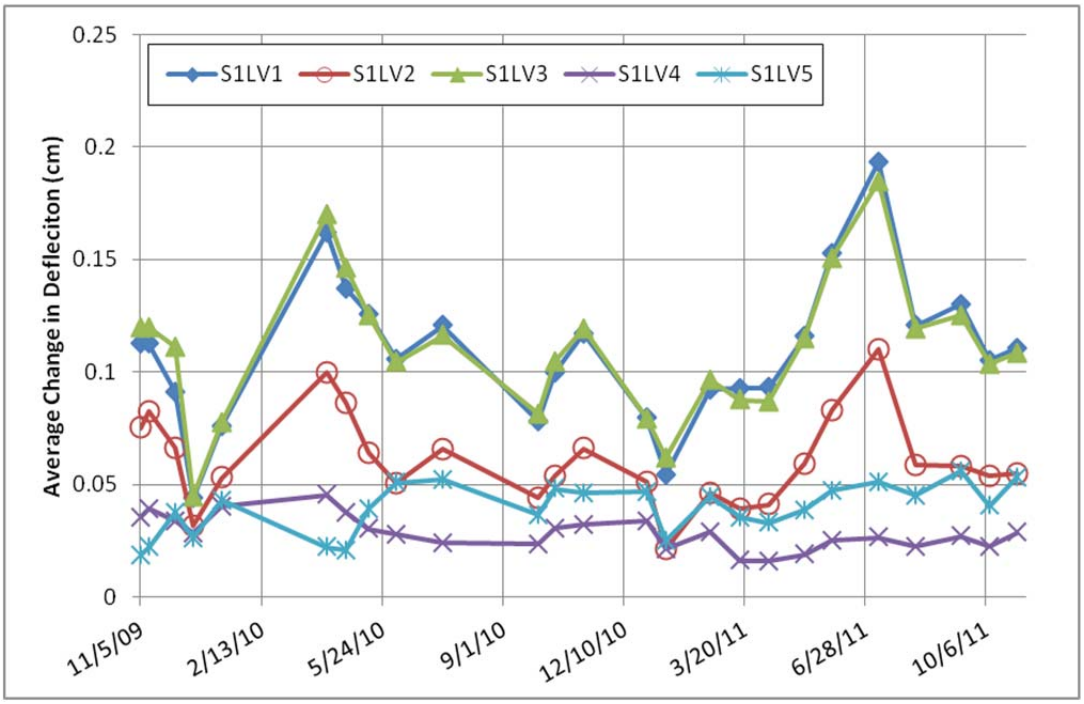

Figure 23 Average daily change in deflection in Section 1 (2.54 cm = 1 in)

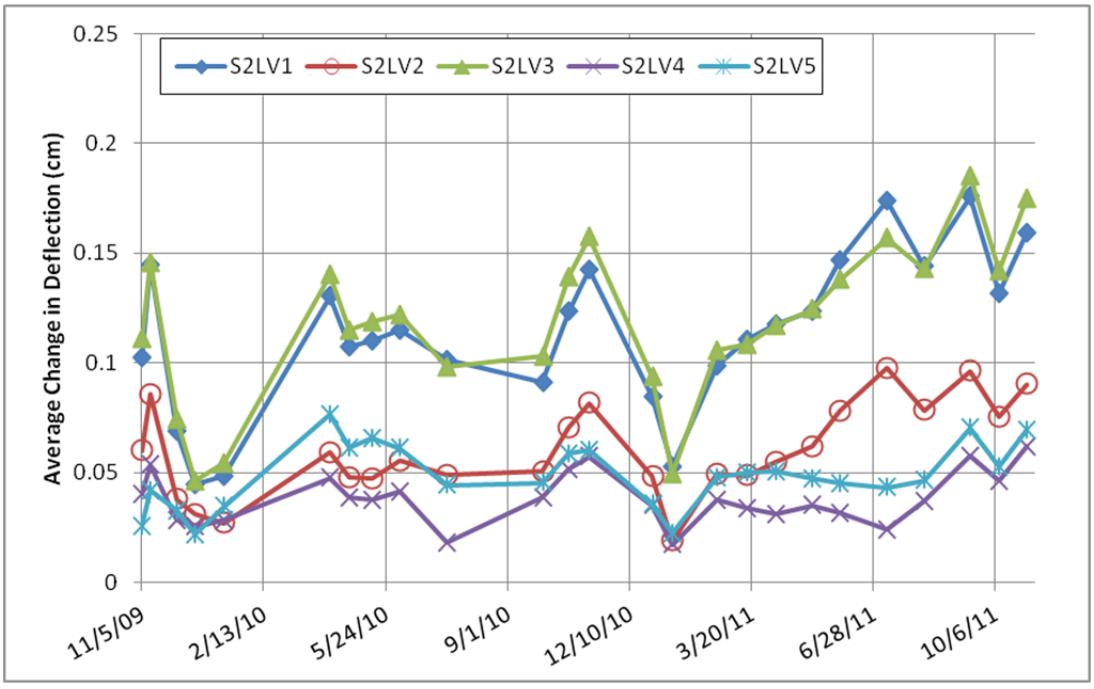

Figure 24 Average daily change in deflection in Section 2 (2.54 cm = 1 in)

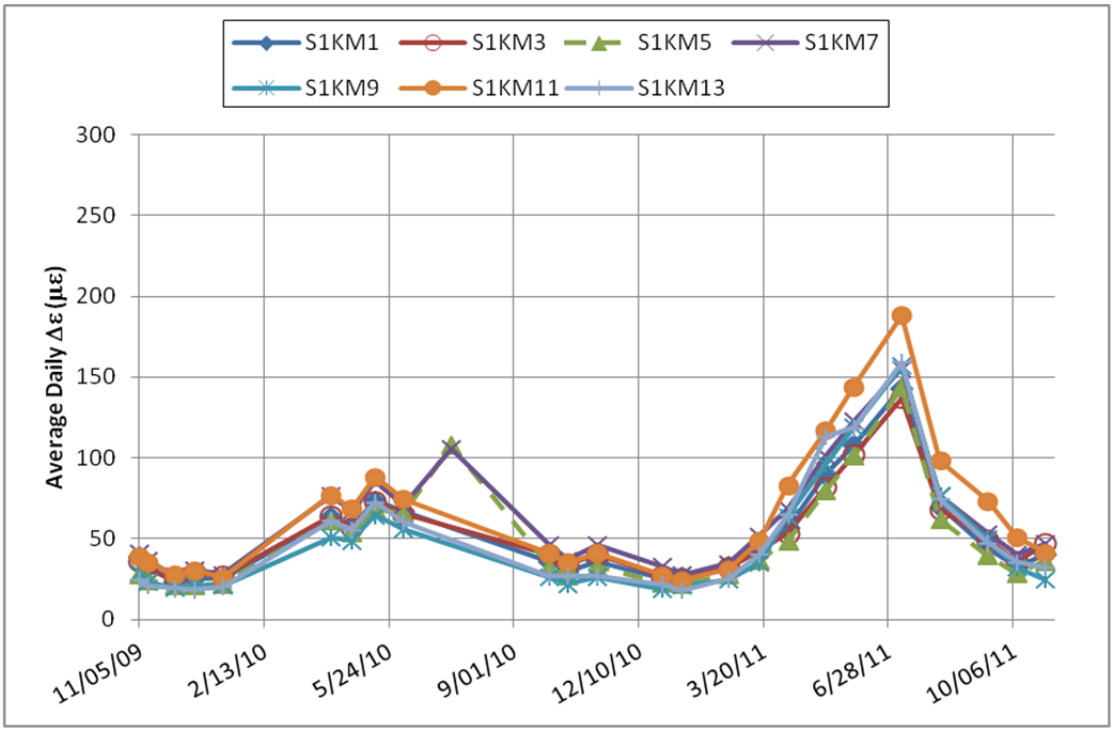

Figure 25 Average daily change in strain in top of slab sensors at Section 1

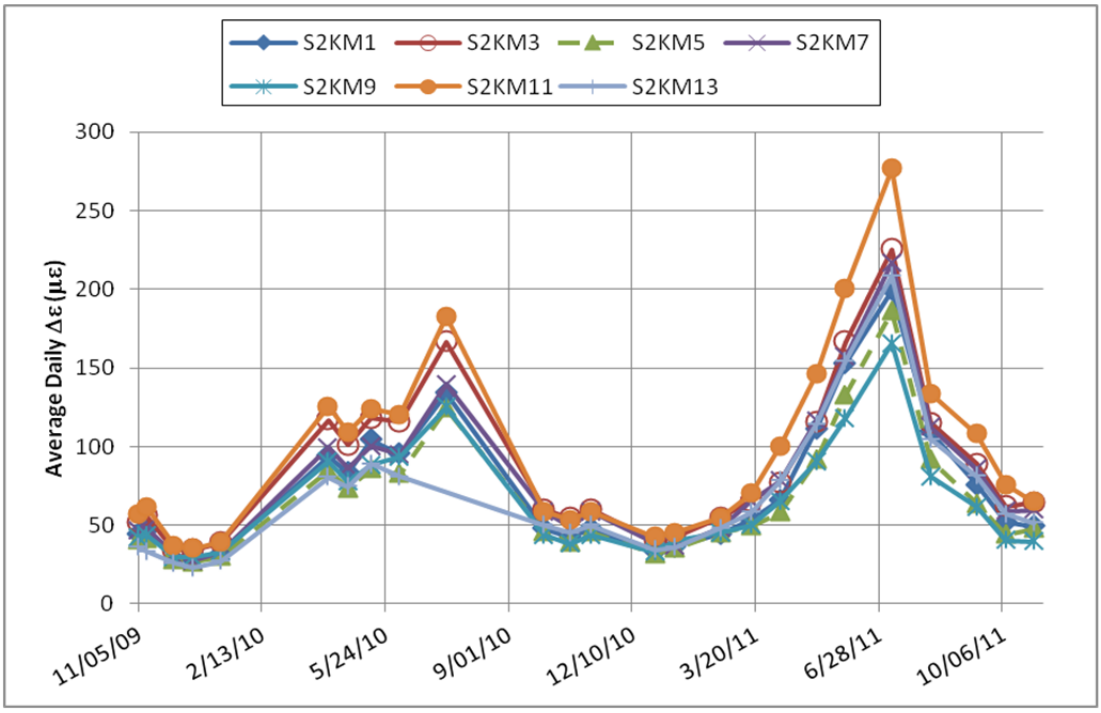

Figure 26 Average daily change in strain in top of slab sensors at Section 2

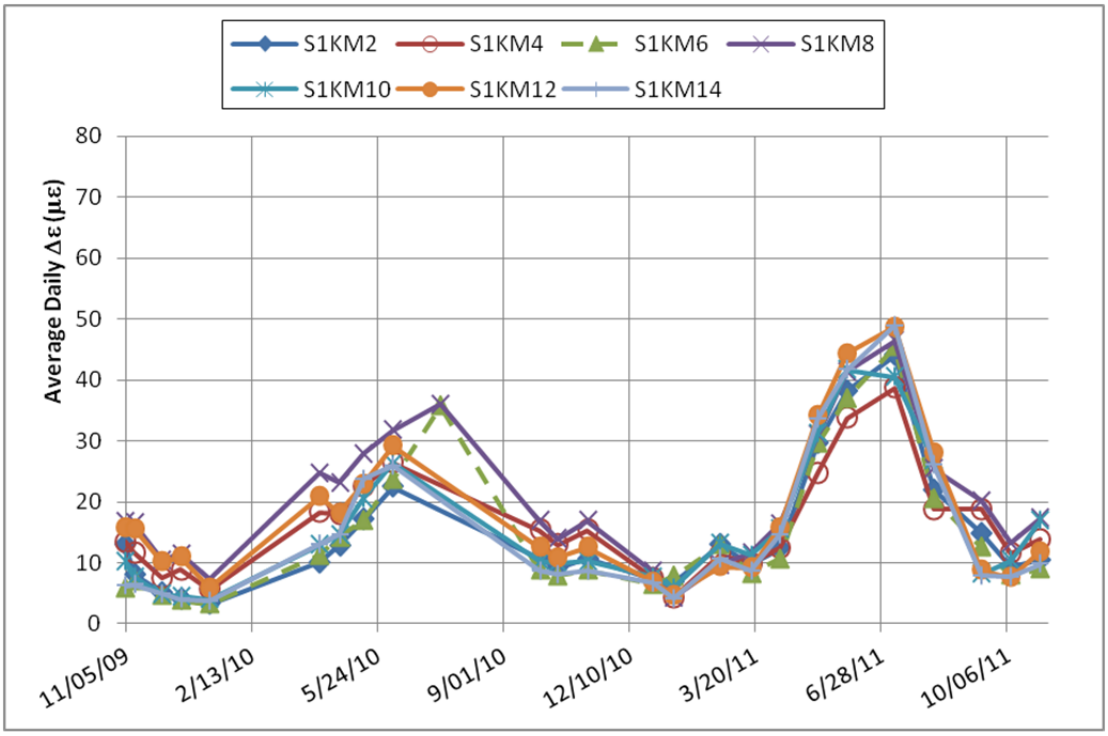

Figure 27 Average daily change in strain in bottom of slab sensors at Section 1

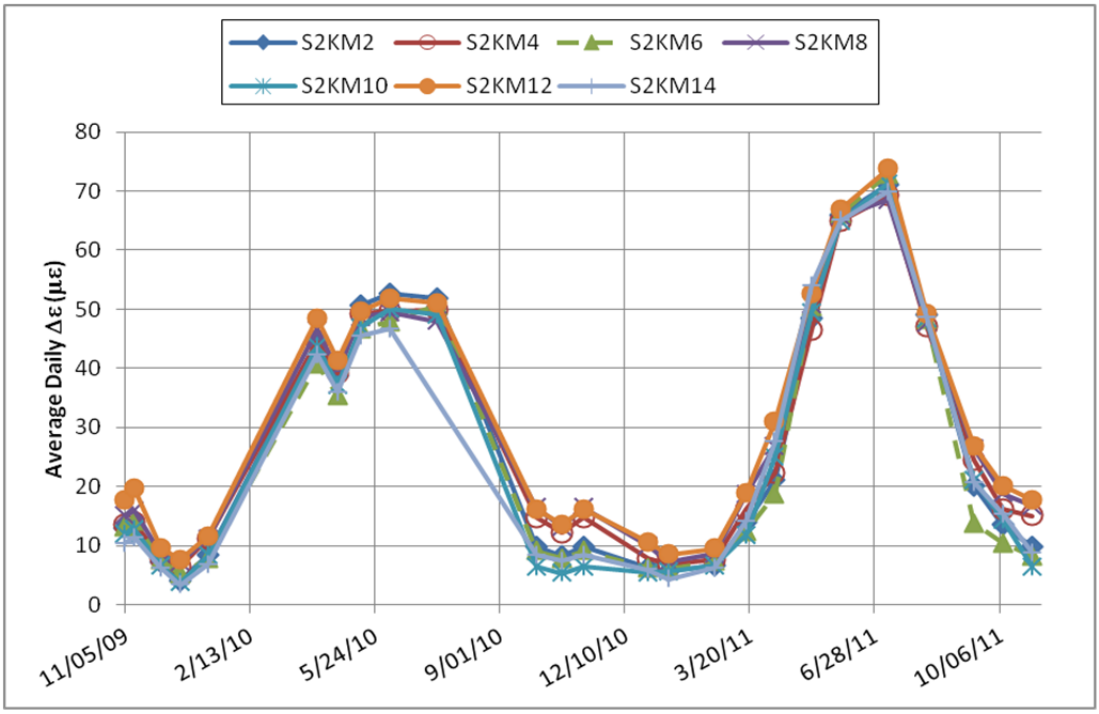

Figure 28 Average daily change in strain in bottom of slab sensors at Section 2

From these figures, the shoulder sensors (LVDT 1, 2 and 3) typically experienced the largest deflections. However, in Section 2, the interior corner (LVDT 5) exceeded the deflections of LVDT 2 during the spring 2010 periods. The spring season recorded some of the largest LTGs, which coincide with the largest deflections along the shoulder in Section 1. However, Section 2 experienced the largest deflections during the fall 2010 season, which had lower LTGs than spring.

Section 1 had larger deflections than Section 2 until after spring 2010. In the subsequent periods, Section 2 followed a different trend than Section 1, and by early fall 2010, Section 2 began to have larger deflections at the slab edges than Section 1.

During all periods, Section 2 recorded larger strains than Section 1. The largest strains were recorded in different locations for either section; however, the top three largest strains in both test sections occurred at mid-slab, at either the slab center, right or left wheel-paths. Section 2 experienced most of the highest strains along the wheel-paths at mid-slab, whereas the greatest strains in Section 1 usually occurred at the slab center.

The largest strains were observed during the summer months, followed by spring. The winter seasons experienced the lowest strains, and the fall and winter seasons produced similar results in the first and second years.

Tie-bars along the longitudinal joint were also instrumented with vibrating-wire (VW) strain gauges. Limited data for similar periods was available due to inconsistent data collection by the data acquisition systems at both test sections. This resulted in smaller and fewer observation periods; however, the data collected does indicate a difference in the two sections. All VW sensors in each section gave similar strain readings; therefore, the mean values are presented for comparison. As with the KM strain gauges, the tie-bar average daily change in load-related strains, herein called "tie-bar strains," were averaged for each period. The tie-bar strains are summarized in Table 13. For all periods observed, Section 2 experienced larger strains than Section 1.

Table 13 Average daily change in tie-bar strains

Season:		Fall 2009	Winter 2009/10	Spring 2010	Summer 2010	Fall 2010
Dates:		Nov 28 - Dec 2	Dec 13-17	May 9-10	July 16-20	*Sept 16-21
Δε (με)	Section 1	4.80	4.38	11.17	7.47	6.84
	Section 2	5.75	5.51	13.04	8.75	7.64

* Section 1 data from VW-4 only

3.3.4 Discussion of Long-term Response

Slab and tie-bar strains in Section 2 were consistently larger than Section 1. During the fall and winter seasons, the slab strains were somewhat similar in both sections. However, in the spring and summer, the strains in Section 2 exceeded those in Section 1 at the top and bottom. This difference in strains was a result of the slab in Section 2 deforming on a rigid base layer and the restraint at the slab/base interface imposed by the CTPB. The strain in Section 2 indicated the slab experienced greater daily changes in stress, and therefore was more likely to experience distress from fatigue loading as a result.

The slab/base interface bond in Section 2 was gradually reduced during spring and summer 2010, which resulted in Section 2 experiencing larger deflections than Section 1. Prior to

summer 2010, Section 1 had typically experienced greater deflections. However, after the April 8 – 14 2010 period, the deflections in Section 2 followed a different trend than Section 1. The shoulder deflections increased over time in Section 2, while the same gauges in Section 1 decreased. By the September 30 – October 6 period, Section 2 was experiencing larger deflections than Section 1, and this trend continued for most of the subsequent periods. In fall 2010, Section 2 recorded larger deflections than in spring 2010, while Section 1 had smaller deflections in the fall than in spring. In particular, the greatest seasonal deflections were recorded during the April 8 – 14 and October 14 – 21 periods for spring and fall, respectively. In Section 1, the deflections decreased by 70% between these two periods; however, in Section 2, the deflections increased by 10%. The average air temperature was the same for these periods, which indicates aggregate interlock was similar. In addition, the LTGs were greater in the spring than the fall, indicating the larger deflections in Section 2 resulted from the slab deforming on the rigid base layer.

This data timeline shows that while the CTPB had restrained deflections early in the pavement's service life, the bond between the CTPB and PCC slab was eventually broken during the high spring seasonal curling deformations. After the slab/base interface restraining forces were reduced, the slab began to experience greater deformations because of the rigid support layer. The slab lost contact with the rigid CTPB base during curling and led to greater deformations; however, the DGAB was flexible and provided more support, which caused smaller deflections. This confirms the conclusions by Sargand and Edwards (2000), which had similar findings. The larger deformations increased the risk of fatigue cracking and structural breaks due to the loss of support.

The location of maximum strains indicates a different strain distribution in both test sections. Section 1 usually experienced the greatest strains at mid-slab center, with the exception of spring 2010 where strains at the slab center and mid-slab right wheel-path were highest. Maximum strains at mid-slab are expected for a slab with an unbonded base. However, Section 2 typically experienced the highest strains at the mid-slab left and right wheel-path. This behavior indicates the slab/base restraint from the CTPB was resisting curling close to the longitudinal edges, resulting in increased slab stresses in these locations.

The two seasons that produce the largest strains were spring and summer, while the greatest deflections were observed during spring, summer, and fall. However, the summer strains were much larger than the spring strains at the slab surface. The winter thaw and spring precipitation increased the subgrade moisture content in the spring. This softened the subgrade, and the lower subgrade modulus resulted in higher strains slab. In the summer, the slabs expanded and engaged aggregate interlock at the transverse joints. This reduced slab deflections, which increased slab strains. In the fall, the subgrade moisture content is lower due to the summer season, which dries the subgrade and increases the modulus. As a result, strains are reduced in the fall, while deflections remain relatively large.

The long-term test section response indicates that initially Section 2 had lower deflections resulting from the PCC mortar bonding with the CTPB during construction. Eventually, this bond deteriorated and deflections increased. Section 2 had greater deflections than Section 1 because the CTPB does not provide uniform slab support for curling deformations. Strains in Section 2 continued to be higher than Section 1, due to the loss of support at the slab edges and slab/base interaction at the slab interior. The restraining forces change the stress distribution

within the slab, which increased strains along the longitudinal edges where curling in the longitudinal direction was restrained. Section 1 indicated an unbonded slab/base interface, and the maximum strains were typically at the center of the slab.

3.3.5 Subgrade Soil Moisture

Sub-base and subgrade moisture content below mid-slab was measured by TDR probes placed at various depths within the sub-base and subgrade layers. The TDR readings were made during site visits and were not continually monitored. Moisture contents typically vary seasonally, and this data provided an instantaneous soil moisture profile for each test section. Figure 29 and Figure 30 summarize the volumetric moisture content (percent water per volume) on the dates data was collected for Section 1 and 2, respectively. The readings on September 25 2009 were the baseline readings taken immediately after instrumentation and prior to pavement construction.

After the initial readings, the moisture content in the Section 1 DGAB layer, located at 0.4-m beneath the pavement, stabilized to around 16%; however, the moisture content in the Section 2 DGAB layer, located at 0.3-m beneath the pavement, fluctuated between 10% and 33%. However, the readings taken directly beneath the DGAB layer at 0.64 and 0.74-m for Section 1 and Section 2, respectively, remained nearly unchanged over time at between 23% and 26%. The soil closest to the DGAB layer is most sensitive to pavement drainage activity; therefore, this data indicates that both pavements were providing equivalent drainage. The subgrade was an A-6 sandy lean clay, which has low permeability. Therefore, the moisture probes at lower depths were more sensitive to natural site conditions rather than the runoff moisture from the pavement.

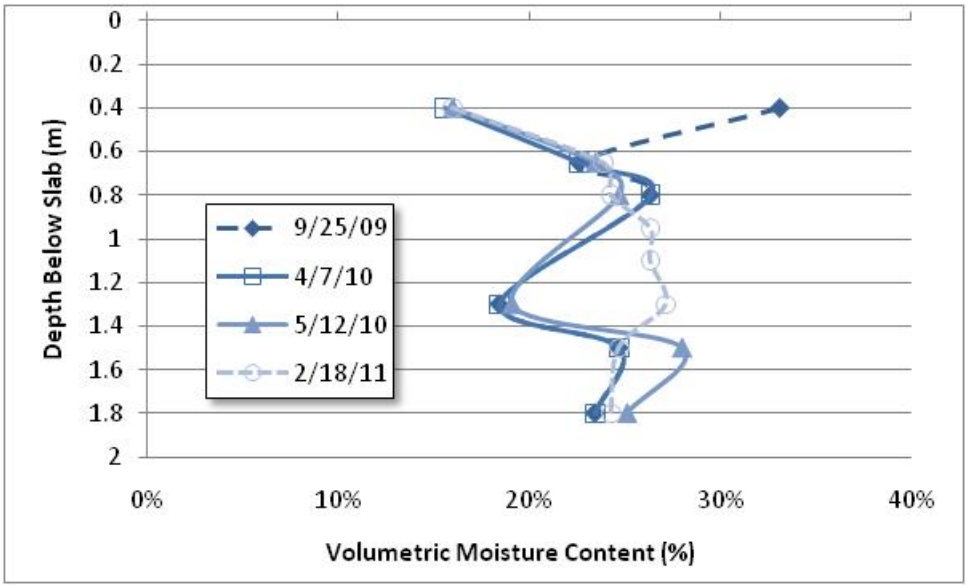

Figure 29 Section 1 volumetric moisture content (1 m = 3.28 ft)

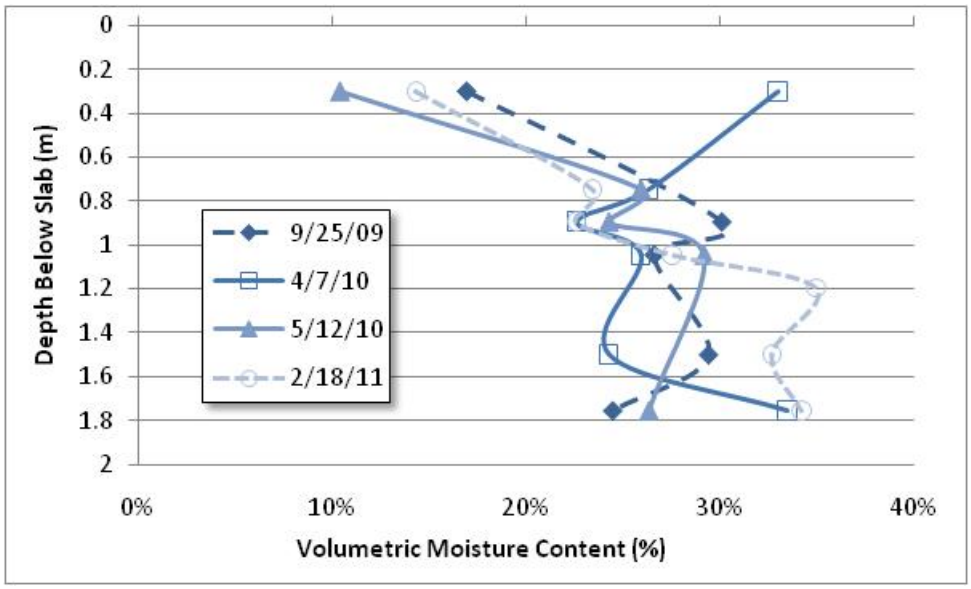

Figure 30 Section 2 volumetric moisture content (1 m = 3.28 ft)

3.4 Falling Weight Deflectometer

In this section, the FWD testing results on the base and pavement are presented and discussed. For the base material test, only deflections at the load center are discussed; however, for the PCC pavement tests, several parameters for pavement stiffness and joint performance are presented for discussion. Additional results and figures are provided in Appendix B.

FWD testing reveals stiffness and joint performance characteristics of pavements and base materials. The device produces a pulse-load by dropping a 250-kg (551 lb) weight onto a 15-cm (6 in) radius plate. For the base testing, eight geophones were used, configured at 0 cm (0 in), 20.3 cm (8 in), 30.5 cm (12 in), 45.7 cm (18 in), 61 cm (24 in), 91.4 cm (36 in), 122 cm (48 in), 152.4 cm (60 in), and 182.9 cm (72 in) from the load center. For testing on PCC pavement, the geophones were spaced at 0 cm (0 in), 30.5 cm (12 in), 45.7 cm (18 in), 61 cm (24 in), 91.4 cm (36 in), 122 cm (48 in), 152.4 cm (60 in), and 182.9 cm (72 in) behind the load plate center, with one geophone 30.5 cm (12 in) in front of the load plate (Figure 12). The loads were applied at 26.7 kN (6.0 kip), 40.0 kN (9.0 kip) and 53.4 kN (12.0 kip) on the base and 40.0 kN (9.0 kip), 53.4 kN (12.0 kip), and 71.2 kN (16 kip) on the pavement. All readings were normalized to 1 kN (0.22 kip, or to 1 kip (4.45 kN)) prior to the analysis to make comparisons between the different loads. The geophone readings at the point of loading (D_0) are representative of the overall pavement stiffness, while readings at 152.4 cm (60 in) from the load (D_{60}) are representative of the subgrade stiffness.

3.4.1 Base Testing

FWD testing was done on the CTPB and DGAB layers in both lanes on October 1 2009, prior to PCC paving. The average normalized D_0 deflections are shown in Figure 31. The separation line between base types shown on this plot is in accordance to site plan dimensions. The CTPB response was less variable than the DGAB, which typically had greater deflections. DGAB deflections increased in the region past station 17+350, which can also be seen in the

pavement tests on this region (see Appendix B). It is important to note again the location of Section 1 and 2 are between stations 17+331.5 to 17+345 and 17+120 to 17+133.5, respectively.

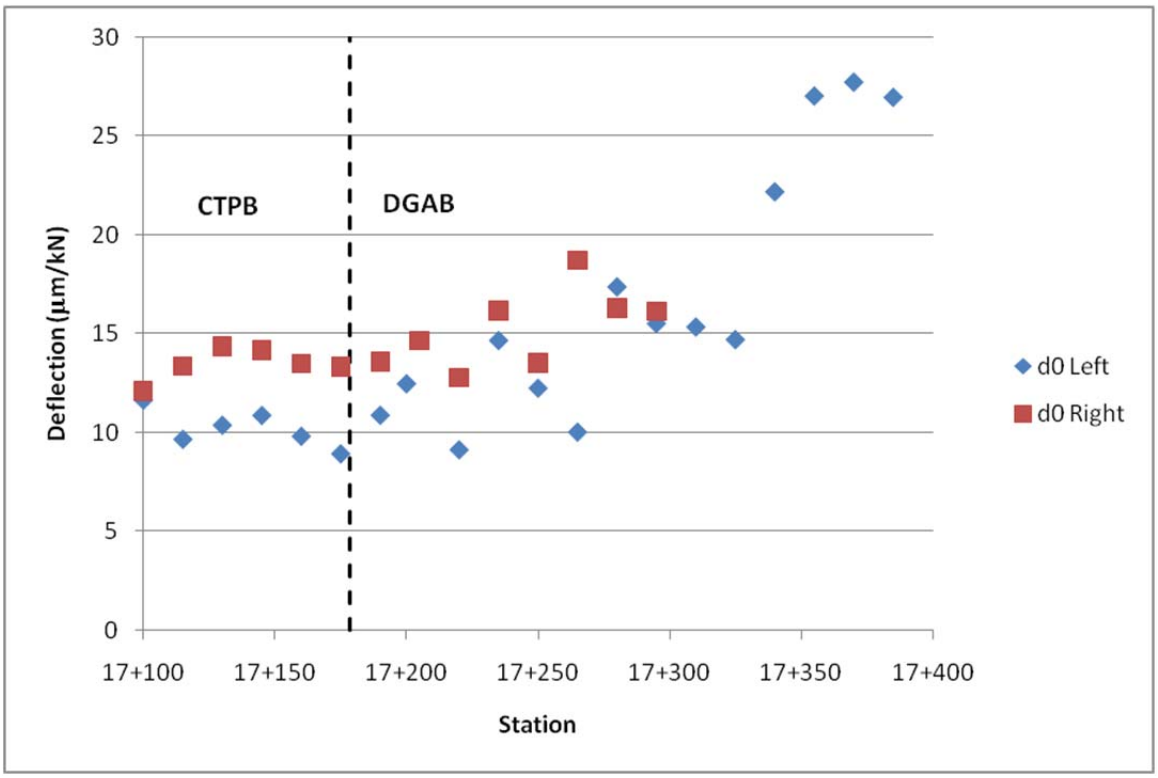

Figure 31 Average normalized D_0 deflections on CTPB and DGAB prior to paving (5.714 µm/kN = 1 mil/kip)

3.4.2 PCC Testing

Early-age FWD tests were performed on the right lane at 21-day curing strength. The thermocouples embedded in the test sections were not recording temperature data during this time due to a power failure. Therefore, the results discussed in terms of the ambient and pavement surface temperatures as recorded by the FWD testing machine. During the test, ambient air temperatures were an average of 12.1°C (53.8°F), and PCC surface temperatures were an average of 12.0°C (53.6°F). The temperatures were nearly constant, indicating slab shape should be constant throughout the test. These results are summarized in Table 14.

After two years in service, additional tests were conducted in November 2011. The results from these tests are shown in Table 15. During the test, ambient air temperatures were an average of 13.6°C (56.5°F), and PCC surface temperatures were an average of 14.2°C (57.6°F).

Tests were done in three positions on each slab: at the joint approach, mid-slab, and joint leave positions. The mid-slab test indicates pavement stiffness, while the joint tests indicate joint performance and support conditions. Additional figures for these results can be found in Appendix B.

Table 14 Summary of FWD results September 29 2011

	Date:		10/29/2009										
	Load		D0 (μm/kN)			D0 (mil/kip)			LTE (%)		JSR	SPR (%)	D3/D0
	(kN)	(kip)	M	JA	JL	M	JA	JL	A	L	M	M	M
Section 1	40	9.0	0.963	1.373	1.412	0.169	0.240	0.247	84.25%	81.06%	1.062	67.97%	0.879
	53	11.9	0.978	1.405	1.428	0.171	0.246	0.250	82.96%	81.96%	1.038	68.54%	0.876
	71	16.0	0.972	1.393	1.407	0.170	0.244	0.246	83.47%	81.79%	1.038	68.25%	0.878
Section 2	40	9.0	0.75	1.44	1.461	0.131	0.252	0.256	82.70%	82.18%	1.057	72.90%	0.885
	53	11.9	0.768	1.464	1.477	0.134	0.256	0.258	83.60%	83.02%	1.066	73.77%	0.88
	71	16.0	0.764	1.441	1.455	0.134	0.252	0.255	84.07%	83.43%	1.069	73.51%	0.889

Note: JA=Joint approach; JL=Joint leave; M=Mid-slab

Table 15 Summary of FWD results November 15 2011

	Date:		11/15/2011										
	Load		D0 (μm/kN)			D0 (mil/kip)			LTE (%)		JSR	SPR (%)	D3/D0
	(kN)	(kip)	M	JA	JL	M	JA	JL	A	L	M	M	M
Section 1	44	9.9	0.963	1.416	1.485	0.169	0.248	0.260	87.11%	79.96%	1.049	70.15%	0.89
	58	13.0	0.974	1.419	1.503	0.170	0.248	0.263	87.43%	80.18%	1.060	70.73%	0.895
	80	18.0	0.987	1.419	1.495	0.173	0.248	0.262	86.64%	79.40%	1.054	69.84%	0.883
Section 2	44	9.9	0.958	1.997	2.111	0.168	0.349	0.369	95.75%	90.24%	1.057	80.49%	0.916
	58	13.0	0.958	2.002	2.104	0.168	0.350	0.368	96.48%	90.16%	1.052	80.46%	0.922
	80	18.0	0.937	1.908	1.997	0.164	0.334	0.349	95.57%	89.48%	1.048	80.00%	0.909

Note: JA=Joint approach; JL=Joint leave; M=Mid-slab

3.4.3 Discussion of FWD Results

From these tables it can be seen that both sections had similar deflections at the joints on the 2009 test conducted 21 days after placement, and that Section 2 had lower mid-slab deflections during the same test. By the Fall of 2011 this trend changes; while the mid-slab deflections are similar, the deflections at the joints are higher for Section 2, which indicates a loss of support at the joints and, confirms the higher readings of LVDT1 and LVDT3 after the Fall of 2010. This loss of support is indicative of the stiffer base in Section 2 and the adhesion that formed initially between the PCC and CTPB

3.5 Truck Load Testing

This section presents the truck testing results from the spring 2010 and fall 2010 tests. Truck testing was performed to verify the environmental monitoring results and to gather load response data for both test sections. In this section, several typical strain and deflection response traces are presented, followed by a summary of the deflection and strain data for the spring and fall tests. Afterwards, the strain and deflection response for both test periods are discussed.

Pressure cells beneath the DGAB layer were also monitored during the tests; however, there was typically no load response from Section 2. This resulted from the depth of the pressure cells below the pavement and the additional stiffness of the CTPB layer. Therefore, the results from the pressure cells shall not be discussed herein. Typical pressure cell traces can be found in the Appendix C for Spring 2010.

3.5.1 Spring 2010 Testing

The spring truck testing was performed on May 12 2010. The morning test was between 8:17 AM and 9:59 AM and the afternoon test was between 2:15 PM and 3:32 PM. The morning and afternoon tests were done to capture the pavement response with a negative and positive temperature gradient, respectively. Light rain fell during the morning test; however, the weather cleared during the afternoon test.

The slab temperature gradients are shown in Figure 32. During the morning test, both sections increased from negative to near-zero temperature gradients. Section 1 indicated a significant positive temperature gradient in the afternoon when the weather cleared and solar radiation increased surface temperatures. The data acquisition in Section 2 stopped recording thermocouple data prior to the afternoon test; however, the temperature gradients in both sections were typically very similar, as shown in Table 11 and Table 12 for the seasonal response data.

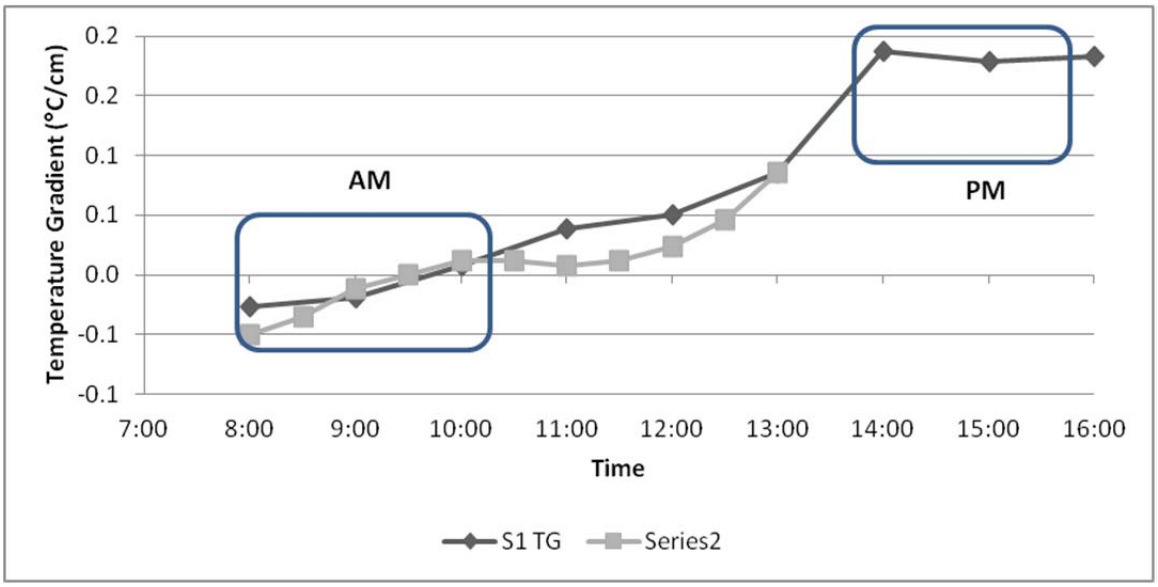

Figure 32 Pavement linear temperature gradients during spring 2010 truck test (1C°/cm = 4.6°F/in)

3.5.1.1 Deflection Response

In this section, slab deflections during truck testing for each LVDT location are presented. The deflection traces at each location show two downward peaks as each axle passes the sensor, with the largest downward deflection under the rear axle. A typical morning deflection trace with the light truck load is shown in Figure 33. No Section 1 deflection data was recorded in the afternoon; therefore, the afternoon results from Section 2 shall be compared to the morning test results. Additional deflection traces and data are presented in the appendices.

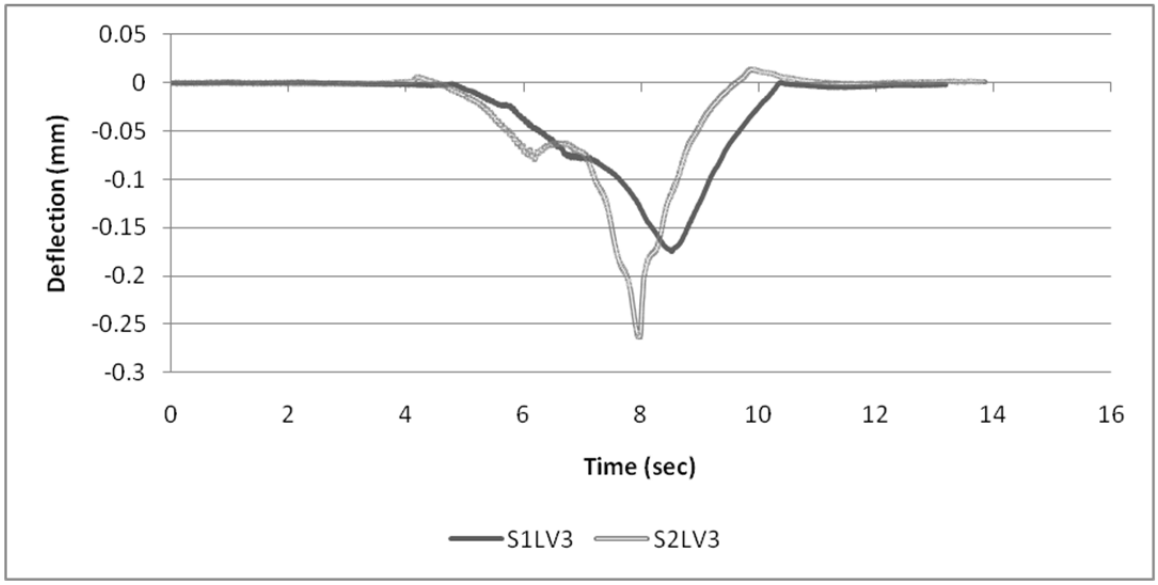

Figure 33 8 km/h (5 mph) light load deflection traces at LVDT3 during morning test (1 mm = 39.4 mil)

The peak deflections were averaged in each direction (positive and negative) for morning and afternoon tests to compare the response of each section and the effect of speed on slab deflections. Average deflections for the light truck load tests are shown in Table 16 in metric units and in

Table 17 in English units. The heavy truck load had similar geometry and produced similar results; therefore, it will not be discussed herein.

Table 16 Average deflections during spring 2010 light truck test (metric units)

Sensor:		LVDT 1 (mm)		LVDT 2 (mm)		LVDT 3 (mm)		LVDT 4 (mm)		LVDT 5 (mm)	
Section:		1	2	1	2	1	2	1	2	1	2
Speed (km/h)		Upward									
AM	8	0.0019	0.0171	0.0014	0.0011	0.0018	0.0119	0.0034	0.0108	0.0033	0.0062
	40	0.0015	0.0178	0.0008	0.0037	0.0007	0.0121	0.0027	0.0102	0.0029	0.0075
	55	0.0018	0.0235	0.0008	0.0025	0.0025	0.0137	0.0031	0.0101	0.0029	0.0066
	70	0.0020	0.0189	0.0007	0.0007	0.0008	0.0130	0.0026	0.0106	0.0025	0.0080
	Downward										
	8	-0.1751	-0.2210	-0.1288	-0.1086	-0.1733	-0.2565	-0.1096	-0.1891	-0.0489	-0.1173
	40	-0.1542	-0.2140	-0.1159	-0.0986	-0.1651	-0.2399	-0.1041	-0.1805	-0.0470	-0.1138
	55	-0.1514	-0.2060	-0.1163	-0.0798	-0.1579	-0.2217	-0.0991	-0.1789	-0.0424	-0.1233
	70	-0.1431	-0.2140	-0.1057	-0.0870	-0.1440	-0.2092	-0.0933	-0.1622	-0.0431	-0.1063
Speed (km/h)		Upward									
PM	8	-	0.0153	-	0.0059	-	0.0119	-	0.0073	-	0.0079
	40	-	0.0124	-	0.0007	-	0.0071	-	0.0052	-	0.0034
	55	-	-	-	-	-	-	-	-	-	-
	70	-	0.0134	-	0.0022	-	0.0077	-	0.0045	-	0.0036
	Downward										
	8	-	-0.1667	-	-0.0849	-	-0.1969	-	-0.1489	-	-0.0996
	40	-	-0.1583	-	-0.0748	-	-0.1732	-	-0.1285	-	-0.0841
	55	-	-0.1503	-	-0.0614	-	-0.1488	-	-0.1191	-	-0.0835
	70	-	-0.1368	-	-0.0549	-	-0.1256	-	-0.1039	-	-0.0776

Table 17 Average deflections during spring 2010 light truck test (English units)

Sensor:		LVDT 1 (mil)		LVDT 2 (mil)		LVDT 3 (mil)		LVDT 4 (mil)		LVDT 5 (mil)	
Section:		1	2	1	2	1	2	1	2	1	2
Speed (mph)		Upward									
AM	5	0.075	0.673	0.055	0.043	0.071	0.469	0.134	0.425	0.130	0.244
	25	0.059	0.701	0.031	0.146	0.028	0.476	0.106	0.402	0.114	0.295
	34	0.071	0.925	0.031	0.098	0.098	0.539	0.122	0.398	0.114	0.260
	43.5	0.079	0.744	0.028	0.028	0.031	0.512	0.102	0.417	0.098	0.315
	Downward										
	5	-6.894	-8.701	-5.071	-4.276	-6.823	-10.098	-4.315	-7.445	-1.925	-4.618
	25	-6.071	-8.425	-4.563	-3.882	-6.500	-9.445	-4.098	-7.106	-1.850	-4.480
	34	-5.961	-8.110	-4.579	-3.142	-6.217	-8.728	-3.902	-7.043	-1.669	-4.854
	43.5	-5.634	-8.425	-4.161	-3.425	-5.669	-8.236	-3.673	-6.386	-1.697	-4.185
Speed (mph)		Upward									
PM	5	-	0.602	-	0.232	-	0.469	-	0.287	-	0.311
	25	-	0.488	-	0.028	-	0.280	-	0.205	-	0.134
	34	-	-	-	-	-	-	-	-	-	-
	43.5	-	0.528	-	0.087	-	0.303	-	0.177	-	0.142
	Downward										
	5	-	-6.563	-	-3.343	-	-7.752	-	-5.862	-	-3.921
	25	-	-6.232	-	-2.945	-	-6.819	-	-5.059	-	-3.311
	34	-	-5.917	-	-2.417	-	-5.858	-	-4.689	-	-3.287
	43.5	-	-5.386	-	-2.161	-	-4.945	-	-4.091	-	-3.055

During the morning tests, Section 2 indicated slight upward deflections at the transverse joints as the truck approached and left the slab. Upward deflection values in Section 1 were miniscule in comparison to Section 2. The slight upward joint deflections in Section 2 were largest in the morning and were reduced during the afternoon test. Section 2 also had larger downward deflections at the transverse joints; however, Section 1 had larger downward deflections at the mid-slab edge location (LVDT 2). In general, increased speed decreased downward deflections; however, upward deflections increased with speed in the morning at Section 2.

3.5.1.2 Strain Response

The embedded KM strain gauges at slab top and bottom recorded the strain response while the trucks drove across the test sections. In this section, typical responses for the light truck along the right wheel-path at mid-slab (KM3 and KM4) are presented. These locations typically experienced the highest strains because the vehicles were driven with their right rear tires centered over the right wheel-path. For additional spring test results please refer to Appendix C.

As the load passed each sensor location, the top of the slab had three positive (tensile) and two negative (compressive) peaks, while the bottom of the slab had two positive peaks and three negative peaks. The maximum peak strains either occurred at a point that both wheels straddled the slab, herein called "Load Condition 1" (LC1), or while the axle load was directly above the sensor, herein called "Load Condition 2" (LC2). See Figure 34 and Figure 35 for typical morning test results with the light load for Sections 1 and 2, respectively.

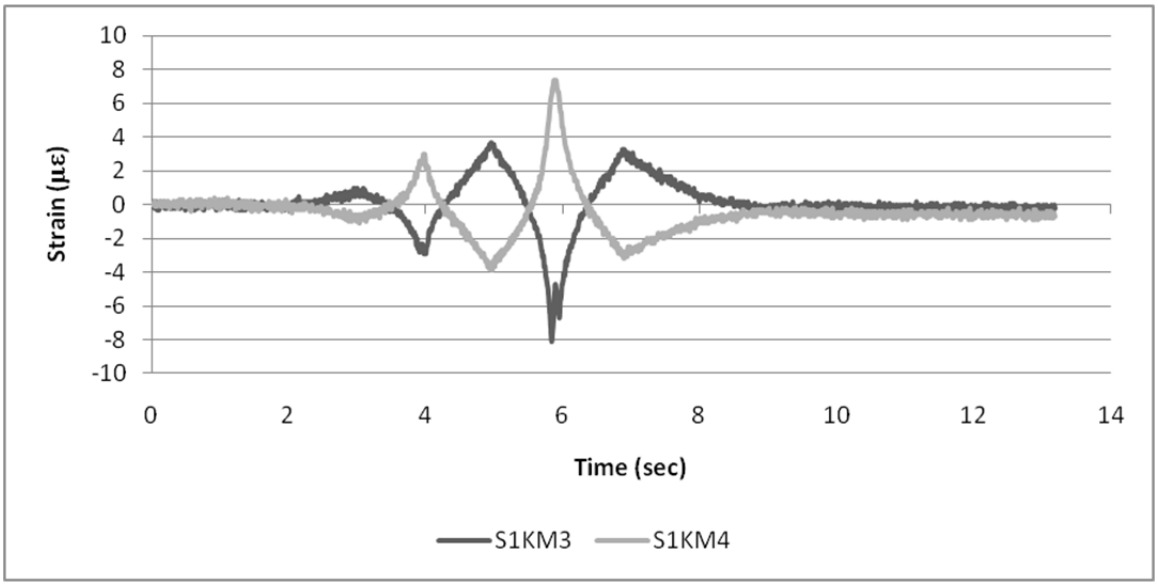

Figure 34 Section 1 light load strain trace at mid-slab wheel-path for AM test

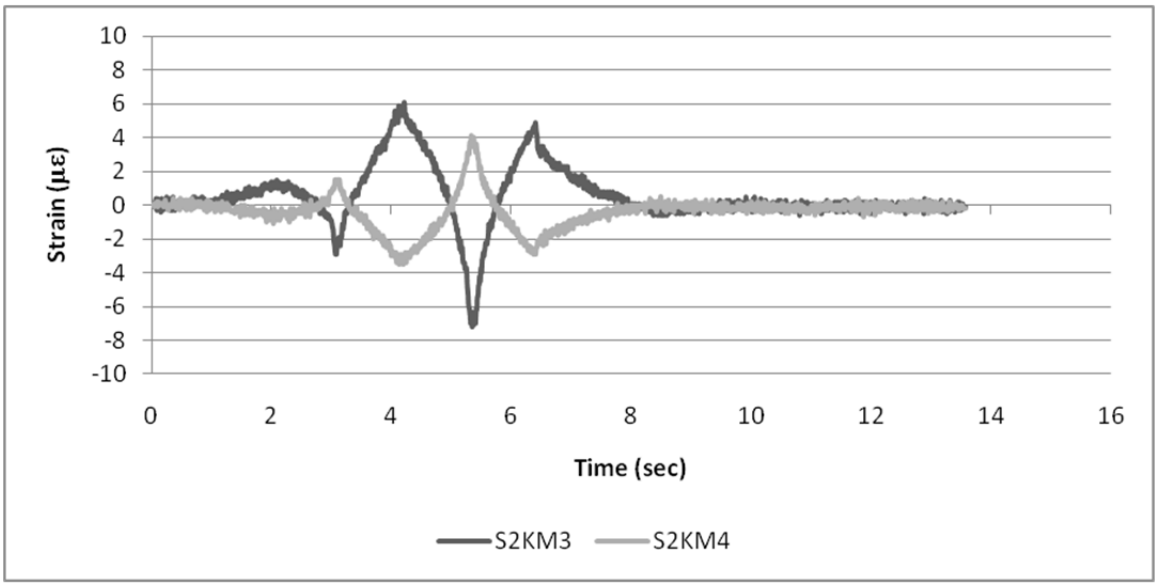

Figure 35 Section 2 light load strain trace at mid-slab wheel-path for AM test

For each test, the maximum tensile and compressive strains for each sensor were identified. The peak strains were averaged in each direction (positive and negative) for each testing period to compare the average response at each section and the effect of speed on strain. Average peak strains from the light truck tests for LC-1 and LC-2 at the mid-slab wheel-path strain gauges are shown in Table 18, where positive and negative strains are tensile and compressive, respectively.

Several trends are observed for the loading conditions above. Section 1 had equal and opposite strains at top and bottom when loaded; however, the top strains in Section 2 were opposite in sign and greater than the bottom strains in magnitude. The average peak compressive strains for each speed were approximately equal in both test sections. In addition, the compressive strains did not vary significantly between morning and afternoon tests. However, the peak tensile strains were dependent on test section and temperature gradients. For LC-1, greater tensile strains were observed in Section 2 at the top sensor, while for LC-2, Section 1 has higher tensile strains at the bottom sensor. Overall, the morning tests resulted in larger strains for LC-1, while larger strains were observed for LC-2 in the afternoon tests. During both testing periods, increased speeds result in decreasing strains.

Table 18 Average peak strain values for LC-1 and LC-2 during spring truck tests

Load Case:			LC-1 Peak Strain (με)				LC-2 Peak Strain (με)			
Test	Speed		Section 1		Section 2		Section 1		Section 2	
	(km/h)	(mph)	KM3	KM4	KM3	KM4	KM3	KM4	KM3	KM4
AM	8	5	3.63	-3.63	6.10	-3.60	-7.60	7.77	-7.43	4.17
	40	25	3.23	-3.07	5.63	-3.13	-7.17	8.30	-7.83	4.43
	55	34	3.40	-3.13	5.27	-2.77	-6.43	7.63	-6.23	3.80
	70	43.5	3.17	-2.83	5.20	-2.90	-6.07	7.23	-6.47	3.90
PM	8	5	2.90	-2.70	4.67	-2.73	-8.65	9.45	-9.07	5.50
	40	25	2.37	-2.37	3.77	-2.30	-7.77	8.40	-7.83	4.33
	55	34	2.43	-2.07	3.83	-2.23	-7.37	8.63	-6.90	4.27
	70	43.5	2.17	-2.07	3.43	-1.90	-6.47	7.93	-7.43	4.20

As mentioned in before, the pavements have two different thicknesses. This results in the sensors measuring strains at different depths in both pavements. While the difference in elevation is small, it follows that these strains should be examined to determine if there are significant differences in the two responses. By linearly extrapolating the strain readings to the pavement surface and bottom, this comparison can be made. This procedure assumes a linear strain distribution occurs throughout the pavement thickness, and under axle loading, this assumption should be sufficient. Using strain data presented in Table 18, the values were extrapolated to the pavement surface and bottom using the strain gradient between the two sensors, shown in Table 19.

Table 19 Extrapolated strain response for KM 3 and 4 8- km/h morning truck tests

Section 1 (KM 3 & 4)			Section 2 (KM 3 & 4)		
Elevation (mm(in))	Strain (με)		Elevation (mm(in))	Strain (με)	
	LC-1	LC-2		LC-1	LC-2
337.5 (13.3) (Top)*	5.01	-7.63	325 (12.8) (Top)*	7.46	-9.05
290 (11.4) (KM3)	3.63	-7.60	290 (11.4) (KM3)	6.10	-7.43
40 (1.6) (KM4)	-3.63	7.77	40 (1.6) (KM4)	-3.60	4.17
0 (0) (Bottom)*	-4.79	7.79	0 (0) (Bottom)*	-5.15	6.03

*Extrapolated data

The extrapolated values in Table 19 indicate there was a similar trend at top and bottom compared to the readings at the sensors. Section 1 maintained similar values top and bottom, while Section 2 had greater strains at the surface for LC-1 and LC-2.

3.5.2 Fall 2010 Testing

The September 22 2010 tests were done during the hours of 8:15 AM to 11:45 AM for the morning tests and 1:30 PM to 2:30 PM for the afternoon tests. Two morning test groups were

performed after the first test was interrupted by rain. The first morning test was from 8:15 AM to 9:00 AM and only recorded responses at speeds of 8 and 40 km/h. The second morning test was from 11:00 AM to 11:45 AM and tested responses at speeds of 8, 40, and 70 km/h. Moisture also compromised some sensor readings following the rain; these tests were removed from the data analysis.

The slab temperature gradient varied during the testing period, as shown in Figure 36. In addition to embedded thermocouples, pavement surface temperatures from Section 2 were measured periodically using an infrared thermometer. The additional readings helped better define the internal pavement temperature gradients. The morning tests maintained a near-zero temperature gradient, due to cloud cover and light precipitation. After the clouds cleared in the afternoon, solar radiation began to heat the slab surface, which created a significant positive temperature gradient.

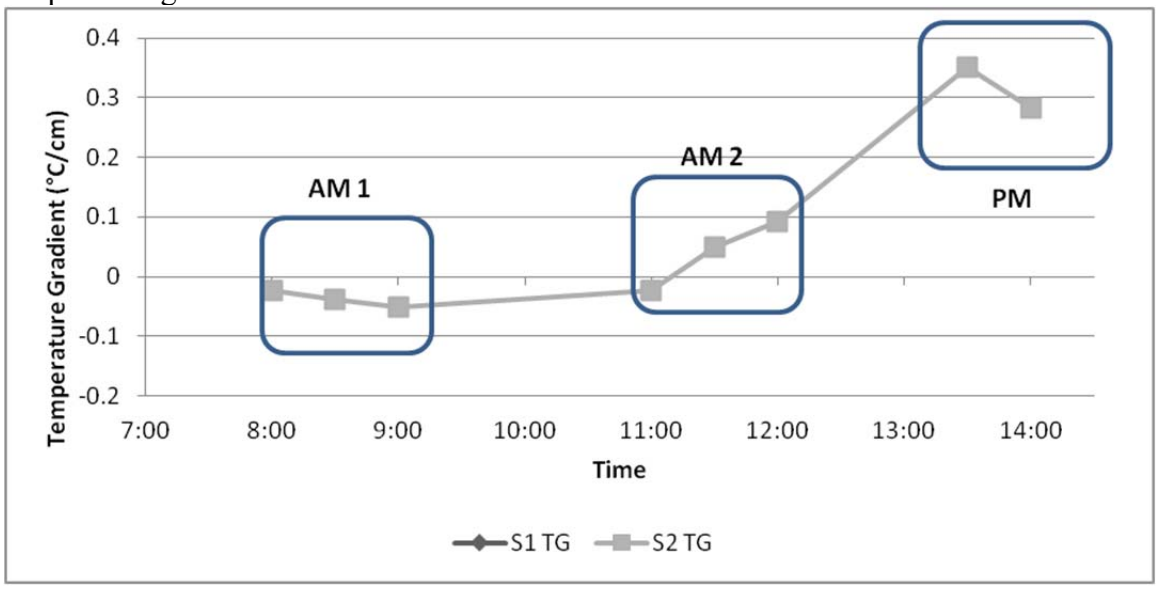

Figure 36 Pavement linear temperature gradients during fall 2010 truck test (1C°/cm = 4.6°F/in)

3.5.2.1 Deflection Response

The Fall 2010 deflection response for the light truck load is summarized in Table 20 and was similar to the spring test results. The heavy truck load was again excluded from this discussion because the geometry was similar and produced proportional responses to the loading applied. Additional test data can be found in Appendix D.

Slight upward deflections were observed at the exterior slab corners in Section 2 during the morning tests, which dissipated in the afternoon. Section 1 had lower deflections at transverse joints and larger deflections at mid-slab along the shoulder, similar to the spring test. During the morning tests, there was a general trend of decreasing deflections with increased vehicle speed. However, in the afternoon, the downward deflections increase with increasing vehicle speeds. This trend differs from the spring test, where increased speed resulted in lower downward deflections.

Table 20 Average deflections during fall 2010 light truck test (metric units)

Sensor:		LVDT 1 (mm)		LVDT 2 (mm)		LVDT 3 (mm)		LVDT 4 (mm)		LVDT 5 (mm)	
Section:		1	2	1	2	1	2	1	2	1	2
Speed (km/h)		Upward									
AM 1	8	0.0012	0.0342	0.0007	0.0022	0.0037	0.0126	0.0052	0.0118	0.0039	0.0124
	40	0.0014	0.0350	0.0009	0.0049	0.0014	0.0152	0.0047	0.0126	0.0038	0.0103
	Downward										
	8	-0.1790	0.2349	-0.1227	-0.0996	-0.1880	-0.2526	-0.1207	-0.2109	-0.0650	-0.1429
	40	-0.1792	0.2365	-0.1318	-0.0861	-0.1986	-0.2311	-0.1150	-0.1982	-0.0521	-0.1356
Speed (km/h)		Upward									
AM 2	8	0.0014	0.0308	0.0008	0.0025	0.0010	0.0099	0.0023	0.0090	0.0023	0.0071
	40	0.0013	0.0224	0.0005	0.0012	0.0009	0.0082	0.0011	0.0081	0.0008	0.0072
	70	0.0036	0.0202	0.0008	0.0020	0.0021	0.0097	0.0010	0.0075	0.0008	0.0048
	Downward										
	8	-0.1745	-0.2068	-0.1224	-0.0855	-0.1786	-0.2186	-0.1083	-0.1909	-0.0538	-0.1413
	40	-0.1314	-0.2107	-0.0859	-0.0885	-0.1214	-0.2074	-0.0854	-0.1647	-0.0462	-0.1081
	70	-0.1103	-0.1779	-0.0621	-0.0721	-0.0829	-0.1553	-0.0687	-0.1300	-0.0373	-0.0898
Speed (km/h)		Upward									
PM	8	0.0008	0.0023	0.0008	0.0009	0.0008	0.0017	0.0005	0.0013	0.0008	0.0012
	40	0.0007	0.0047	0.0006	0.0007	0.0010	0.0014	0.0007	0.0014	0.0006	0.0010
	70	0.0006	0.0010	0.0006	0.0006	0.0007	0.0013	0.0008	0.0008	0.0007	0.0008
	Downward										
	8	-0.0325	-0.0481	-0.0371	-0.0258	-0.0367	-0.0465	-0.0575	-0.0786	-0.0335	-0.0701
	40	-0.0309	-0.0565	-0.0351	-0.0271	-0.0367	-0.0513	-0.0559	-0.0787	-0.0316	-0.0660
	70	-0.0393	-0.0637	-0.0413	-0.0319	-0.0419	-0.0517	-0.0555	-0.0721	-0.0273	-0.0564

Table 21Average deflections during fall 2010 light truck test (English units)

Sensor:		LVDT 1 (mil)		LVDT 2 (mil)		LVDT 3 (mil)		LVDT 4 (mil)		LVDT 5 (mil)	
Section:		1	2	1	2	1	2	1	2	1	2
Speed (mph)		Upward									
AM 1	5	0.047	1.346	0.028	0.087	0.146	0.496	0.205	0.465	0.154	0.488
	25	0.055	1.378	0.035	0.193	0.055	0.598	0.185	0.496	0.150	0.406
	Downward										
	5	-7.047	9.248	-4.831	-3.921	-7.402	-9.945	-4.752	-8.303	-2.559	-5.626
	25	-7.055	9.311	-5.189	-3.390	-7.819	-9.098	-4.528	-7.803	-2.051	-5.339
Speed (mph)		Upward									
AM 2	5	0.055	1.213	0.031	0.098	0.039	0.390	0.091	0.354	0.091	0.280
	25	0.051	0.882	0.020	0.047	0.035	0.323	0.043	0.319	0.031	0.283
	43.5	0.142	0.795	0.031	0.079	0.083	0.382	0.039	0.295	0.031	0.189
	Downward										
	5	-6.870	-8.142	-4.819	-3.366	-7.031	-8.606	-4.264	-7.516	-2.118	-5.563
	25	-5.173	-8.295	-3.382	-3.484	-4.780	-8.165	-3.362	-6.484	-1.819	-4.256
	43.5	-4.343	-7.004	-2.445	-2.839	-3.264	-6.114	-2.705	-5.118	-1.469	-3.535
Speed (mph)		Upward									
PM	5	0.031	0.091	0.031	0.035	0.031	0.067	0.020	0.051	0.031	0.047
	25	0.028	0.185	0.024	0.028	0.039	0.055	0.028	0.055	0.024	0.039
	43.5	0.024	0.039	0.024	0.024	0.028	0.051	0.031	0.031	0.028	0.031
	Downward										
	5	-1.280	-1.894	-1.461	-1.016	-1.445	-1.831	-2.264	-3.094	-1.319	-2.760
	25	-1.217	-2.224	-1.382	-1.067	-1.445	-2.020	-2.201	-3.098	-1.244	-2.598
	43.5	-1.547	-2.508	-1.626	-1.256	-1.650	-2.035	-2.185	-2.839	-1.075	-2.220

3.5.2.2 Strain Response

The average strain measurements for LC-1 and LC-2 at the mid-slab wheel-path location for the light truck test are shown in Table 22. The integrity of strain gauge data collected during the second morning test (AM2) was poor until the 70 km/h (43.5 mph) tests at the end of the session; therefore, only the 70 km/h (43.5 mph) results are presented herein. Additional sensors and truck test data can be found in the appendices.

Table 22 Average peak strain values for LC-1 and LC-2 during fall 2010 truck tests

Load Case:		LC-1 Peak Strain (με)				LC-2 Peak Strain (με)			
Test	Speed (km/h (mph))	Section 1		Section 2		Section 1		Section 2	
		KM3	KM4	KM3	KM4	KM3	KM4	KM3	KM4
AM 1	8 (5)	4.30	-4.00	7.00	-3.78	-7.40	7.78	-8.33	4.30
	40 (25)	3.73	-3.63	6.37	-3.63	-7.60	7.87	-7.57	4.00
AM 2	70 (43.5)	2.60	-2.47	4.53	-2.50	-6.70	7.63	-7.57	4.23
PM	8 (5)	1.93	-1.70	2.47	-1.50	-9.23	9.47	-7.60	4.67
	40 (25)	1.73	-1.53	2.67	-1.47	-8.97	9.27	-8.47	4.97
	70 (43.5)	2.00	-1.57	2.80	-1.50	-7.57	8.80	-7.97	4.43

The spring and fall 2010 tests produced similar results. LC-1 resulted in higher tensile surface strains at Section 2, and LC-2 resulted in higher tensile bottom strains for Section 1. Section 1 still indicated equal and opposite strains at top and bottom, while Section 2 had higher absolute values of strains at the top of the slab. The effects of speed vary somewhat, depending on the testing time and sensor location. In the morning, increased speed decreased strains; however, in the afternoon, surface strains increased with speed for LC-1, while most others decreased with speed.

The strains were extrapolated to the pavement top and bottom for the morning test for LC-1 and LC-2, shown in Table 23. These results were similar to the spring tests, and indicated the strain distribution shown from the KM strain gauges was similar to the extrapolated strain distribution at slab top and bottom.

Table 23 Extrapolated strain response for KM 3 and 4 8- km/h AM1 truck tests

Section 1 (KM 3 & 4)			Section 2 (KM 3 & 4)		
Elevation (mm (in))	Strain (με)		Elevation (mm (in))	Strain (με)	
	LC-1	LC-2		LC-1	LC-2
337.5 (13.3) (Top)*	5.88	-10.28	325 (12.8) (Top)*	8.51	-10.10
290 (11.4) (KM3)	4.30	-7.40	290 (11.4) (KM3)	7.00	-8.33
40 (1.6) (KM4)	-4.00	7.78	40 (1.6) (KM4)	-3.78	4.30
0 (0) (Bottom)*	-5.33	10.21	0 (0) (Bottom)*	-5.50	6.32

*Extrapolated data

3.5.3 Fall 2011 Truck Testing

Additional tests were conducted on November 15 and 16 2011. These tests included both single-and dual-axle trucks. The results from these tests produced responses similar to previous tests. Therefore, they shall not be discussed herein, and the results can be found in Appendix E.

3.5.4 Discussion of Truck Testing

Higher deflections and slight upward deflections at the transverse joints in Section 2 show the CTPB contributed to higher deflections and a loss of support. In Section 1, there were no upward deflections and the downward deflections at the transverse joints were smaller. The deflections in Section 2 were larger because the slab was deforming on a rigid base layer, which did not provide continuous support when the slab curled. The reduced edge support led to greater downward deflections and slight upward movement at the joints. The greater deflections in Section 2 under traffic load increase the risk of structural breaks due to the loss of support at the edges.

The DGAB in Section 1 maintained support beneath the slab when traffic loads passed over the section, indicating that the DGAB flexibility improves slab support. This was demonstrated by the lack of upward deflections and smaller joint deflections in Section 1. Section 1 experienced larger downward deflections at the mid-slab shoulder location (LVDT 2) because of the more flexible DGAB layer. This was expected, however, because at this location there was minimal curling deformation, which made the deflection response dependent on the base stiffness.

The CTPB stiffness contributed to between 40% and 50% larger tensile strains at the slab surface when compared to the DGAB. Greater surface tensile strains can increase the risk of top-down cracking over time through fatigue loading. In the morning, the environmental curling deformations caused a loss of support in Section 2 because the CTPB does not provide uniform support when the slab curls. When the slab was loaded at the edges (LC-1), the cantilevered slab edges caused higher tensile strains at the mid-slab surface. Section 1 had lower surface tensile strains for LC-1 because the DGAB was more flexible and provided uniform slab edge support.

The strain response in each test section indicated a different slab/base interface condition in both test sections. In Section 1, the strains top and bottom of the slab were nearly equal in magnitude and opposite in direction. This condition corresponds to an unbonded slab/base interface. In Section 2, the magnitude of surface strains was greater than bottom strains, which indicated a bonded slab/base interface condition. The unbalanced strains indicate that the neutral axis had shifted downward because of the slab/base interaction.

The temperature gradient and resulting slab shape played a crucial role in the magnitude of strains and deflections from traffic loads. In the morning, the slab edges were curled upwards due to the negative temperature gradient. This resulted in the largest transverse joint deflections, and the greatest strains were experienced when the edges were loaded in LC-1. In the afternoon, the slab edges were curled downwards due to the positive temperature gradient. The upward curling decreased downward deflections and eliminated the upward deflections in Section 2. The upward curling also decreased support at mid-slab, and the highest strains in the afternoon occurred with LC-2, when the rear axle was at mid-slab.

The variation of deflection with vehicle speed was dependent on the slab temperature gradient. In the morning tests, the downward deflections decreased with increased speed. This results from the time-dependent nature of the deflection response, where less contact time decreases the deflection. In the spring, the afternoon deflections also decreased with increase speeds; however, this trend was not prevalent during the fall afternoon test. The temperature gradient during the fall afternoon test was greater than the spring afternoon gradient, which increased the contact between the slab edges and the base. This resulted in increased deflections with increased speeds, due to the vehicle impact loading. Hall et al. (1997) indicated that the dynamic subgrade k-value is twice as large as the static k-value; therefore, increasing speeds causes a greater deflection response due to the increasing k-value.

Strains tend to decrease with increased vehicle speed due to the shorter contact time between the vehicle and slab. As the speed increases, the pavement has less time to react to the load, and smaller strains result.

The difference in pavement thickness between the two test sections did not significantly alter the results. By extrapolating the strain to the slab top and bottom, it was shown that the difference in thickness was not the cause of different strain readings from either section. This confirms that the CTPB experienced slab/base interaction, which shifts the neutral axis downwards, while the DGAB performs as an unbonded pavement.

The truck testing was performed to examine the traffic load response for both test sections and to corroborate the environmental monitoring findings. From the testing, it was shown that the CTPB was causing a loss of support at the transverse joints, which leads to slight upward joint deflections, greater downward joint deflections, and higher mid-slab surface tensile strains. The DGAB had smaller joint deflections, which shows that DGAB provided improved slab support, and reduced joint deflections and mid-slab strains. The mid-slab shoulder deflections were slightly greater in the DGAB section, which show it was a more flexible material.

Chapter 4 Summary and Conclusions

4.1 Conclusions on Environmental Response

Embedded strain gauges and LVDTs have continually monitored the environmental response of the test sections since their placement in October 2009. Based on the short-term and long-term pavement response, the following conclusions have been made:

- Daily changes in deflection in Section 2 (CTPB) were initially smaller than Section 1 (DGAB); however, over the course of less than one year, the deflections in Section 2 became greater than Section 1.
- The higher change in deflection in Section 2 was a result of the slab deforming on a rigid base. The stiff CTPB does not provide uniform support when the slab edges curl. This confirms the findings of Sargand and Edwards (2000).
- The DGAB was more flexible and provided better edge support as the slab curls, which decreases deflections and strains.
- Section 2 (CTPB) had greater daily changes in load-related strain. This resulted from loss of support at the slab edges due to the rigid base in addition to higher slab/base interaction, which increased restraining forces.
- The higher deformations and strains in Section 2 indicate the CTPB increased the risk of cracking due to fatigue and loss of support.
- The CTPB layer did not influence subgrade moisture content, and both test sections had similar subgrade moisture contents directly beneath the DGAB layer.
- The difference in strain distributions for both sections was due to different slab/base interface conditions. Section 1 had peak strains at slab center, which was anticipated for an un-bonded slab/base interface. Section 2 had peak strains at mid-slab along the wheel-paths, indicating the longitudinal curling was restrained and increased strains at these locations.
- The initial curing strain response indicated higher slab/base interaction in Section 2.
- Summer and spring were the two critical season for slab strains. The subgrade modulus was lower in the spring season, which resulted in larger slab strains. In the summer, aggregate interlock restrained slab movement, which increased slab strains.
- Spring, summer, and fall were critical seasons for curling deflections. Some of the largest temperature gradients occurred during these seasons, which led to greater slab curling deformations.

4.2 Conclusions on FWD Response

Falling weight deflectometer tests were performed on the base materials prior to paving and on the PCC pavement after 14 and 21 days of curing. From these tests, the following conclusions have been made:

- The CTPB increased the overall pavement stiffness.
- The joint conditions in the CTPB section were more susceptible to changes in temperature.

- The DGAB had lower and more variable joint load transfer values; however, the joint efficiency was comparable to the CTPB section.
- The subgrade soil had uniform stiffness properties throughout the test section.

4.3 Conclusions on Dynamic Truck Testing

Truck testing was performed during the spring and fall seasons to verify the environmental monitoring data and to collect load response data for each test section. Based on these tests, the following conclusions have been made:

- The loss of support caused Section 2 (CTPB) to have slight upward deflections and larger downward deflections at the transverse joints than Section 1 (DGAB).
- Section 1 had smaller joint deflections and no upward deflections because the DGAB was more flexible and provided more uniform support conditions.
- Section 2 (CTPB) had larger tensile surface strains at mid-slab than Section 1 (DGAB). This was a result of the loss of support at the slab edges, which created a cantilevered beam effect and increased mid-slab strains when loaded.
- The loss of support and larger tensile strains in Section 2 (CTPB) increased the risk of fatigue cracking and structural breaks under traffic loading.
- Section 2 (CTPB) had higher slab/base interaction under traffic loads, which changed the strain distribution in the slab.
- Section 1 (DGAB) behaved as an unbonded pavement, as indicated by the equal and opposite strains at top and bottom.
- The morning surface tensile strains were greater than those in the afternoon due to the upward curling, which reduced slab support conditions.
- The temperature gradients determined the critical loading condition. In the morning, the critical loading was with both axles placed at the slab edges. In the afternoon, the critical loading was with the rear axle placed at mid-slab.
- The temperature gradients affected the deflection responses. The deflections were greater in the morning because the slab edges were curled upwards. In the afternoon, the slab curled downward, and joint deflections were reduced as the slab edges made contact with the base.
- Vehicle speed affected slab strains and deflections. Strains typically decreased with increasing speed, as the load was present for a shorter period. Generally, deflections decreased with speed, but the trend was also dependent on slab shape.

4.4 General Conclusions

Chapter 5 The environmental analysis indicates that the pavement placed on CTPB initially has smaller deflections than the pavement placed on DGAB. However, over time, the bond at the slab/base interface deteriorated such that the pavement deflections of the CTPB section surpassed those of the DGAB section. The truck testing has proven that there was a loss of support at the transverse joints in the CTPB section, which resulted in greater joint deflections under traffic loads. Thus the DGAB provided more uniform slab support, which resulted in lower strains and deflections in the pavement.

Chapter 6 The average daily changes in strain were higher in Section 2, which resulted from unsupported slab edges and higher restraining stresses at the slab/base interface. Surface tensile

strains under traffic loads were also higher in Section 2, resulting from the unsupported slab edges. The bonding between the CTPB and PCC slab occurred during pavement construction. This engaged restraining forces at the slab/base interface which affected pavement deformations and increased slab strains. Over time, this bonding was weakened, which led to higher joint deflections. However, truck tests indicate that at the strain gage locations, there was significant slab/base interaction. This research supports the conclusions from Yu et al. (1998), which found that the slab/base interface can be un-bonded under curling deformations and bonded under traffic loads, even in the absence of a physical bond between layers. However, this premise was only true for the CTPB section, since the DGAB has limited capabilities for shear stress transfer. Therefore, for this interaction to occur, the underlying layer must be bonded and capable of shear stress transfer. In addition, the results of this study confirmed those of previous studies in Ohio by ORITE that indicated that the base layer should be selected based on permeability, stiffness, and constructability.

Chapter 7 The CTPB layer increased slab surface tensile strains and joint deflections, compared to those of the DGAB section. The impact of higher slab strains and edge deflections is an increased risk of mid-slab cracking due to fatigue loading, and structural breaks at the joints due to a loss of support. Therefore, the CTPB had no positive influence on the pavement and had negative impacts on the load response. The subgrade moisture under the two sections was similar.

7.1 Implementation

Based on the conclusions above, it is recommended to utilize a DGAB base under PCC pavements instead of CPTB. At the very least, the NYSDOT can specify DGAB as a preferred base material in plans and specifications pertaining to JPCP pavements.

References

American Concrete Pavement Association. (2007). *Subgrades and subbases for concrete pavements*. Skokie, IL.

ASTM Standard C469/C469M, (2010). *Standard test method for static modulus of elasticity and Piosson's ratio of concrete in compression*. DOI: 10.1420/C0033-03. West Conshohocken, PA: ASTM International.

Beckemeyer, C. A., Khazanovich, L., & Yu, H. T. (2002). Determining amount of built-in curling in jointed plain concrete pavements: Case study of Pennsylvania I-80. *Transportation Research Record: Journal of the Transportation Research Bard, 1809*, 85-92.

Elfino, M. K. & Hossain, M. S. (2007). Subsurface drainage and premature distresses in concrete pavement: A case study in Virginia. *Transportation Research Record: Journal of the Transportation Research Board, 2004*, 141-149.

Fekrat, A. Q. (2010). Calibration and validation of EverFE2.24: A finite element analysis program for jointed plain concrete pavements. Unpublished master's thesis, Ohio University.

FHWA. (1990). Concrete Pavement Joints. Technical Advisory 5040.30, In FHWA Pavement Notebook Federal Highway Administration, Washington, D.C.

Hall, K. T., Darter, M. I., Hoerner, T. E., and Khazanovich, L. (1997). LTPP data analysis phase I: Validation of guidelines for k-value selection and concrete pavement performance prediction (Report No. FHWA-RD-96-198). McLean, VA: Turner-Fairbank Highway Research Center.

Hopkins, E. J. (2005). WES supplemental information: DataStreme WES week ten: 7-11 November 2005, Calendars and meteorological seasons [WWW Document] URL http://www.aos.wisc.edu/~hopkins/wes/fall_05/wesf05supl10.html (visited 2011, April 13).

Jensen, E. A. & Hansen, W. (2006). Nonlinear aggregate interlock model for concrete pavements. *International Journal of Pavement Engineering, 7*(4), 261-273.

Jeong, J. H. & Zollinger, D. G. (2005). Environmental effects on the behavior of jointed plain concrete pavements. *Journal of Transportation Engineering, ASCE, 131*(2), 140-148.

Mahboub, K. C., Liu, Y., & Allen, D. (2004). Evaluation of temperature responses in concrete pavement. *Journal of Transportation Engineering, ASCE, 130*(3), 395-401.

New York State Department of Transportation, Design Division & Technical Services Division (2002). Comprehensive pavement design manual. Albany, NY.

New York State Department of Transportation, Engineering Division – Office of Technical Services. *Highway Data Services Bureau.* [WWW Document] URL http://www.nysdot.gov/divisinos/engineering/technical-services/highway-data-services (visited 2011, June 1).

New York State Thruway Authority. *Interchange 39-40 reconstruction* [WWW Document] URL http://www.thruway.ny.gov/projectsandstudies/projects/i39-i40/index.html (visited 2010, April 2).

Pierce, L. M. (1999). Development of a computer program for the determination of the area value and subgrade modulus using dynatest FWD. Wisconsin State Department of Transportation.

Rasmussen, R.O. & Rozycki, D.K. (2001). Characterization and modeling of axial slab-support restraint. *Transportation Research Record: Journal of the Transportation Research Board, 1778*, 26-32.

Rufino, D. & Roesler, J. (2006). Effect of slab-base interaction on measured concrete pavement responses. *Journal of Transportation Engineering, ASCE, 132*(5), 425-434.

Rutkowski, T.S., Shober, S.F., & Schmeidlin, R.B. (1998). *Performance evaluation of drained pavement structures.* (Research Project #WI 87-05). Madison, WI: Wisconsin Department of Transportation.

Sargand, S. M. (2002). Determination of pavement layer stiffness on the Ohio SHRP test road using non-destructive testing techniques. Federal Highway Administration Report FHWA/OH-2002/031.

Sargand, S. M. & Abdalla, B. (2006). Truck/pavement/economic modeling and in-situ field test data analysis applications – Volume 2: Verification and validation of finite element models for rigid pavement using in-situ data – Selection of joint spacing. Federal Highway Administration Report FHWA/OH-2006/3B.

Sargand, S. M. & Beegle, D. (1995). *Three dimensional modeling of rigid pavement*. (Final Report, State Job No. 14537(0)). Athens, OH: Ohio University Civil Engineering Department.

Sargand, S. M. & Edwards, W. F. (2000). *Effectiveness of base type on the performance of PCC pavement on ERI/LOR 2.* (Interim Report, State Job #14652(0)). Athens, OH: Ohio Research Institute for Transportation and the Environment.

Sargand, S. M., Swanlund, M., Wise, J., & Edwards, W. F. (2005). Evaluation of slab shape under controlled environmental conditions. *ACI Structural Journal, 102*(4), 588-595.

Sargand, S. M., Wu, S., & Figueroa, J. L. (2006). Rational approach for base type selection. *Journal of Transportation Engineering, ASCE, 132*(10), 753-762.

Sayers, M. W. & Karamihas, S. M. (1998). The little book of profiling. Michigan: University of Michigan Transportation Research Institute.

Shoukry, S. N., William, G. W., & Riad, M. (2003). Nonlinear temperature gradient effects in dowel jointed concrete slabs. *International Journal of Pavement Engineering, 4*(3), 131-142.

Shoukry, S. N., William, G. W., & Riad, M. (2007). Effect of thermal stresses on mid-slab cracking in dowel jointed concrete pavement. *Structure and Infrastructure Engineering, 3*(1), 43-51.

Teller, L.W. & Sutherland, E. C. (1935). The structural design of concrete pavements. Part 2: Observed effects of variations in temperature and moisture on the size, shape and stress resistance of concrete pavement slabs. *Public Roads, 16*(9), 169-197.

Westergaard, H. M. (1927). Theory of concrete pavement design. *Proc., Highway Research Board*, Part I, Washington DC., 175-181.

Yang, H. H. (2004). Pavement Analysis and Design (2nd ed.). Upper Saddle River, NJ: Pearson Prentice Hall.

Yoder, E.J. & Witczak, M.W. (1975). Principles of Pavement Design (2nd ed.). New York: Wiley-Interscience.

Yu. H.T., Khazanovich, L., Darter, M.I., & Ardani, A. (1998). Analysis of concrete pavement responses to temperature and wheel loads measured from instrumented slabs. *Transportation Research Record: Journal of the Transportation Research Board, 1639*, 94-101.

Zhang, J. & Li, V. C. (2001). Influence of supporting base characteristics on shrinkage-induced stresses in concrete pavements. *Journal of Transportation Engineering, ASCE, 127*(6), 455-462.

Appendix A Supplemental Environmental Response Data

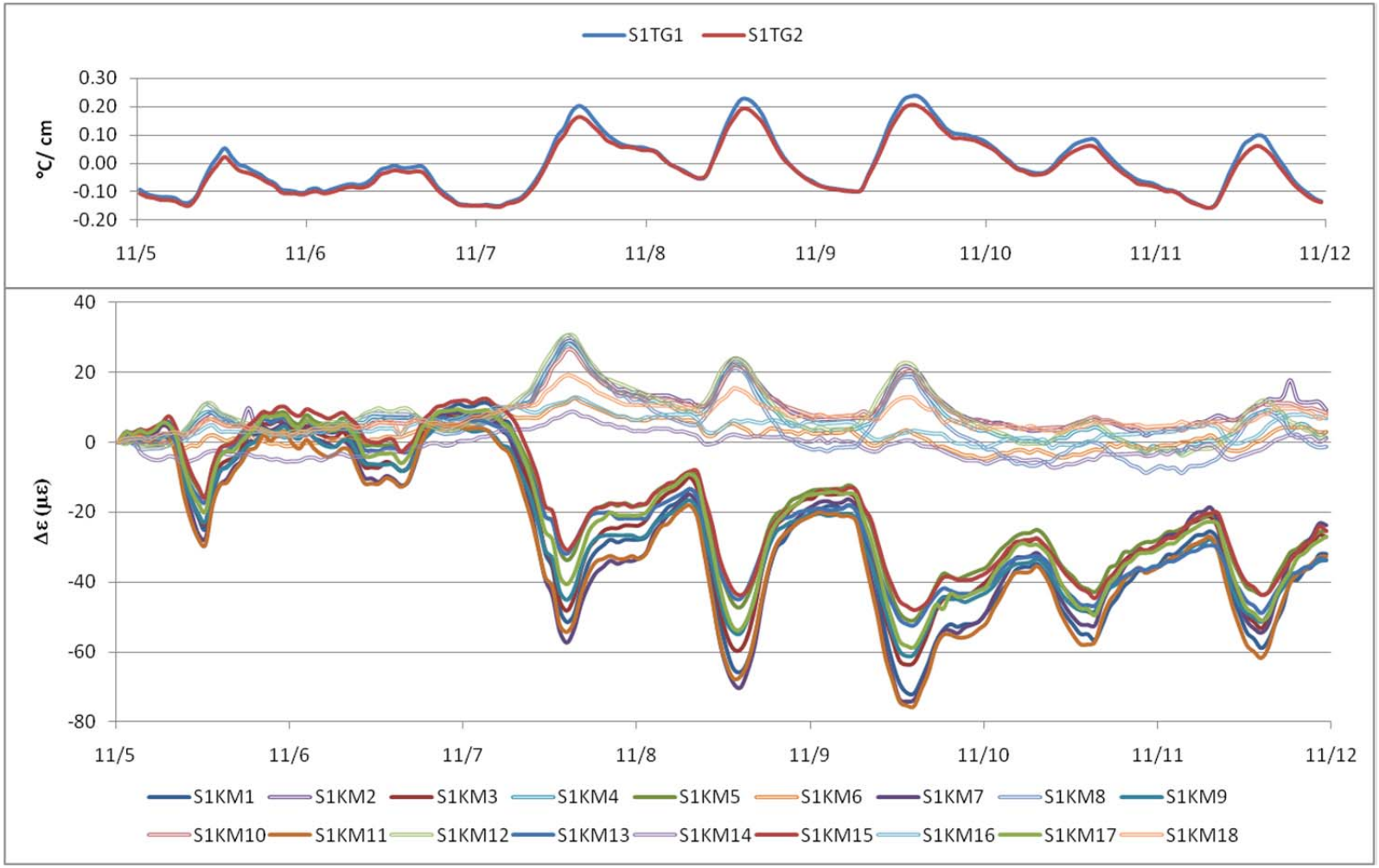

Section 1 - Load-related strains – Fall 2009 (11/5 – 11/11) (1 C°/cm = 4.6°F/in)

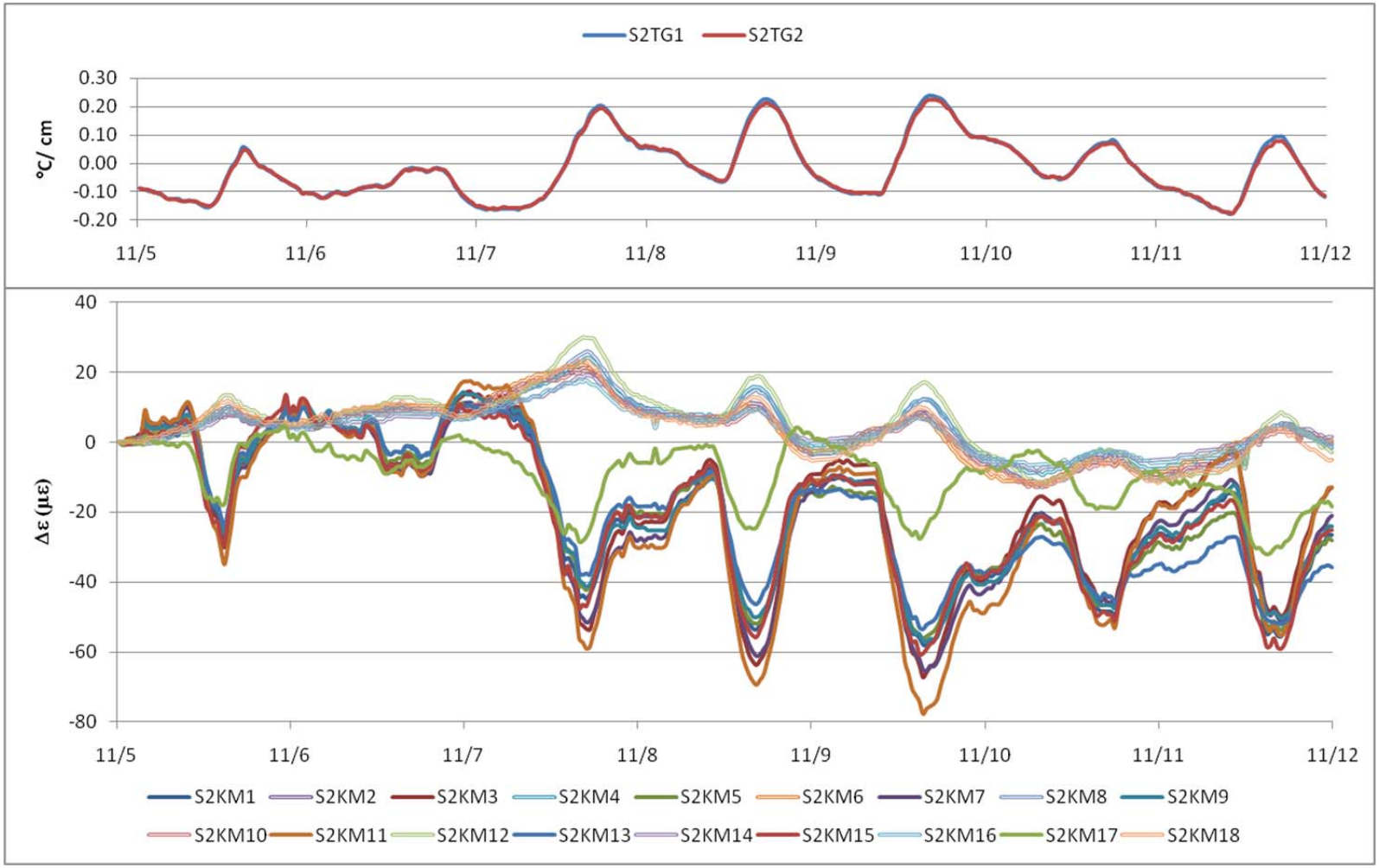

Section 2 - Load-related strains – Fall 2009 (11/5 – 11/11) (1 C°/cm = 4.6°F/in)

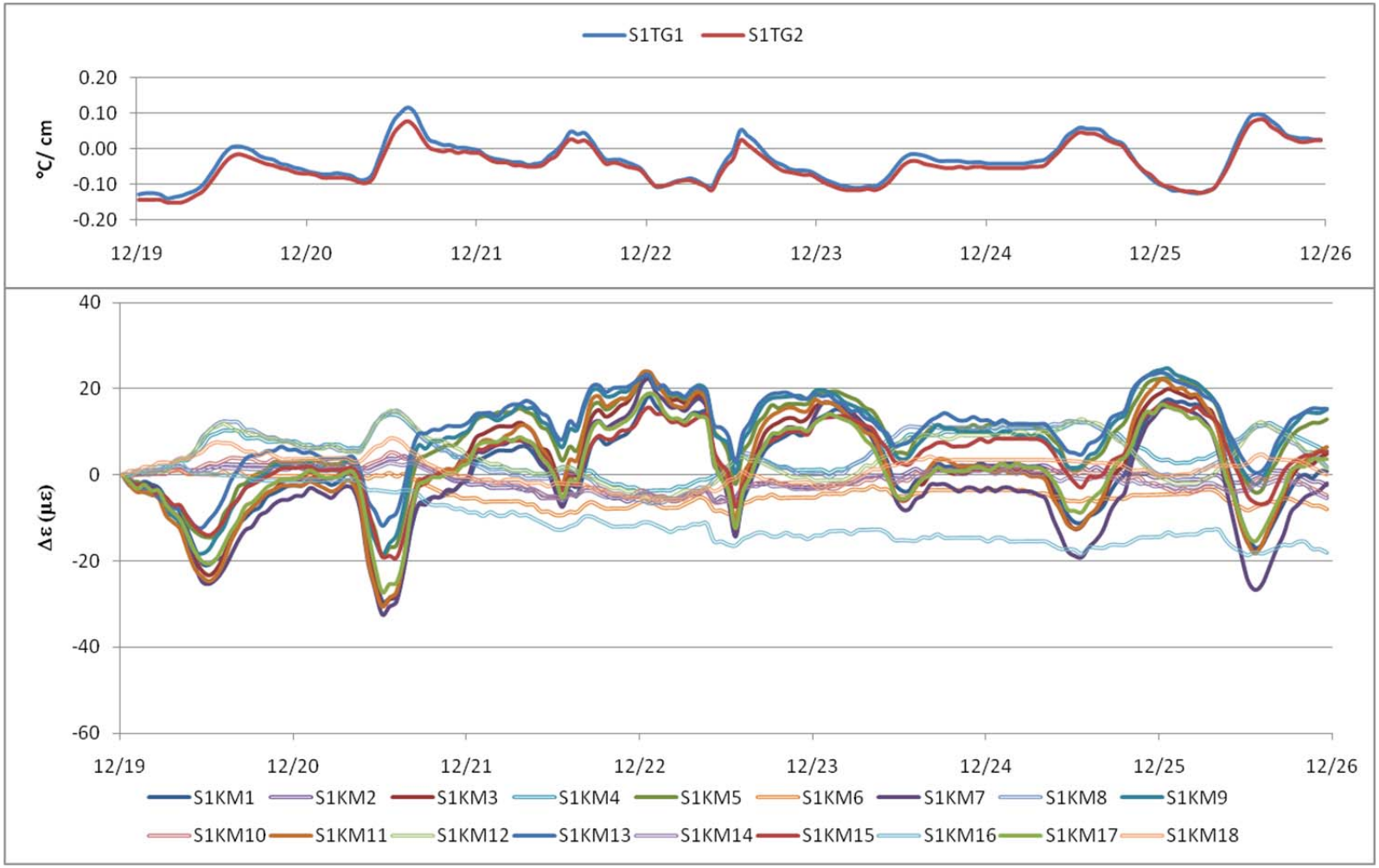

Section 1 - Load-related strains – Winter 2009-10 (12/19 – 12/25) (1 C°/cm = 4.6°F/in)

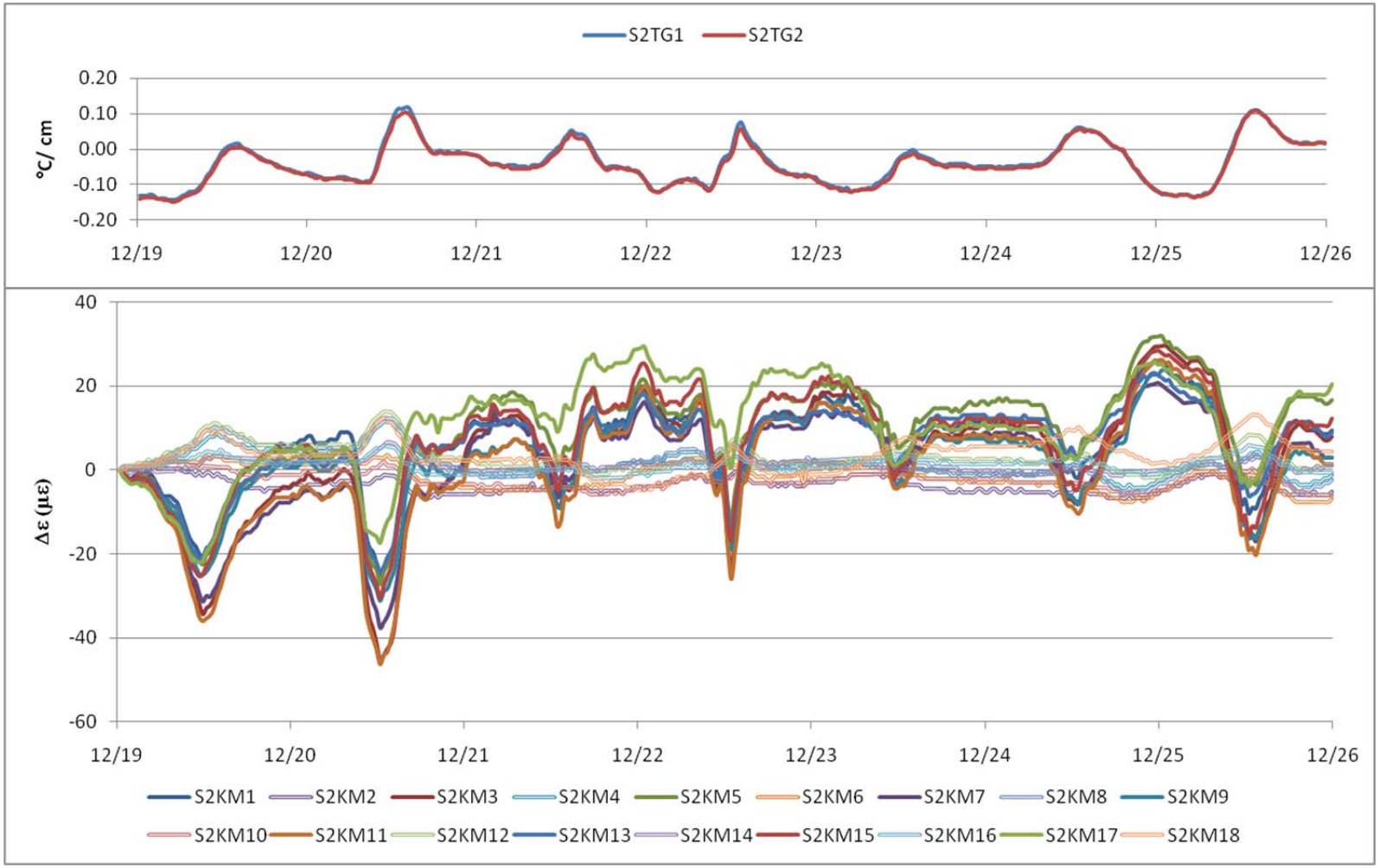

Section 2 - Load-related strains – Winter 2009-10 (12/19 – 12/25) (1 C°/cm = 4.6°F/in)

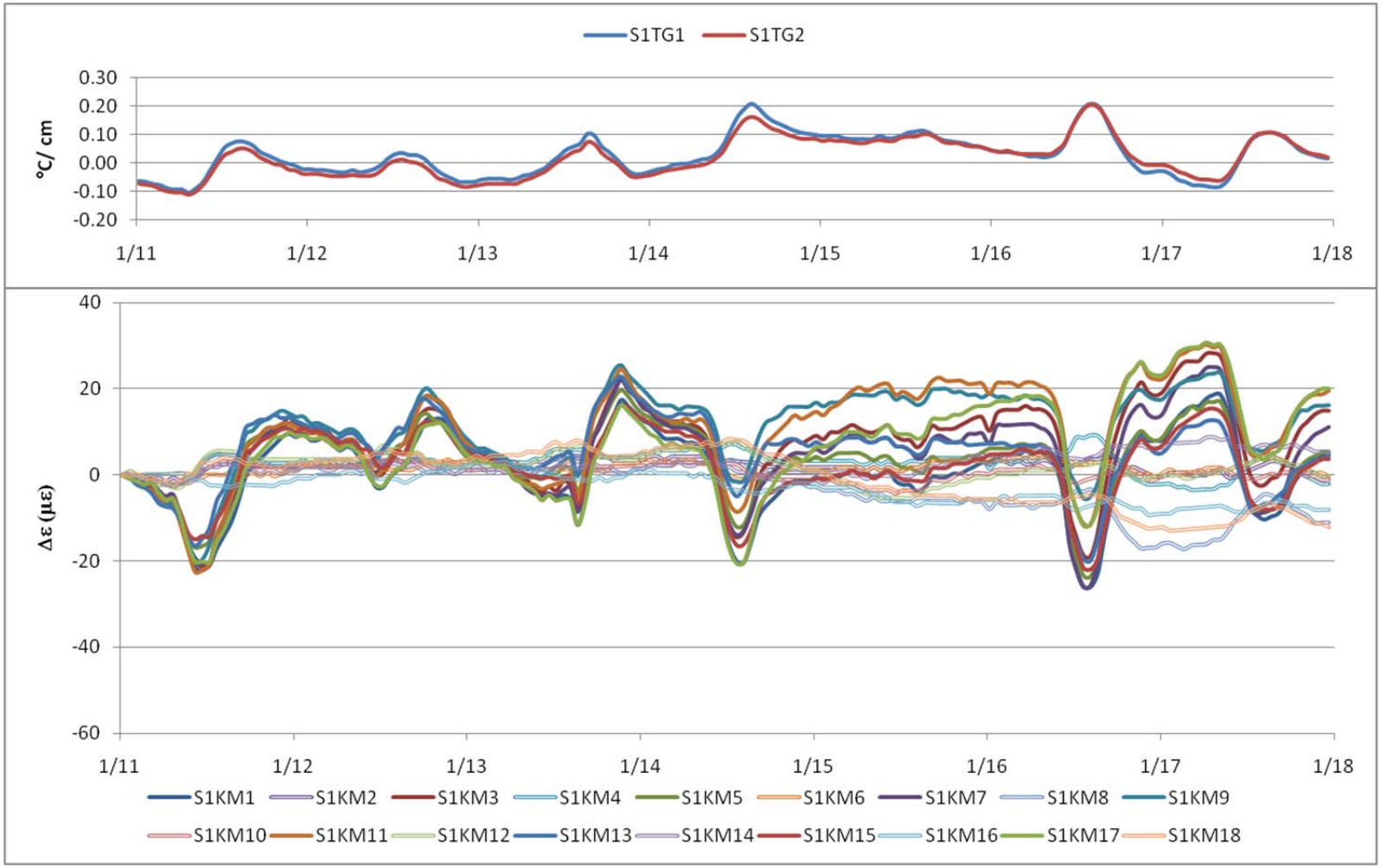

Section 1 - Load-related strains – Winter 2009-10 (1/11 – 1/17) (1 C°/cm = 4.6°F/in)

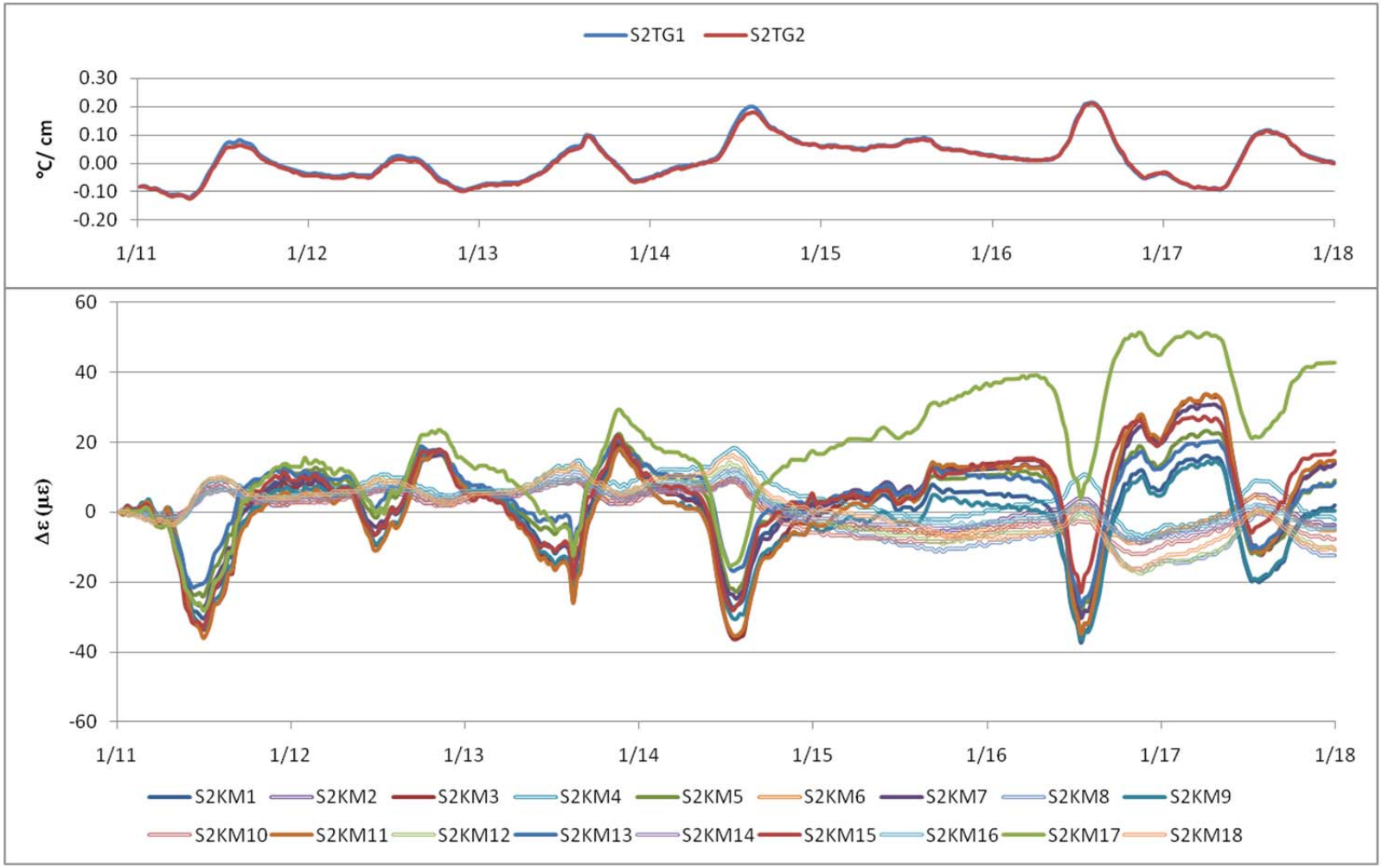

Section 2 - Load-related strains – Winter 2009-10 (1/11 – 1/17) (1 C°/cm = 4.6°F/in)

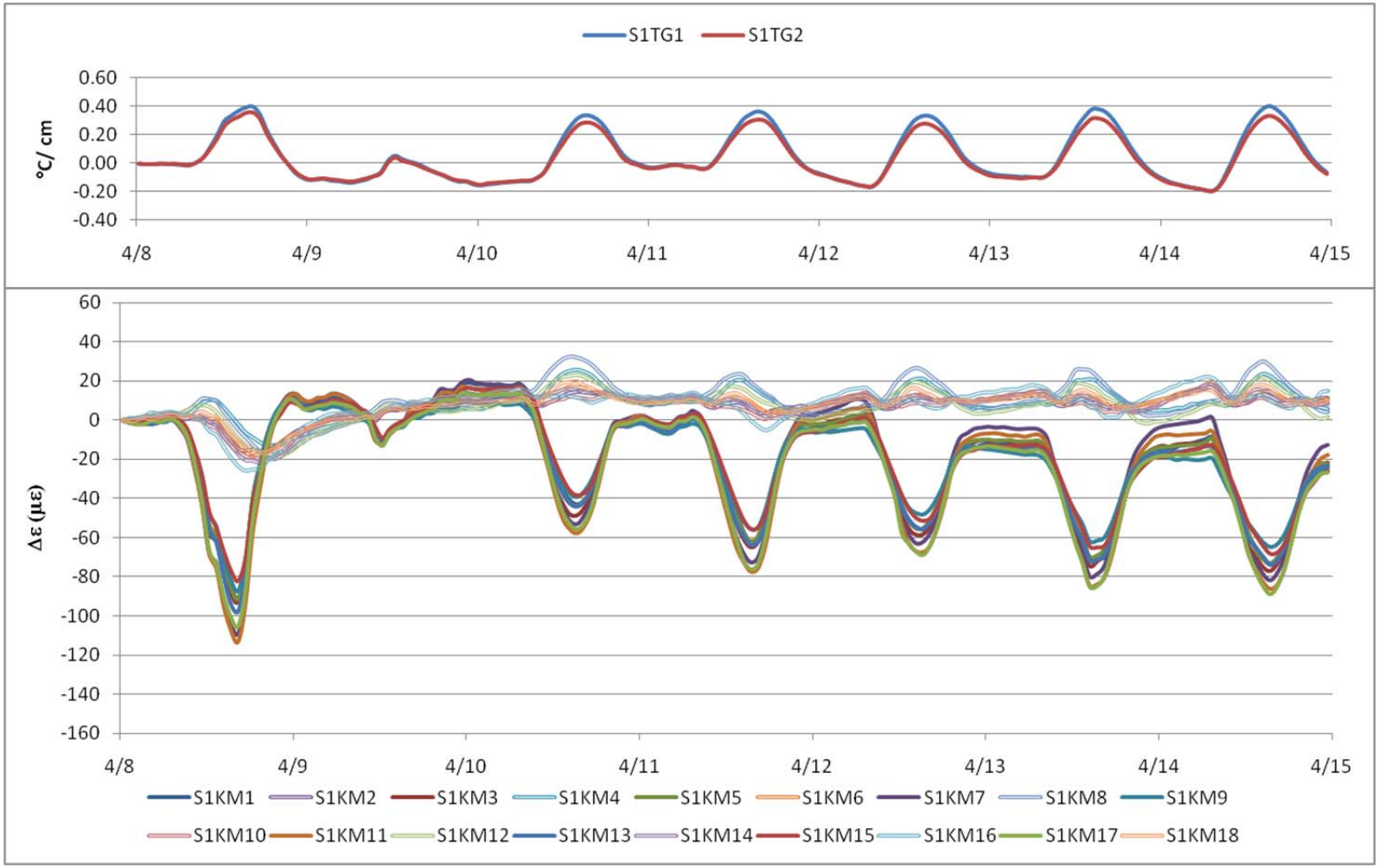

Section 1 - Load-related strains – Spring 2010 (4/8 – 4/14) (1 C°/cm = 4.6°F/in)

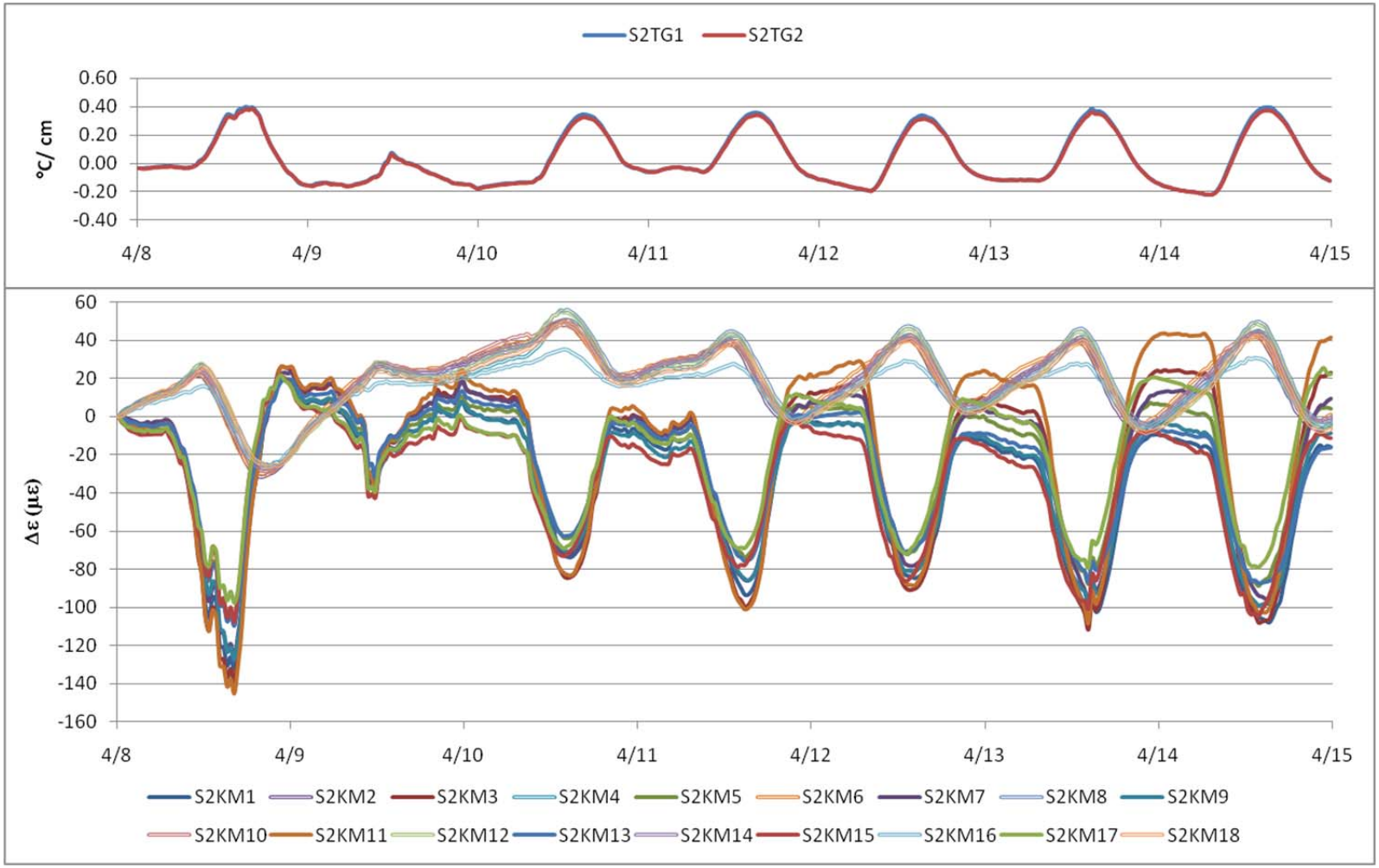

Section 2 - Load-related strains – Spring 2010 (4/8 – 4/14) (1 C°/cm = 4.6°F/in)

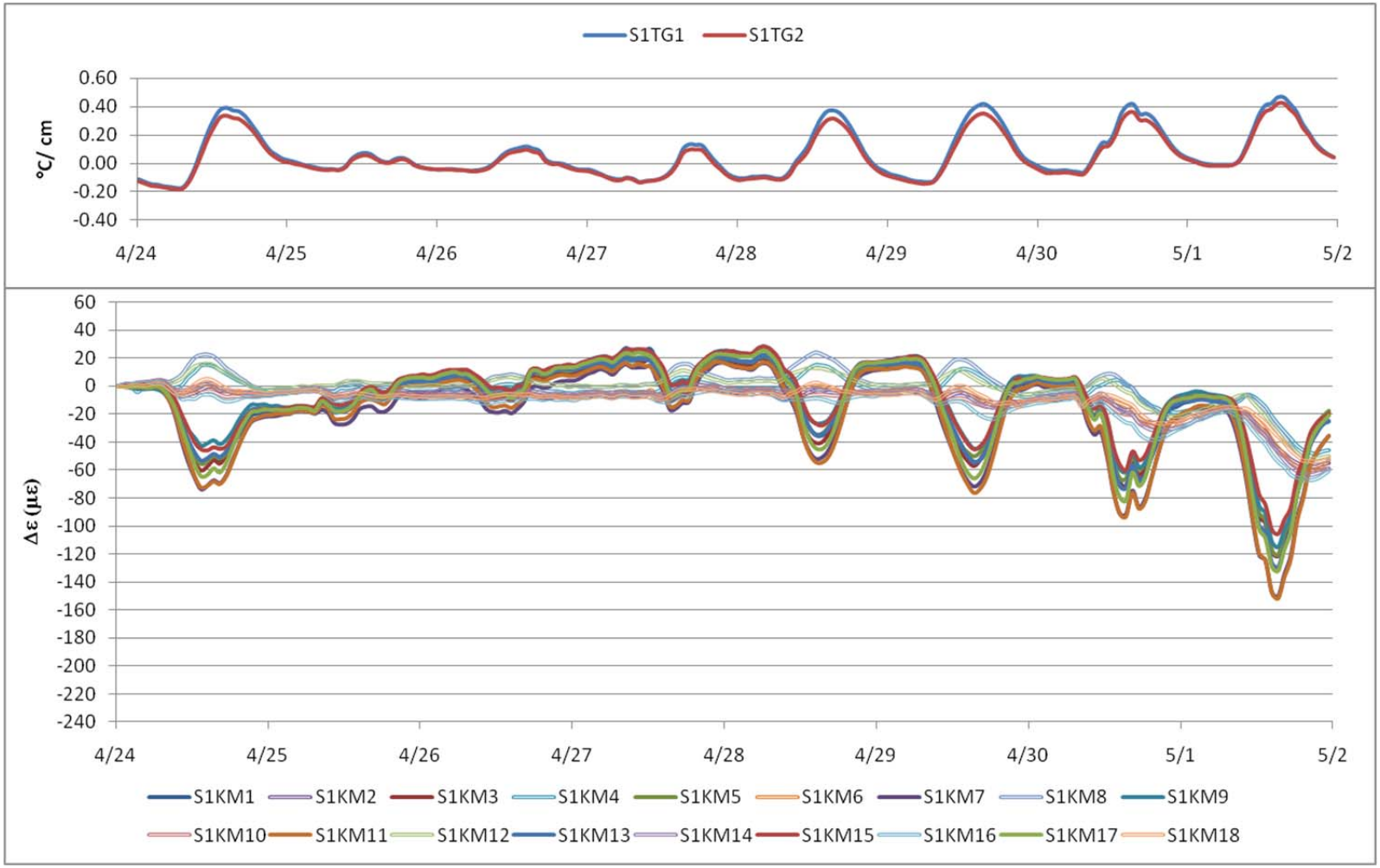

Section 1 - Load-related strains – Spring 2010 (4/24 – 4/30) (1 C°/cm = 4.6°F/in)

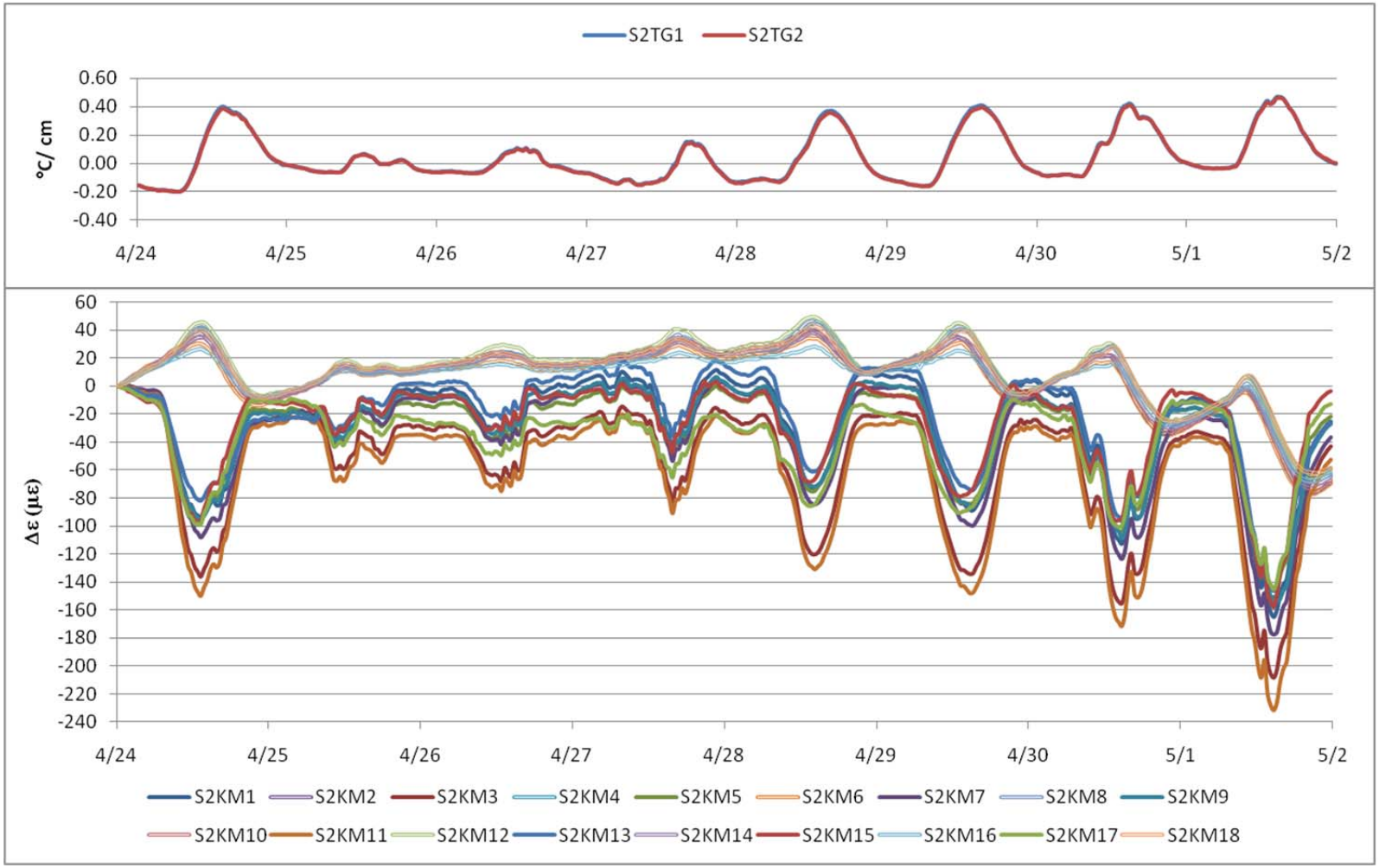

Section 2 - Load-related strains – Spring 2010 (4/24 – 4/30) (1 C°/cm = 4.6°F/in)

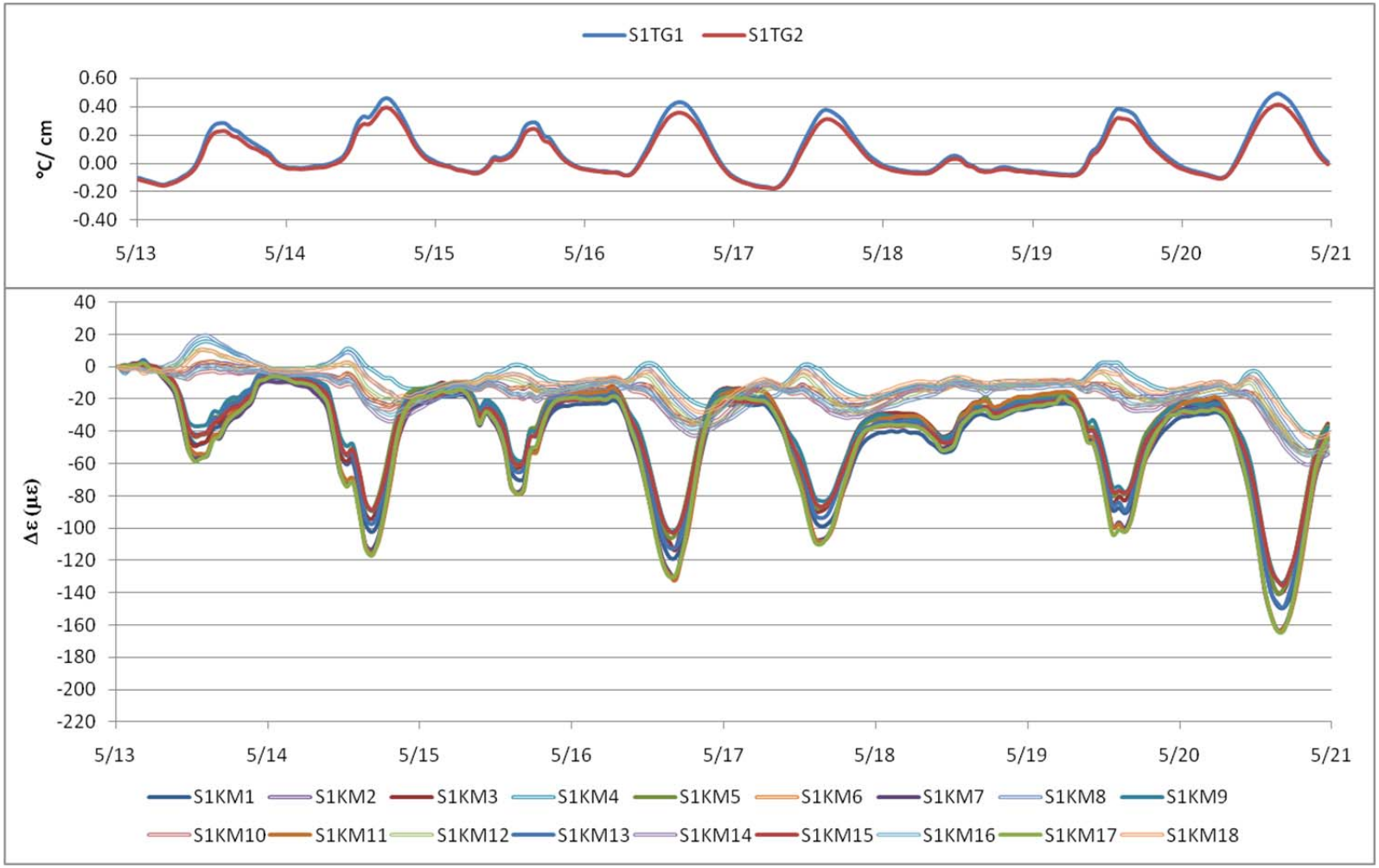

Section 1 - Load-related strains – Spring 2010 (5/13 – 5/19) (1 C°/cm = 4.6°F/in)

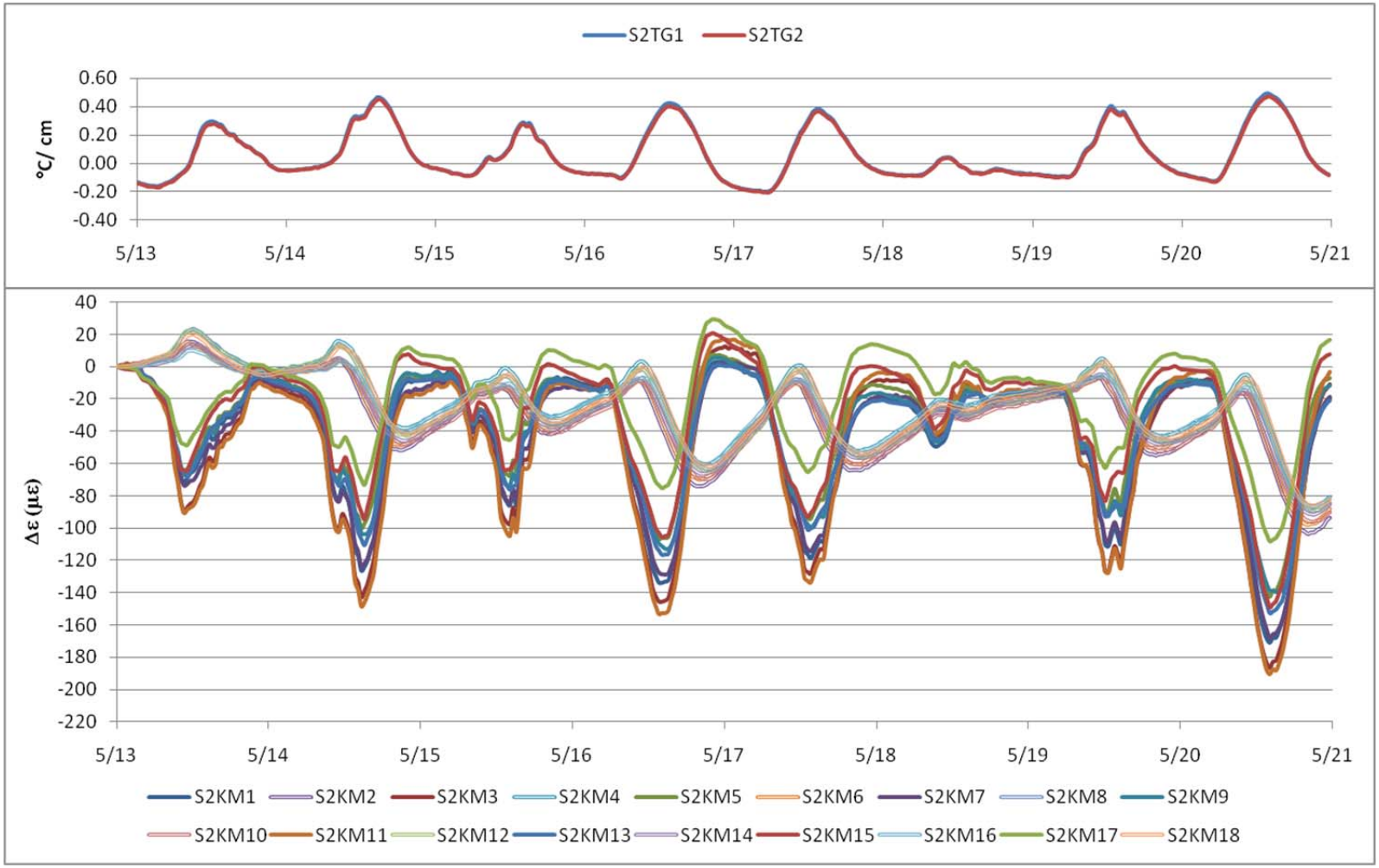

Section 2 - Load-related strains – Spring 2010 (5/13 – 5/19) (1 C°/cm = 4.6°F/in)

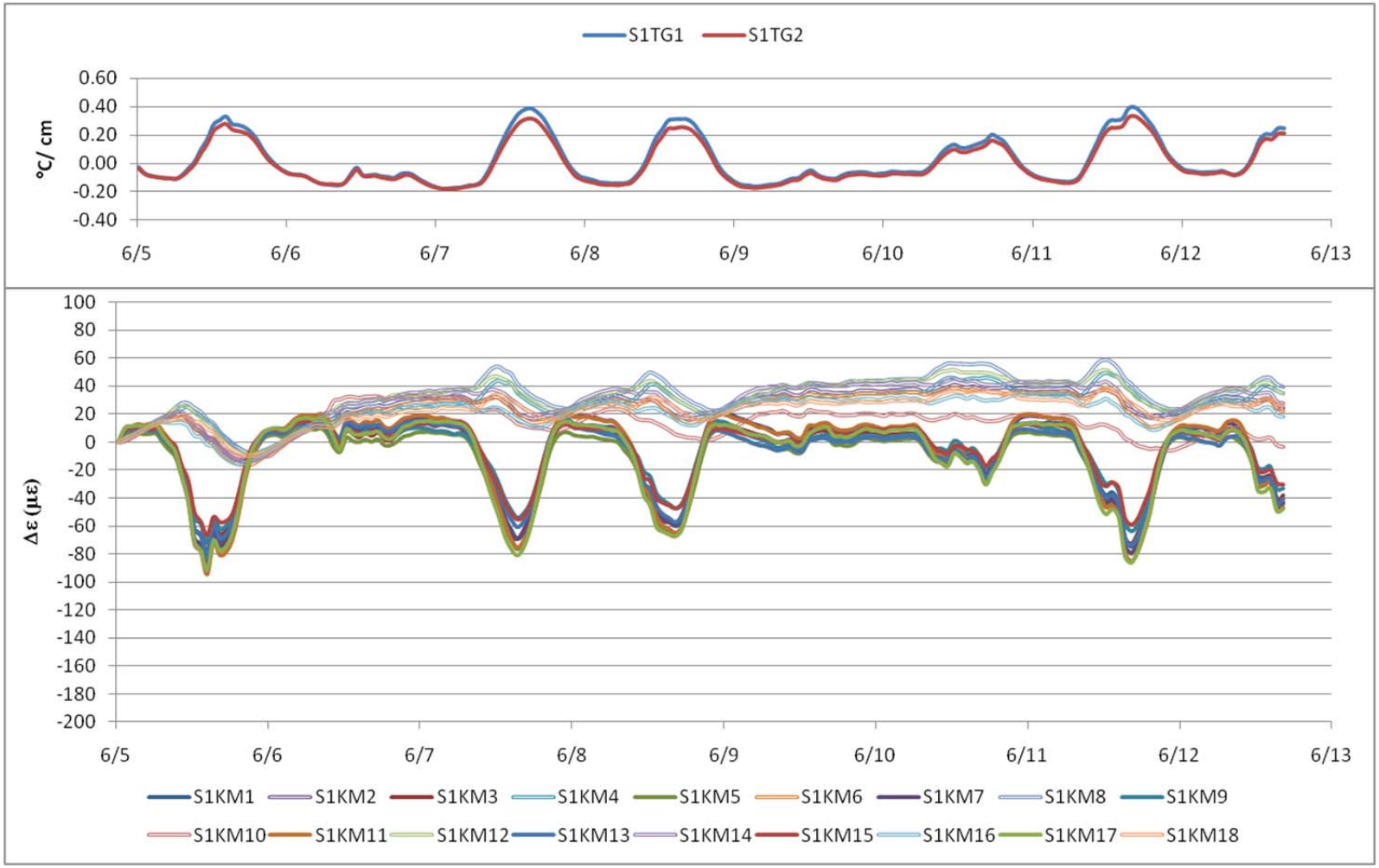

Section 1 - Load-related strains – Summer 2010 (6/5 – 6/11) (1 C°/cm = 4.6°F/in)

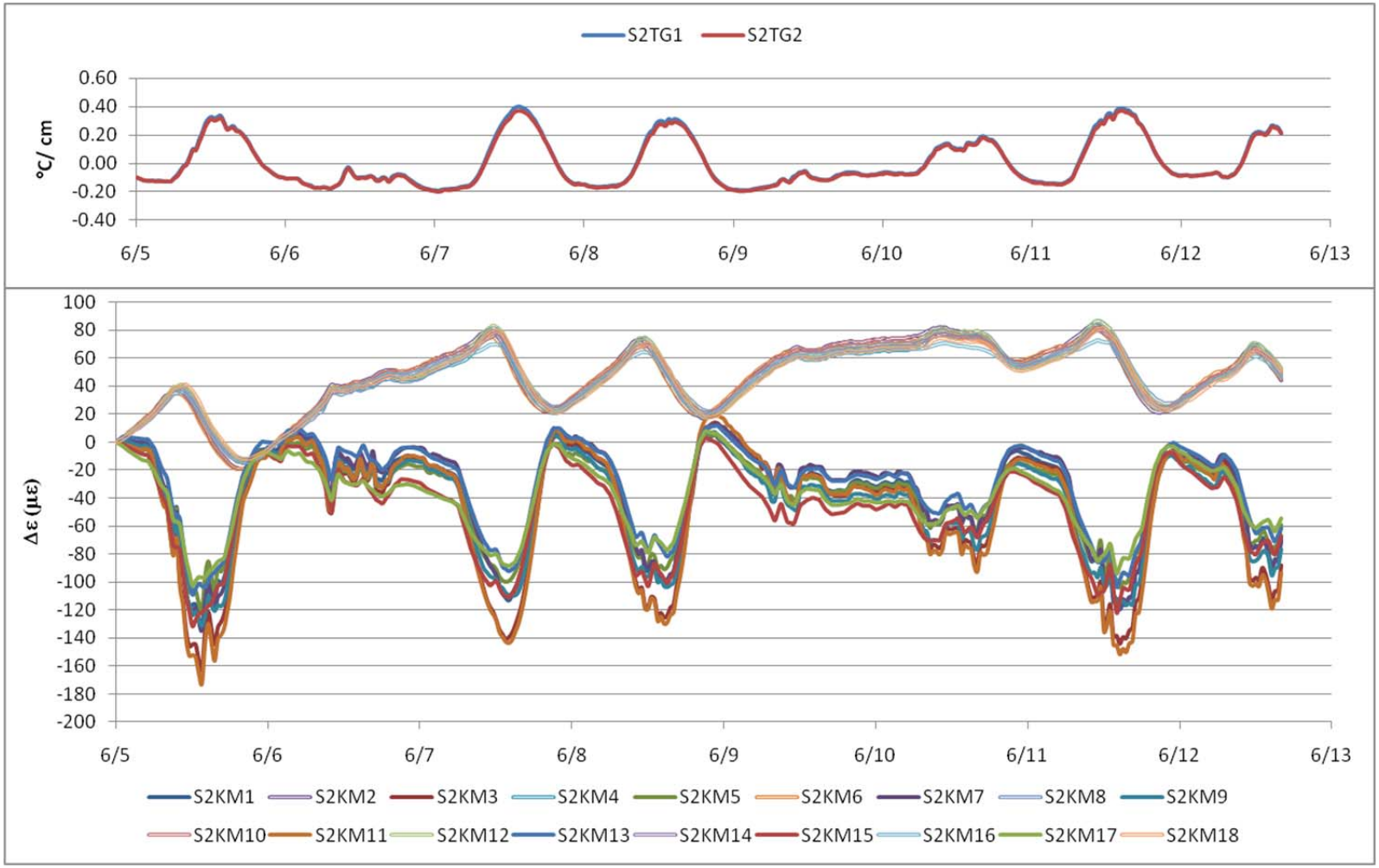

Section 2 - Load-related strains – Summer 2010 (6/5 – 6/11) (1 C°/cm = 4.6°F/in)

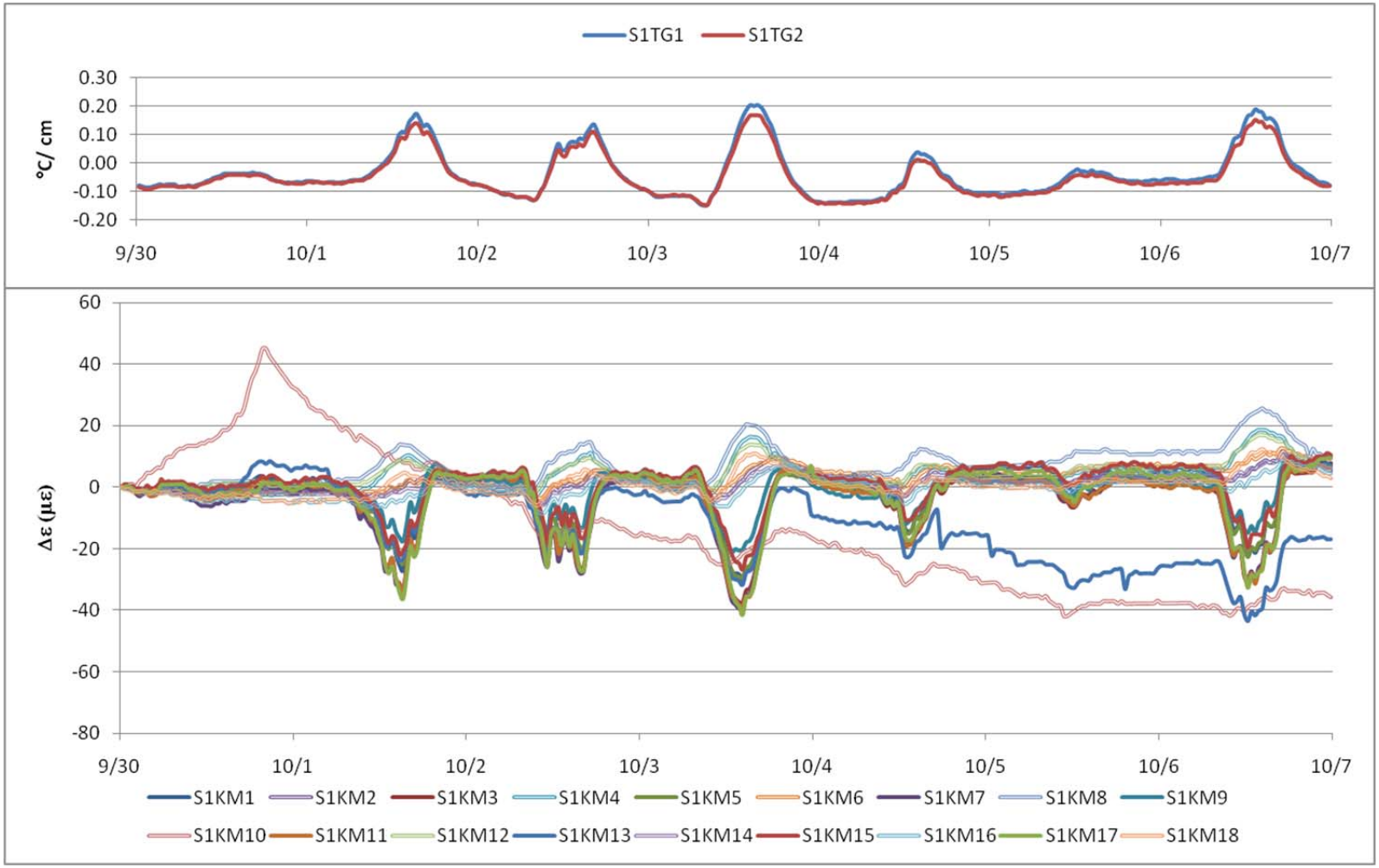

Section 1 - Load-related strains – Fall 2010 (9/30 – 10/6) (1 C°/cm = 4.6°F/in)

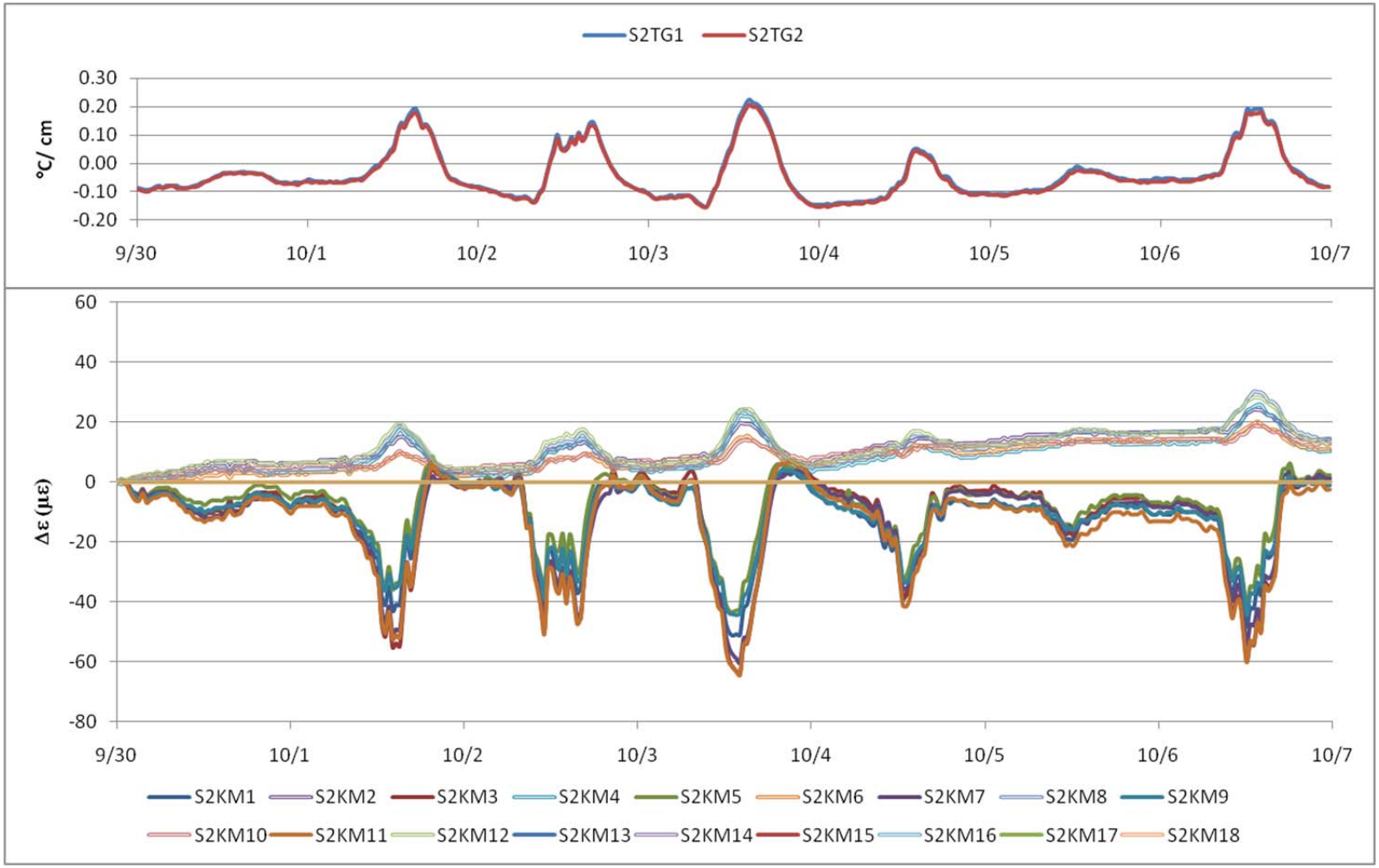

Section 2 - Load-related strains – Fall 2010 (9/30 – 10/6) (1 C°/cm = 4.6°F/in)

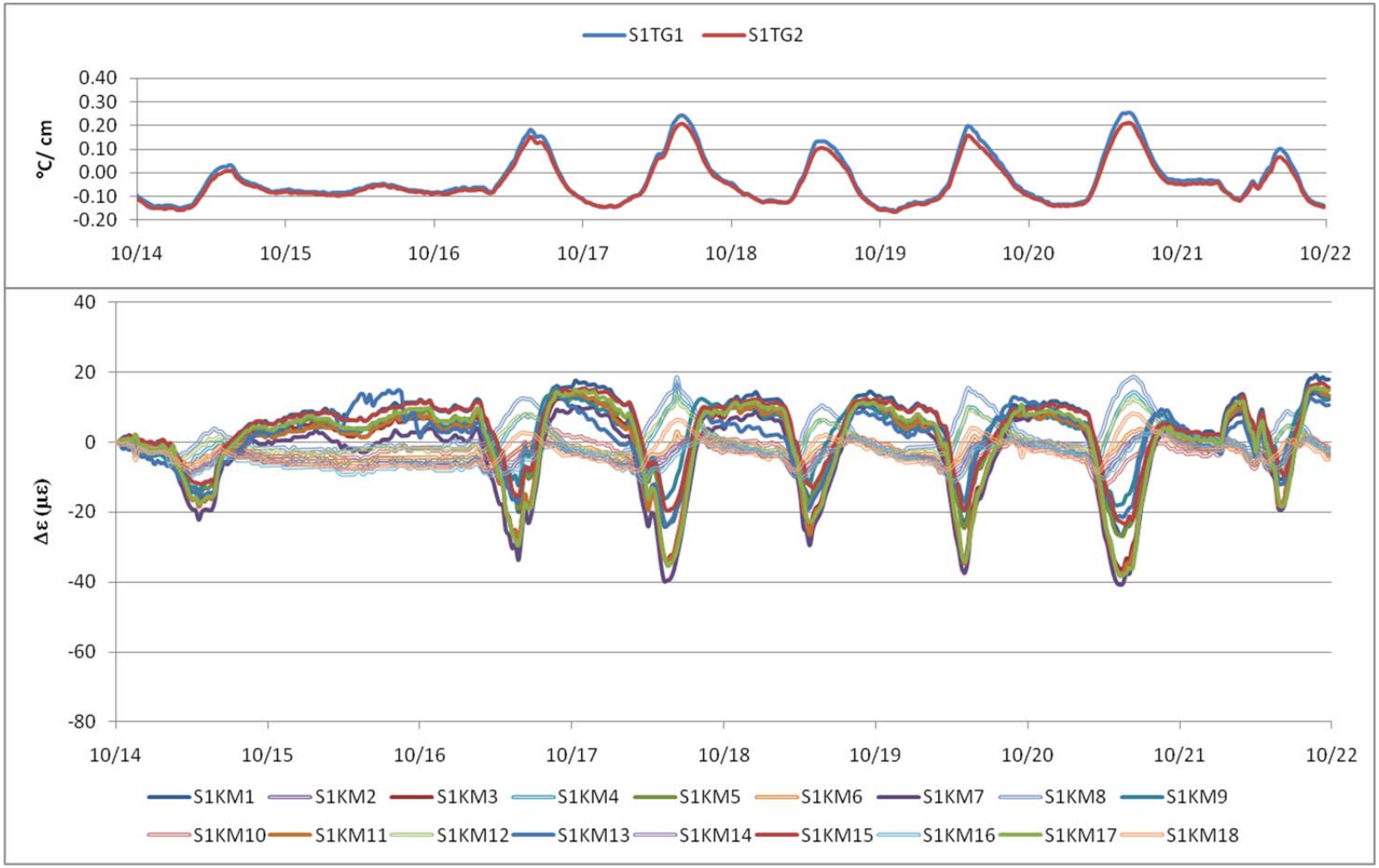

Section 1 - Load-related strains – Fall 2010 (10/14 – 10/22) (1 C°/cm = 4.6°F/in)

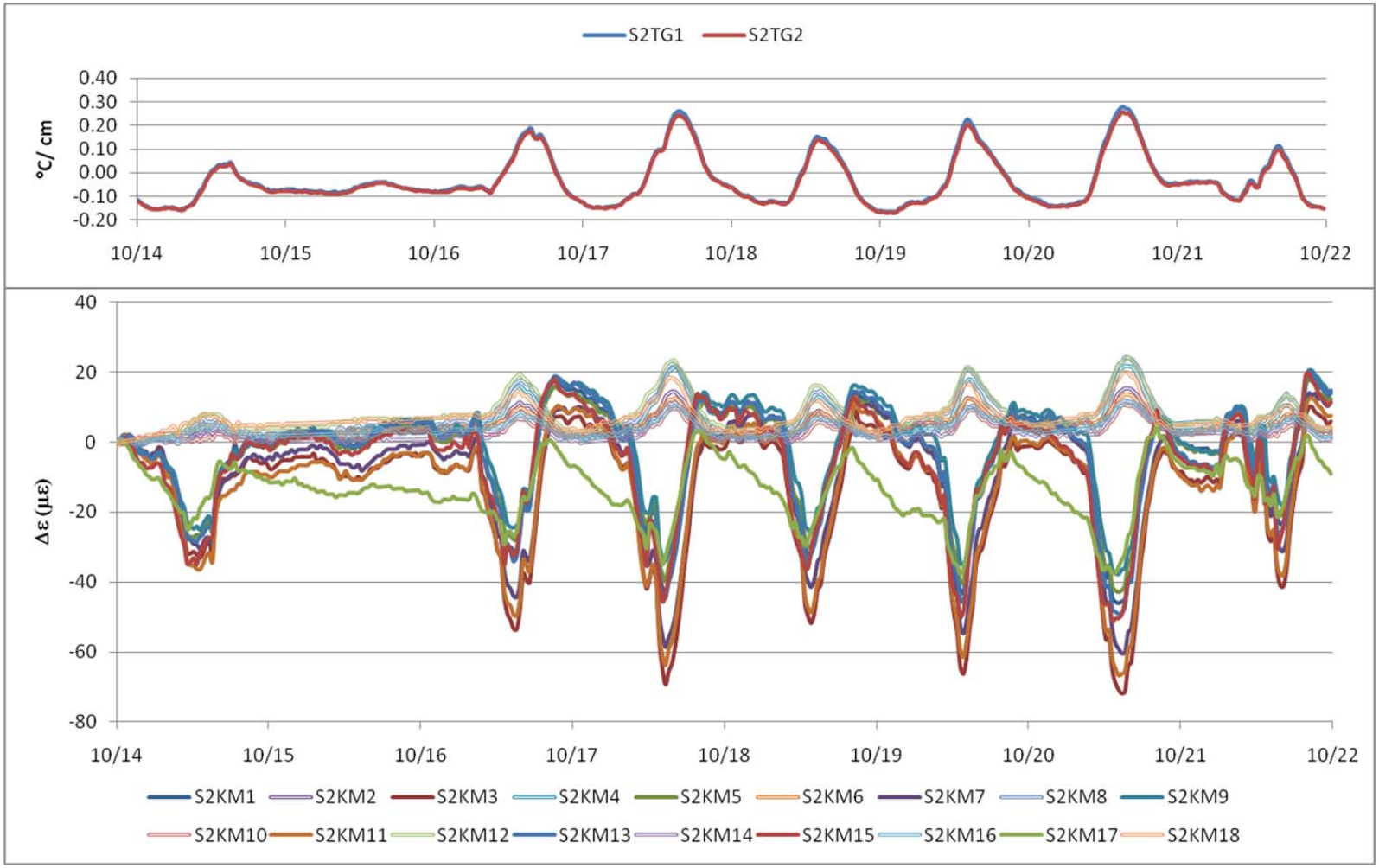

Section 2 - Load-related strains – Fall 2010 (10/14 – 10/22) (1 C°/cm = 4.6°F/in)

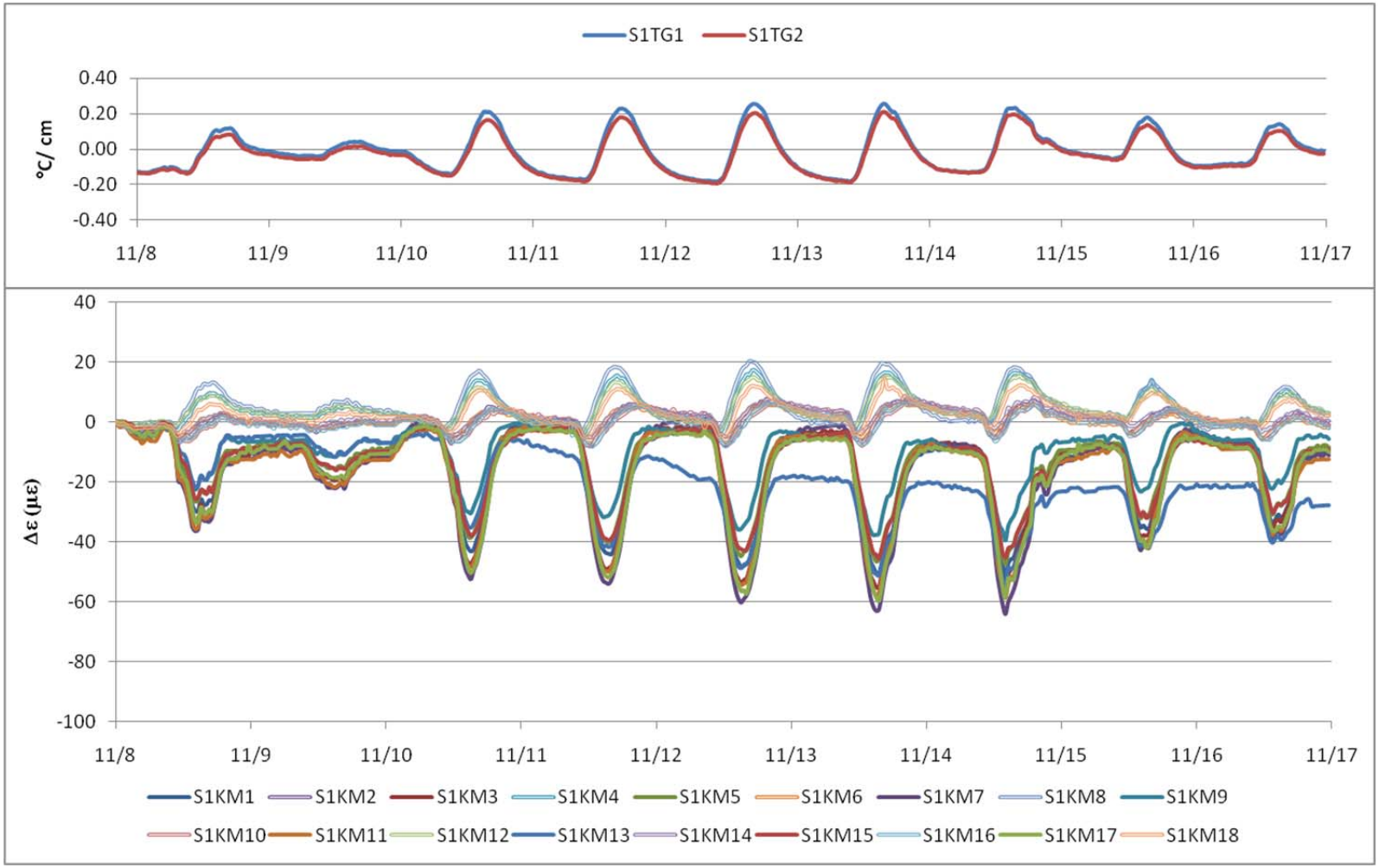

Section 1 - Load-related strains – Fall 2010 (11/8 – 11/16) (1 C°/cm = 4.6°F/in)

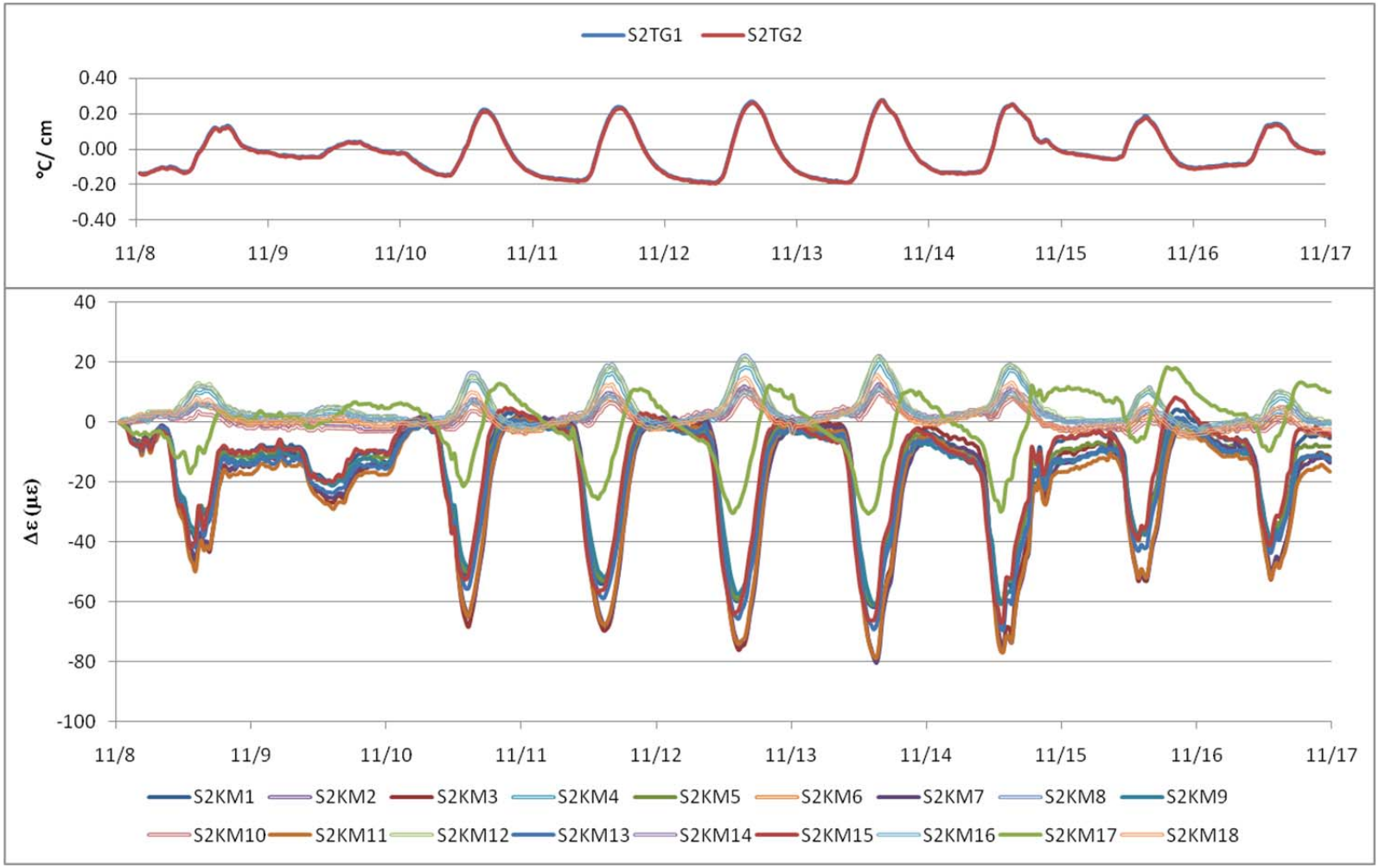

Section 2 - Load-related strains – Fall 2010 (11/8 – 11/16) (1 C°/cm = 4.6°F/in)

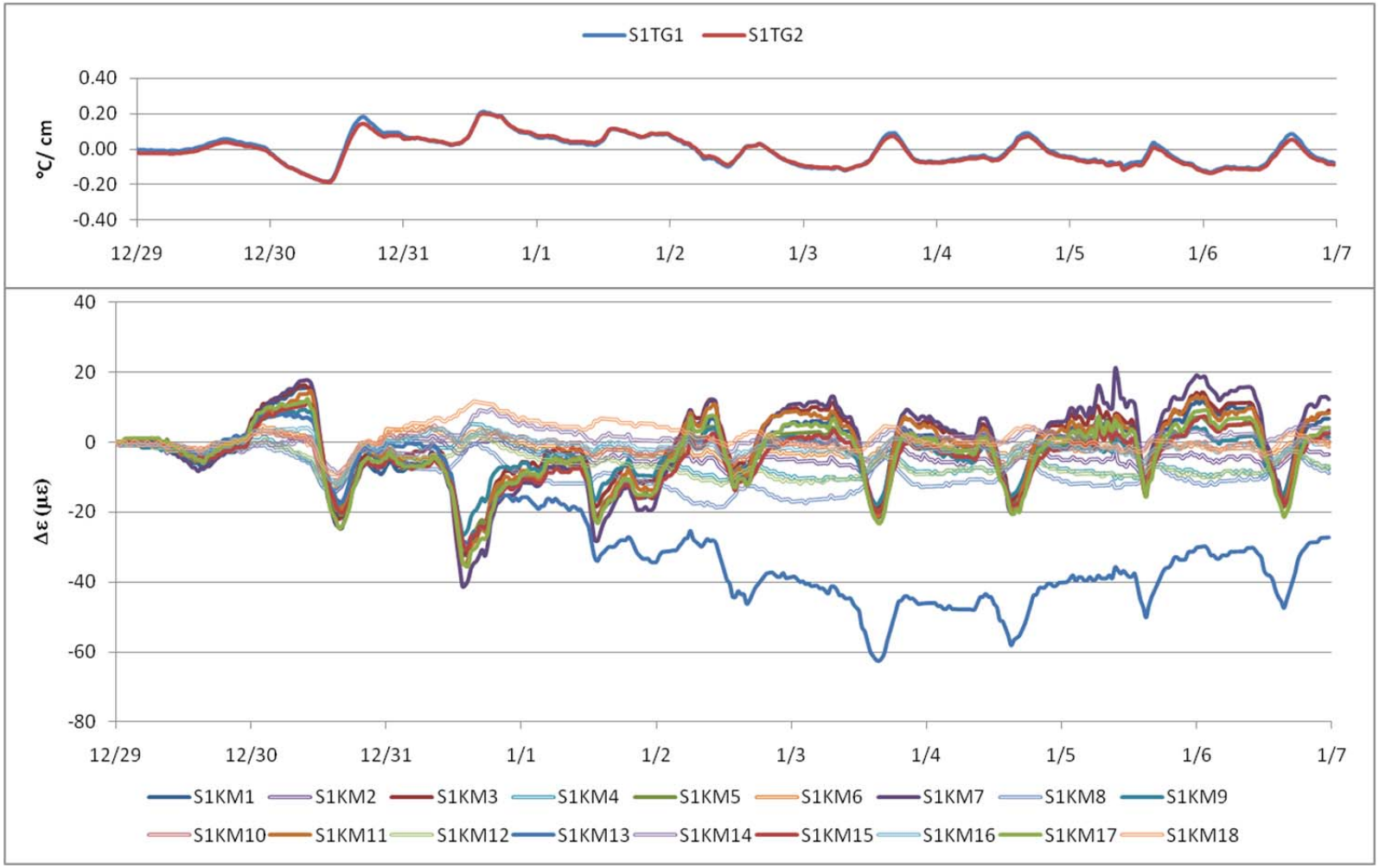

Section 1 - Load-related strains – Winter 2010-11 (12/29 – 1/6) (1 C°/cm = 4.6°F/in)

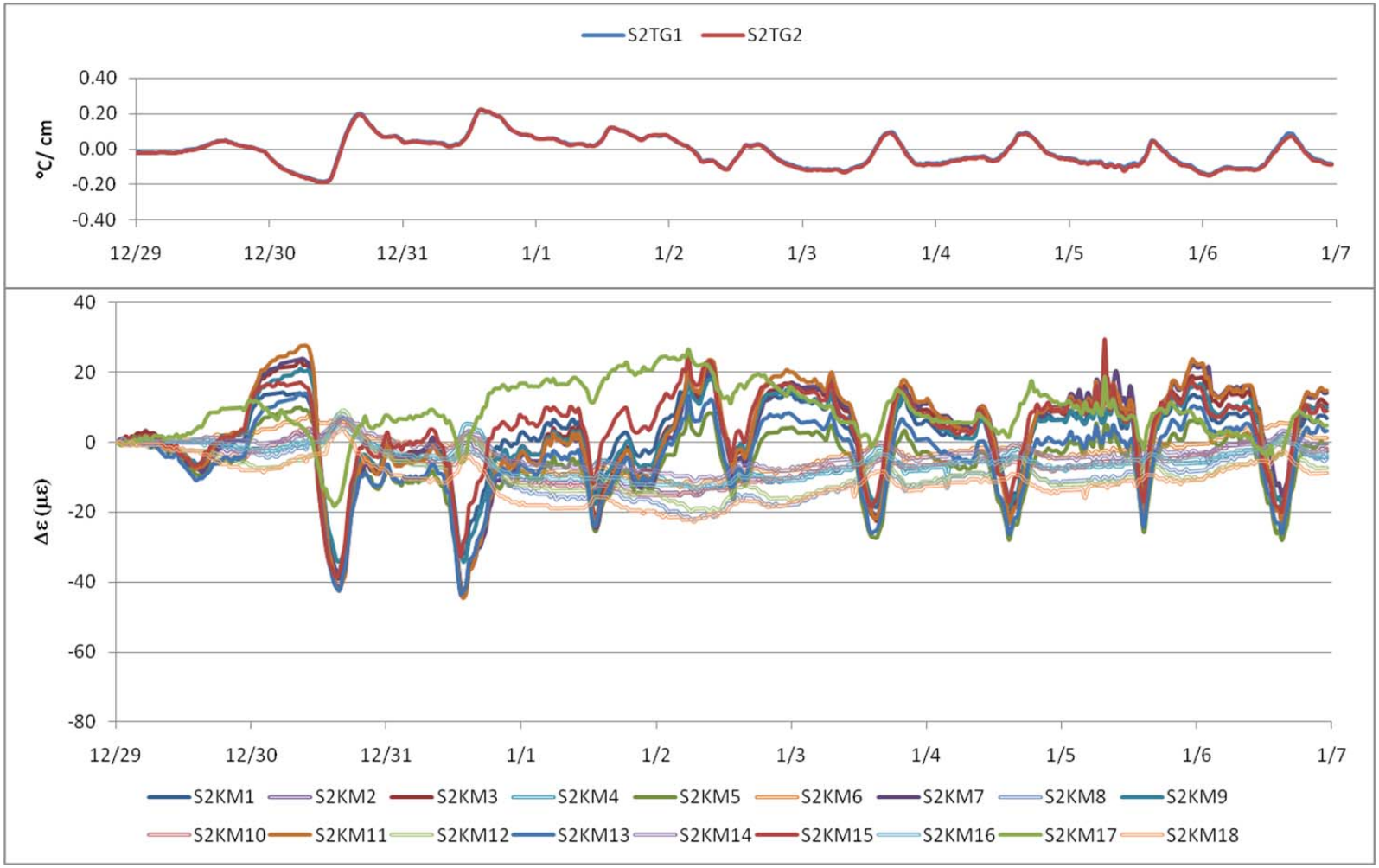

Section 2 - Load-related strains – Winter 2010-11 (12/29 – 1/6) (1 C°/cm = 4.6°F/in)

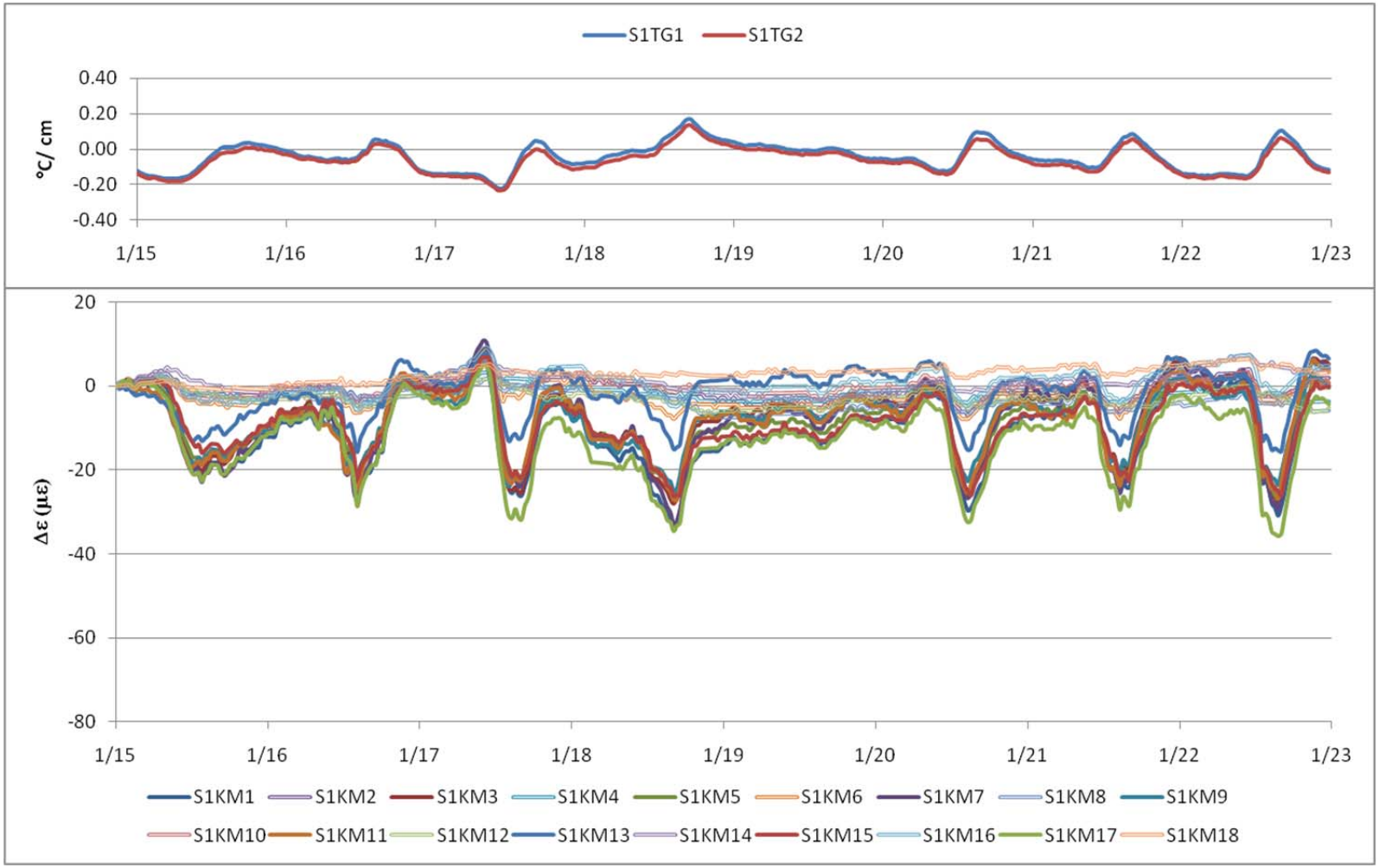

Section 1 - Load-related strains – Winter 2010-11 (1/15 – 1/22) (1 C°/cm = 4.6°F/in)

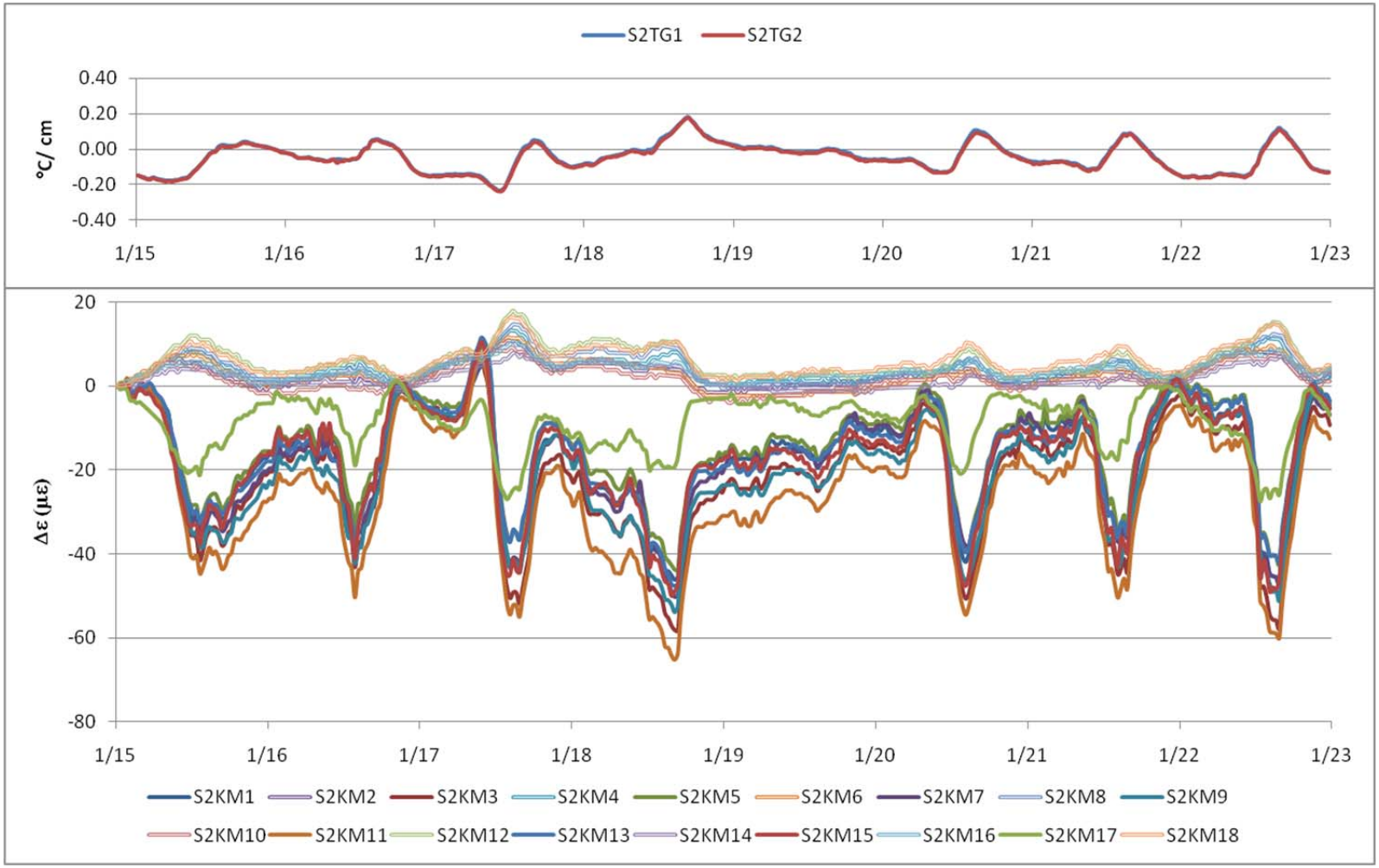

Section 2 - Load-related strains – Winter 2010-11 (1/15 – 1/22) (1 C°/cm = 4.6°F/in)

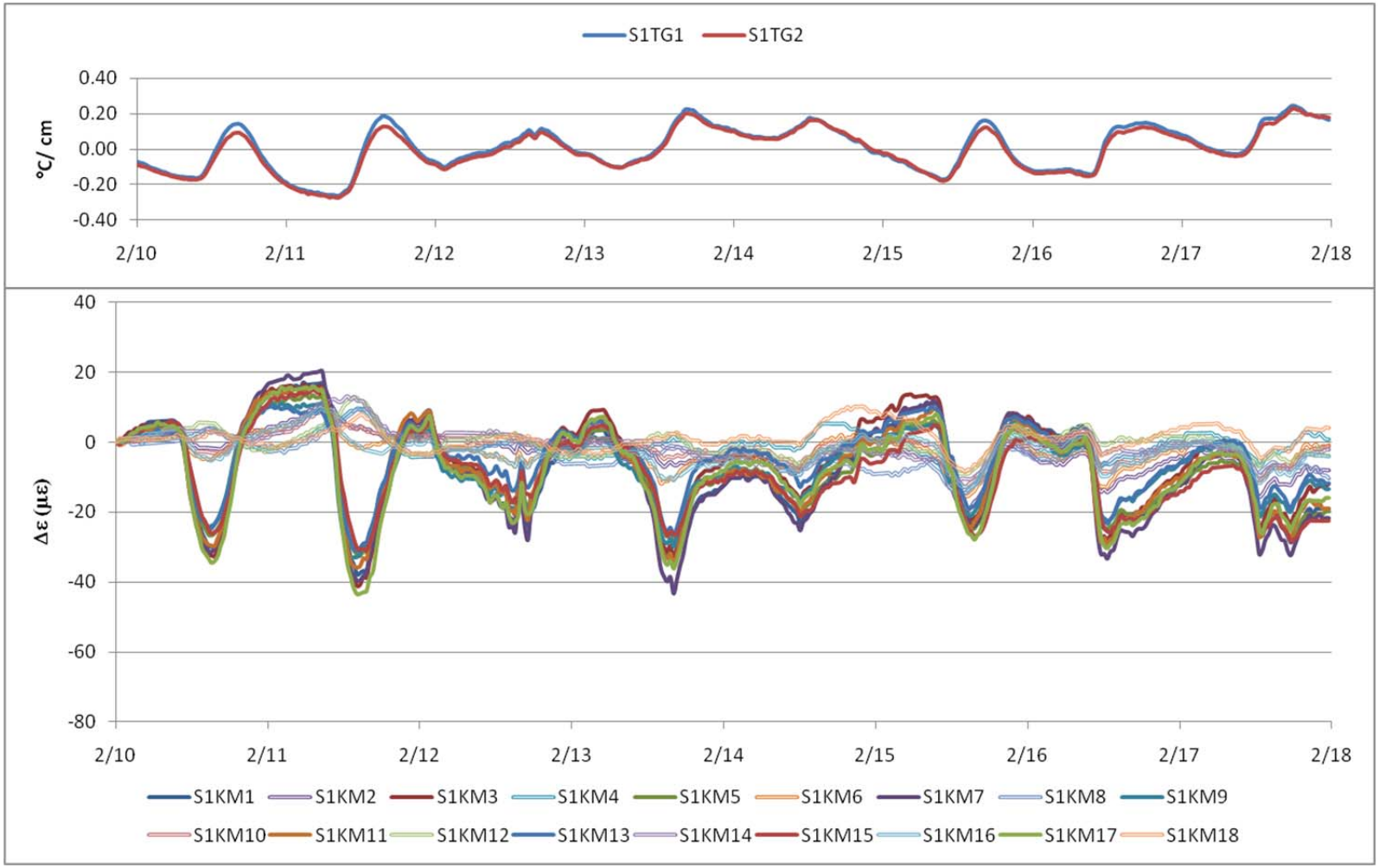

Section 1 - Load-related strains – Winter 2010-11 (2/10 – 2/17) (1 C°/cm = 4.6°F/in)

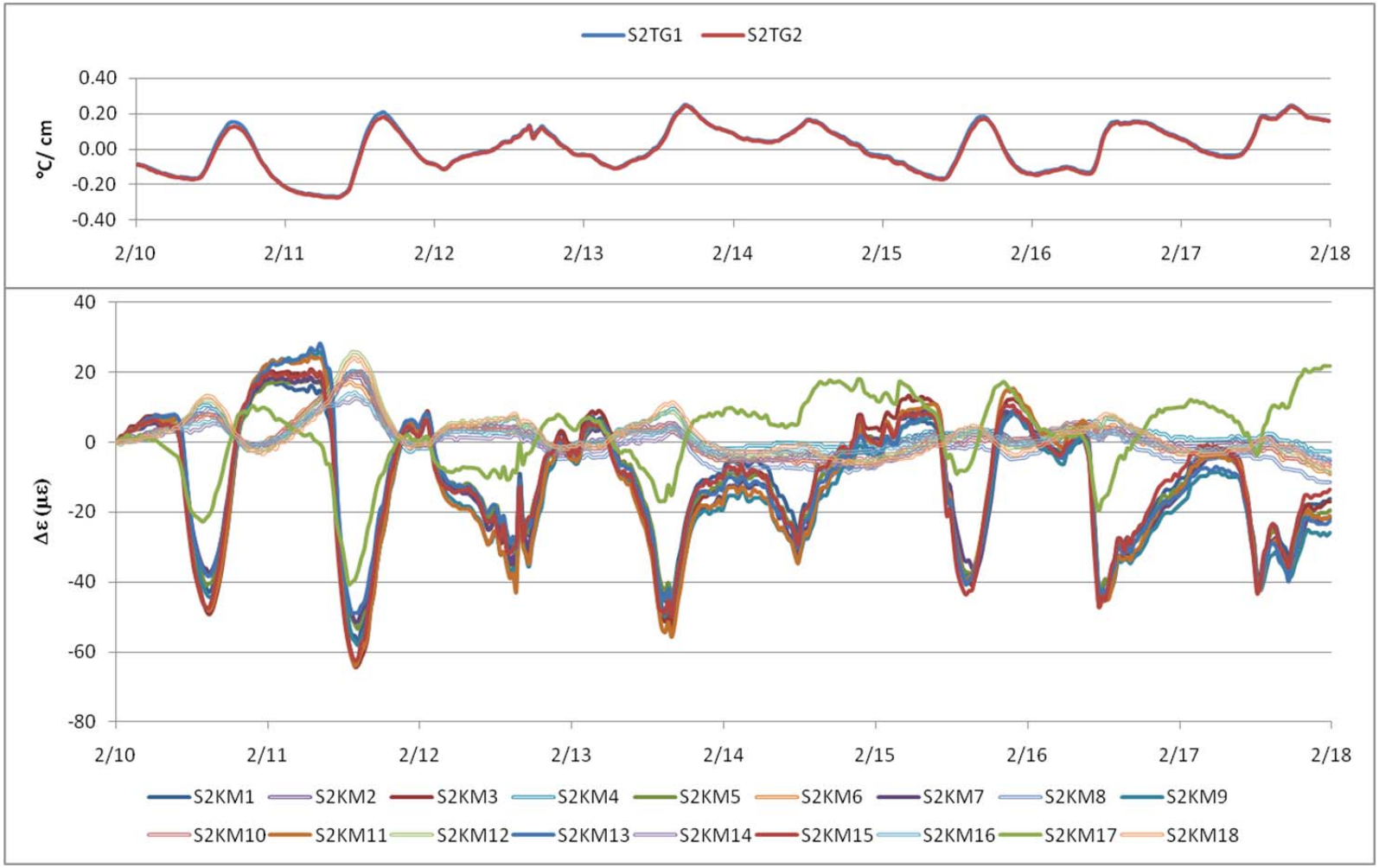

Section 2 - Load-related strains – Winter 2010-11 (2/10 – 2/17) (1 C°/cm = 4.6°F/in)

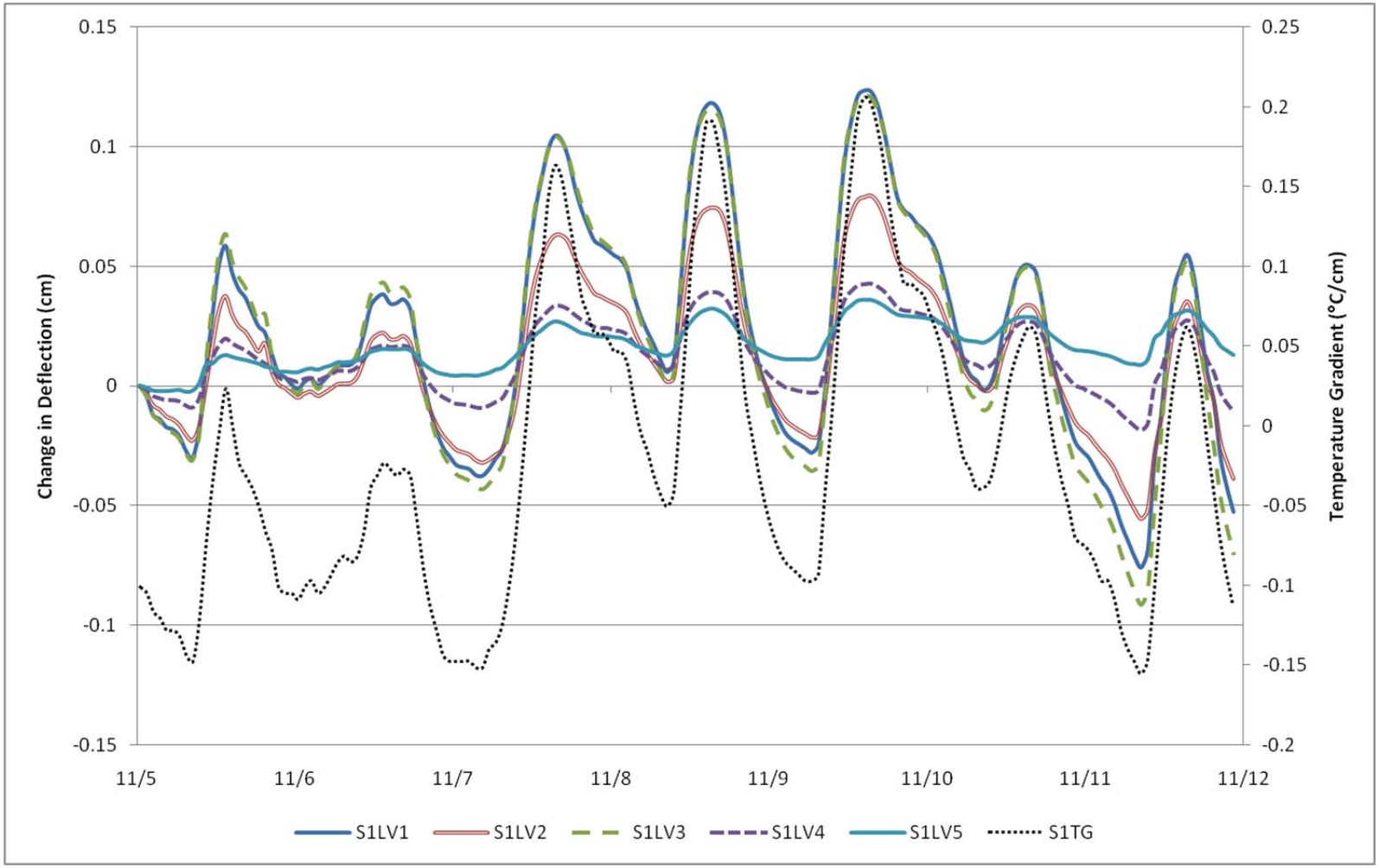

Section 1 – Change in Deflections – Fall 2009 (11/5 – 11/11) (2.54 cm = 1 in; 1 C°/cm = 4.6°F/in)

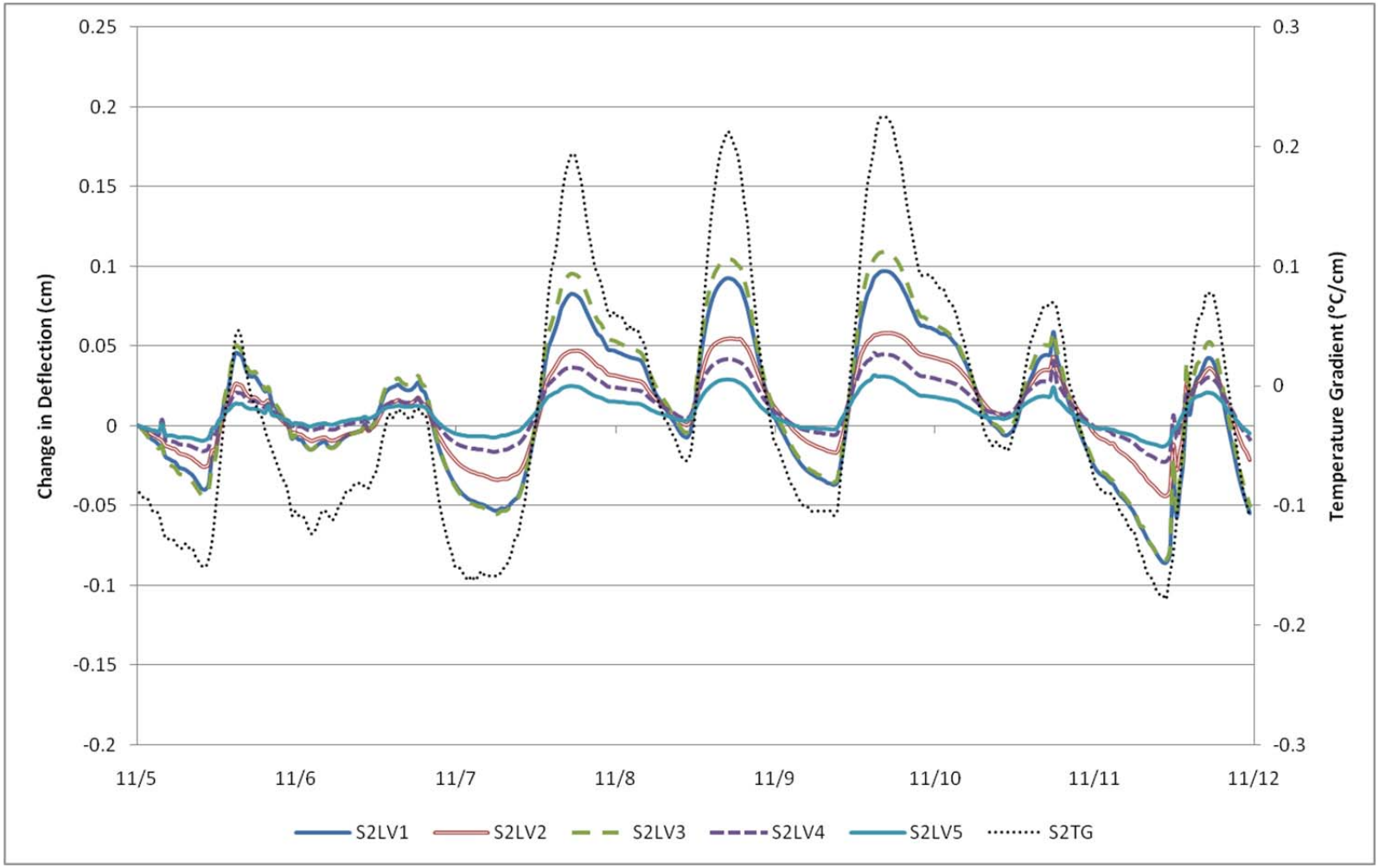

Section 2 – Change in Deflections – Fall 2009 (11/5 – 11/11) (2.54 cm = 1 in; 1 C°/cm = 4.6°F/in)

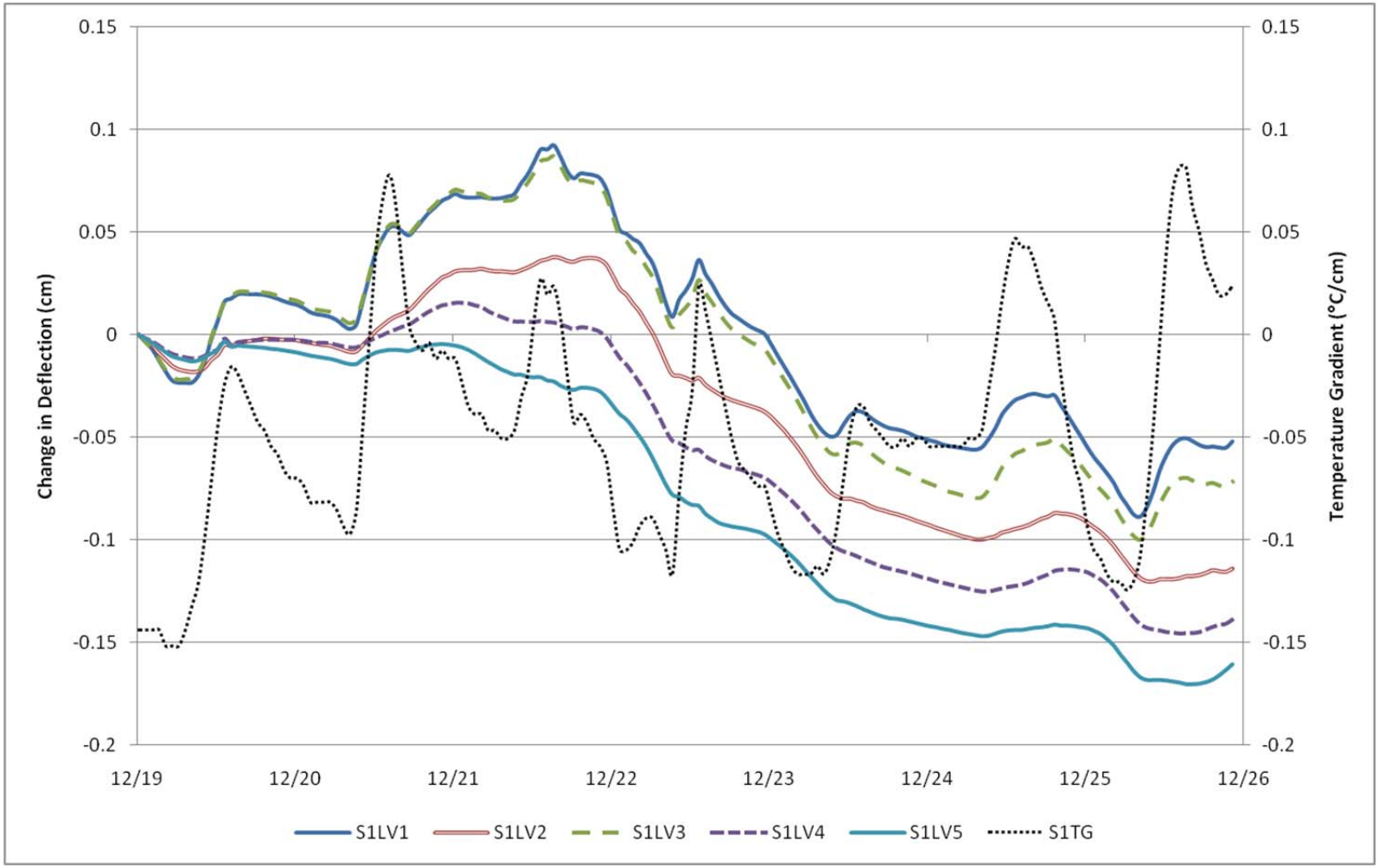

Section 1 – Change in Deflections – Winter 2009/10 (12-19 – 12/25) (2.54 cm = 1 in; 1 C°/cm = 4.6°F/in)

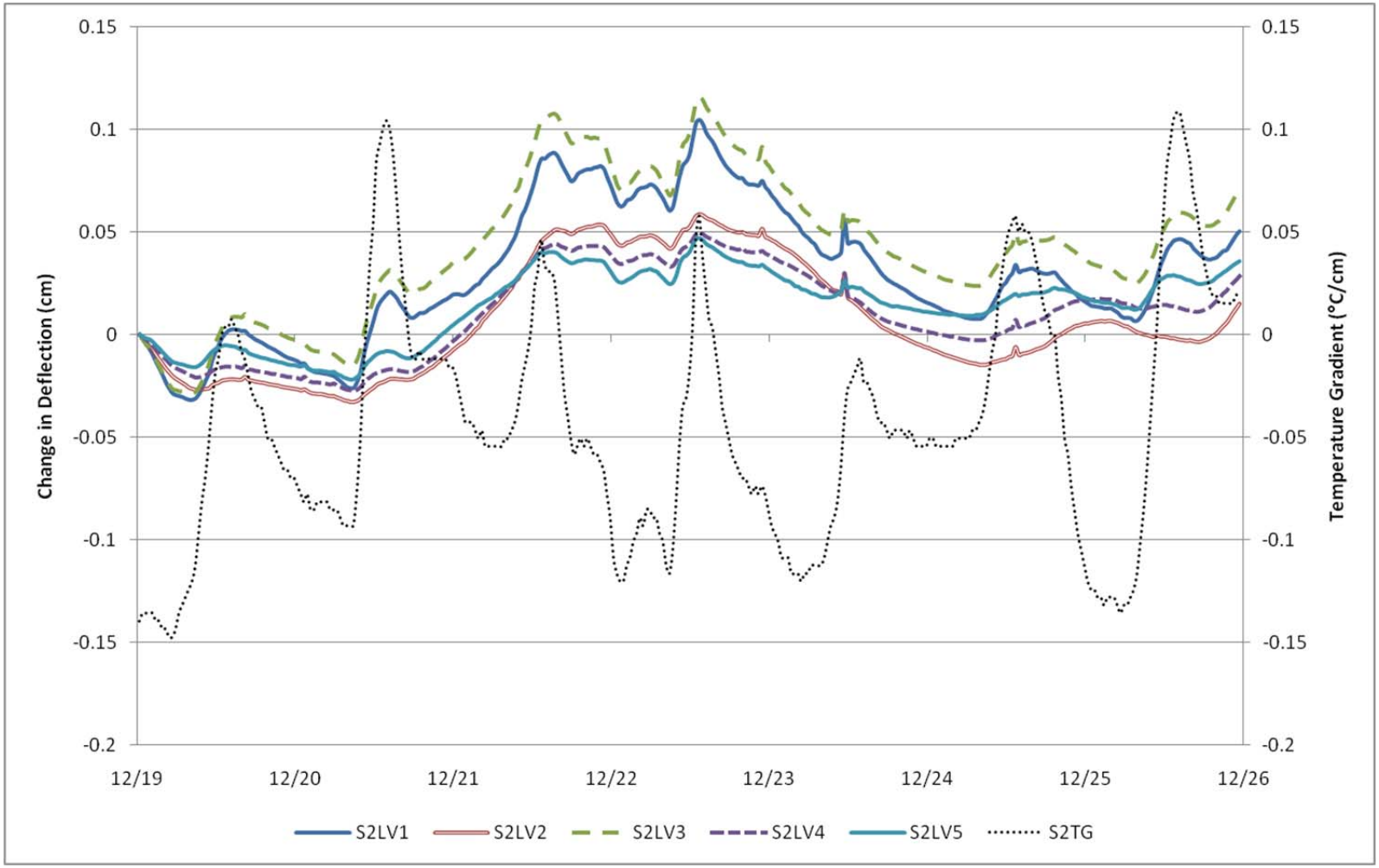

Section 2 – Change in Deflections – Winter 2009/10 (12-19 – 12/25) (2.54 cm = 1 in; 1 C°/cm = 4.6°F/in)

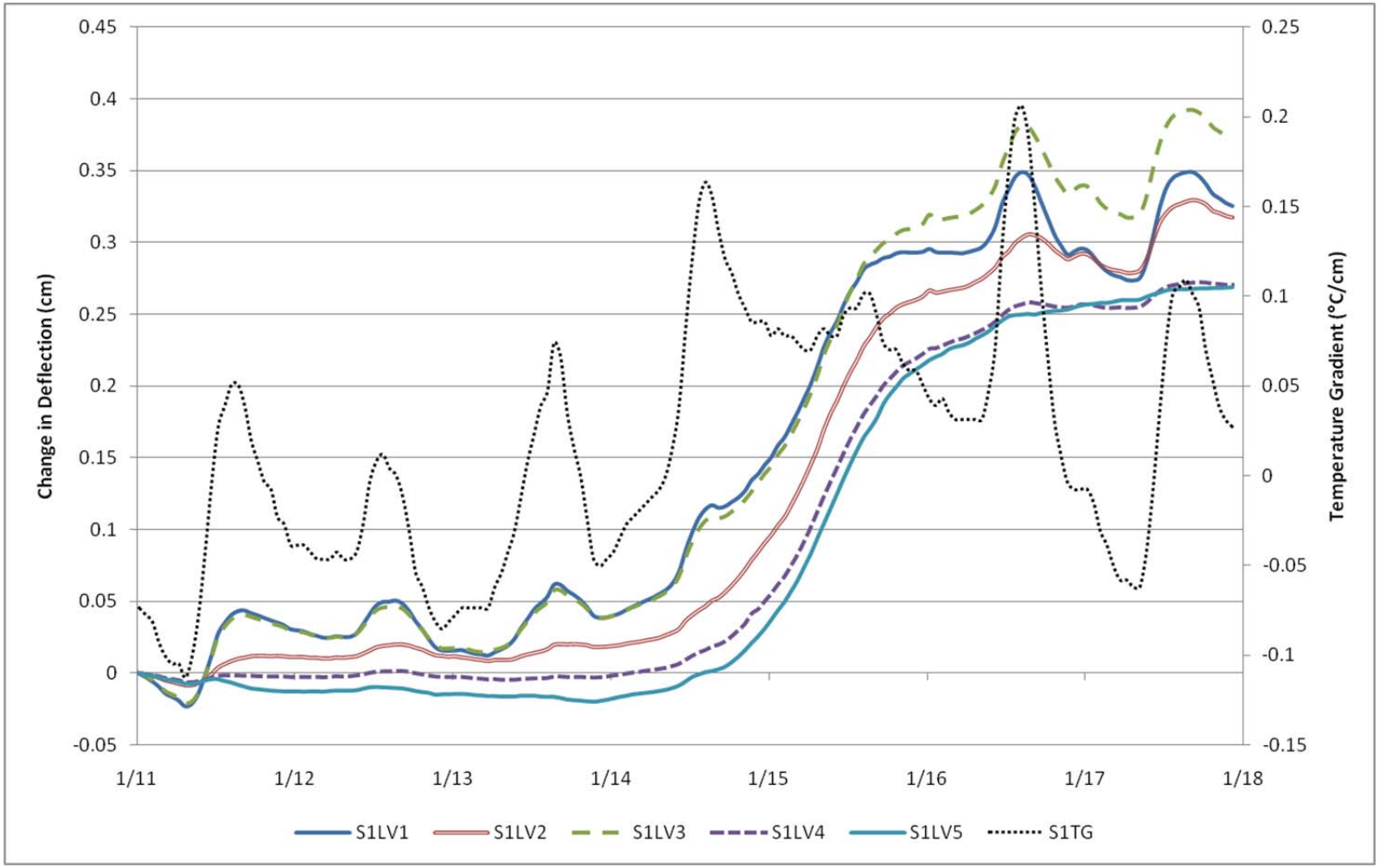

Section 1 – Change in Deflections – Winter 2009/10 (1/11 – 1/17) (2.54 cm = 1 in; 1 C°/cm = 4.6°F/in)

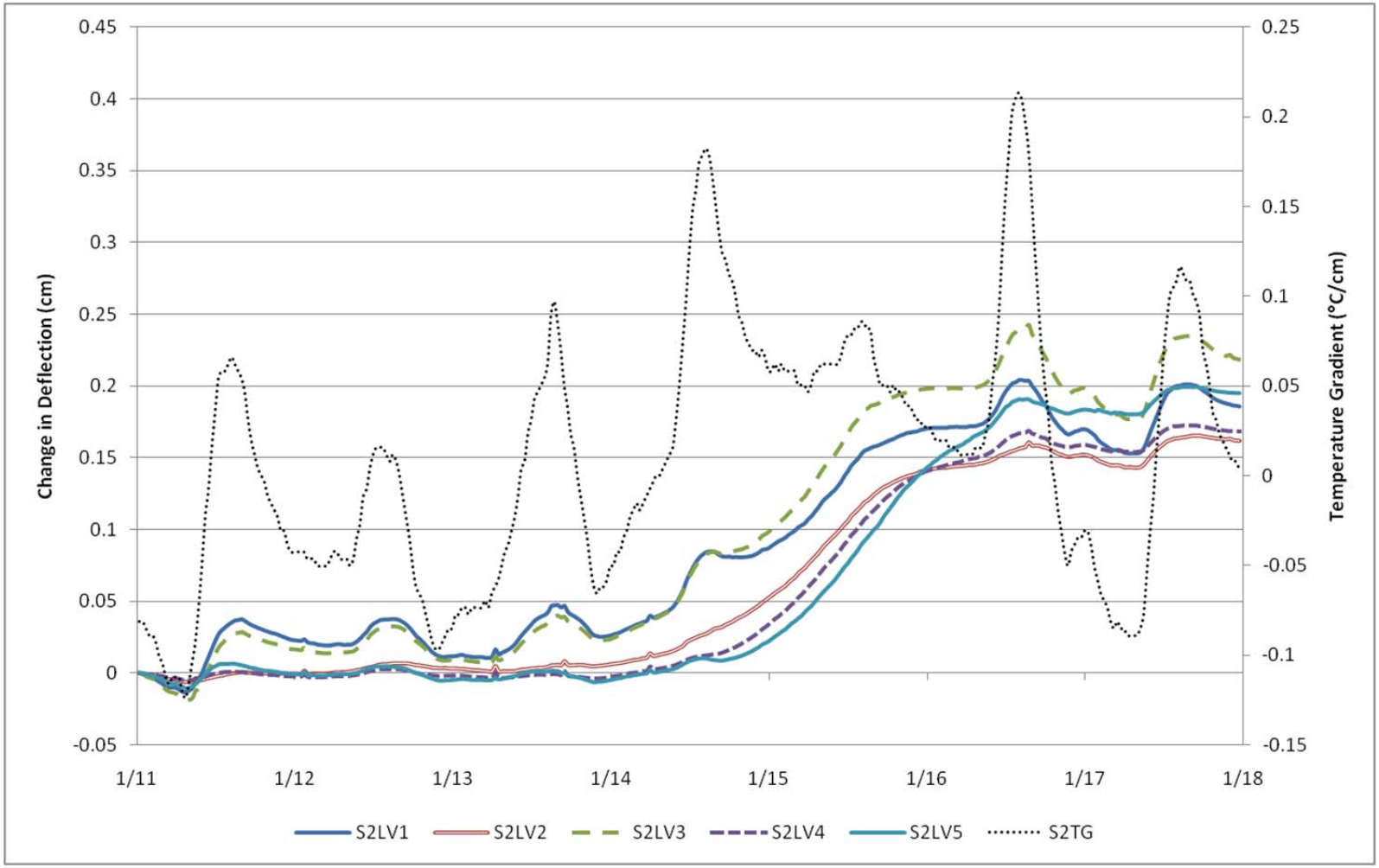

Section 2 – Change in Deflections – Winter 2009/10 (1/11 – 1/17) (2.54 cm = 1 in; 1 C°/cm = 4.6°F/in)

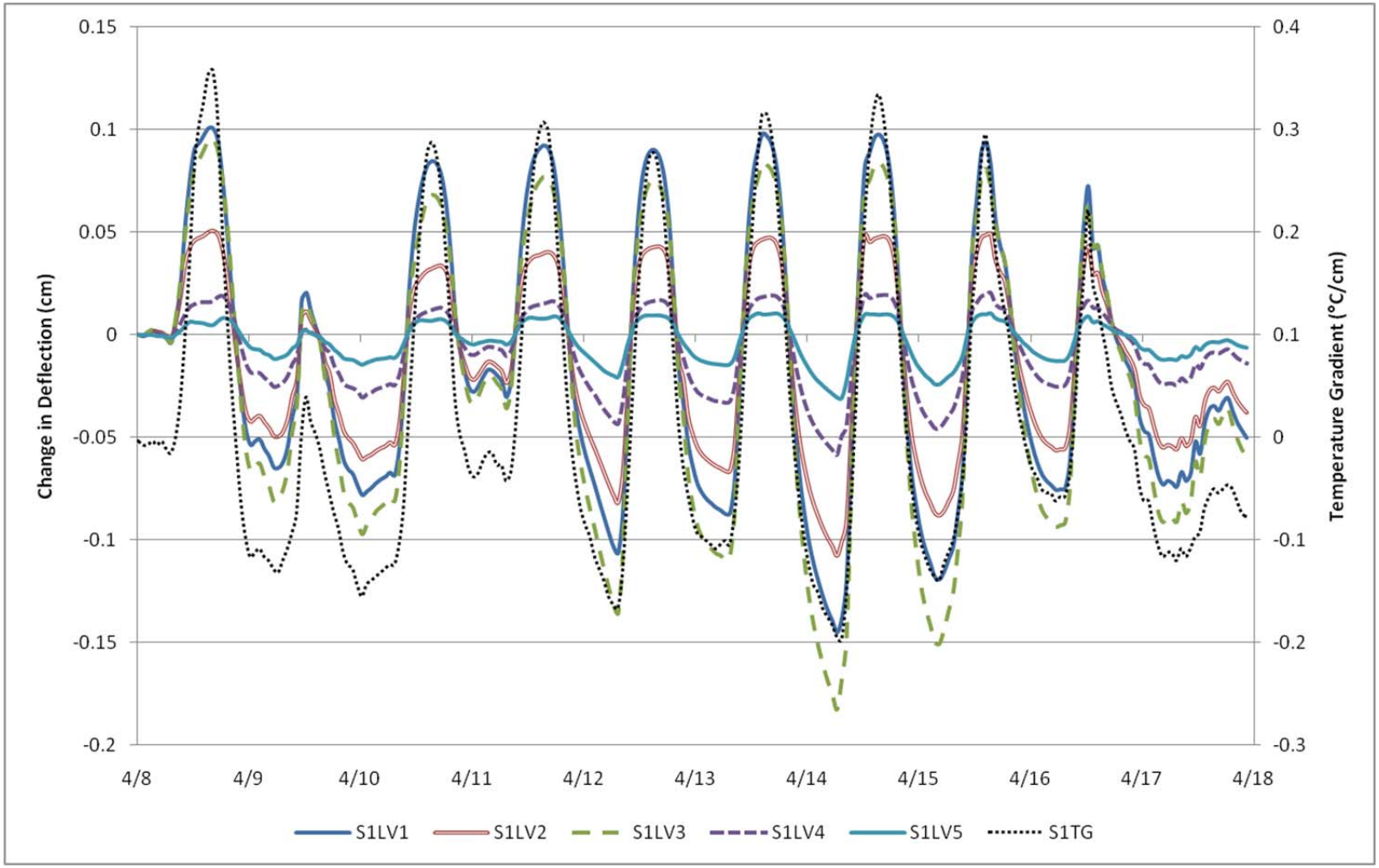

Section 1 – Change in Deflections – Spring 2010 (4/8 – 4/14) (2.54 cm = 1 in; 1 C°/cm = 4.6°F/in)

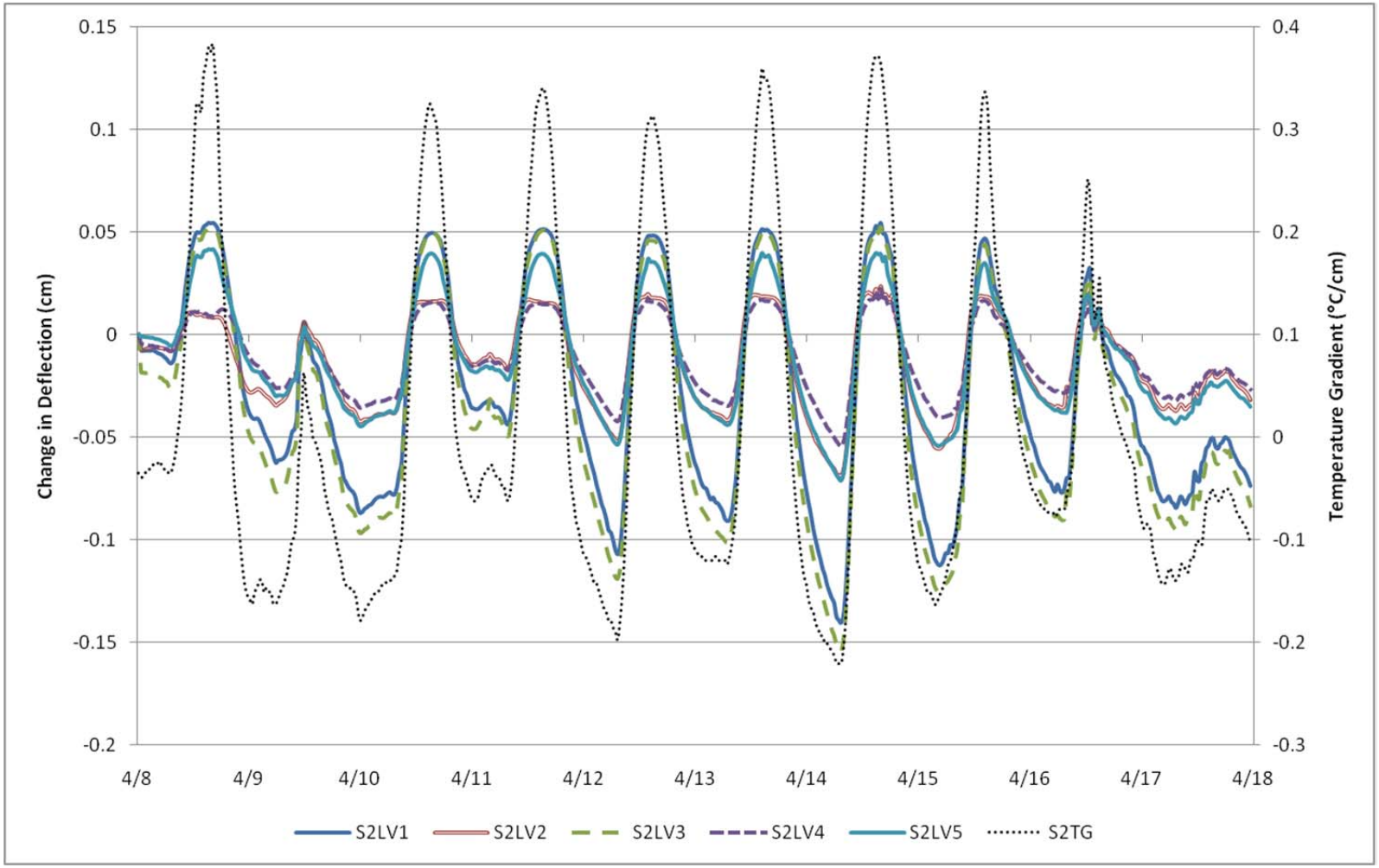

Section 2 – Change in Deflections – Spring 2010 (4/8 – 4/14) (2.54 cm = 1 in; 1 C°/cm = 4.6°F/in)

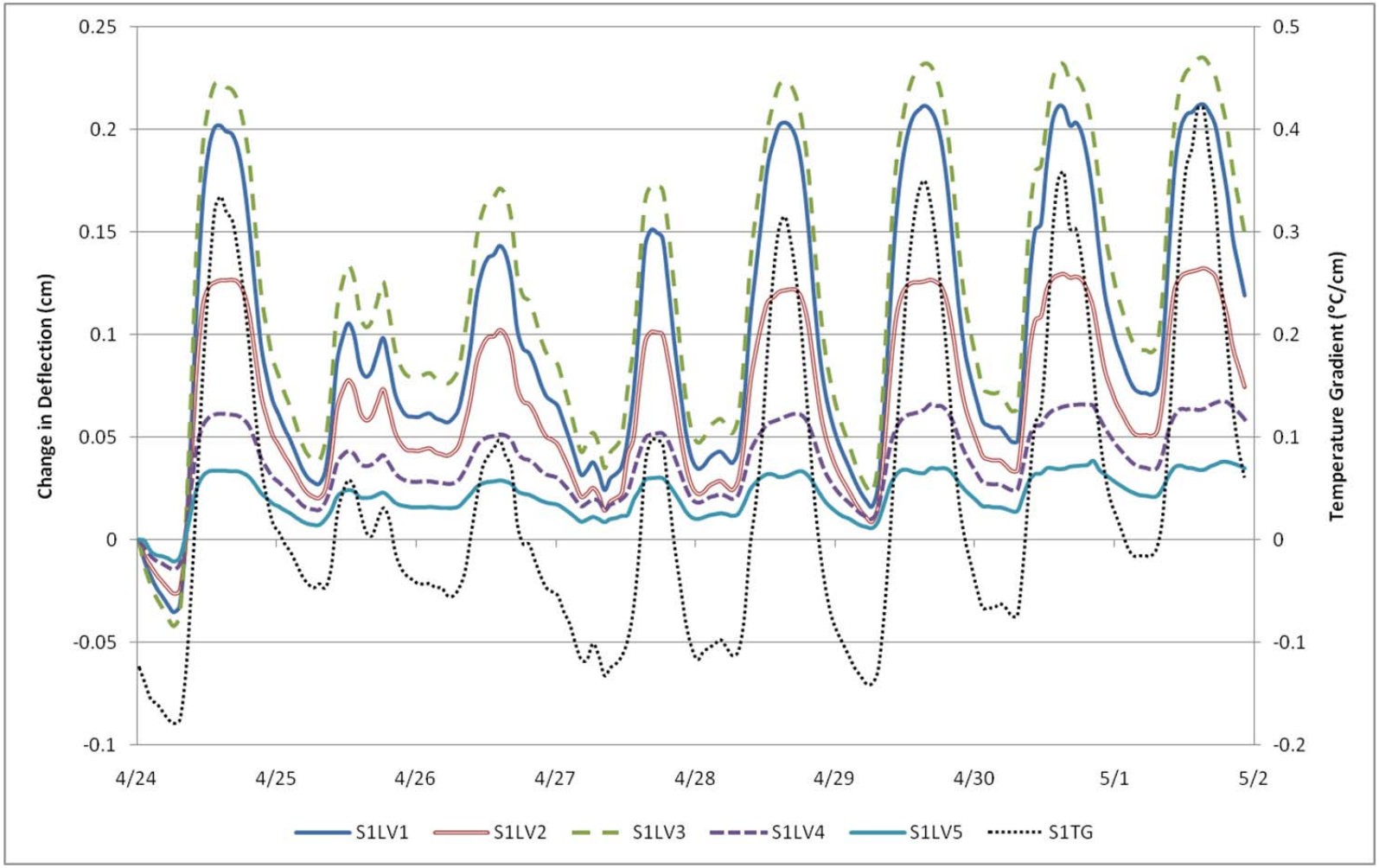

Section 1 – Change in Deflections – Spring 2010 (4/24 – 5/1) (2.54 cm = 1 in; 1 C°/cm = 4.6°F/in)

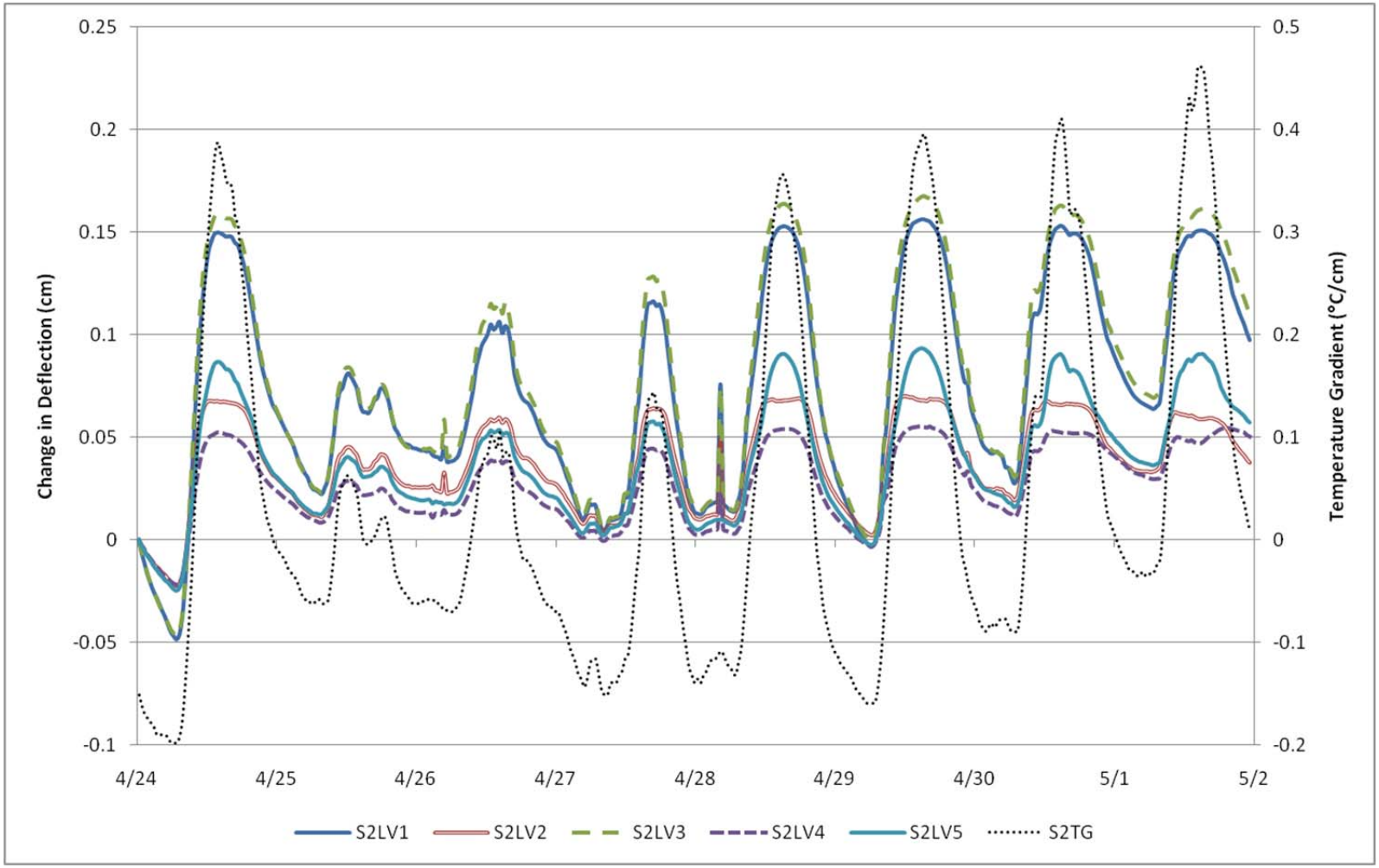

Section 2 – Change in Deflections – Spring 2010 (4/24 – 5/1) (2.54 cm = 1 in; 1 C°/cm = 4.6°F/in)

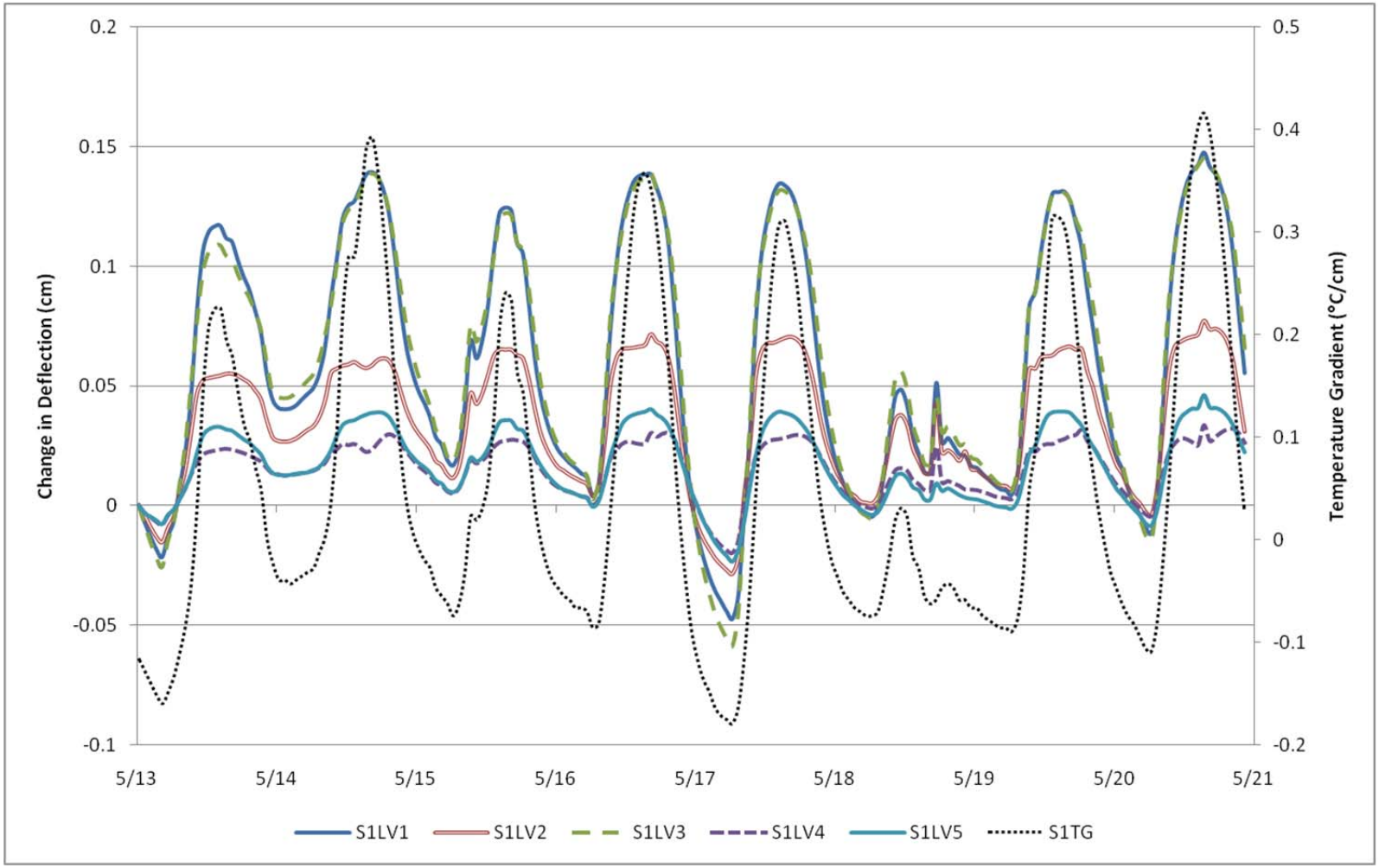

Section 1 – Change in Deflections – Spring 2010 (5/13 – 5/20) (2.54 cm = 1 in; 1 C°/cm = 4.6°F/in)

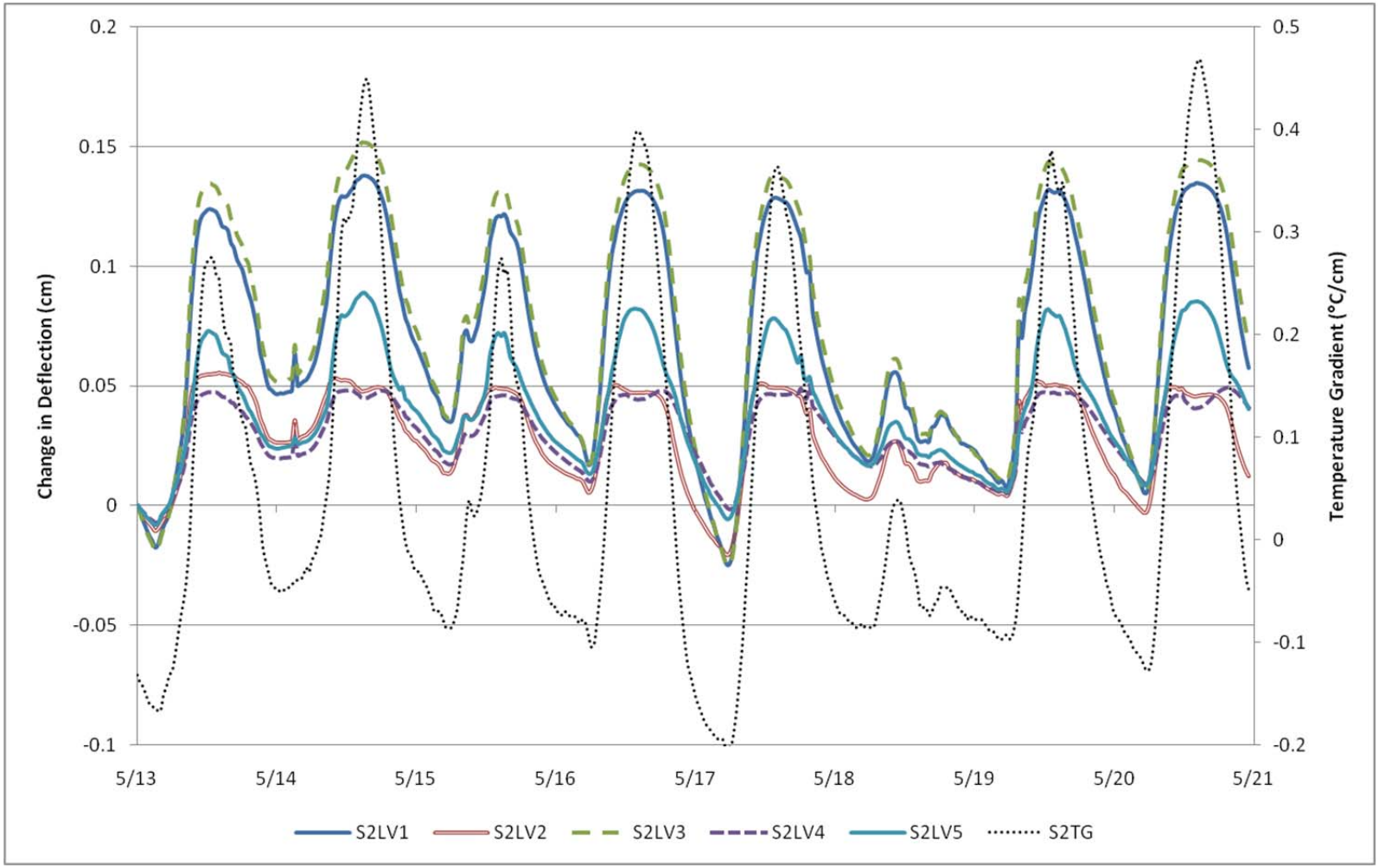

Section 2 – Change in Deflections – Spring 2010 (5/13 – 5/20) (2.54 cm = 1 in; 1 C°/cm = 4.6°F/in)

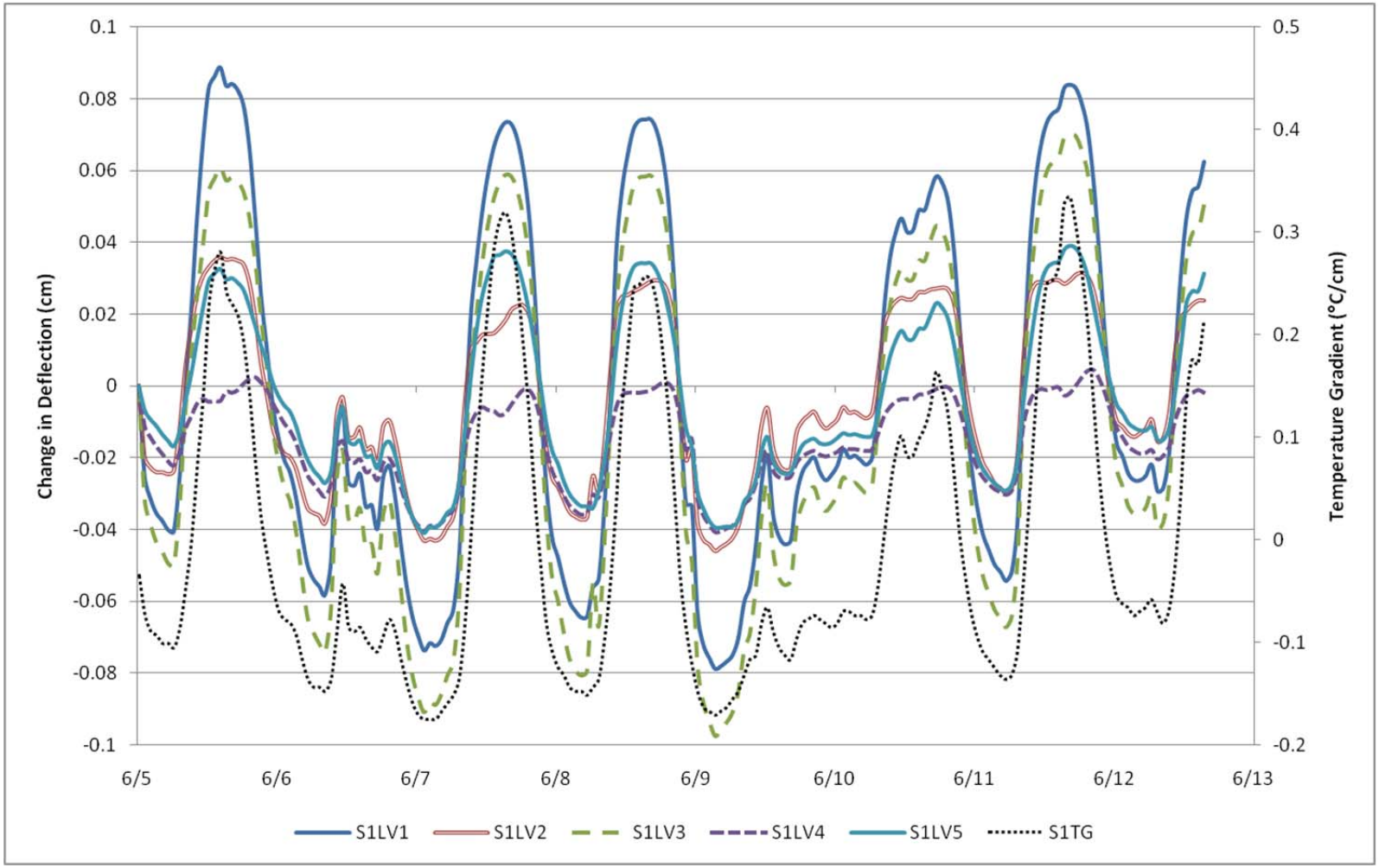

Section 1 – Change in Deflections – Summer 2010 (6/5 – 6/12) (2.54 cm = 1 in; 1 C°/cm = 4.6°F/in)

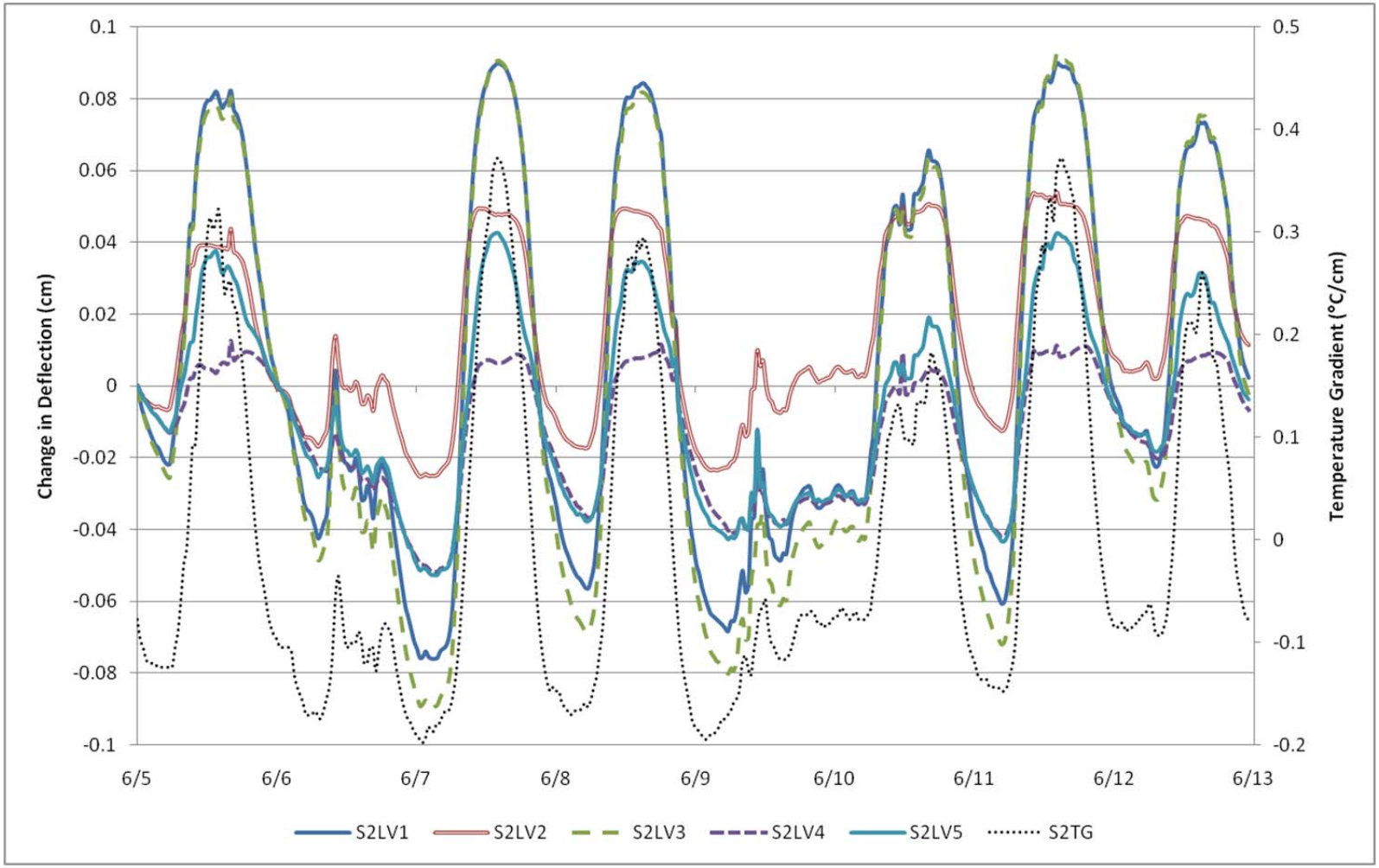

Section 2 – Change in Deflections – Summer 2010 (6/5 – 6/12) (2.54 cm = 1 in; 1 C°/cm = 4.6°F/in)

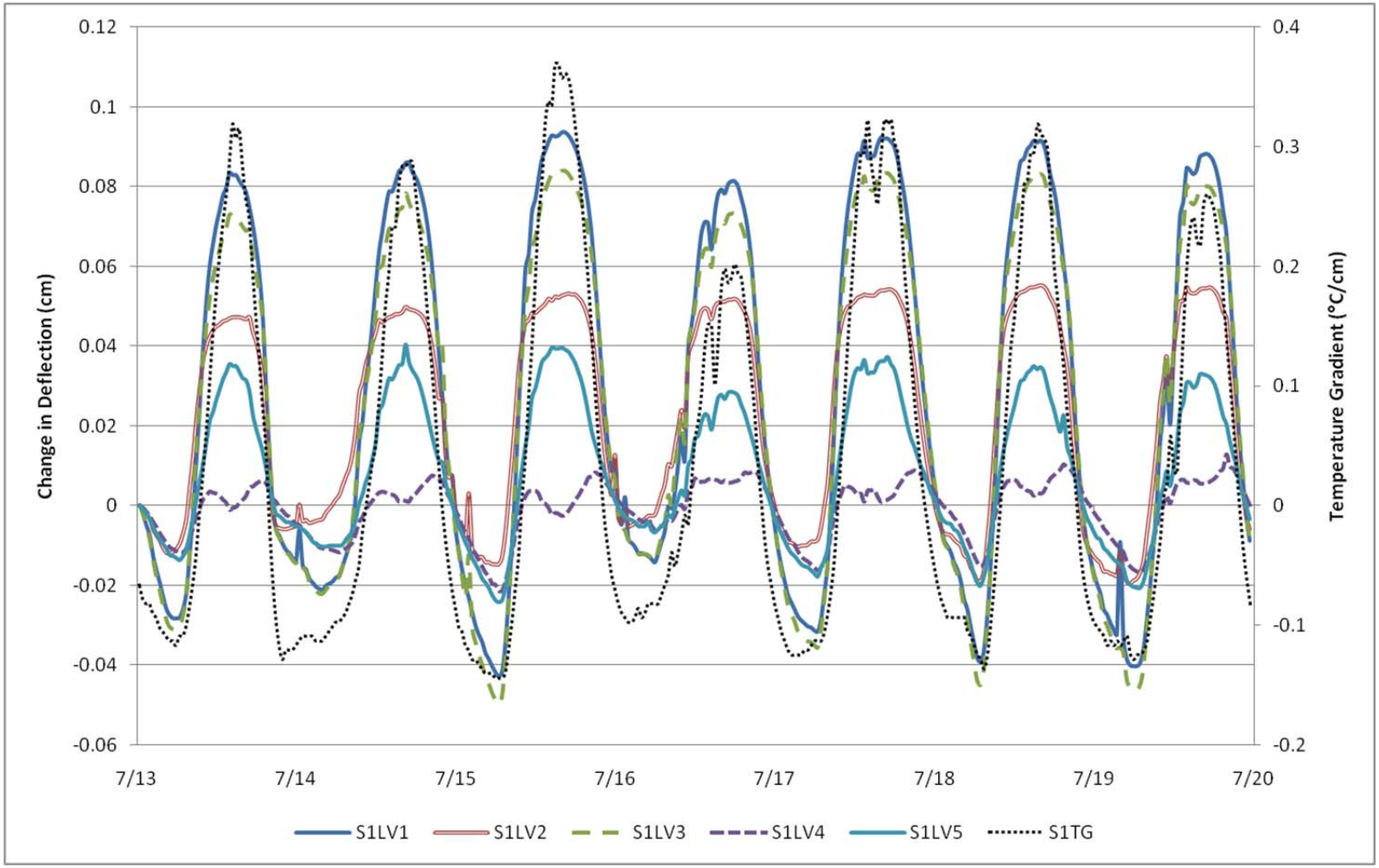

Section 1 – Change in Deflections – Summer 2010 (7/13 – 7/20) (2.54 cm = 1 in; 1 C°/cm = 4.6°F/in)

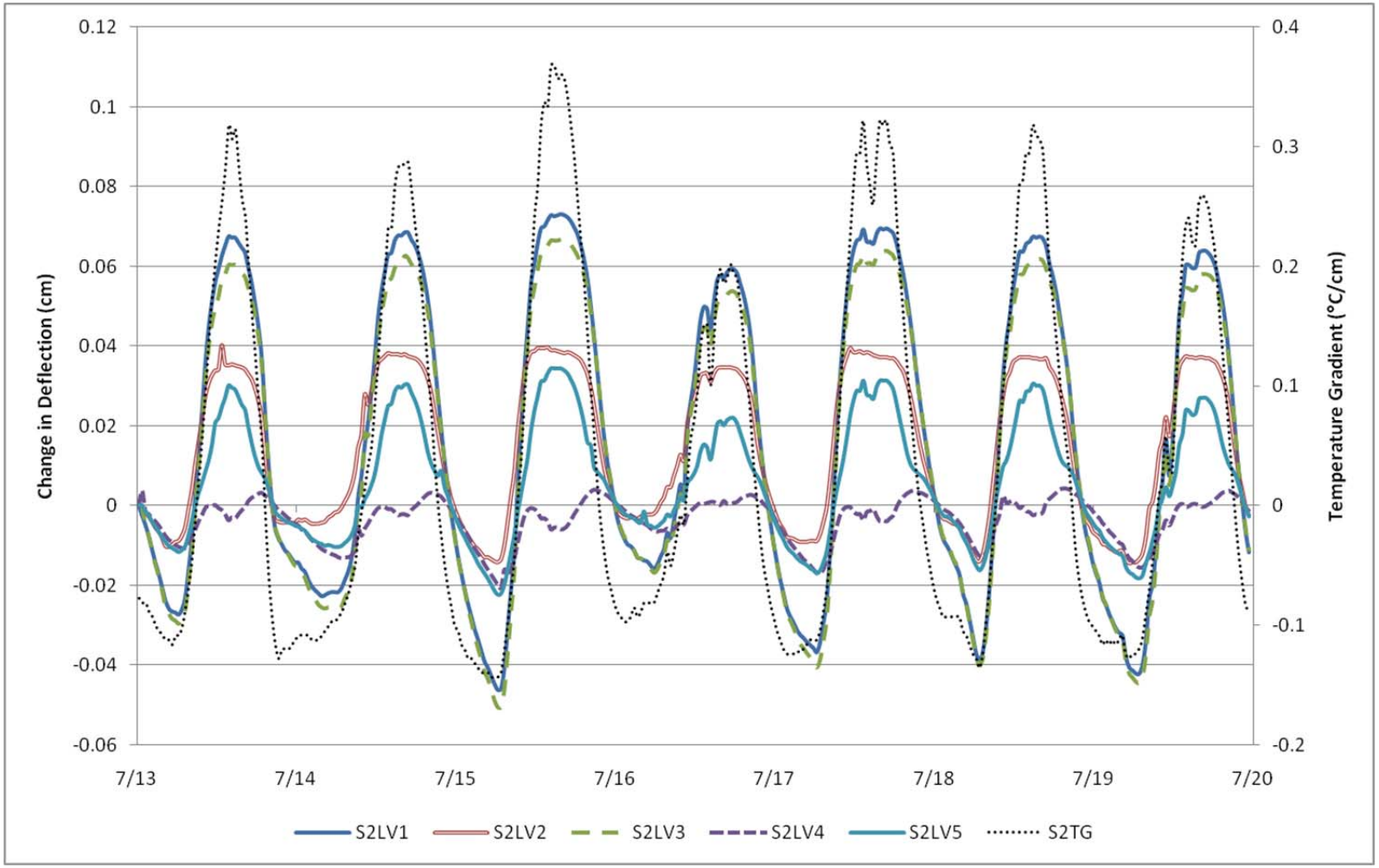

Section 2 – Change in Deflections – Summer 2010 (7/13 – 7/20) (2.54 cm = 1 in; 1 C°/cm = 4.6°F/in)

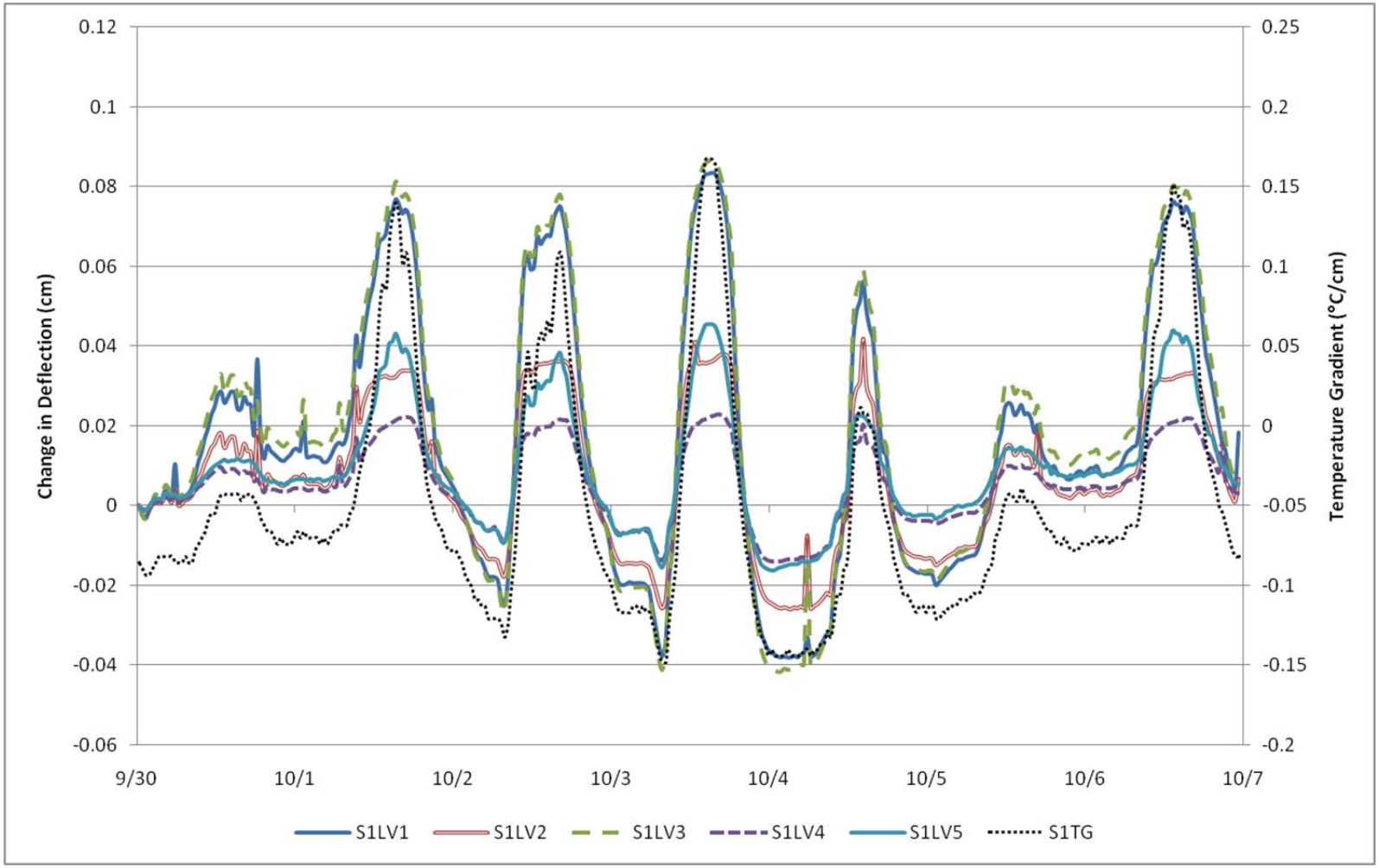

Section 1 – Change in Deflections – Fall 2010 (9/30 – 10/6) (2.54 cm = 1 in; 1 C°/cm = 4.6°F/in)

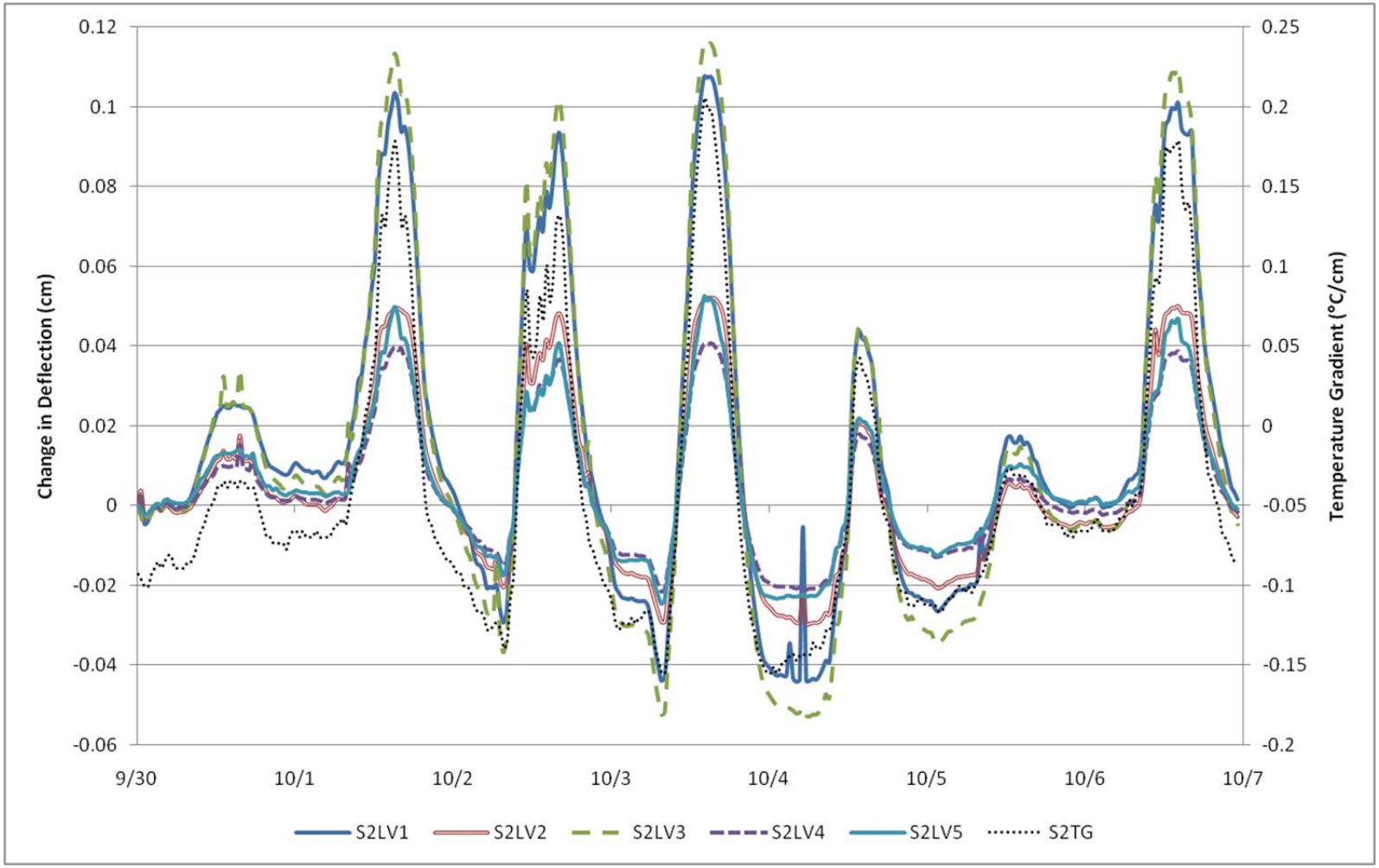

Section 2 – Change in Deflections – Fall 2010 (9/30 – 10/6) (2.54 cm = 1 in; 1 C°/cm = 4.6°F/in)

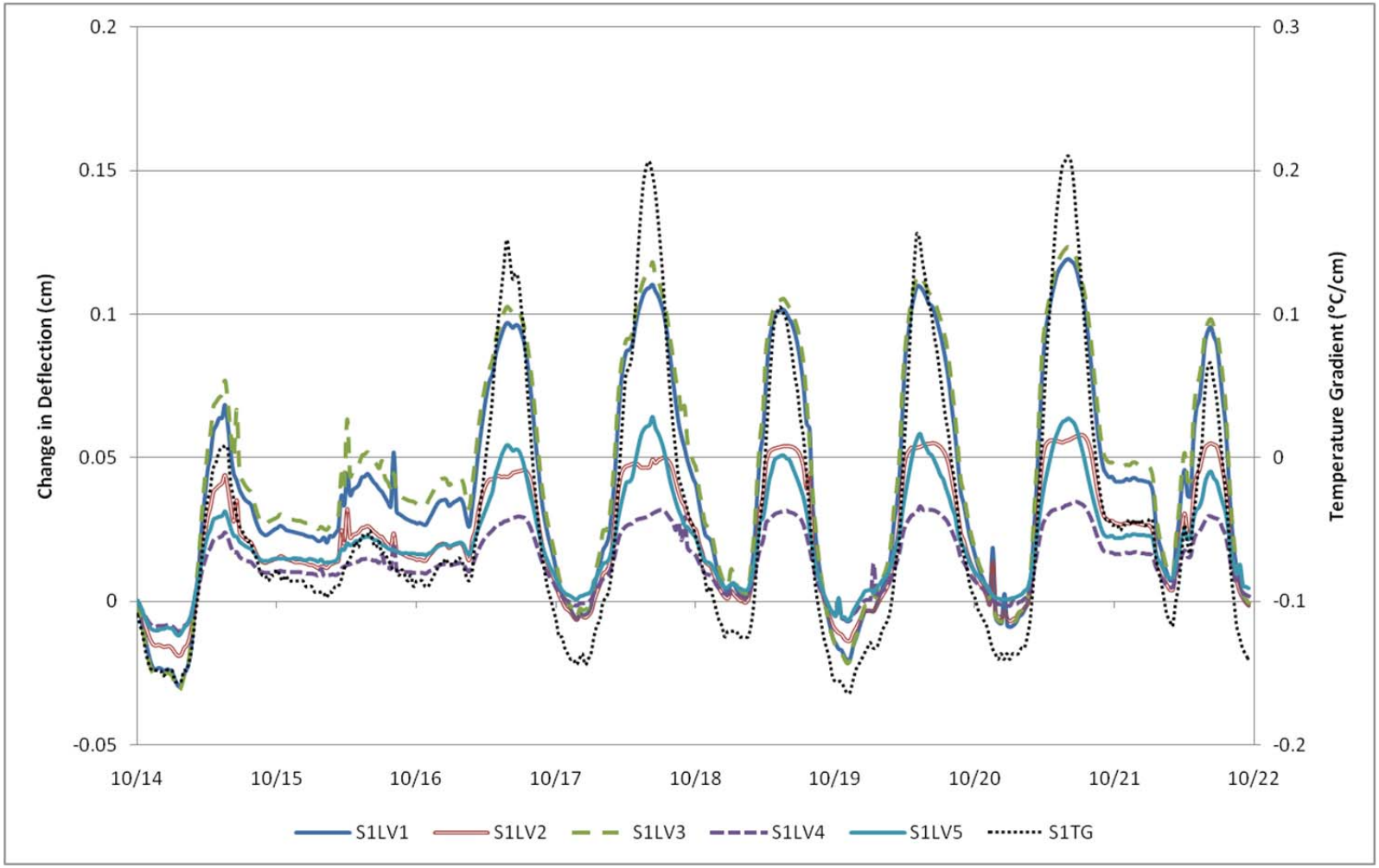

Section 1 – Change in Deflections – Fall 2010 (10/14 – 10/21) (2.54 cm = 1 in; 1 C°/cm = 4.6°F/in)

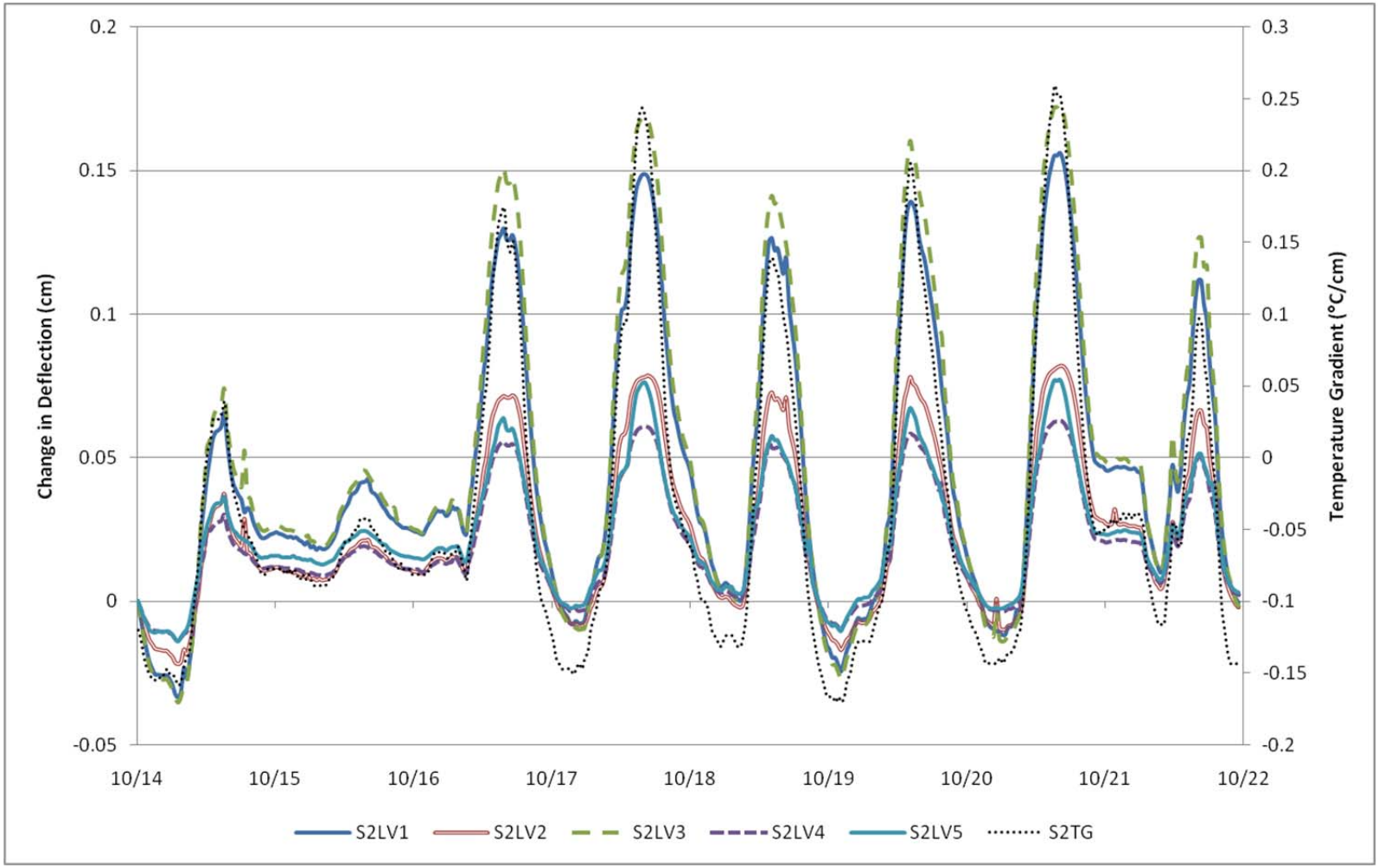

Section 2 – Change in Deflections – Fall 2010 (10/14 – 10/21) (2.54 cm = 1 in; 1 C°/cm = 4.6°F/in)

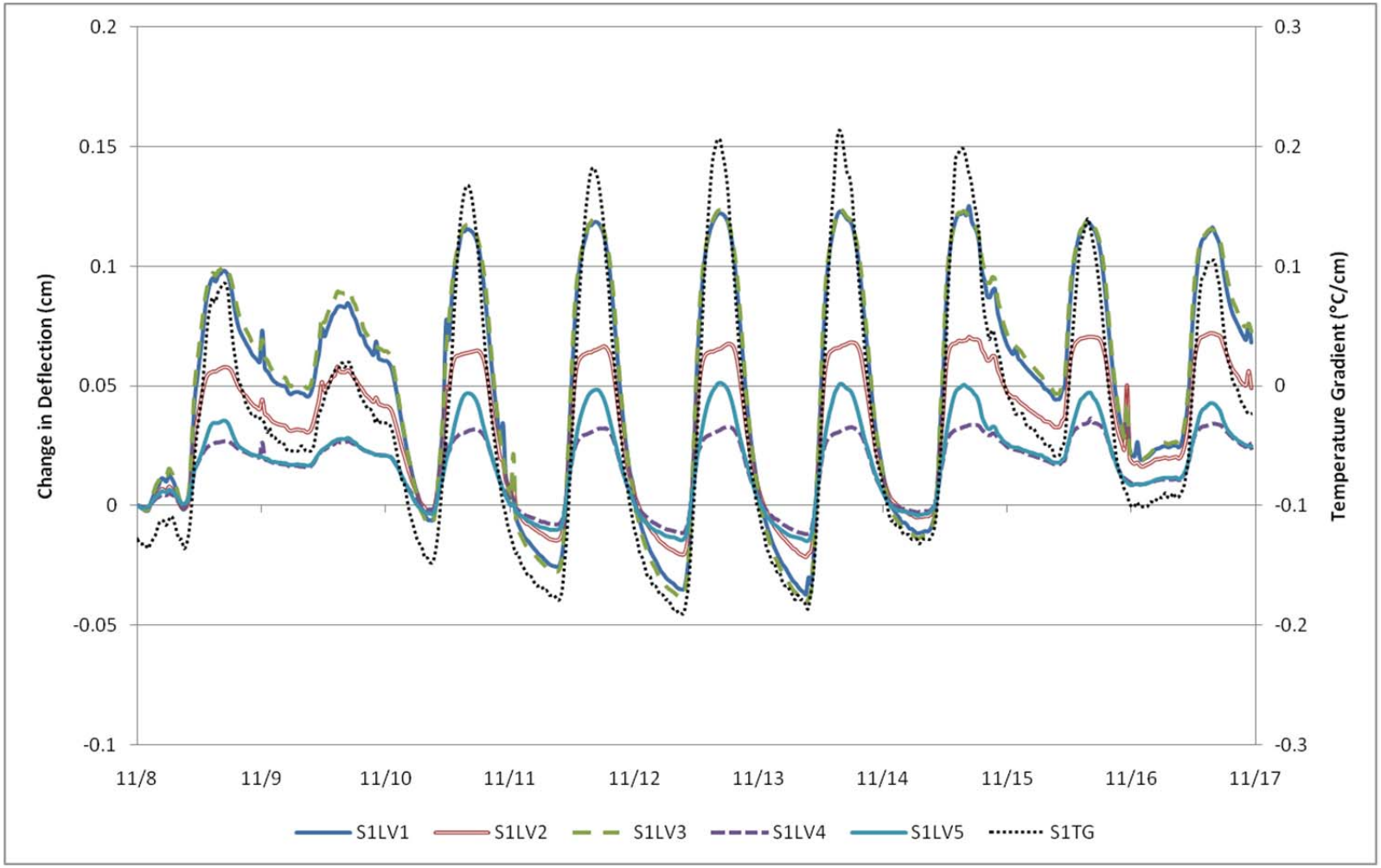

Section 1 – Change in Deflections – Fall 2010 (11/8 – 11/16) (2.54 cm = 1 in; 1 C°/cm = 4.6°F/in)

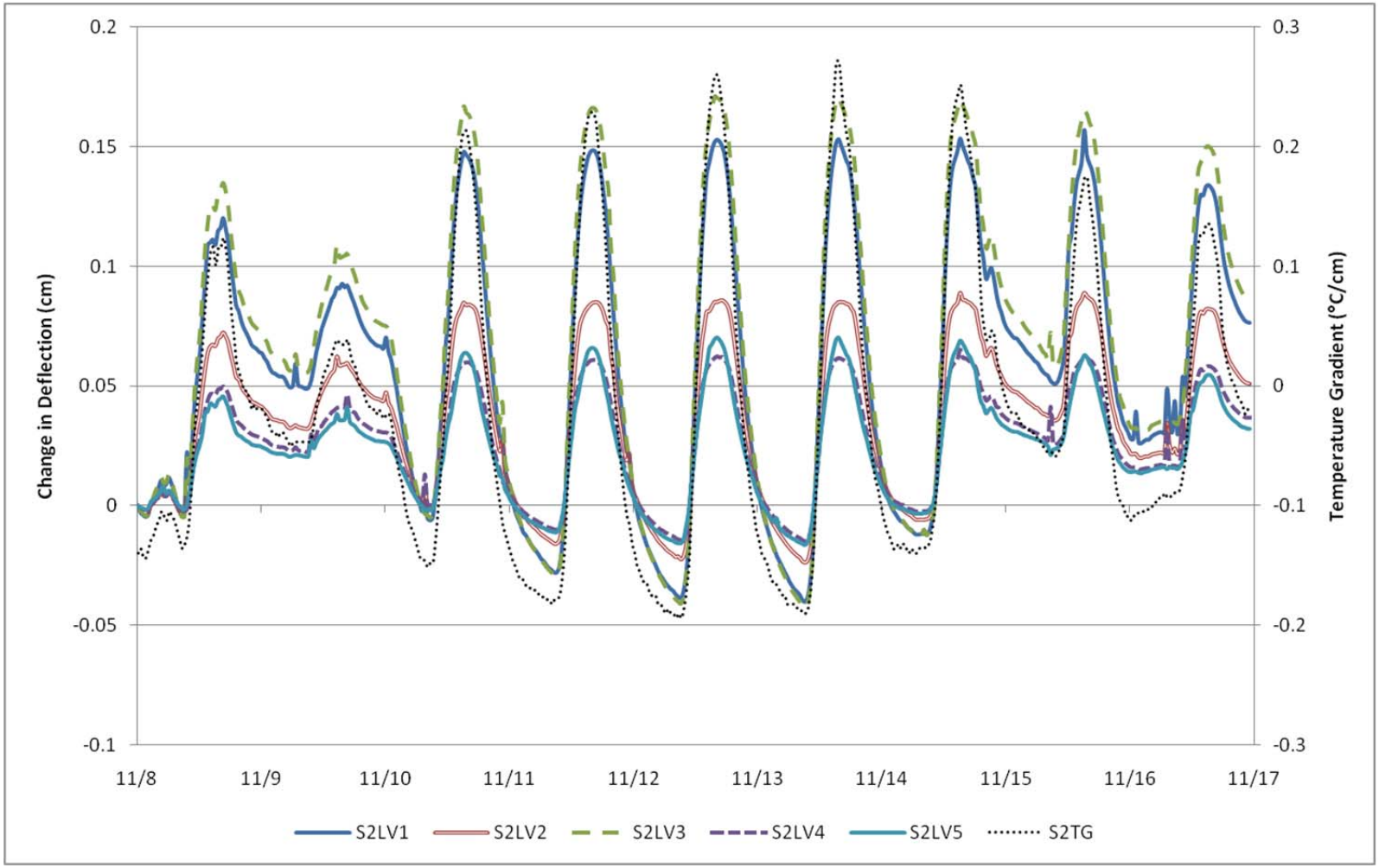

Section 2 – Change in Deflections – Fall 2010 (11/8 – 11/16) (2.54 cm = 1 in; 1 C°/cm = 4.6°F/in)

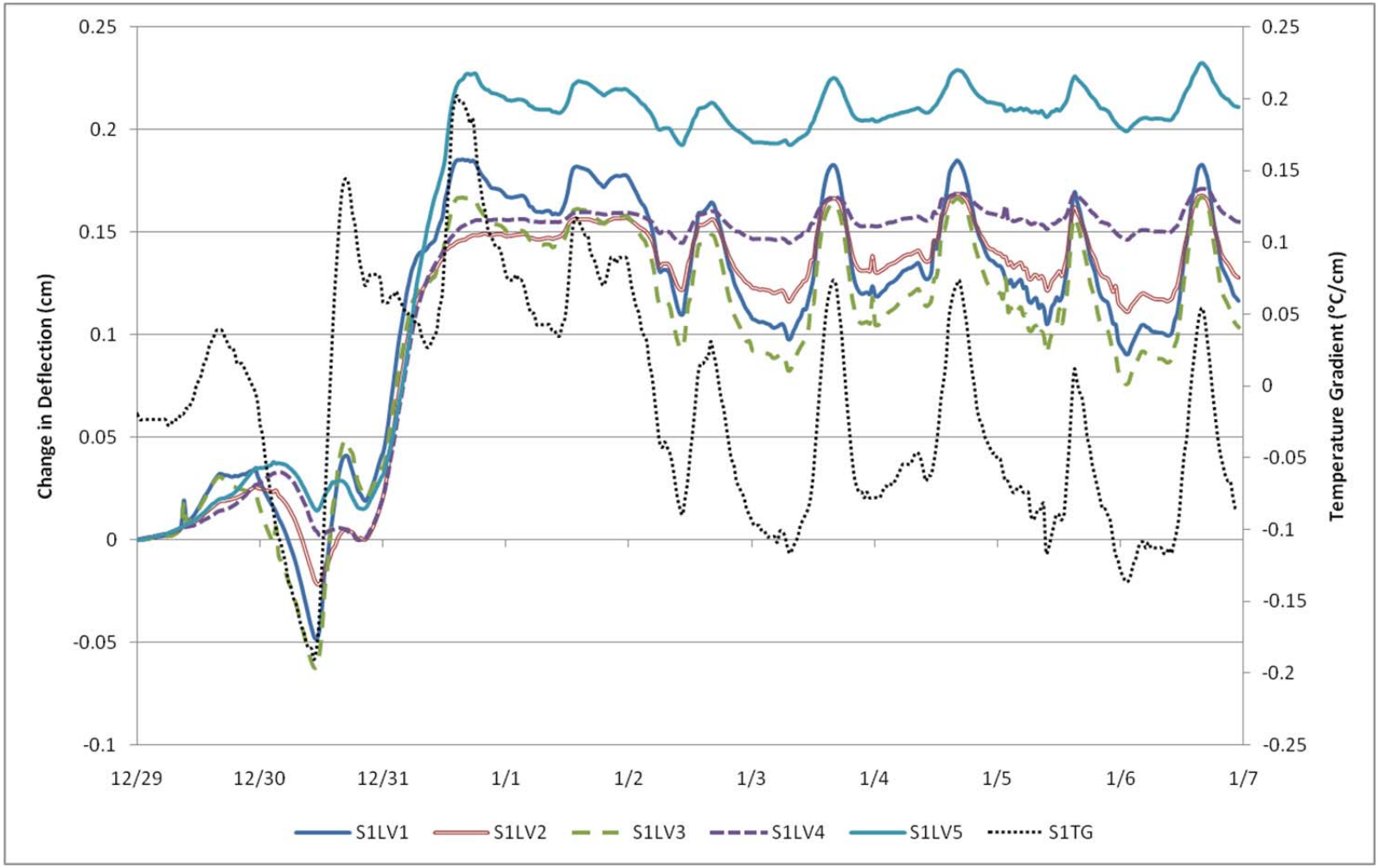

Section 1 – Change in Deflections – Winter 2010/11 (12/29 – 1/6) (2.54 cm = 1 in; 1 C°/cm = 4.6°F/in)

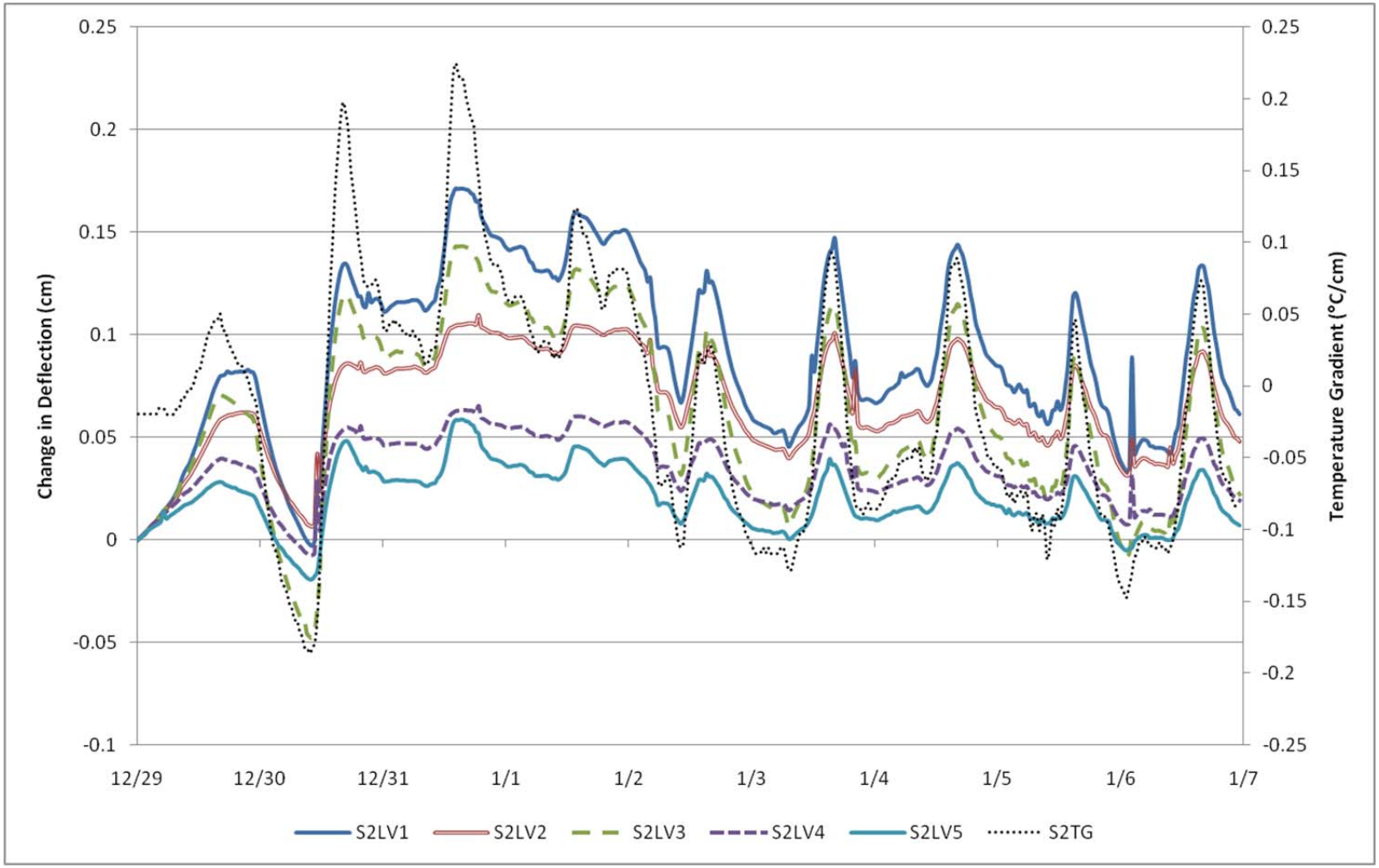

Section 2 – Change in Deflections – Winter 2010/11 (12/29 – 1/6) (2.54 cm = 1 in; 1 C°/cm = 4.6°F/in)

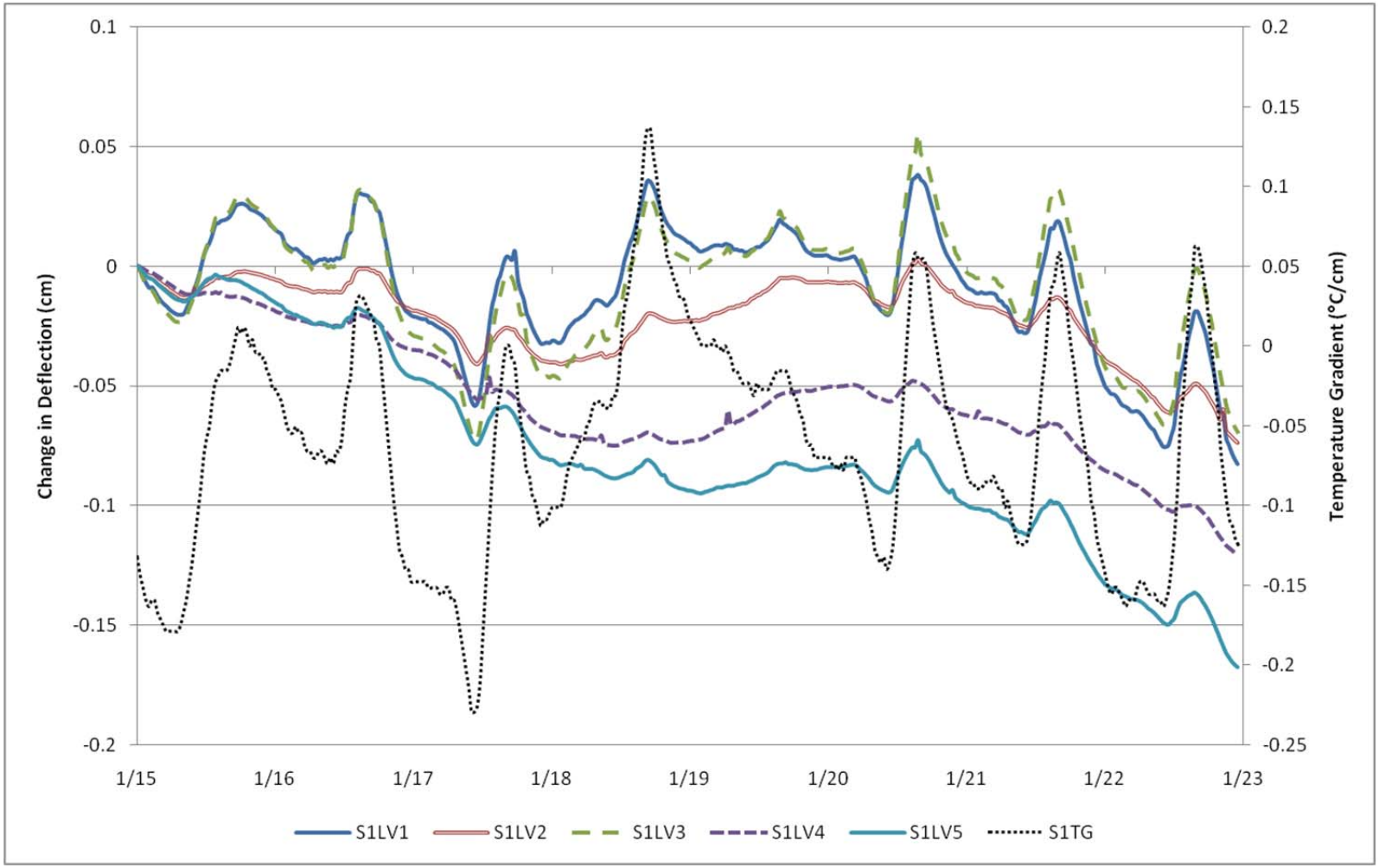

Section 1 – Change in Deflections – Winter 2010/11 (1/15 – 1/22) (2.54 cm = 1 in; 1 C°/cm = 4.6°F/in)

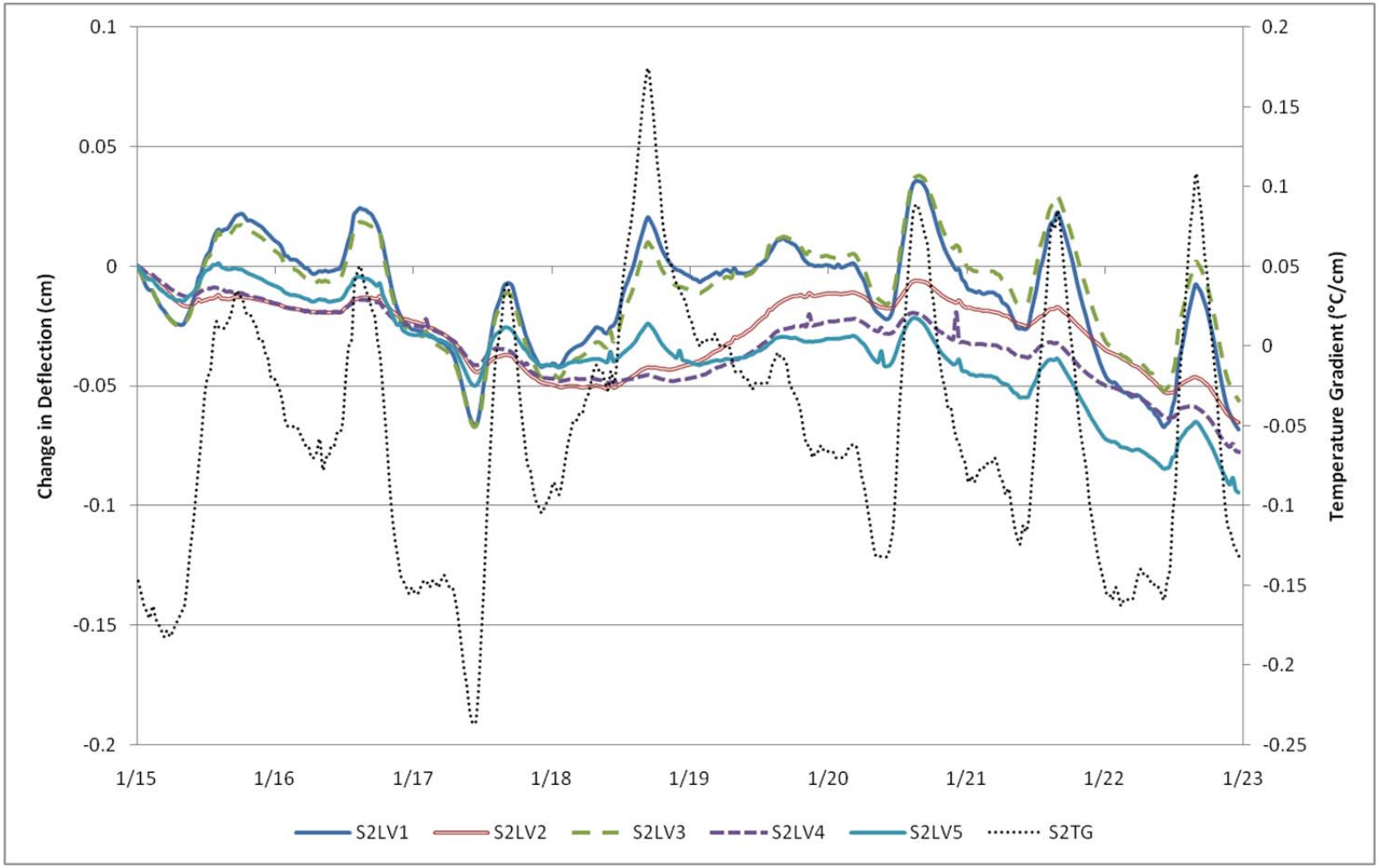

Section 2 – Change in Deflections – Winter 2010/11 (1/15 – 1/22) (2.54 cm = 1 in; 1 C°/cm = 4.6°F/in)

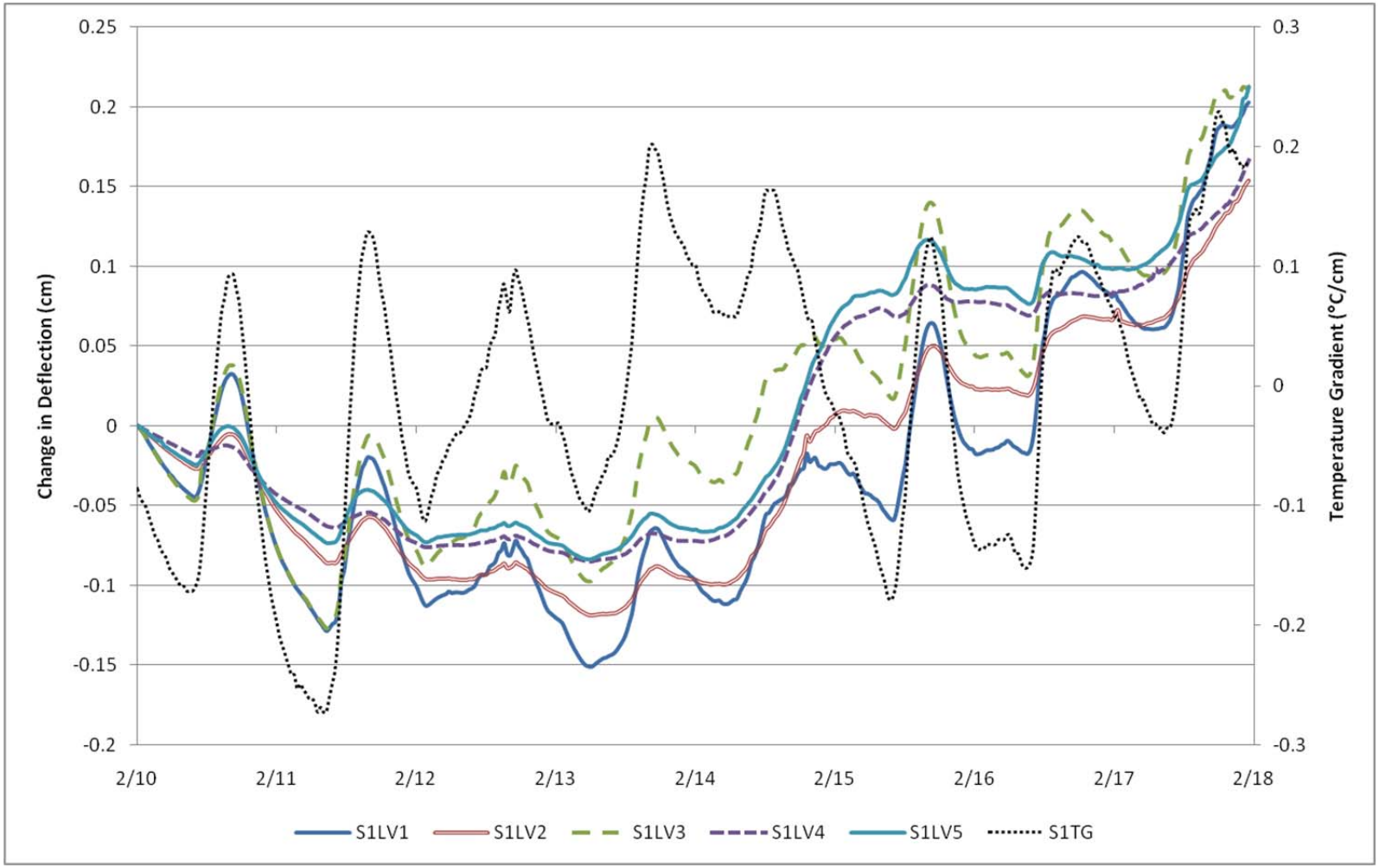

Section 1 – Change in Deflections – Winter 2010/11 (2/10 – 2/17) (2.54 cm = 1 in; 1 C°/cm = 4.6°F/in)

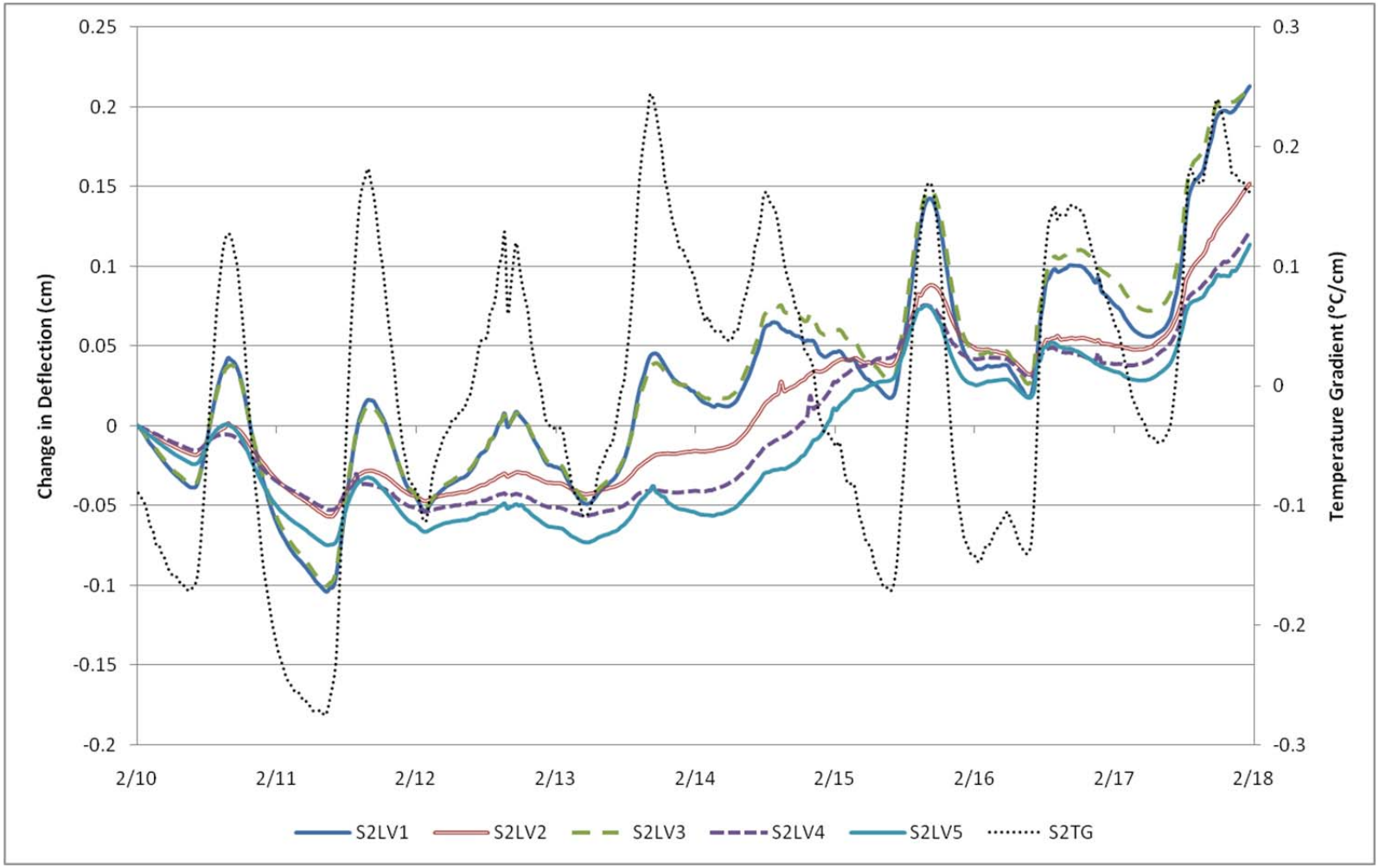

Section 2 – Change in Deflections – Winter 2010/11 (2/10 – 2/17) (2.54 cm = 1 in; 1 C°/cm = 4.6°F/in)

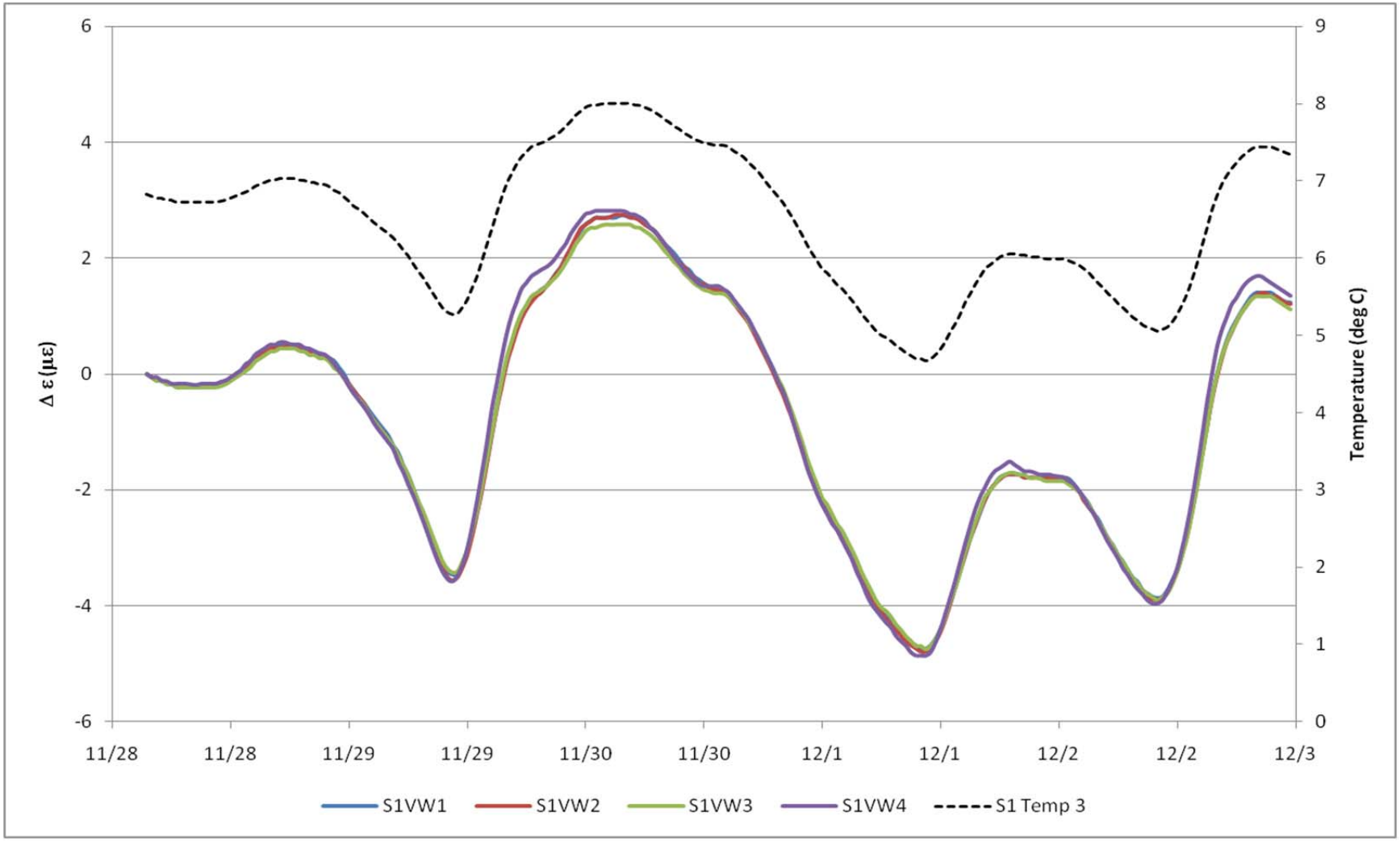

Section 1 – Tie-bar change in load-related strain – Fall 2009 (11/28 – 12/2) (0 °C = 32°F, 9°C = 48.2°F)

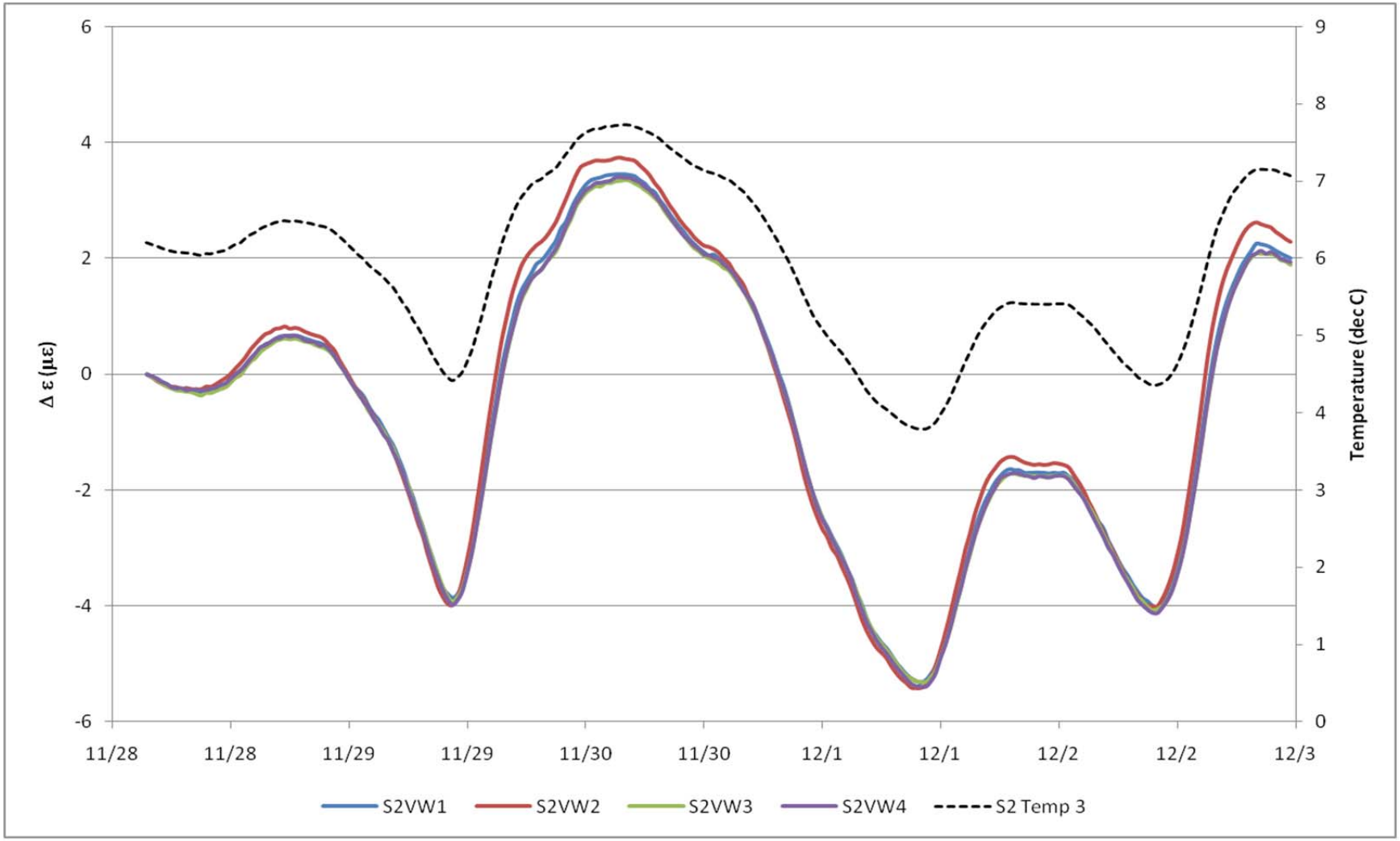

Section 2 – Tie-bar change in load-related strain – Fall 2009 (11/28 – 12/2) (0 °C = 32°F, 9°C = 48.2°F)

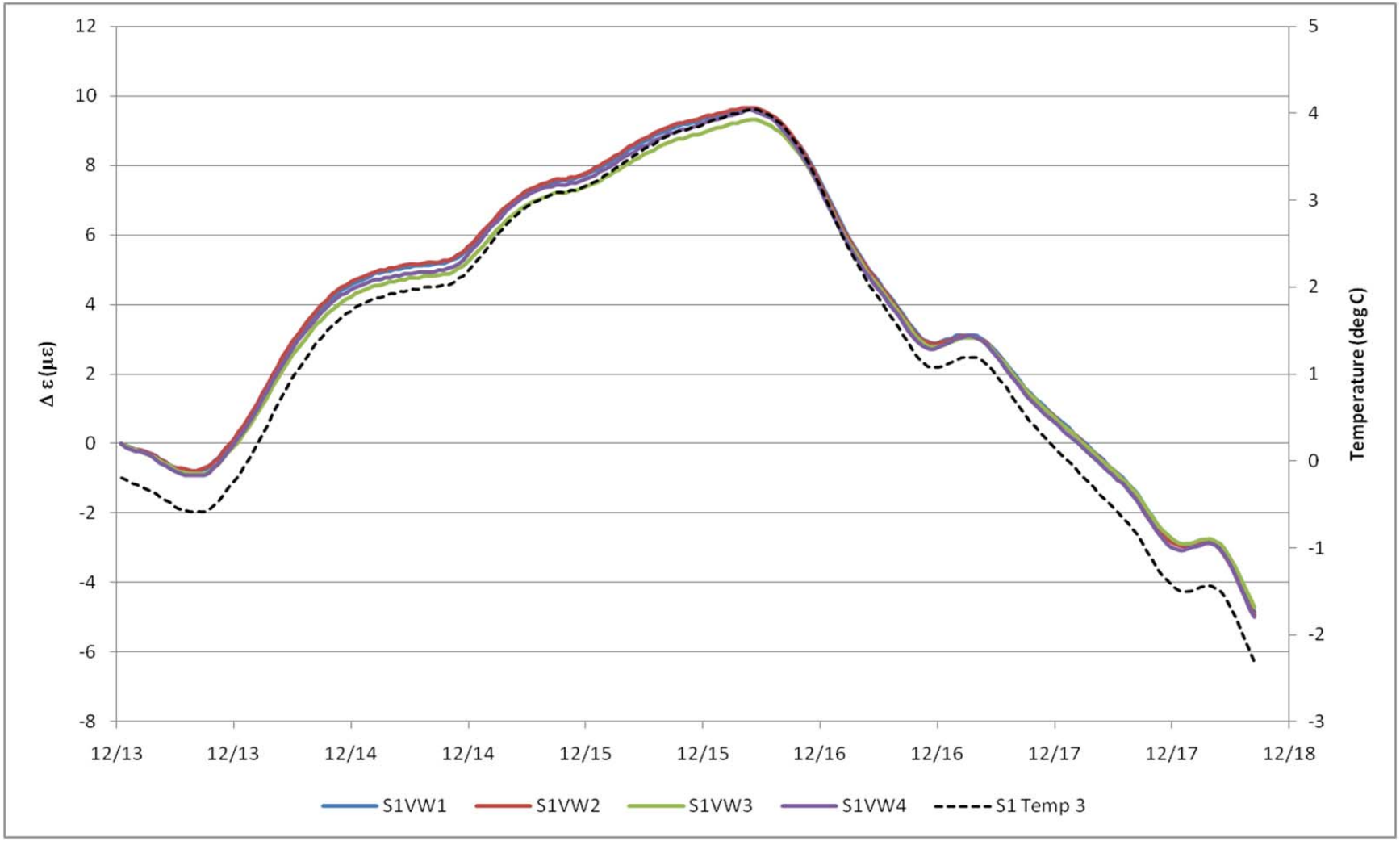

Section 1 – Tie-bar change in load-related strain – Winter 2009/10 (12/13 – 12/17) (-3 °C = 26.6°F, 9°C = 41.0°F)

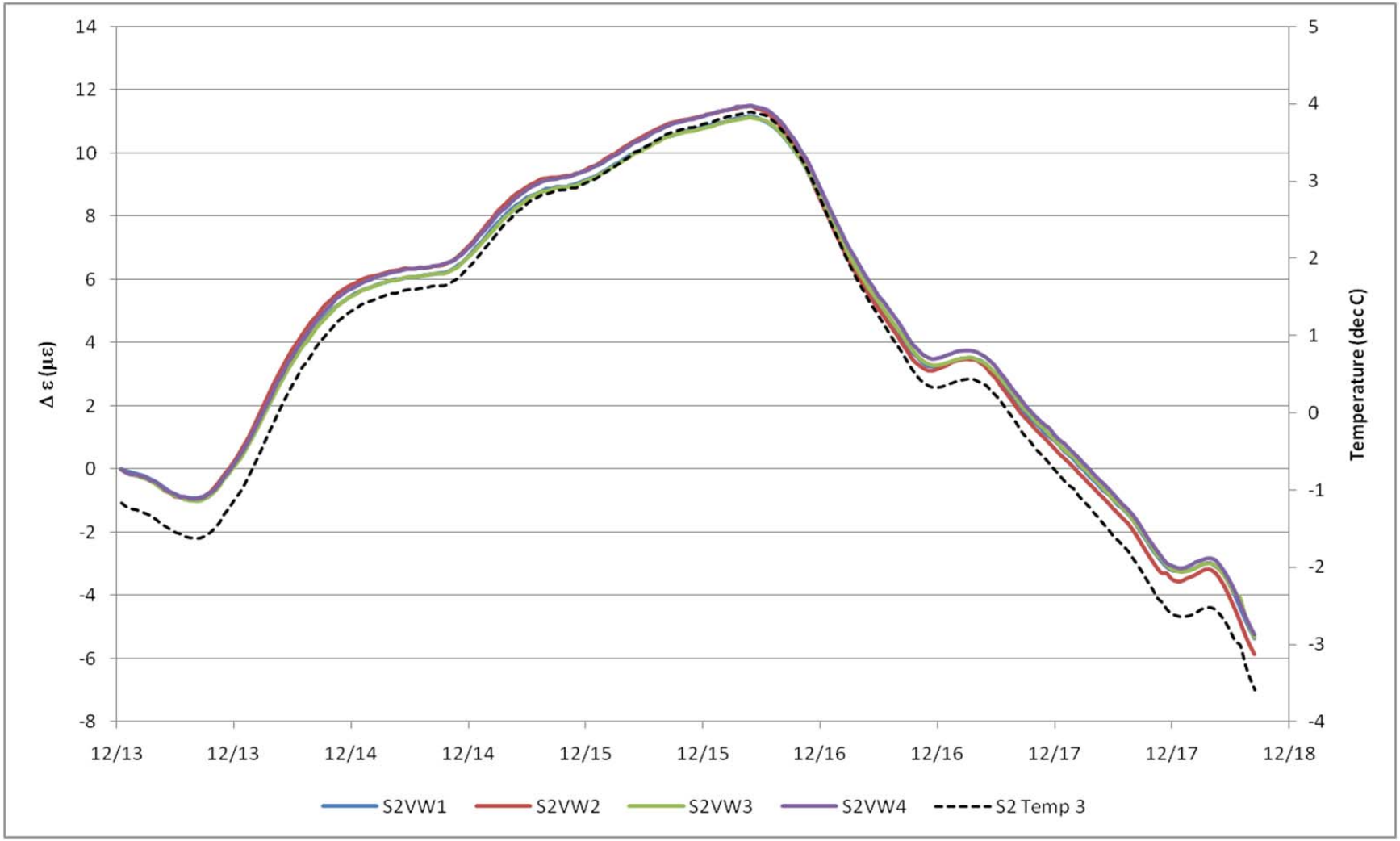

Section 2 – Tie-bar change in load-related strain – Winter 2009/10 (12/13 – 12/17) (-3 °C = 26.6°F, 9°C = 41.0°F)

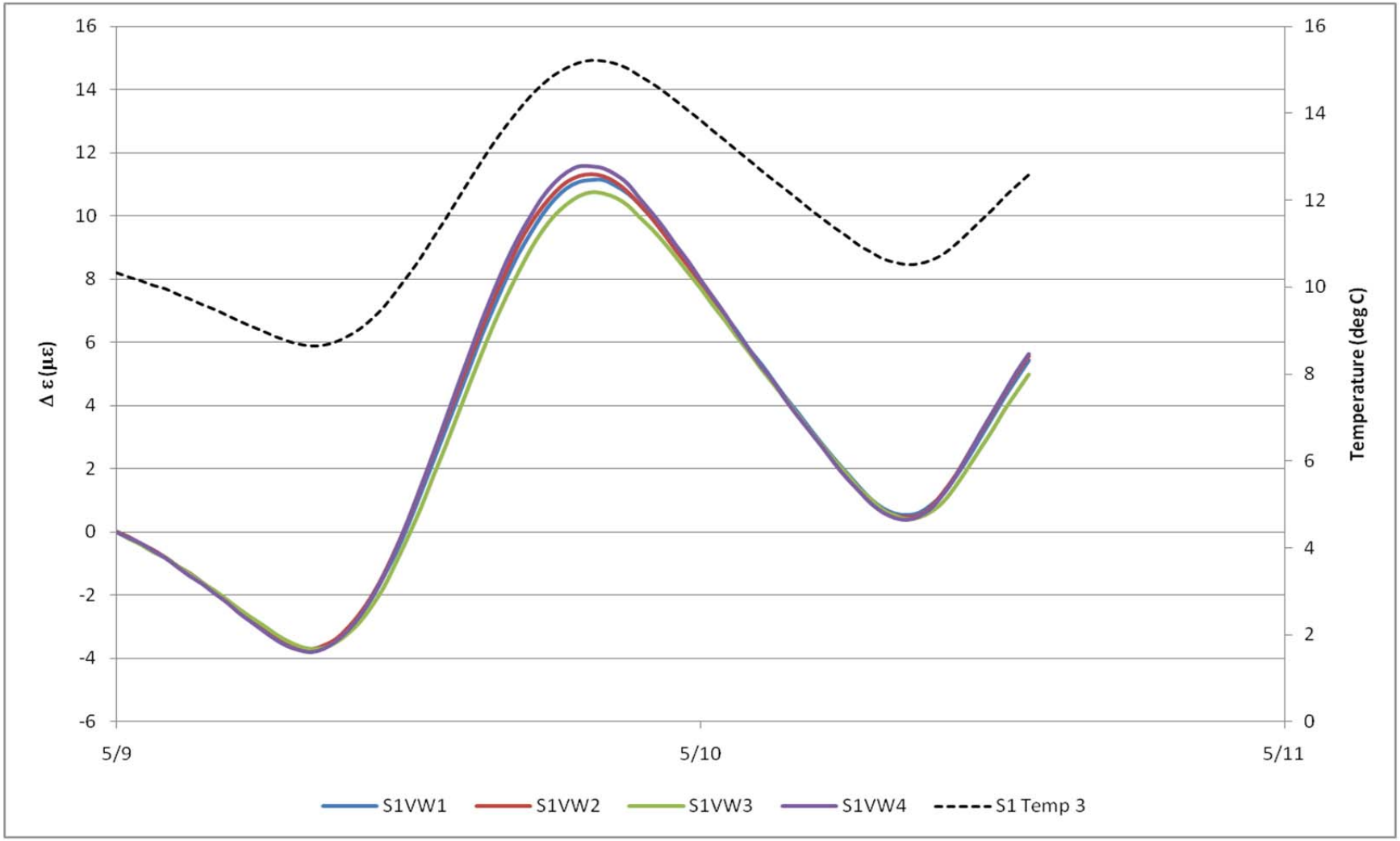

Section 1 – Tie-bar change in load-related strain – Spring 2010 (5/9 – 5/10) (0°C = 32°F, 16°C = 60.8°F)

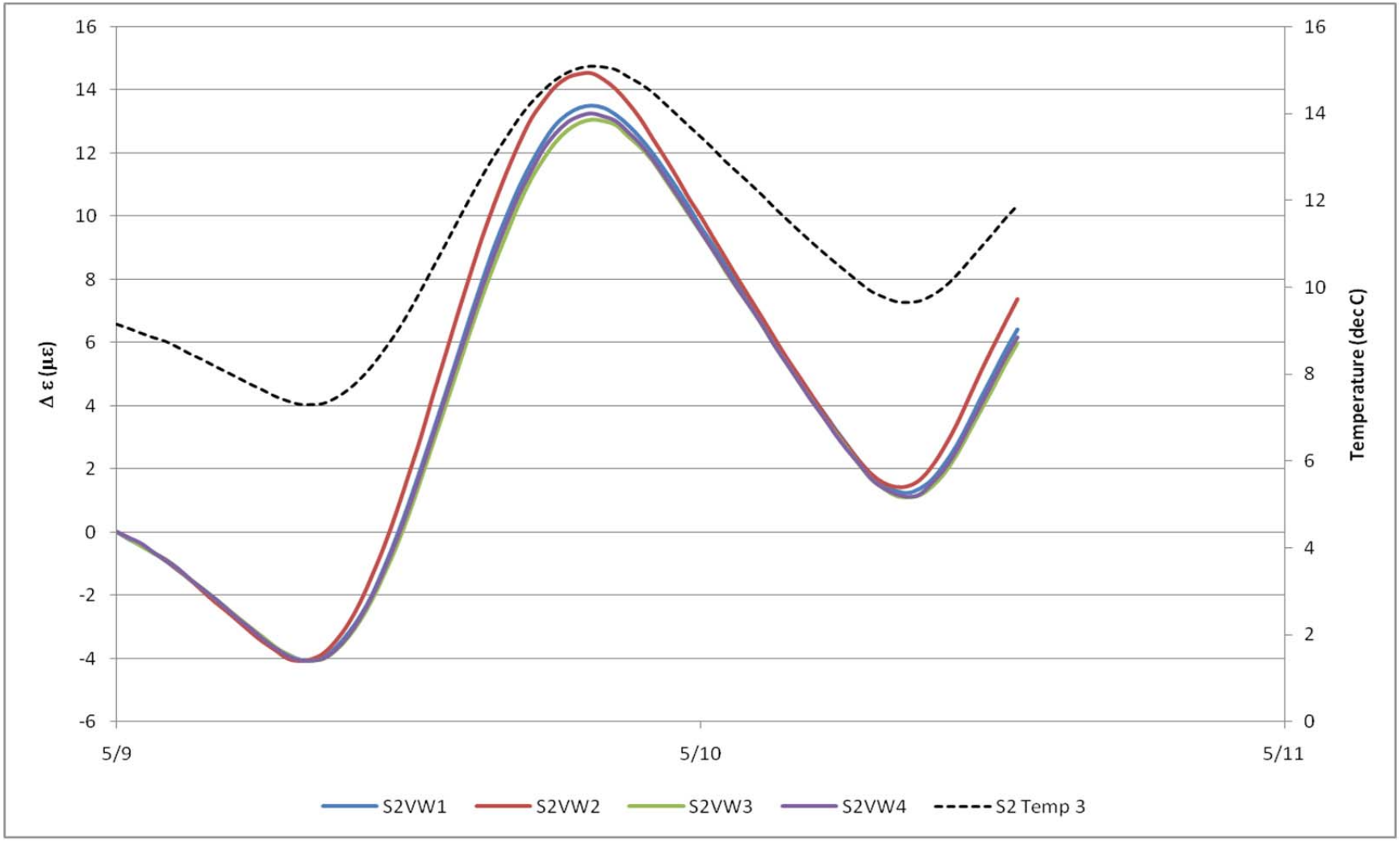

Section 2 – Tie-bar change in load-related strain – Spring 2010 (5/9 – 5/10) (0°C = 32°F, 16°C = 60.8°F)

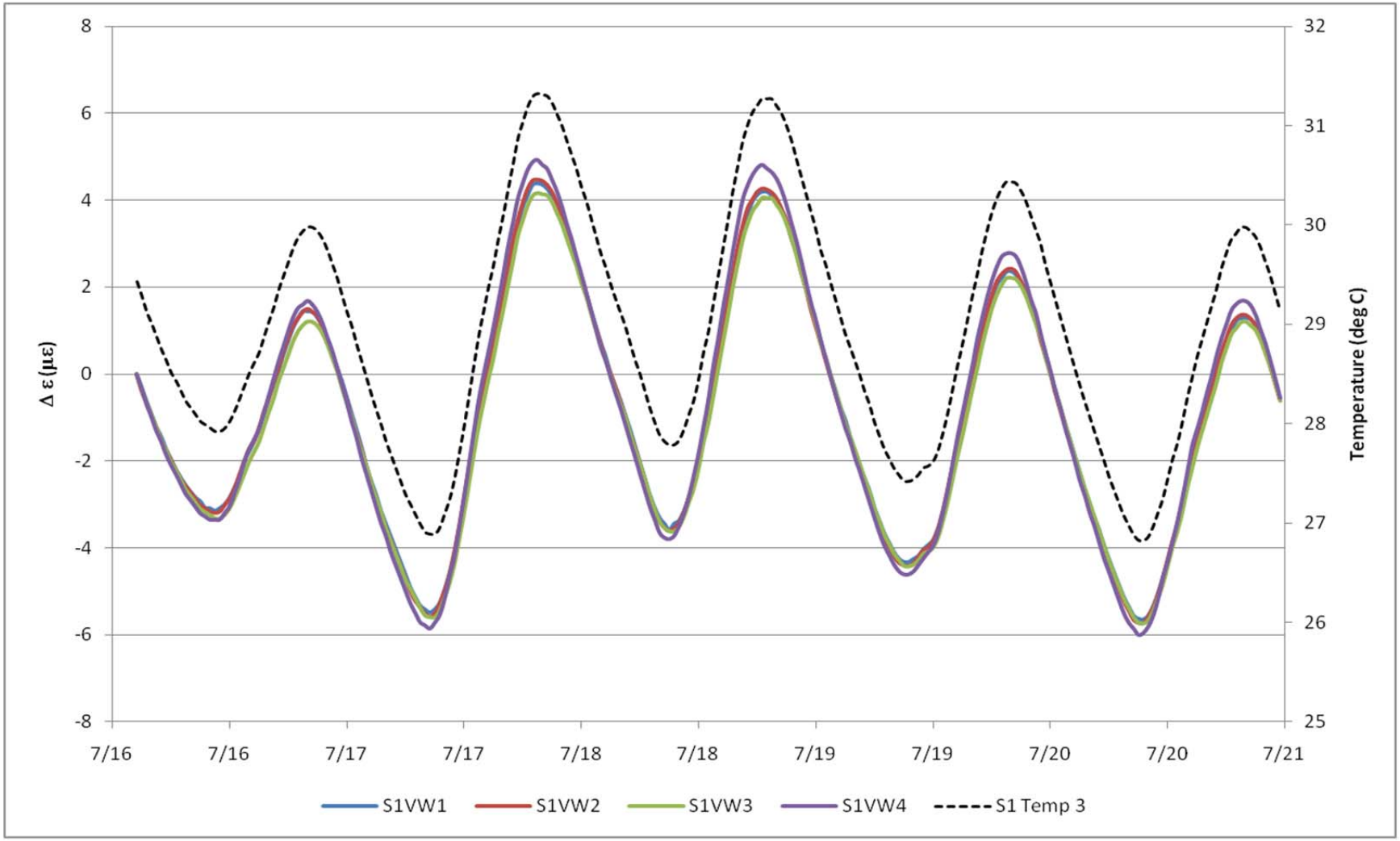

Section 1 – Tie-bar change in load-related strain – Summer 2010 (7/16 – 7/20) (25°C = 77°F, 32°C = 89.6°F)

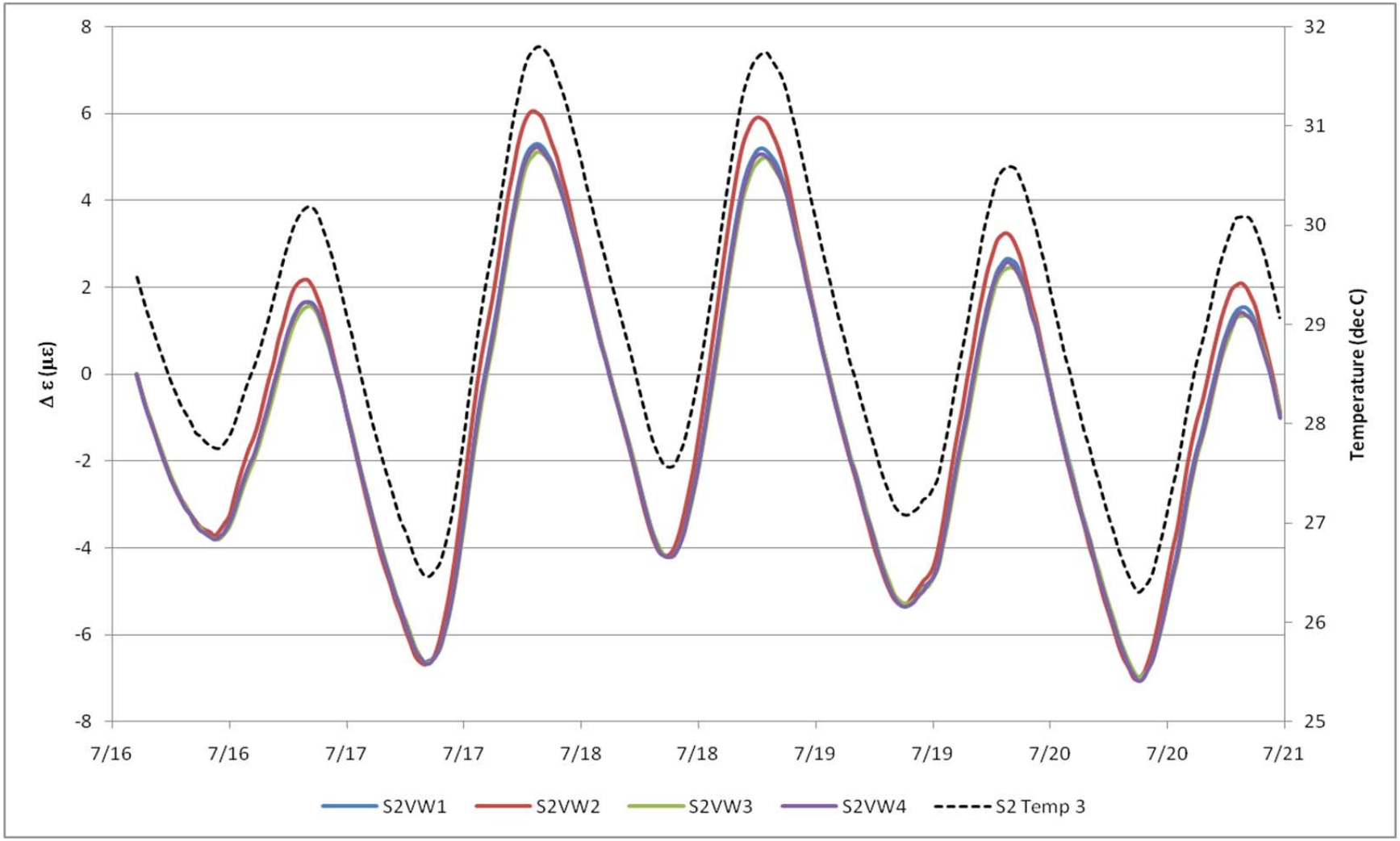

Section 2 – Tie-bar change in load-related strain – Summer 2010 (7/16 – 7/20) (25°C = 77°F, 32°C = 89.6°F)

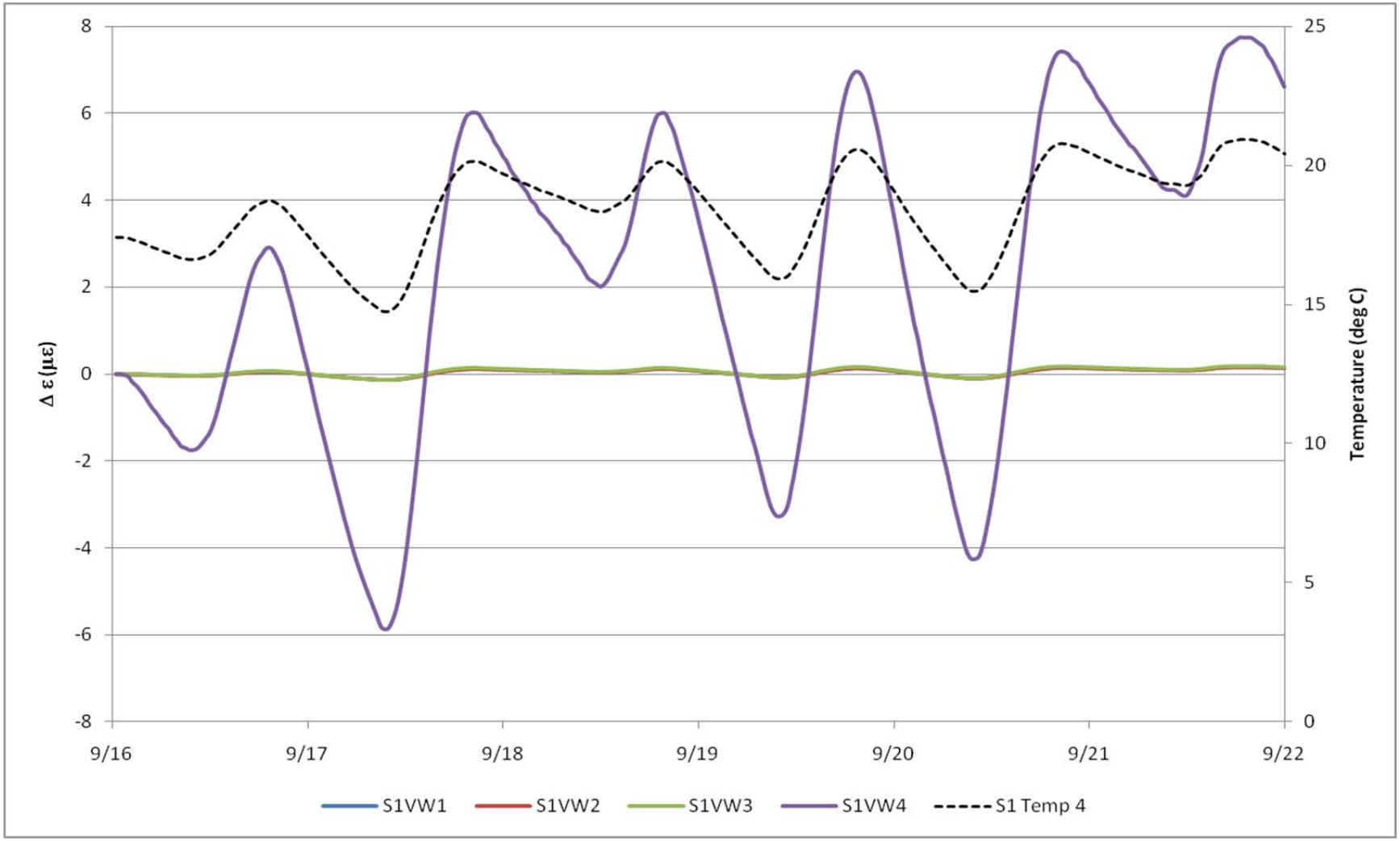

Section 1 – Tie-bar change in load-related strain – Fall 2010 (9/16 – 9/21) (0°C = 32°F, 25°C = 77°F)

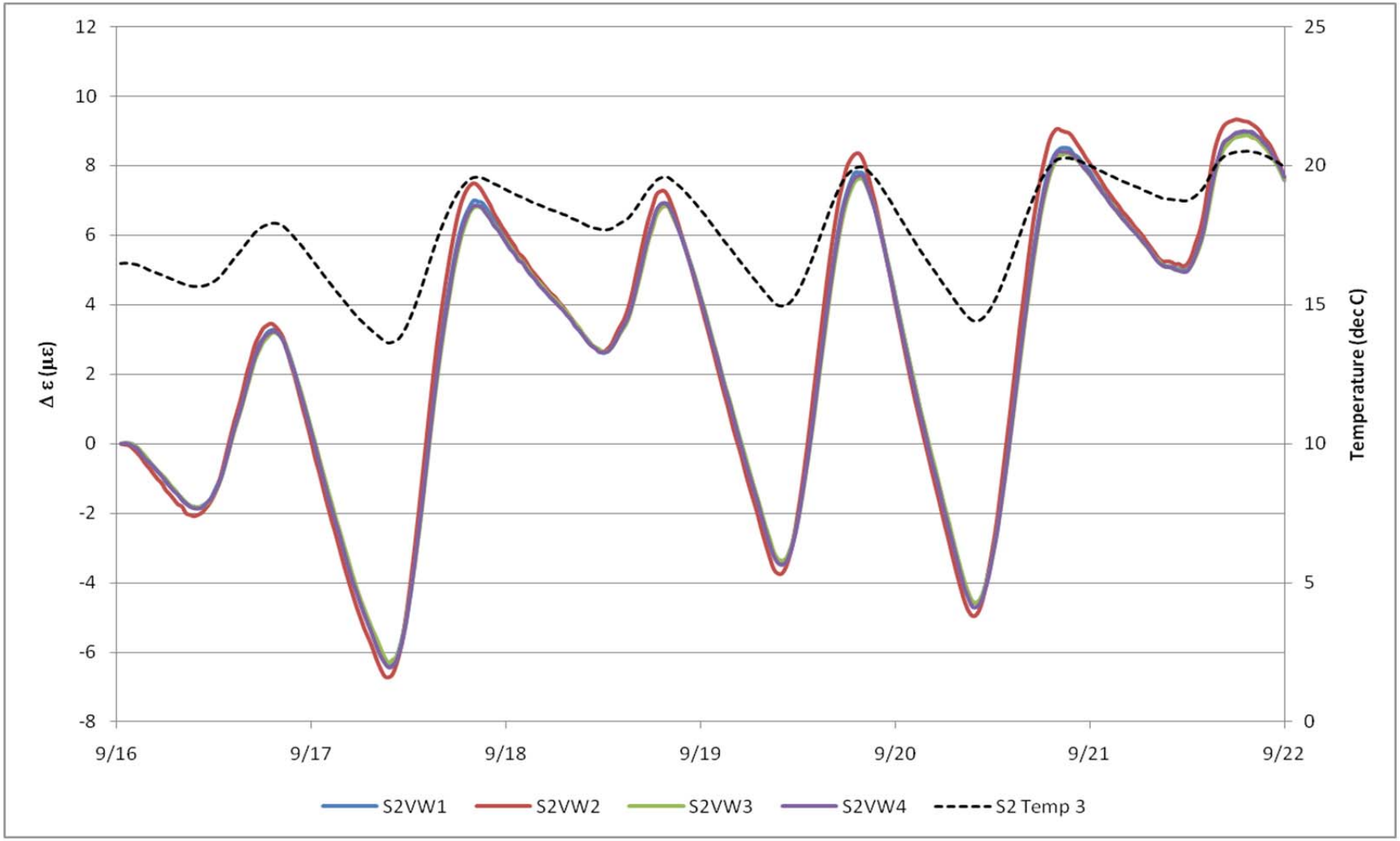

Section 2 – Tie-bar change in load-related strain – Fall 2010 (9/16 – 9/21) (0°C = 32°F, 25°C = 77°F)

Appendix B Supplemental FWD Response Data

FWD Test Results – PCC Pavement

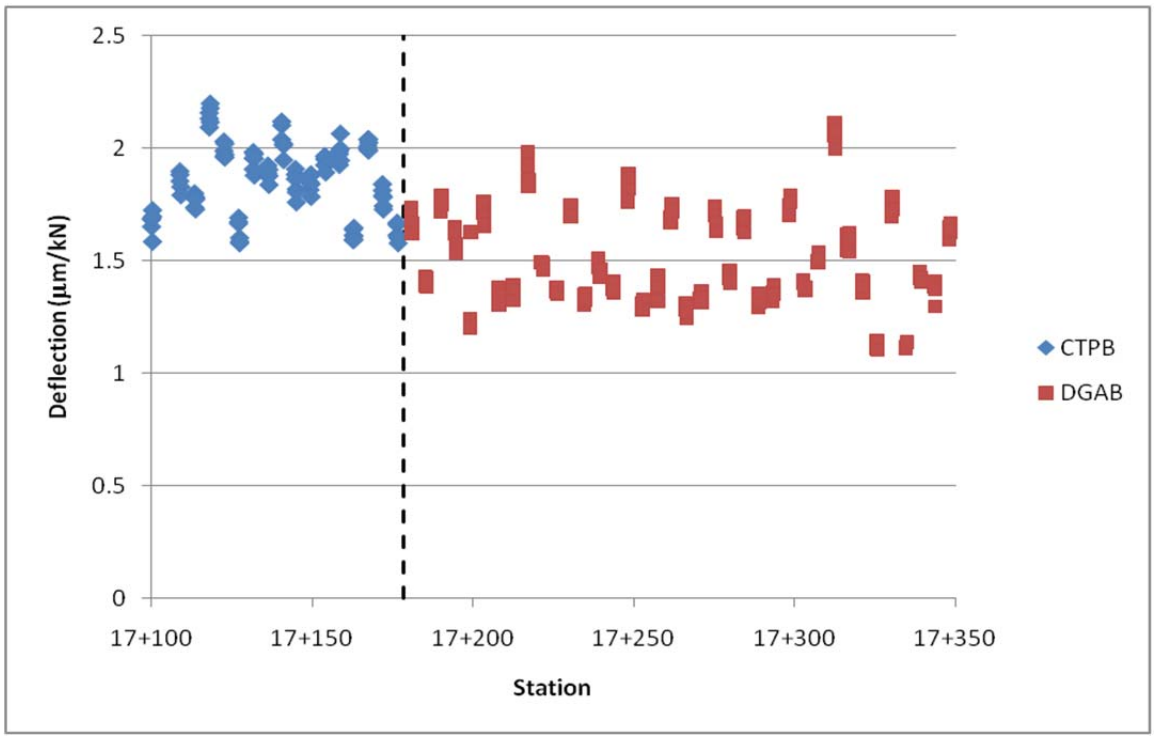

D_0 at joints – Left lane (5.714µm/kN = 1 mil/kip)

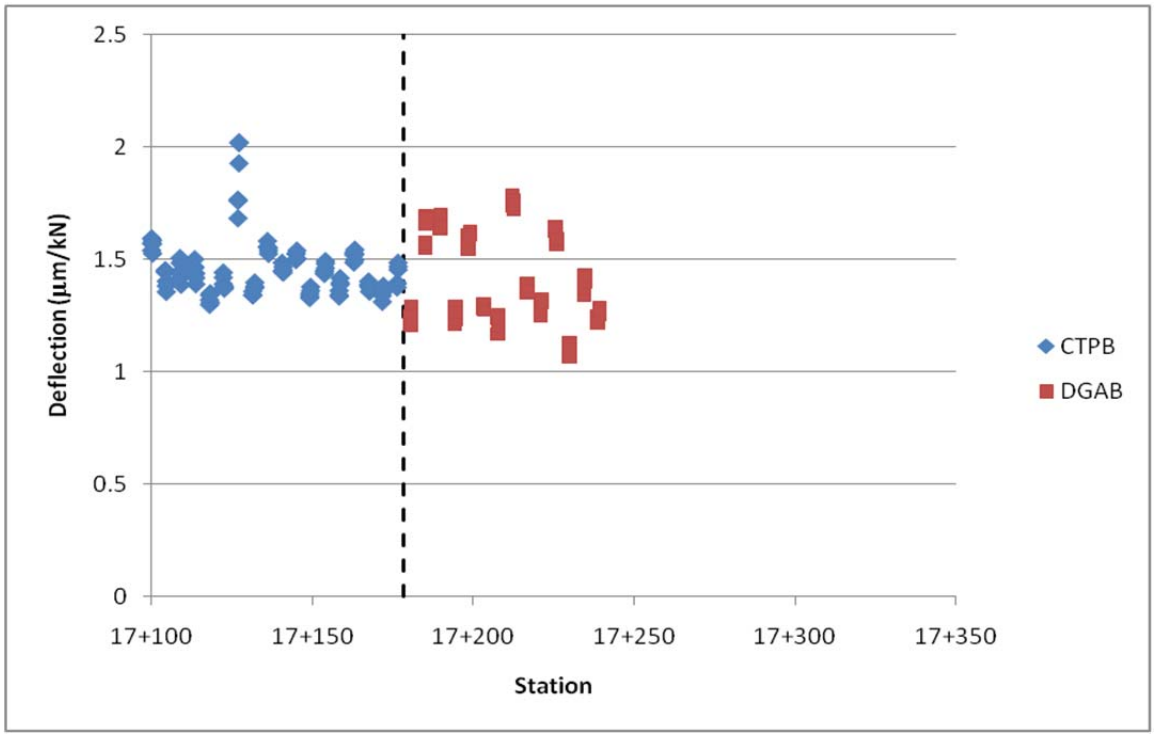

D_0 at joints – Right lane (5.714µm/kN = 1 mil/kip)

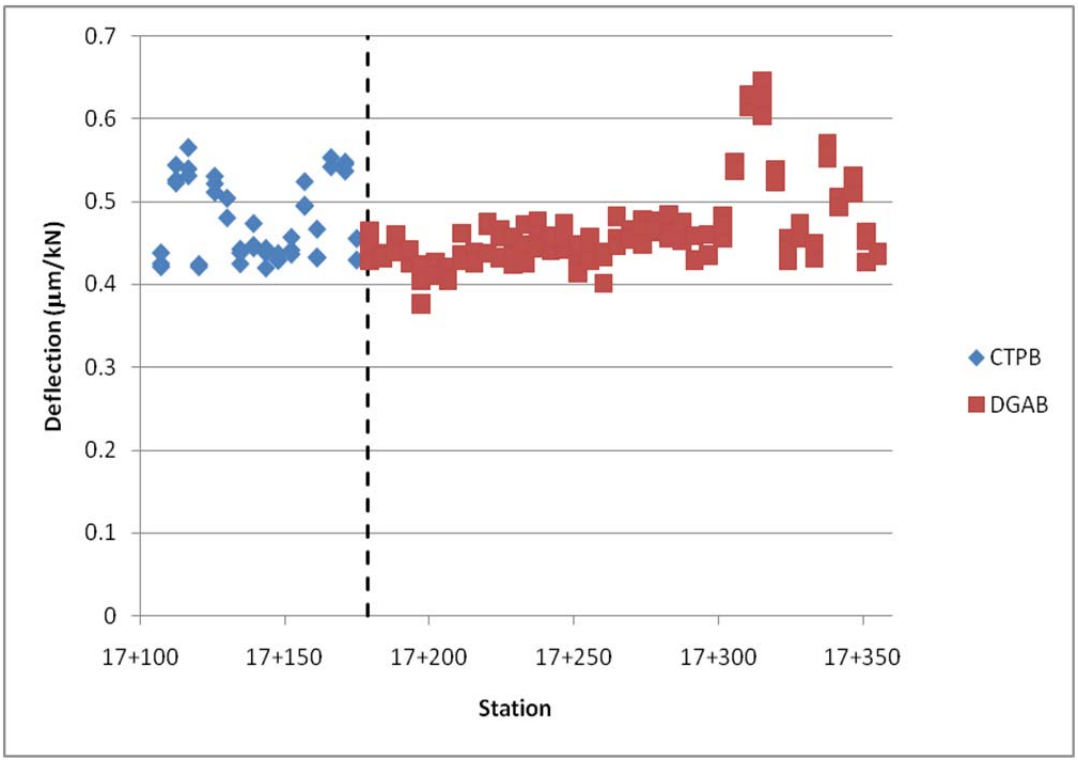

D_{60} at mid-slab – Left lane (5.714µm/kN = 1 mil/kip)

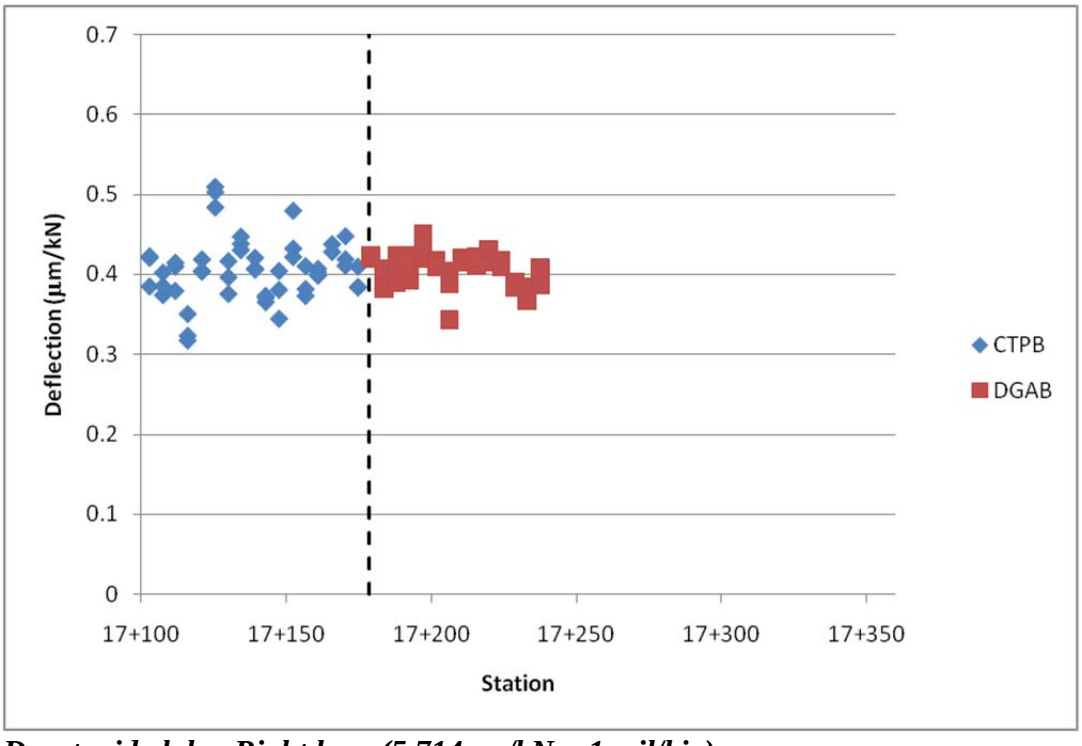

D_{60} at mid-slab – Right lane (5.714µm/kN = 1 mil/kip)

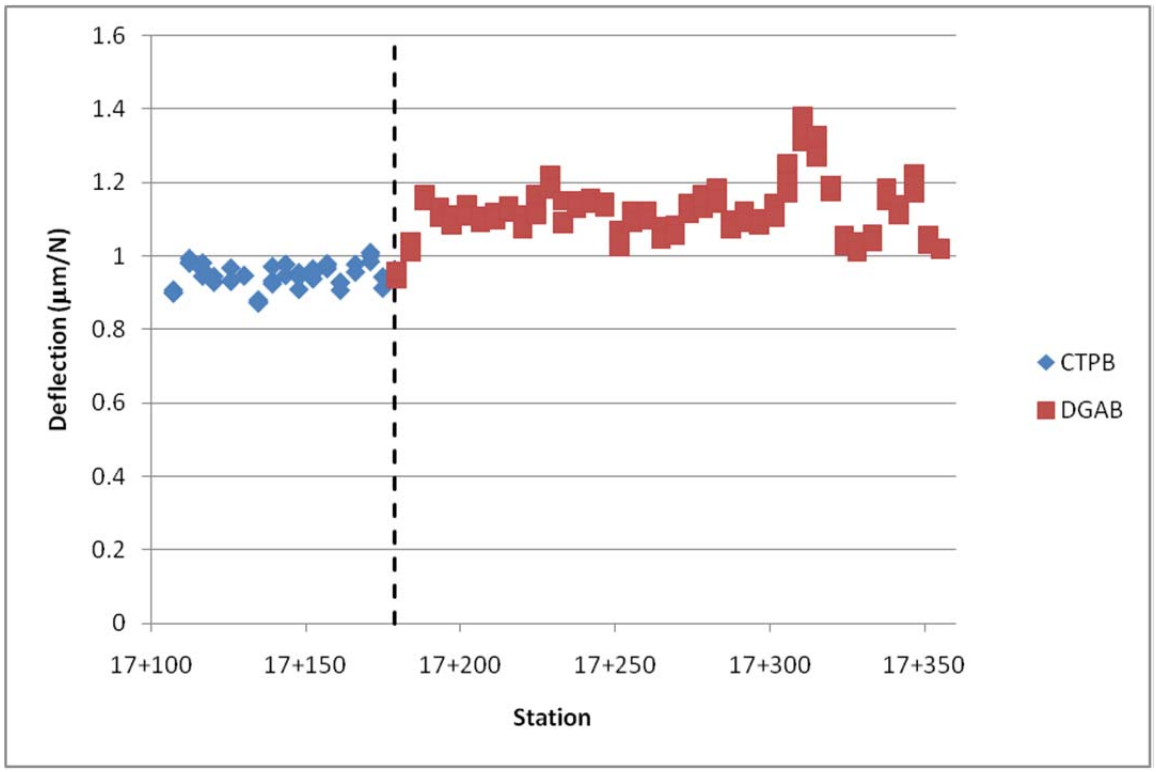

D_0 at mid-slab – Left lane (5.714µm/kN = 1 mil/kip)

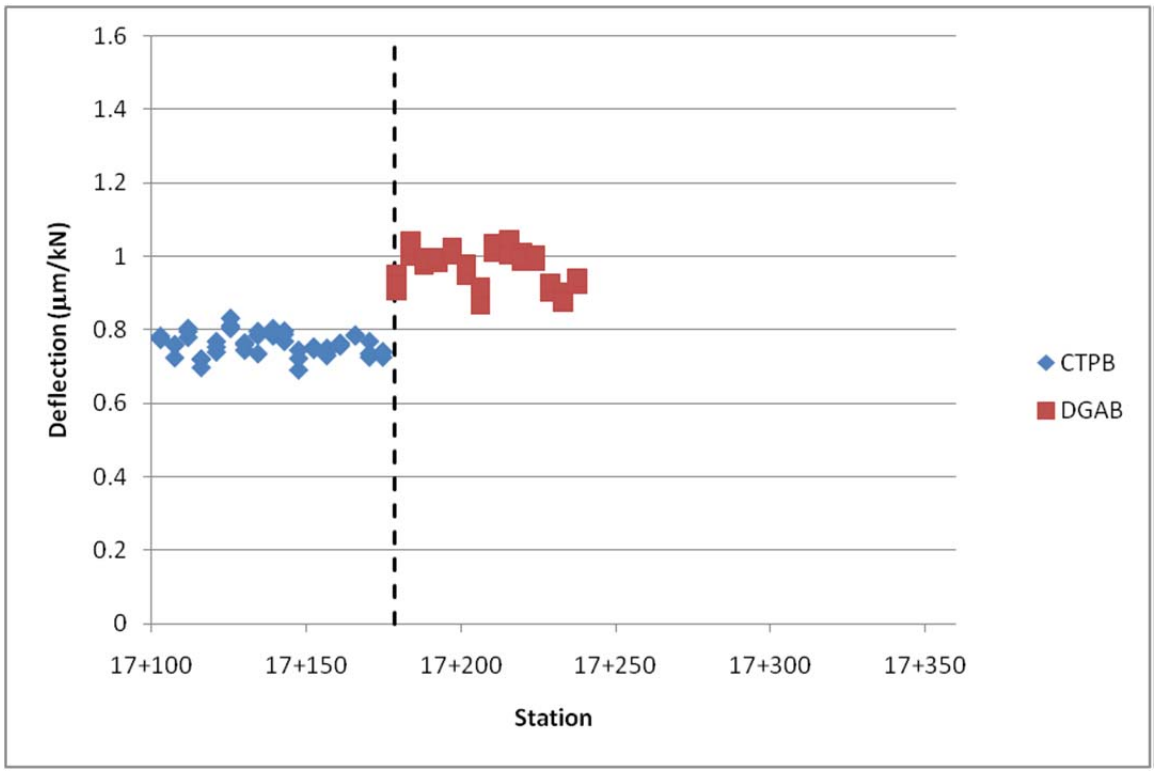

D_0 at mid-slab – Right lane (5.714µm/kN = 1 mil/kip)

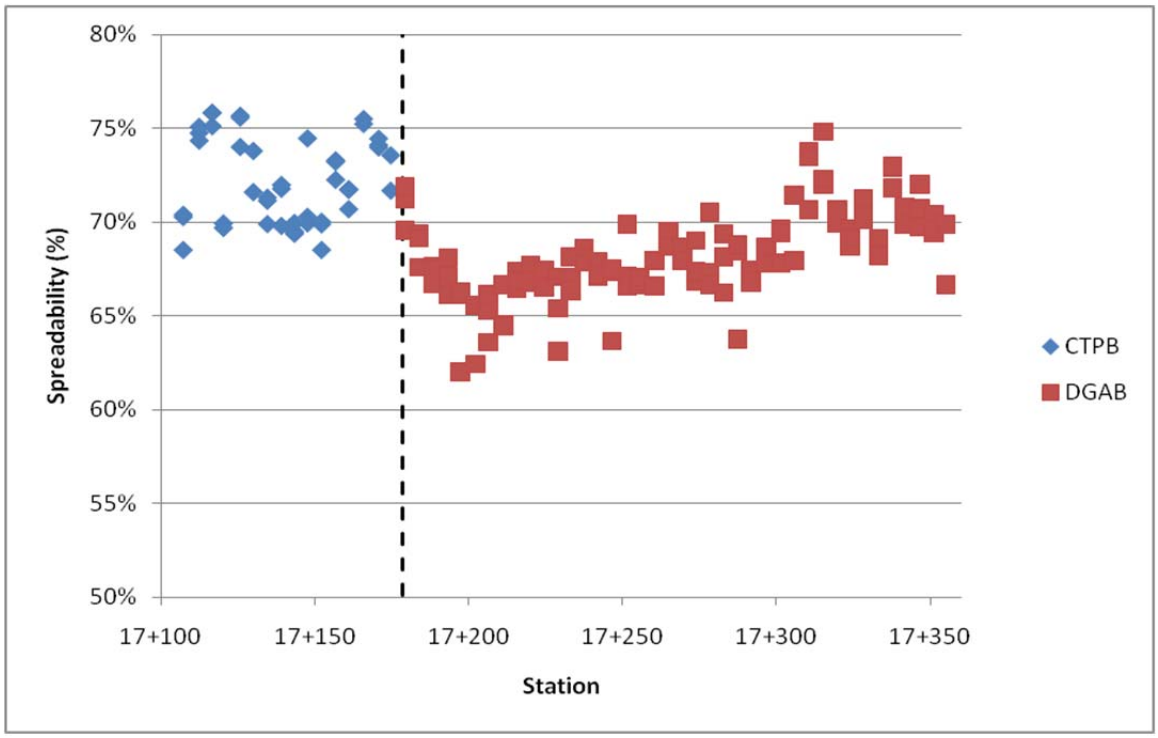

Spreadability – Left lane

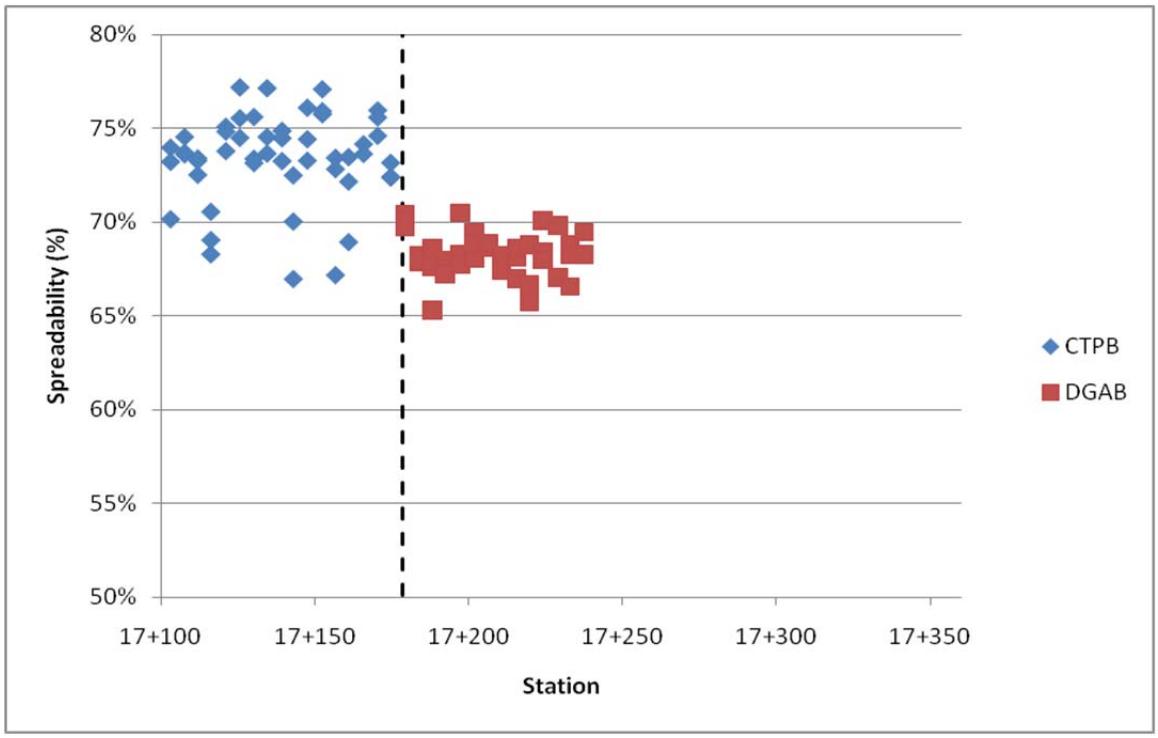

Spreadability – Right lane

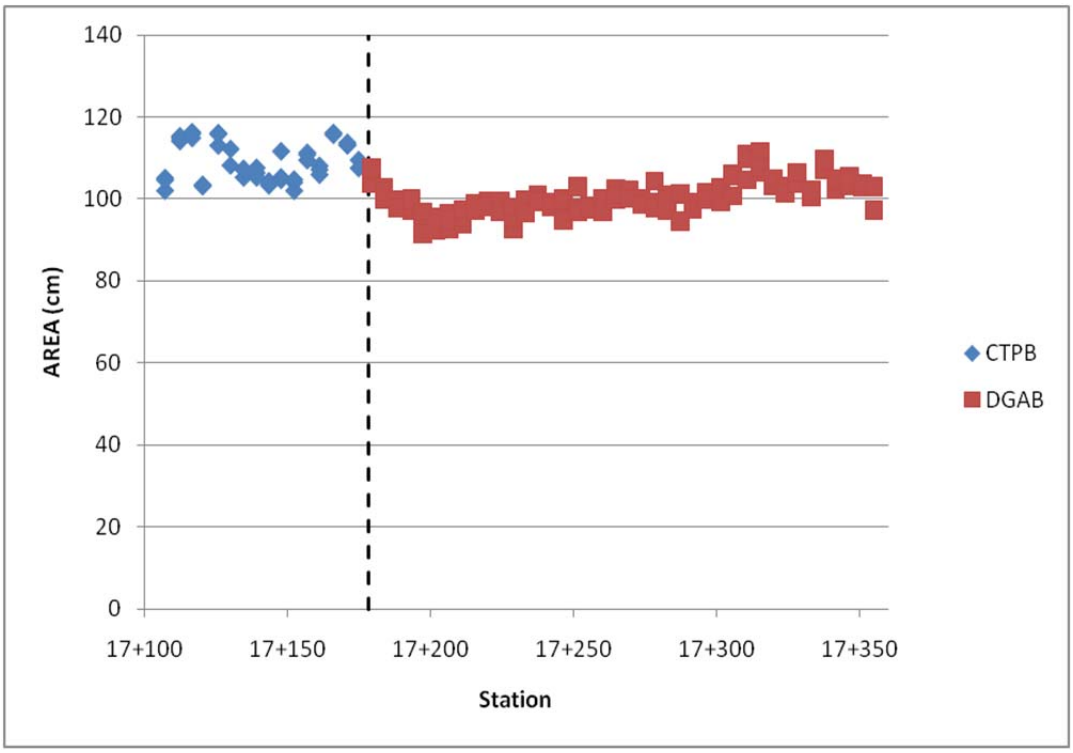

AREA$_{72}$ – Left lane (2.54cm = 1 in)

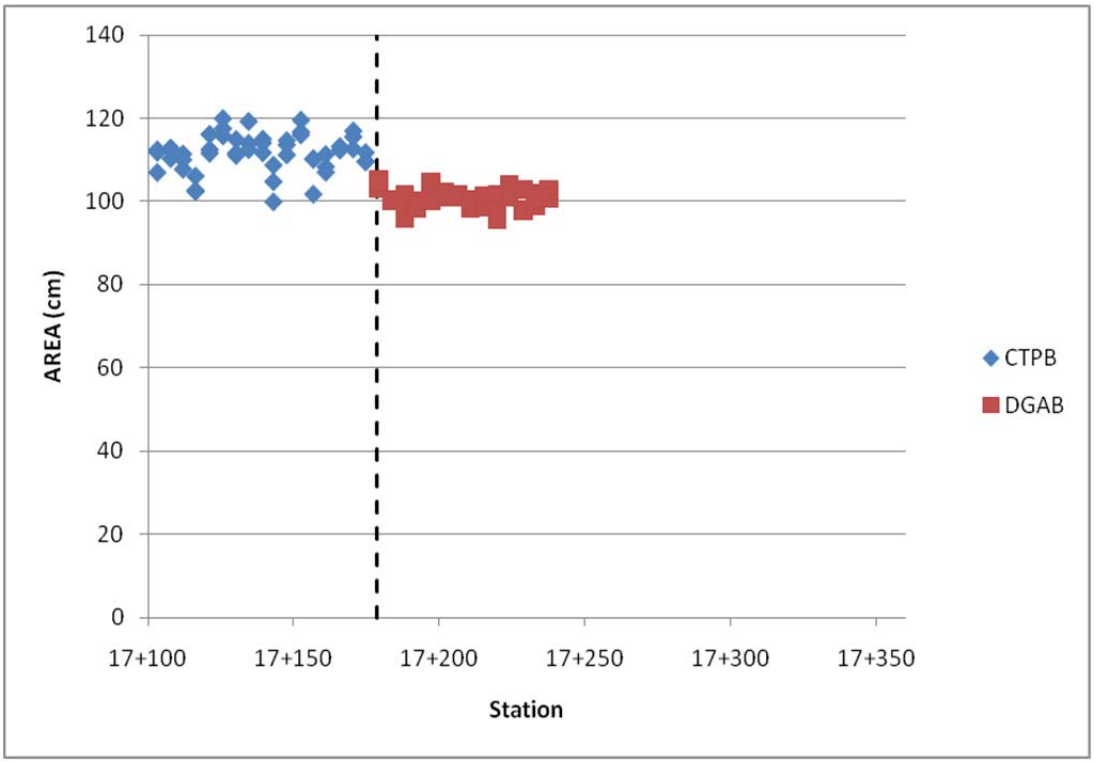

AREA$_{72}$ – Right lane (2.54cm = 1 in)

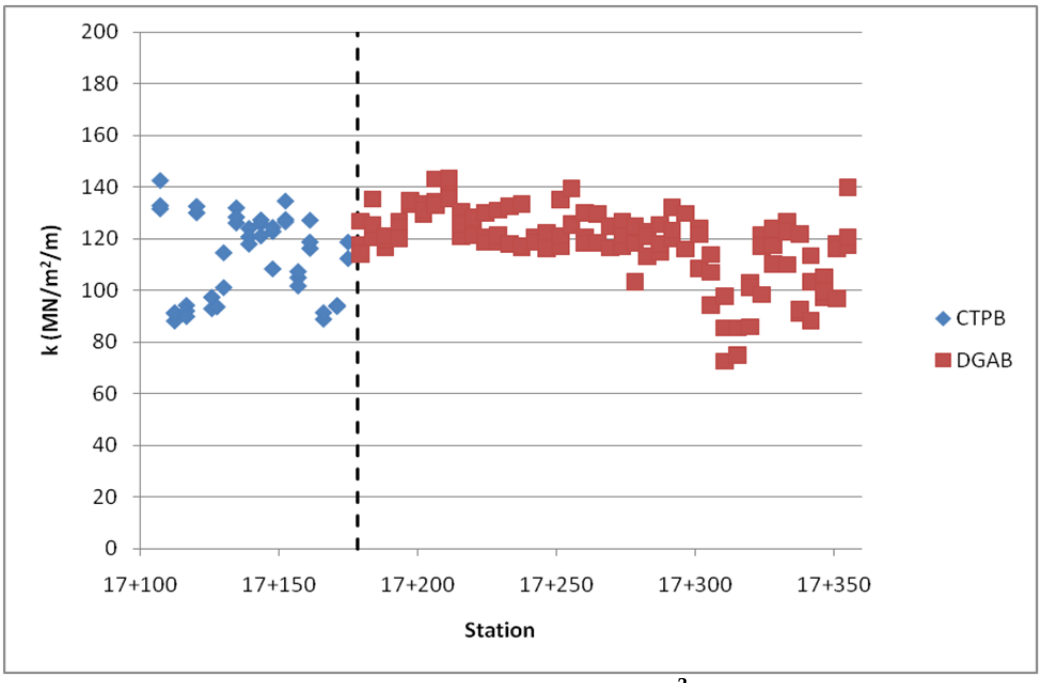

Subgrade k-value – Left lane (1MPa/m = 3.70 lb/in^3)

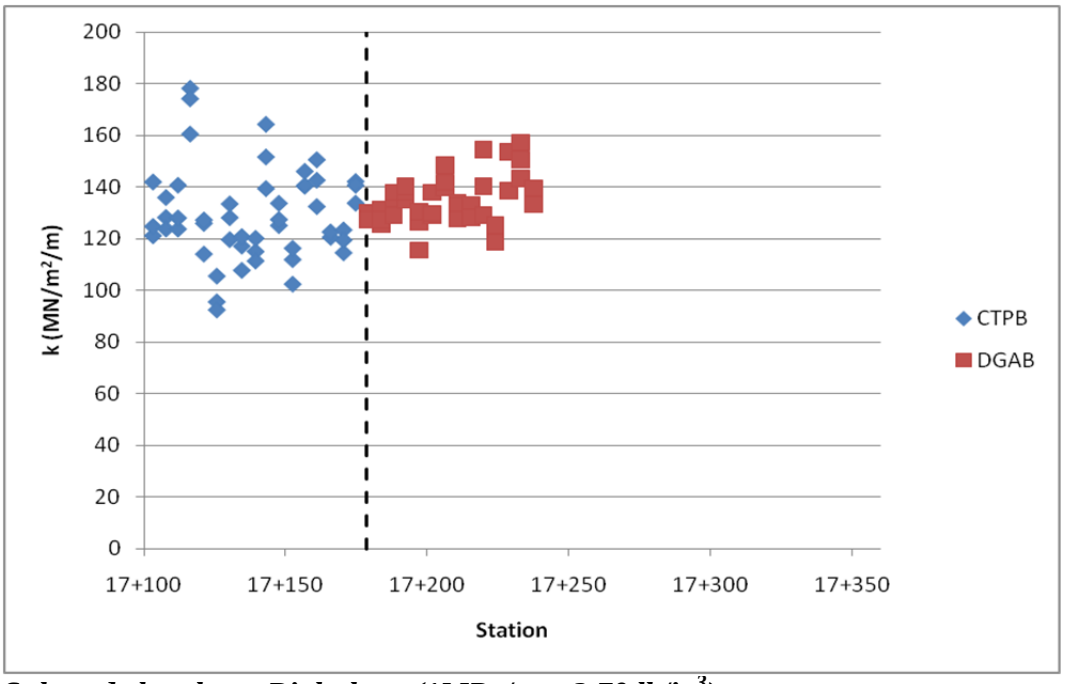

Subgrade k-value – Right lane (1MPa/m = 3.70 lb/in^3)

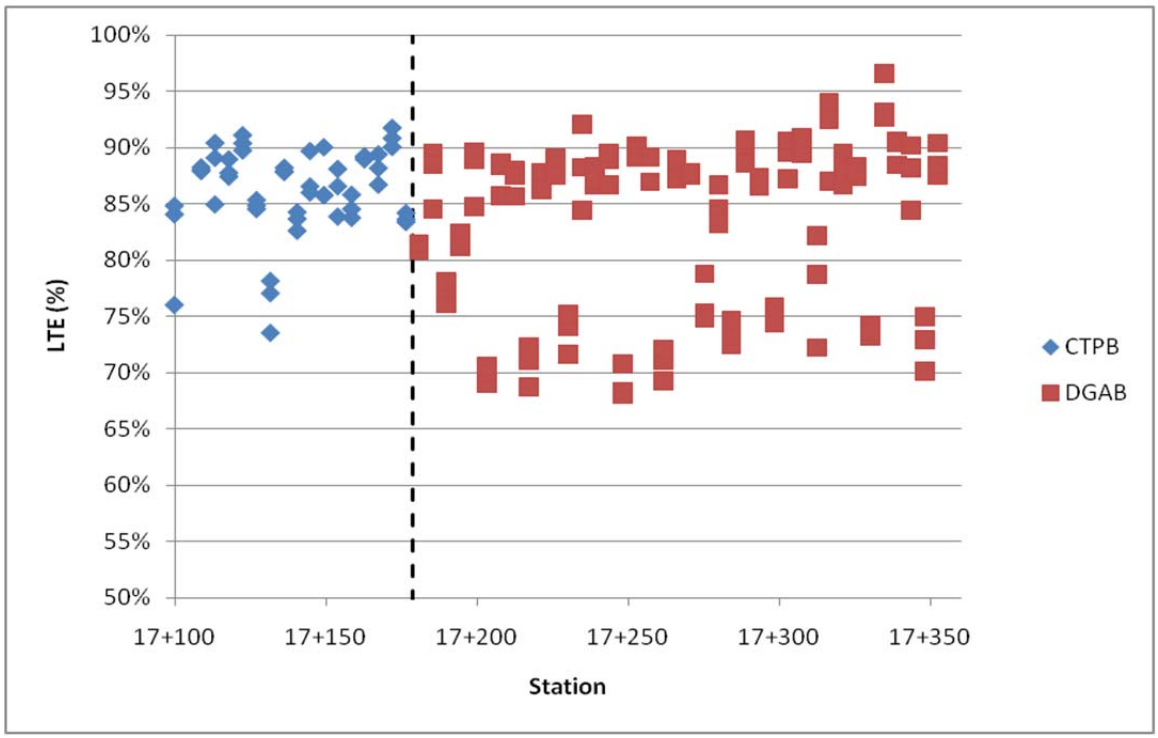

LTE approach position – Left lane

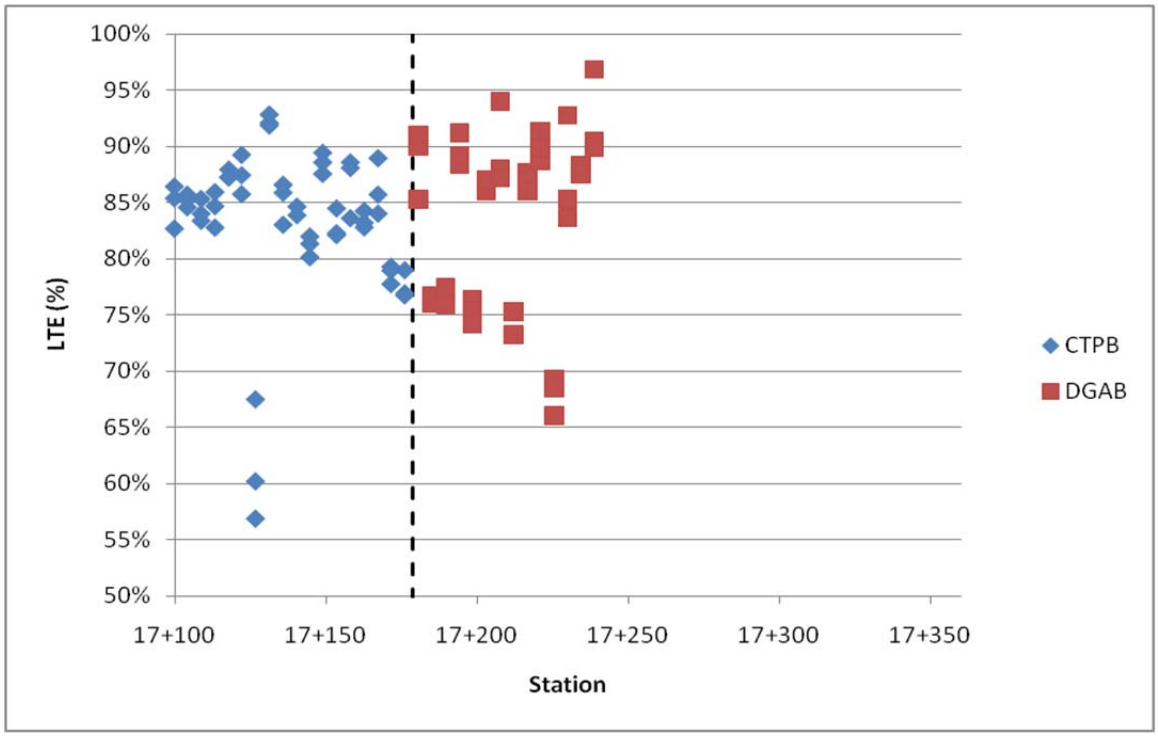

LTE approach position – Right lane

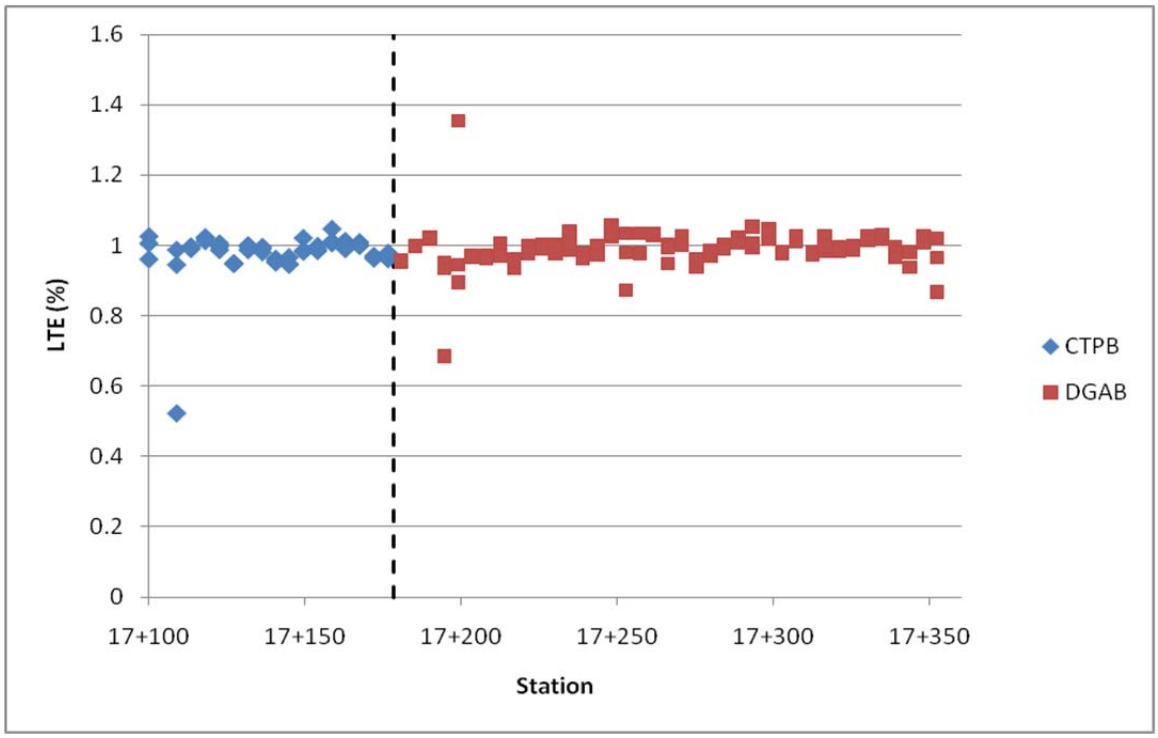

JSR – Left lane

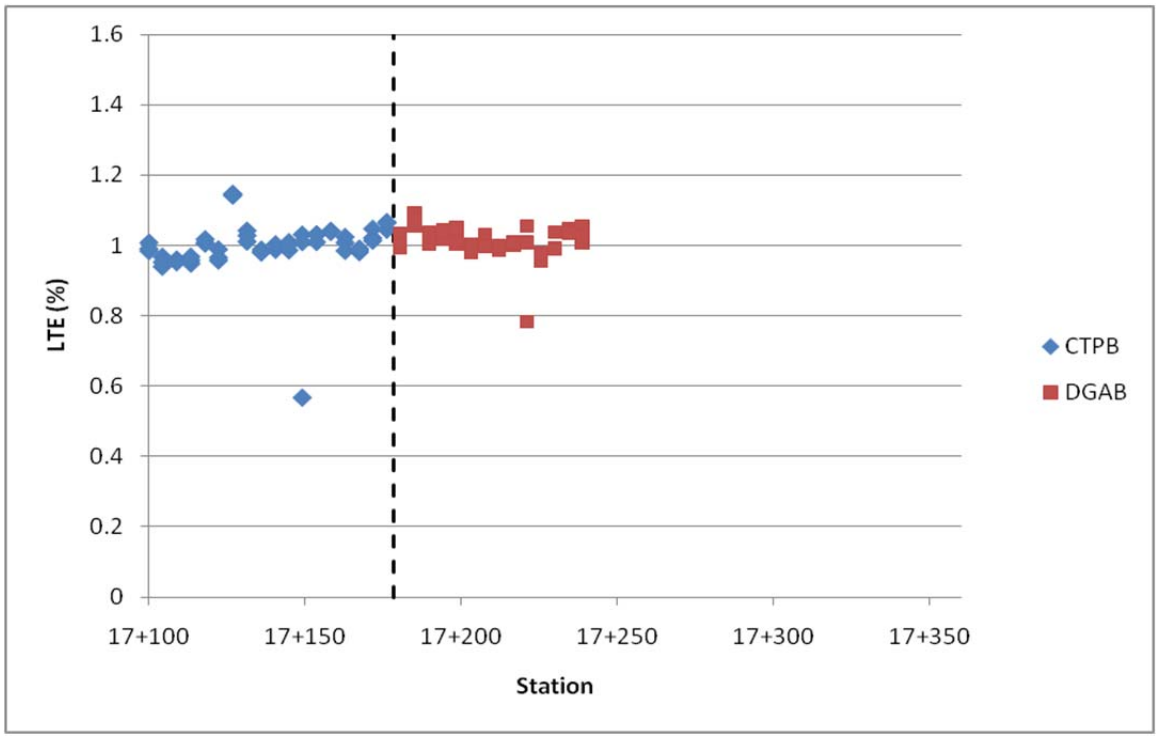

JSR – Right lane

Appendix C Supplemental Spring 2010 Truck Testing Data

Typical Strain Response – Morning Test – 8 km/h (5 mph) – Light Truck

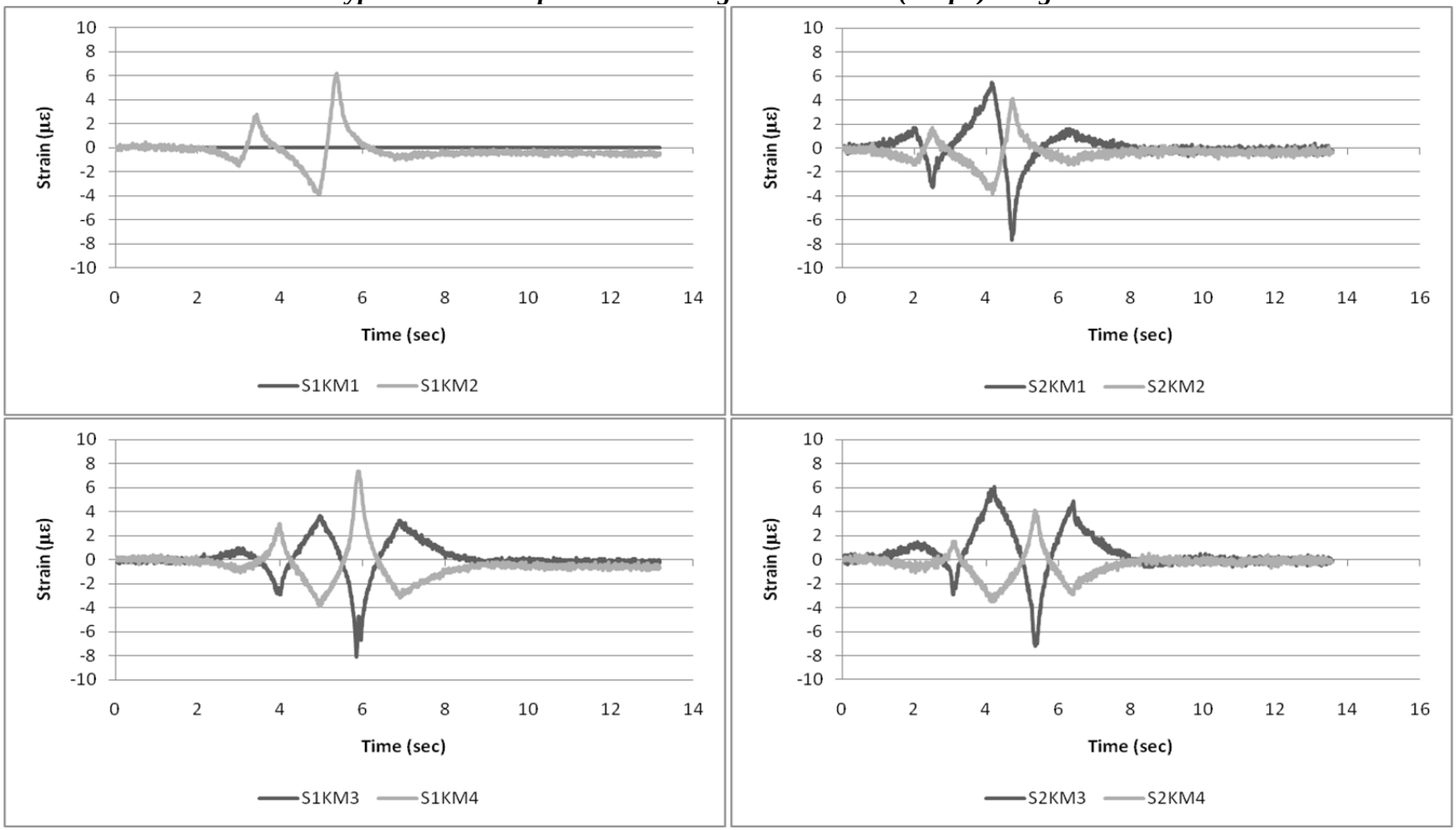

Typical Strain Response – Morning Test – 8 km/h (5 mph) – Light Truck

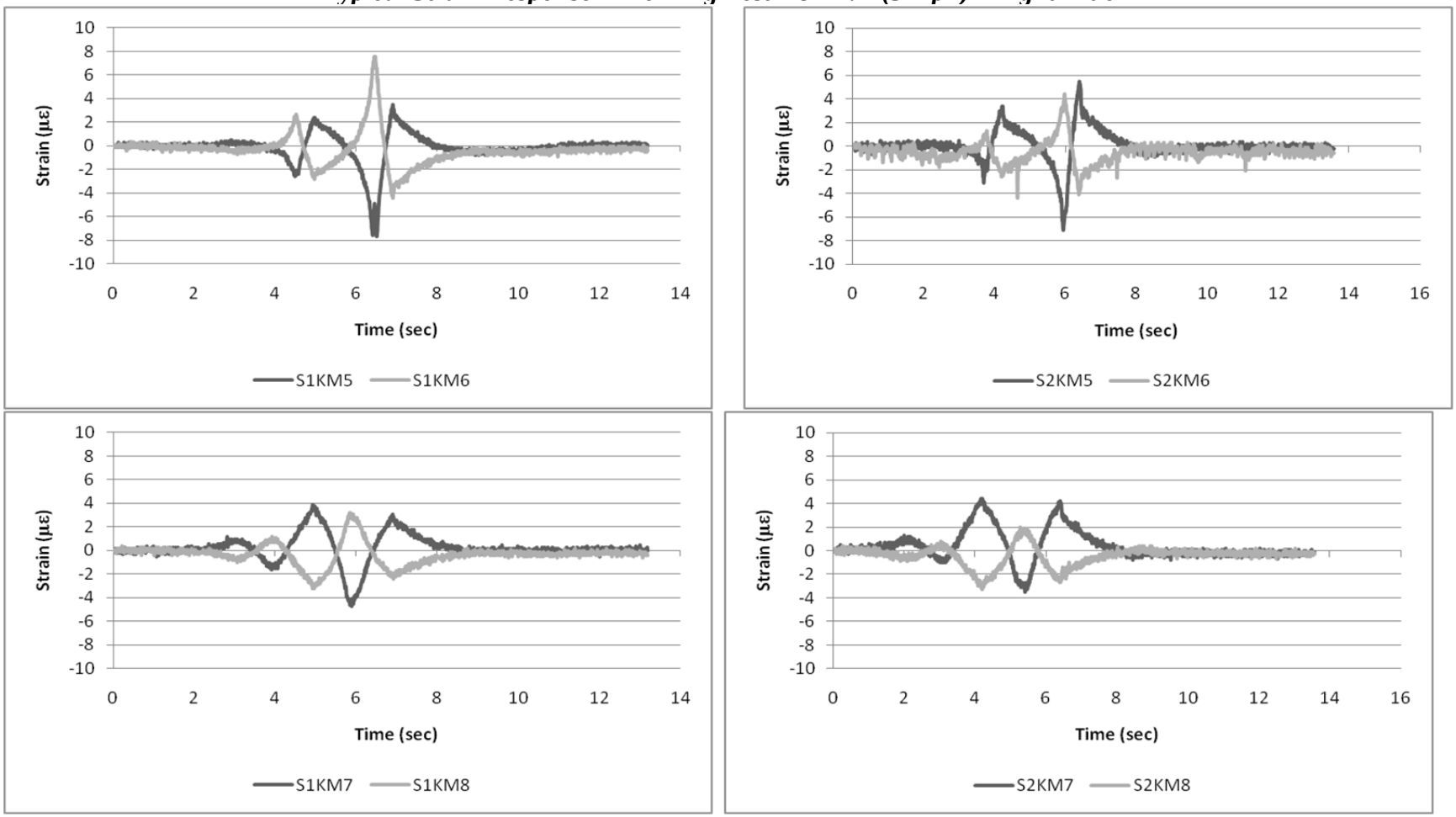

Typical Strain Response – Morning Test – 8 km/h(5 mph) – Light Truck

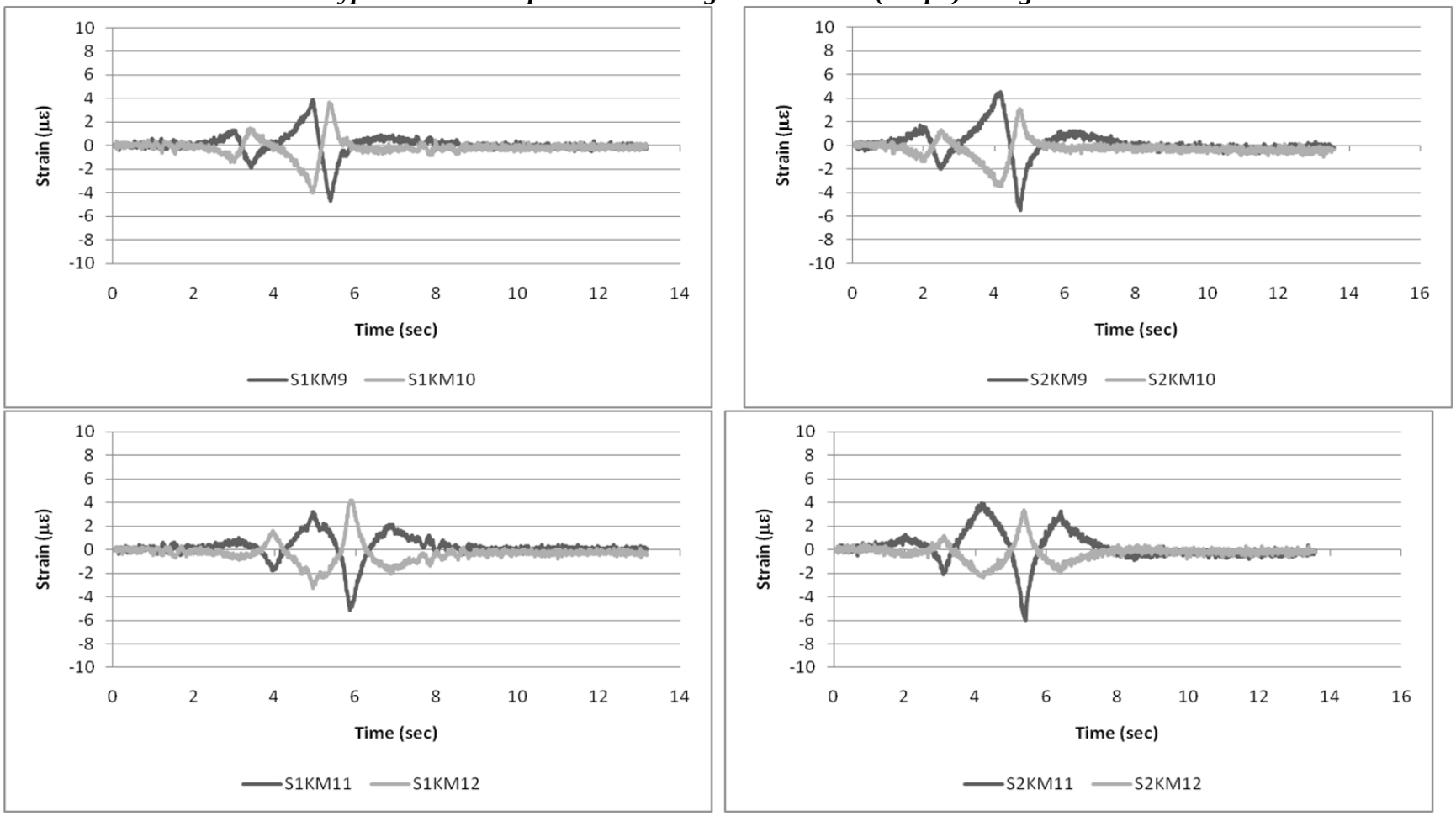

Typical Strain Response – Morning Test – 8 km/h (5 mph) – Light Truck

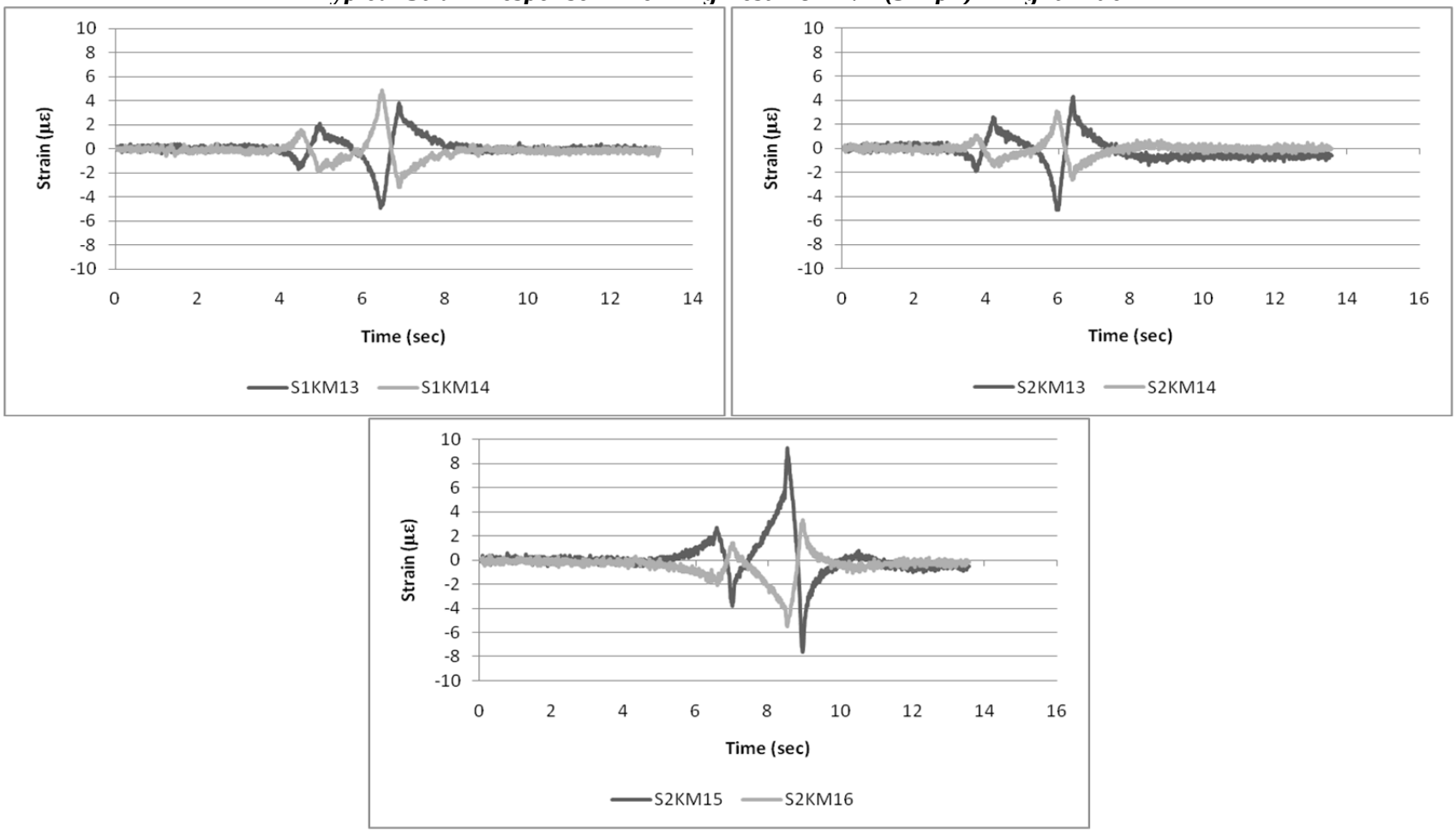

Typical Strain Response – Morning Test – 8 km/h (5mph) – Light Truck

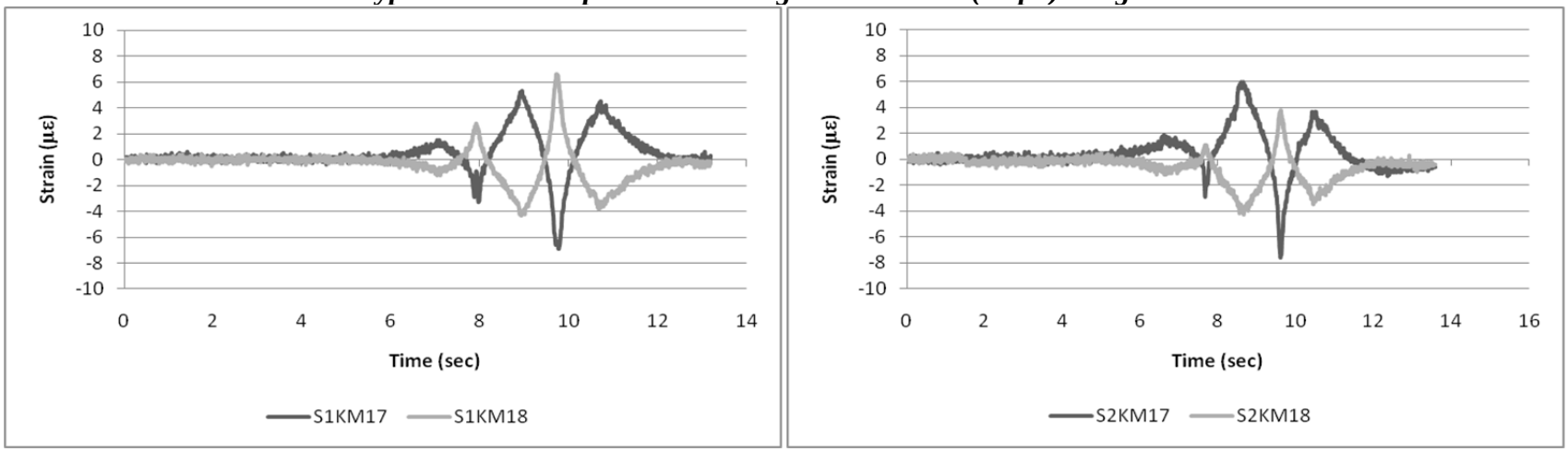

Typical Strain Response – Afternoon Test – 8 km/h (5 mph) – Light Truck

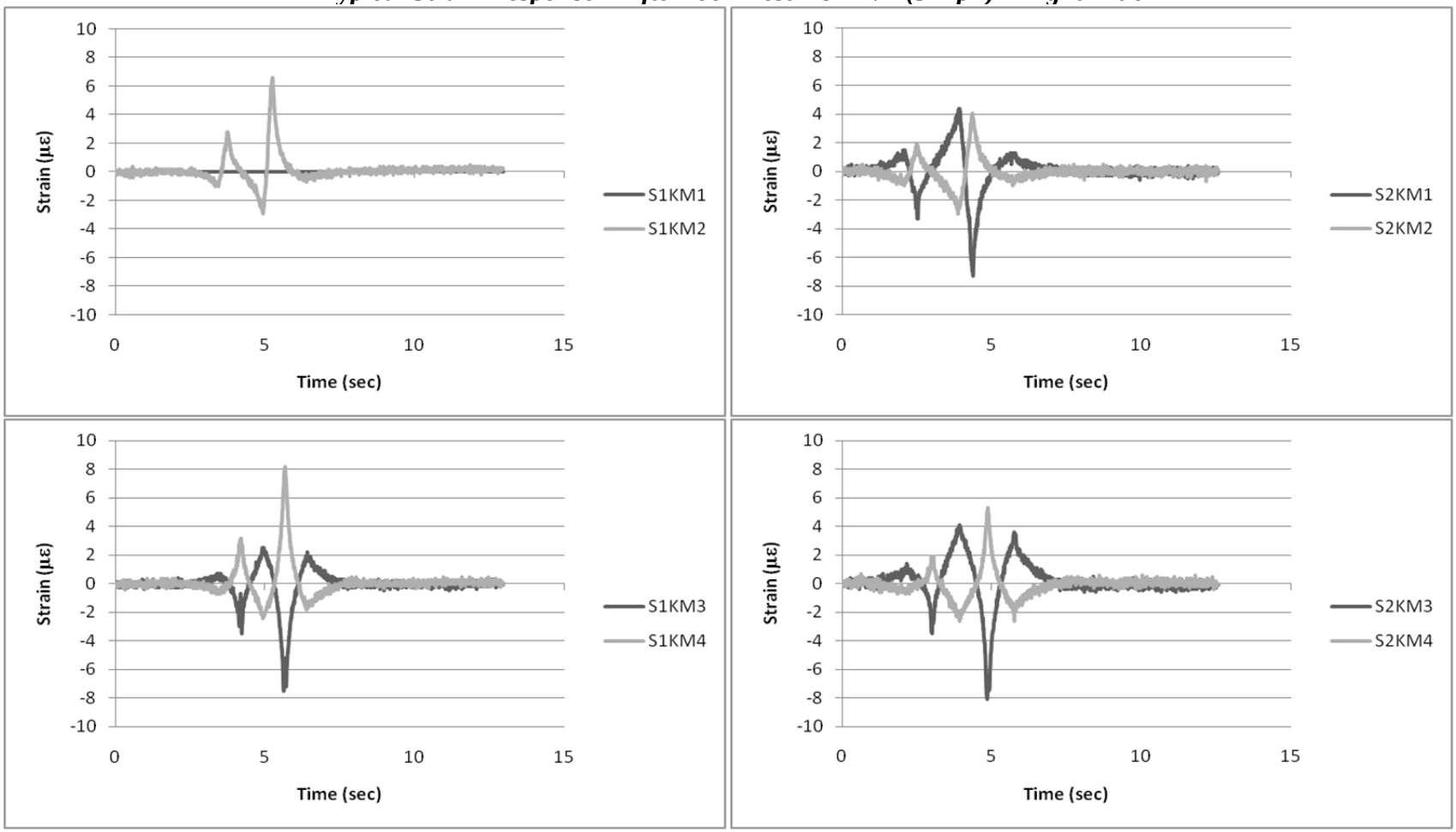

Typical Strain Response – Afternoon Test – 8 km/h (5 mph) – Light Truck

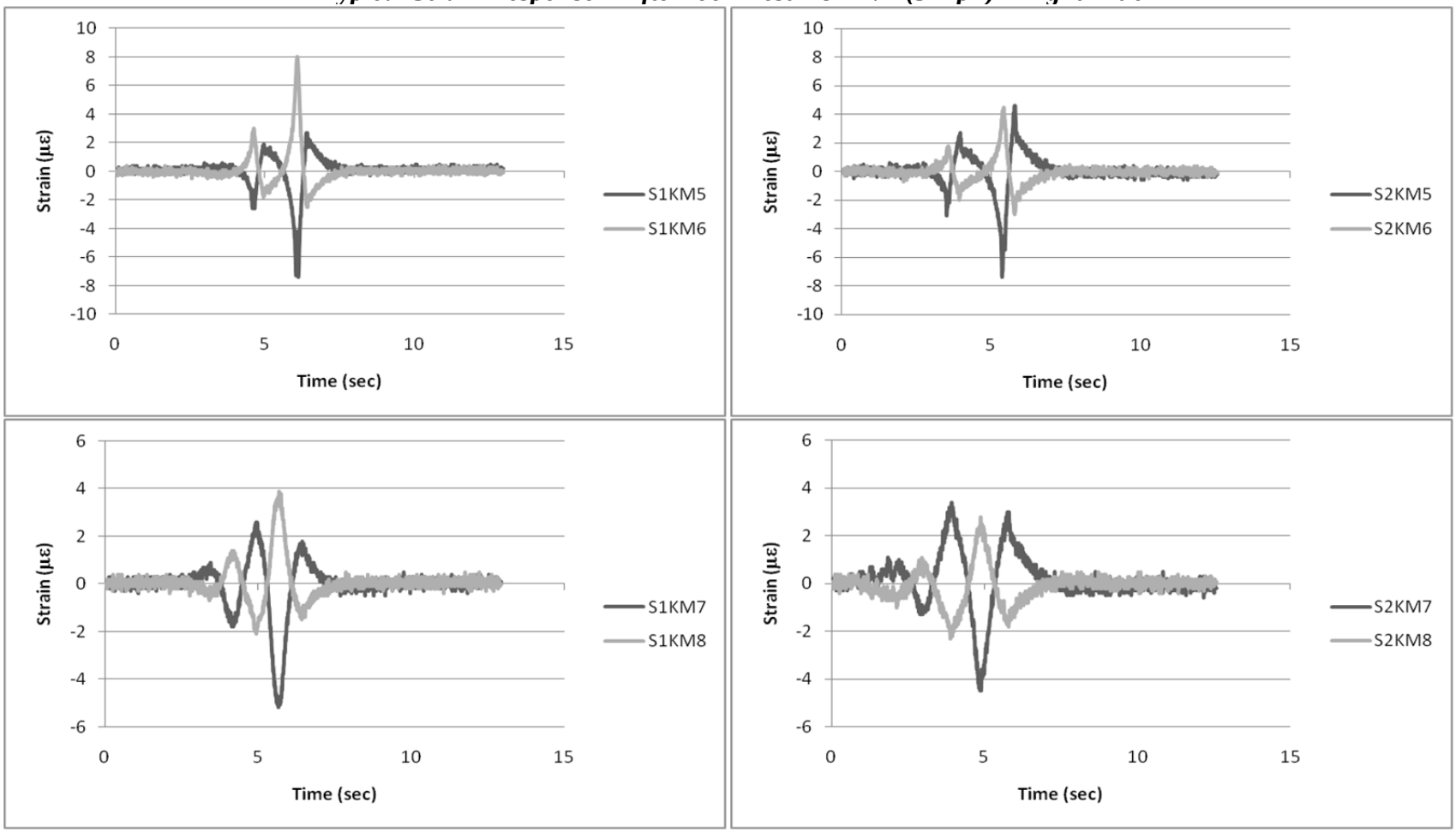

Typical Strain Response – Afternoon Test – 8 km/h (5 mph) – Light Truck

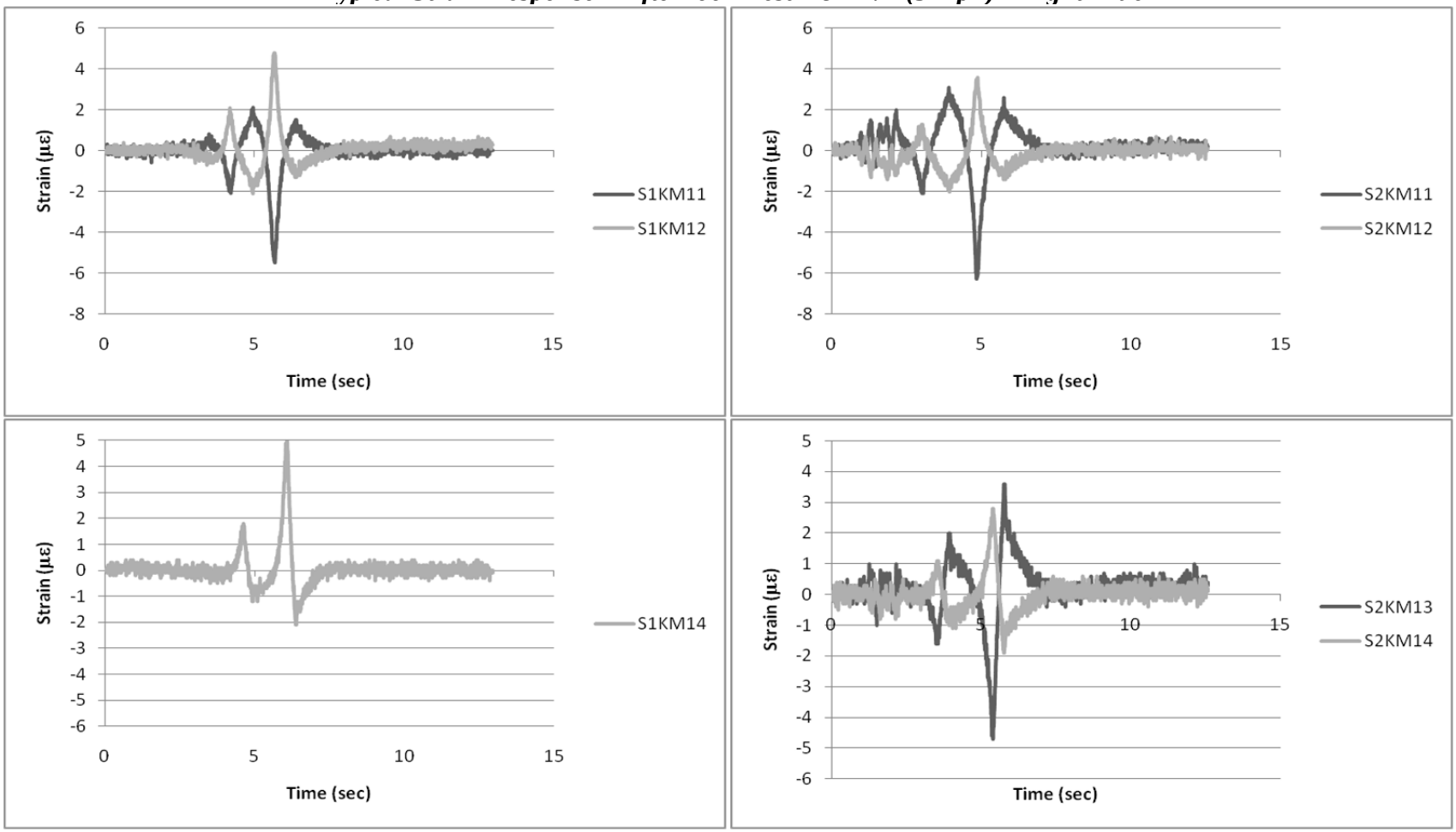

Typical Strain Response – Afternoon Test – 8 km/h (5 mph) – Light Truck

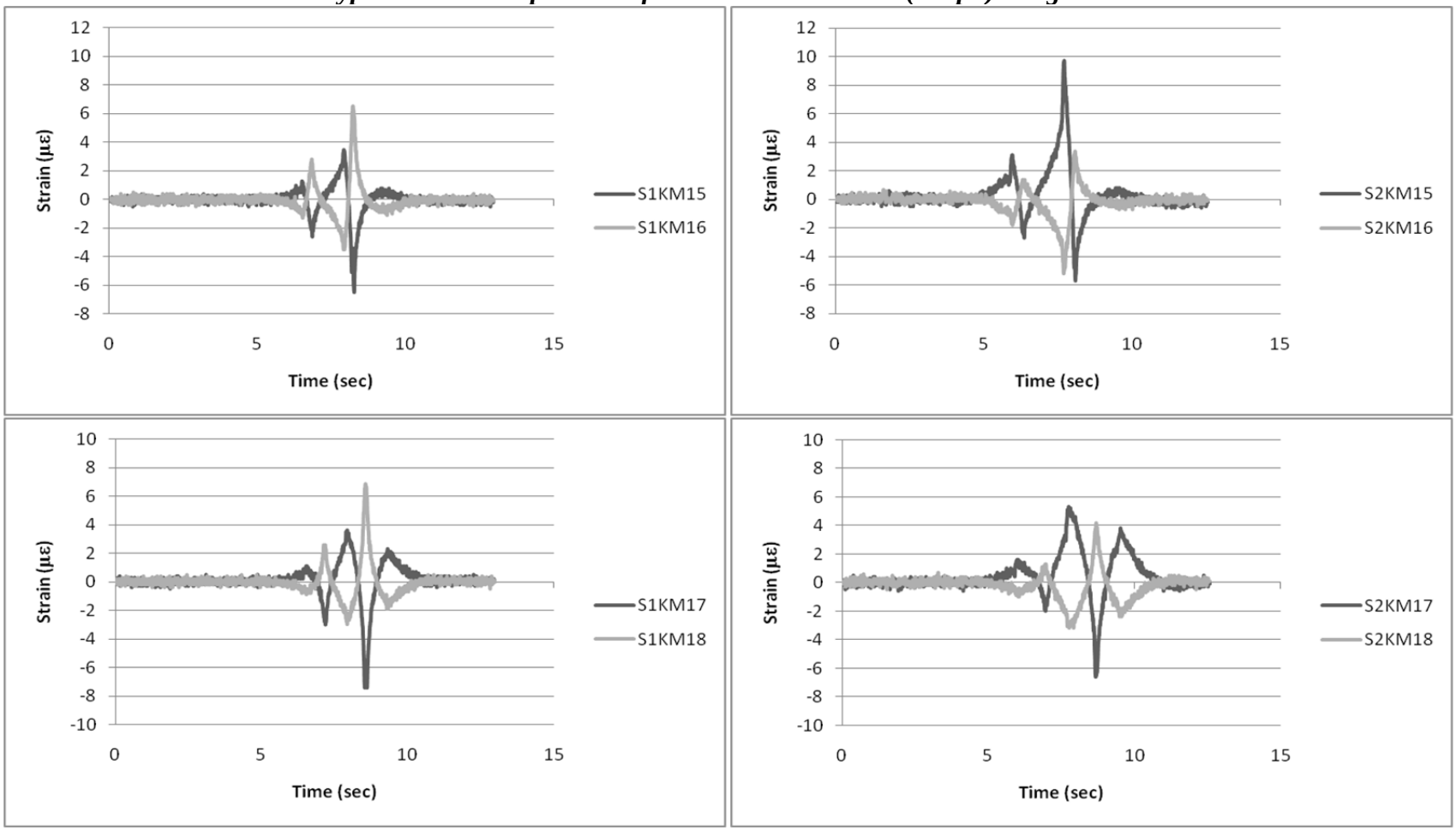

Typical Deflection Response – Morning Test – 8 km/h (5 mph) – Light Truck (1 mm =39.4 mil)

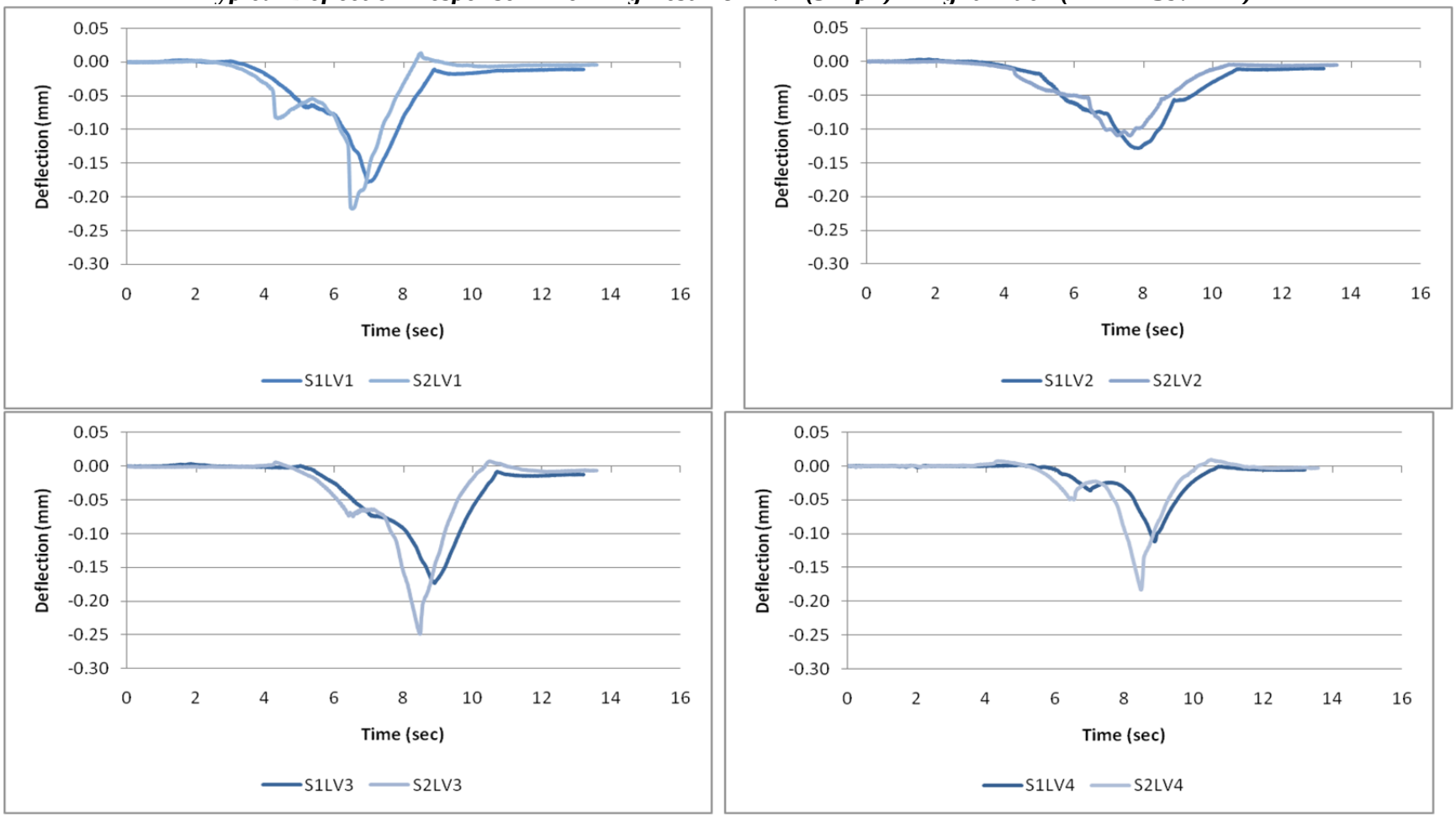

Typical Deflection Response – Morning Test – 8 km/h (5 mph) – Light Truck (1 mm =39.4 mil)

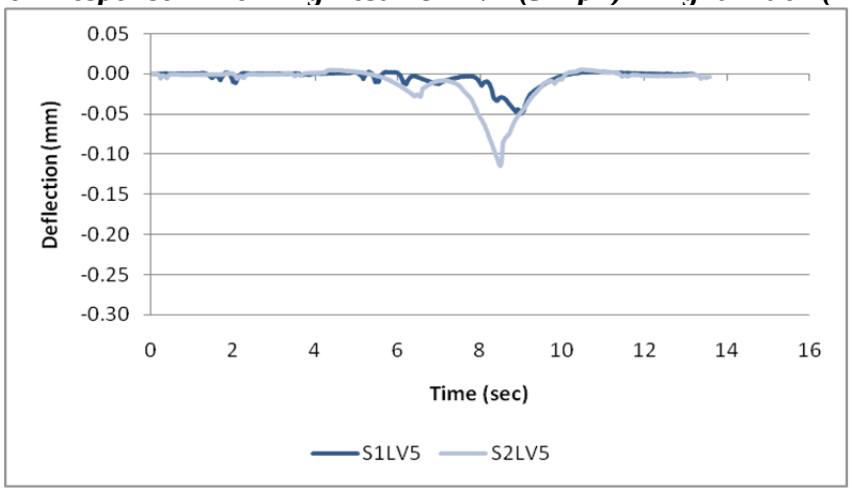

Typical Deflection Response – Afternoon Test – 8 km/h (5 mph) – Light Truck (1 mm =39.4 mil)

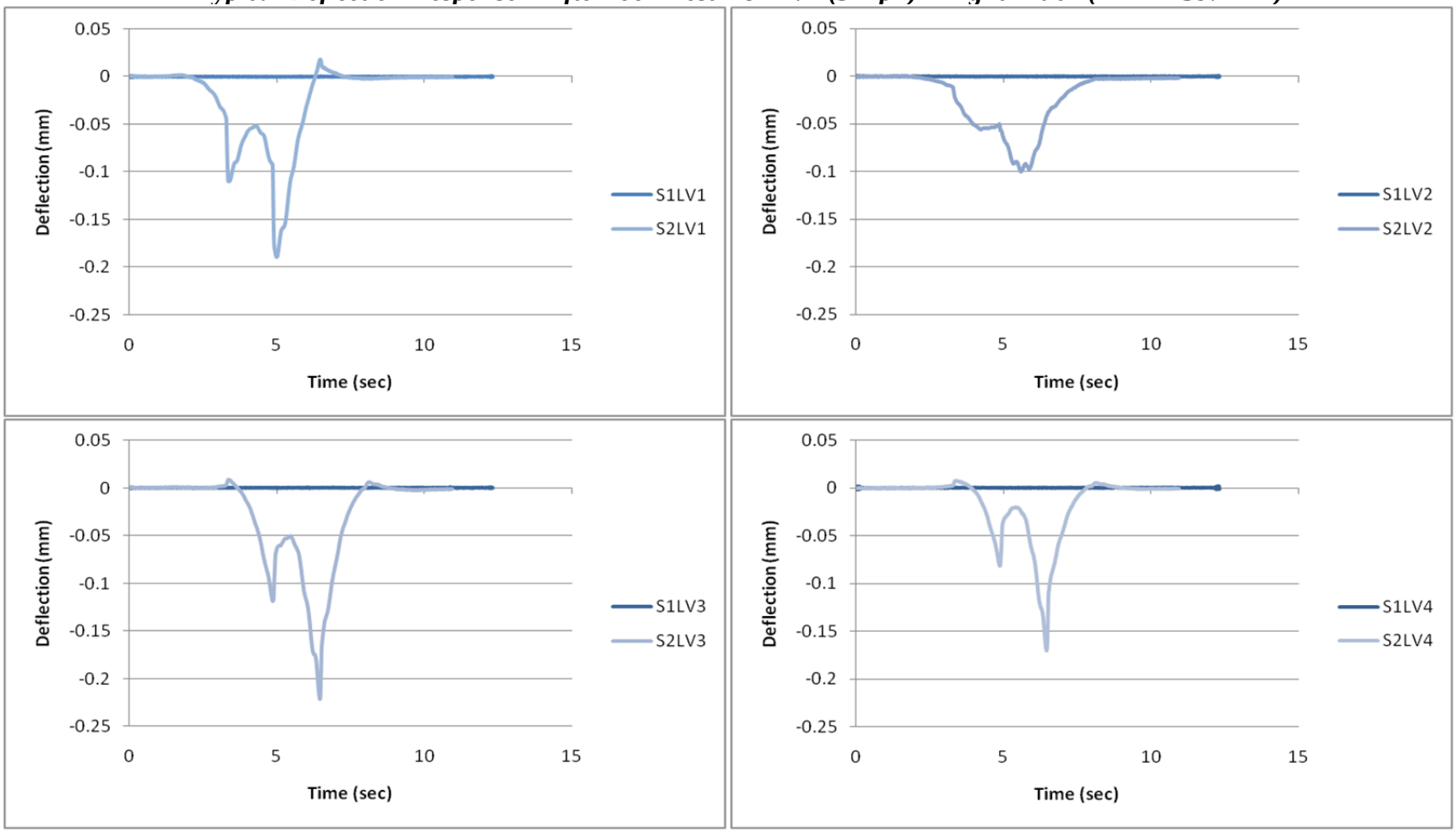

Typical Deflection Response – Afternoon Test – 8 km/h (5 mph) – Light Truck (1 mm =39.4 mil)

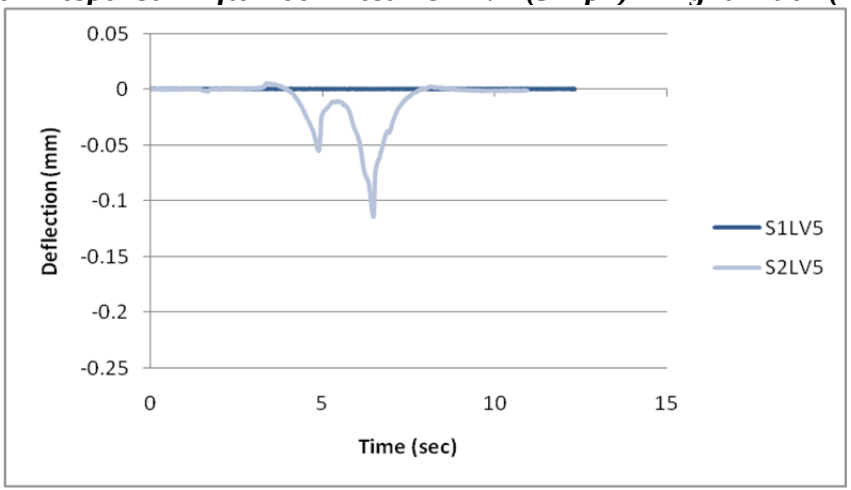

Typical Pressure Cell Response – Morning Test – 8 km/h (5 mph) – Light Truck (1 psi = 6.89 kPa)

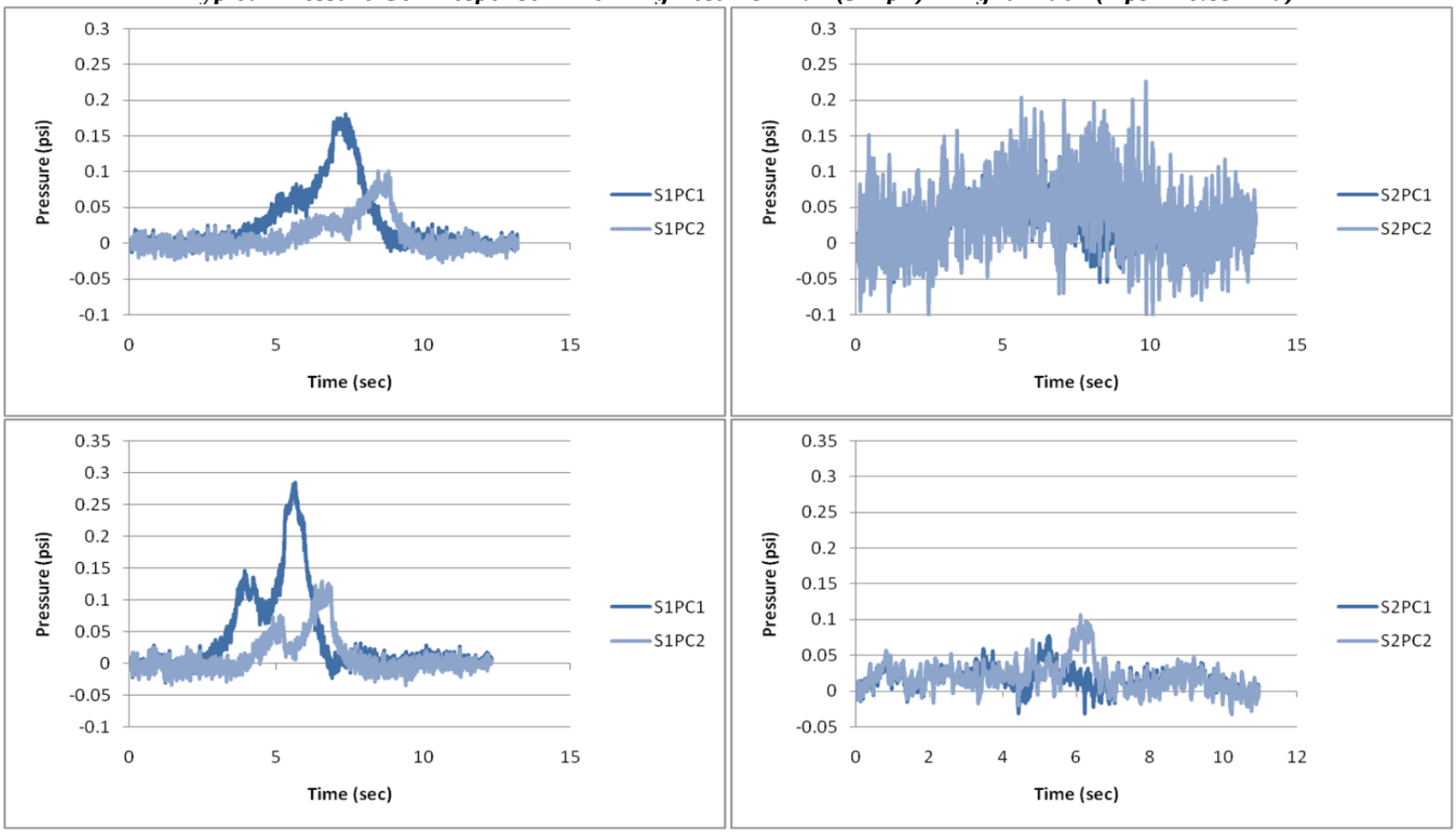

Deflection Response – Heavy Truck Load

Sensor:		**LVDT 1 (mm)**		**LVDT 2 (mm)**		**LVDT 3 (mm)**		**LVDT 4 (mm)**		**LVDT 5 (mm)**	
Section:		**1**	**2**	**1**	**2**	**1**	**2**	**1**	**2**	**1**	**2**
Speed (km/h)		**Upward**									
AM	**8**	0.0026	0.0203	0.0014	0.0017	0.0019	0.0160	0.0052	0.0145	0.0045	0.0117
	40	0.0028	0.0213	0.0014	0.0019	0.0021	0.0124	0.0029	0.0135	0.0052	0.0100
	55	0.0018	0.0207	0.0007	0.0010	0.0007	0.0158	0.0034	0.0164	0.0038	0.0123
	70	0.0021	0.0157	0.0008	0.0006	0.0019	0.0102	0.0027	0.0105	0.0021	0.0081
	-	**Downward**									
	8	-0.2269	-0.2671	-0.1736	-0.1411	-0.2191	-0.3123	-0.1391	-0.2277	-0.0582	-0.1353
	40	-0.2162	-0.2484	-0.1610	-0.1288	-0.2128	-0.2907	-0.1313	-0.2168	-0.0503	-0.1344
	55	-0.2253	-0.2947	-0.1661	-0.1254	-0.2143	-0.3047	-0.1311	-0.2221	-0.0509	-0.1312
	70	-0.1638	-0.1744	-0.1305	-0.0742	-0.1606	-0.1741	-0.1168	-0.1356	-0.0577	-0.0877
Speed (km/h)		**Upward**									
PM	**8**	0.0010	0.0144	0.0007	0.0008	0.0008	0.0091	0.0017	0.0084	0.0008	0.0066
	40	-	0.0161	-	0.0024	-	0.0116	-	0.0093	-	0.0077
	55	-	-	-	-	-	-	-	-	-	-
	70	0.0012	0.0139	0.0011	0.0008	0.0012	0.0084	0.0018	0.0069	0.0011	0.0064
	-	**Downward**									
	8	-0.0010	-0.1935	-0.0007	-0.1021	-0.0008	-0.2238	-0.0019	-0.1680	-0.0007	-0.1080
	40	-	-0.1902	-	-0.0979	-	-0.2132	-	-0.1570	-	-0.0985
	55	-0.0012	-0.1930	-0.0010	-0.0824	-0.0009	-0.1947	-0.0017	-0.1505	-0.0010	-0.0987
	70	-0.0012	-0.1784	-0.0009	-0.0734	-0.0008	-0.1666	-0.0015	-0.1303	-0.0011	-0.0823

Sensor:		LVDT 1 (mil)		LVDT 2 (mil)		LVDT 3 (mil)		LVDT 4 (mil)		LVDT 5 (mil)	
Section:		1	2	1	2	1	2	1	2	1	2
Speed (mph)		Upward									
AM	5	0.102	0.799	0.055	0.067	0.075	0.630	0.205	0.571	0.177	0.461
	25	0.110	0.839	0.055	0.075	0.083	0.488	0.114	0.531	0.205	0.394
	34	0.071	0.815	0.028	0.039	0.028	0.622	0.134	0.646	0.150	0.484
	43.5	0.083	0.618	0.031	0.024	0.075	0.402	0.106	0.413	0.083	0.319
		Downward									
	5	-8.933	-10.516	-6.835	-5.555	-8.626	-12.295	-5.476	-8.965	-2.291	-5.327
	25	-8.512	-9.780	-6.339	-5.071	-8.378	-11.445	-5.169	-8.535	-1.980	-5.291
	34	-8.870	-11.602	-6.539	-4.937	-8.437	-11.996	-5.161	-8.744	-2.004	-5.165
	43.5	-6.449	-6.866	-5.138	-2.921	-6.323	-6.854	-4.598	-5.339	-2.272	-3.453
Speed (mph)		Upward									
PM	5	0.039	0.567	0.028	0.031	0.031	0.358	0.067	0.331	0.031	0.260
	25	-	0.634	-	0.094	-	0.457	-	0.366	-	0.303
	34	-	-	-	-	-	-	-	-	-	-
	43.5	0.047	0.547	0.043	0.031	0.047	0.331	0.071	0.272	0.043	0.252
		Downward									
	5	-0.039	-7.618	-0.028	-4.020	-0.031	-8.811	-0.075	-6.614	-0.028	-4.252
	25	-	-7.488	-	-3.854	-	-8.394	-	-6.181	-	-3.878
	34	-0.047	-7.598	-0.039	-3.244	-0.035	-7.665	-0.067	-5.925	-0.039	-3.886
	43.5	-0.047	-7.024	-0.035	-2.890	-0.031	-6.559	-0.059	-5.130	-0.043	-3.240

Strain Response – Heavy Truck Test

Load Case:		LC-1 Strain (με)				LC-2 Strain (με)			
Section		Section 1		Section 2		Section 1		Section 2	
Test	Speed (km/h (mph))	KM1	KM2	KM1	KM2	KM1	KM2	KM1	KM2
AM	8 (5)	-	-4.67	7.30	-4.43	-	7.03	-7.47	4.47
	40 (25)	-	-4.40	6.87	-4.10	-	8.07	-7.80	4.67
	55 (34)	-	-4.57	7.10	-4.33	-	7.53	-7.57	4.47
	70 (43.5)	-	-4.30	4.30	-2.53	-	7.40	-5.20	3.10
PM	8 (5)	-	-3.40	5.73	-3.40	-	7.30	-7.73	4.50
	40 (25)	-	-	-	-	-	-	-	-
	55 (34)	-	-	-	-	-	-	-	-
	70 (43.5)	-	-2.83	4.63	-2.47	-	7.97	-7.60	4.60
		KM3	KM4	KM3	KM4	KM3	KM4	KM3	KM4
AM	8 (5)	4.83	-4.70	8.10	-4.60	-9.23	10.23	-9.80	5.60
	40 (25)	4.37	-4.20	7.50	-4.13	-8.30	9.37	-9.60	5.30
	55 (34)	4.63	-4.37	7.60	-4.27	-7.83	9.30	-8.00	4.60
	70 (43.5)	4.17	-4.00	4.63	-2.80	-8.57	9.87	-5.87	3.50
PM	8 (5)	3.37	-3.10	5.73	-3.23	-9.87	10.77	-10.80	6.37
	40 (25)	3.20	-3.40	5.30	-2.97	-9.40	9.70	-9.80	5.53
	55 (34)	3.20	-2.93	5.33	-2.80	-8.73	10.13	-8.93	5.00
	70 (43.5)	2.93	-2.77	4.73	-2.57	-9.40	10.83	-9.20	5.40
		KM5	KM6	KM5	KM6	KM5	KM6	KM5	KM6
AM	8 (5)	4.40	-4.10	6.70	-3.93	-8.40	9.20	-8.10	5.70
	40 (25)	4.07	-4.03	5.77	-3.63	-8.30	9.27	-8.53	5.67
	55 (34)	3.83	-3.77	6.50	-4.07	-8.37	9.87	-8.47	5.30
	70 (43.5)	3.23	-3.40	4.30	-2.50	-7.60	8.67	-5.13	3.70
PM	8 (5)	3.53	-3.23	5.37	-3.50	-8.70	9.37	-8.77	5.30
	40 (25)	-	-	-	-	-	-	-	-
	55 (34)	-	-	-	-	-	-	-	-
	70 (43.5)	2.63	-2.33	4.77	-2.67	-8.07	9.40	-8.43	5.73
		KM7	KM8	KM7	KM8	KM7	KM8	KM7	KM8
AM	8 (5)	4.83	-3.73	6.13	-4.07	-6.23	4.67	-4.80	2.87
	40 (25)	4.33	-3.47	5.73	-3.53	-5.83	4.50	-4.60	2.90
	55 (34)	4.33	-3.57	5.80	-3.67	-5.67	4.23	-3.97	2.30
	70 (43.5)	4.20	-3.37	3.80	-2.33	-6.27	4.87	-2.90	1.90
PM	8 (5)	3.40	-2.43	4.57	-2.77	-7.37	5.80	-5.60	3.47
	40 (25)	-	-	-	-	-	-	-	-
	55 (34)	-	-	-	-	-	-	-	-
	70 (43.5)	2.97	-2.33	3.63	-2.17	-7.13	5.60	-5.03	3.07

Strain Response – Heavy Truck Test

Load Case:		LC-1 Strain (με)				LC-2 Strain (με)			
Section		Section 1		Section 2		Section 1		Section 2	
Test	Speed (km/h (mph))	KM9	KM10	KM9	KM10	KM9	KM10	KM9	KM10
AM	8 (5)	4.13	-4.17	5.50	-4.43	-5.27	4.10	-5.43	2.90
	40 (25)	4.00	-4.00	5.47	-3.97	-5.23	4.23	-6.30	3.37
	55 (34)	3.73	-3.77	5.57	-4.20	-4.40	3.50	-5.77	3.27
	70 (43.5)	4.10	-4.20	3.53	-2.70	-6.70	5.20	-4.57	2.50
PM	8 (5)	13.60	-6.90	4.33	-3.17	-12.87	0.00	-5.27	3.63
	40 (25)	-	-	-	-	-	-	-	-
	55 (34)	-	-	-	-	-	-	-	-
	70 (43.5)	-	-	3.37	-2.37	-	-	-5.33	3.13
		KM11	KM12	KM11	KM12	KM11	KM12	KM11	KM12
AM	8 (5)	3.47	-3.10	5.30	-3.27	-6.27	5.50	-7.17	3.60
	40 (25)	3.03	-2.83	5.13	-2.67	-6.27	5.77	-7.17	4.03
	55 (34)	2.97	-2.77	5.20	-2.97	-5.63	4.97	-5.80	3.00
	70 (43.5)	2.93	-2.77	3.53	-1.90	-6.60	6.83	-4.83	2.67
PM	8 (5)	2.60	-2.53	3.97	-2.30	-7.23	6.50	-7.20	4.17
	40 (25)	-	-	-	-	-7.23	-	-7.20	-
	55 (34)	-	-	-	-	-	-	-	-
	70 (43.5)	2.30	-2.20	3.23	-1.83	-7.07	6.53	-6.07	3.10
		KM13	KM14	KM13	KM14	KM13	KM14	KM13	KM14
AM	8 (5)	4.37	-3.43	5.43	-3.37	-5.70	5.30	-5.27	3.17
	40 (25)	4.00	-3.13	4.90	-2.87	-5.50	5.53	-6.37	3.77
	55 (34)	3.03	-2.97	5.47	-3.07	-6.47	5.07	-5.37	3.27
	70 (43.5)	3.47	-2.87	3.63	-2.00	-6.20	6.33	-4.43	2.73
PM	8 (5)	-	-2.80	4.30	-2.23	-	5.80	-5.43	3.27
	40 (25)	-	-	-	-	-	-	-	-
	55 (34)	-	-	-	-	-	-	-	-
	70 (43.5)	2.17	-1.77	2.90	-1.93	-6.03	5.63	-5.67	3.20
		KM15	KM16	KM15	KM16	KM15	KM16	KM15	KM16
AM	8 (5)	5.80	-5.80	12.40	-6.90	-7.63	7.70	-8.30	4.27
	40 (25)	5.47	-5.27	12.33	-6.57	-6.70	7.20	-7.13	3.93
	55 (34)	5.57	-5.37	12.60	-6.63	-6.97	7.73	-7.80	3.90
	70 (43.5)	4.83	-4.77	7.63	-4.07	-5.93	6.63	-4.87	2.77
PM	8 (5)	4.60	-4.50	11.83	-6.23	-7.23	7.60	-7.37	4.00
	40 (25)	-	-	-	-	-	-	-	-
	55 (34)	-	-	-	-	-	-	-	-
	70 (43.5)	3.53	-3.53	10.50	-5.37	-6.37	7.40	-7.50	3.90

Strain Response – Heavy Truck Test

Load Case:		**LC-1 Strain (με)**				**LC-2 Strain (με)**			
Section		**Section 1**		**Section 2**		**Section 1**		**Section 2**	
Test	**Speed (km/h (mph))**	**KM17**	**KM18**	**KM17**	**KM18**	**KM17**	**KM18**	**KM17**	**KM18**
AM	**8 (5)**	6.90	-5.60	9.10	-5.67	-8.53	8.10	-8.10	4.83
	40 (25)	6.50	-5.27	8.73	-5.13	-8.90	8.37	-7.93	4.80
	55 (34)	6.33	-5.17	8.93	-5.33	-7.47	7.33	-7.10	4.30
	70 (43.5)	5.33	-4.47	5.40	-3.43	-7.13	6.80	-4.90	3.23
PM	**8 (5)**	4.60	-3.77	7.10	-4.33	-9.20	8.33	-9.23	5.20
	40 (25)	-	-	-	-	-	-	-	-
	55 (34)	-	-	-	-	-	-	-	-
	70 (43.5)	3.73	-	5.93	-	-8.33	-	-8.83	-

Strain Response – Light Truck Test

Load Case:		**LC-1 Strain (με)**				**LC-2 Strain (με)**			
Section		**Section 1**		**Section 2**		**Section 1**		**Section 2**	
Test	**Speed (km/h (mph))**	**KM1**	**KM2**	**KM1**	**KM2**	**KM1**	**KM2**	**KM1**	**KM2**
AM	**8 (5)**	-	-3.80	5.70	-3.67	-	-3.10	4.80	-3.17
	40 (25)	-	-3.37	5.60	-3.13	-	-	-	-
	55 (34)	-	-3.47	5.47	-3.13	-	-	-	-
	70 (43.5)	-	-3.27	5.03	-3.17	-	-2.47	3.67	-2.03
PM	**8 (5)**	-	6.10	-7.43	4.07	-	6.95	-7.33	4.17
	40 (25)	-	6.37	-6.63	3.70	-	-	-	-
	55 (34)	-	5.70	-5.67	3.23	-	-	-	-
	70 (43.5)	-	5.07	-5.83	3.50	-	5.53	-6.37	3.67
		KM3	**KM4**	**KM3**	**KM4**	**KM3**	**KM4**	**KM3**	**KM4**
AM	**8 (5)**	3.63	-3.63	6.10	-3.60	2.90	-2.70	4.67	-2.73
	40 (25)	3.23	-3.07	5.63	-3.13	2.37	-2.37	3.77	-2.30
	55 (34)	3.40	-3.13	5.27	-2.77	2.43	-2.07	3.83	-2.23
	70 (43.5)	3.17	-2.83	5.20	-2.90	2.17	-2.07	3.43	-1.90
PM	**8 (5)**	-7.60	7.77	-7.43	4.17	-8.65	9.45	-9.07	5.50
	40 (25)	-7.17	8.30	-7.83	4.43	-7.77	8.40	-7.83	4.33
	55 (34)	-6.43	7.63	-6.23	3.80	-7.37	8.63	-6.90	4.27
	70 (43.5)	-6.07	7.23	-6.47	3.90	-6.47	7.93	-7.43	4.20
		KM5	**KM6**	**KM5**	**KM6**	**KM5**	**KM6**	**KM5**	**KM6**
AM	**8 (5)**	3.60	-4.10	5.70	-6.70	3.10	-2.85	4.87	-3.07
	40 (25)	3.20	-3.33	4.97	-3.07	-	-	-	-
	55 (34)	2.97	-2.97	4.77	-2.07	-	-	-	-
	70 (43.5)	2.87	-2.93	4.63	-2.80	2.13	-1.97	3.43	-1.93
PM	**8 (5)**	-7.30	7.53	-6.93	4.70	-7.95	8.60	-7.63	4.63
	40 (25)	-6.57	7.30	-7.00	4.37	-	-	-	-
	55 (34)	-6.33	7.33	-5.03	3.60	-	-	-	-
	70 (43.5)	-6.00	7.40	-5.60	3.97	-6.50	7.83	-6.20	4.63
		KM7	**KM8**	**KM7**	**KM8**	**KM7**	**KM8**	**KM7**	**KM8**
AM	**8 (5)**	3.77	-3.03	4.40	-3.23	3.00	-2.40	3.80	-2.43
	40 (25)	3.53	-2.70	4.30	-2.80	-	-	-	-
	55 (34)	3.27	-2.63	4.27	-2.70	-	-	-	-
	70 (43.5)	3.23	-2.40	4.03	-2.67	2.27	-1.63	2.80	-1.70
PM	**8 (5)**	-4.77	3.33	-3.70	2.07	-6.35	4.65	-4.90	3.03
	40 (25)	-4.97	3.57	-3.50	2.17	-	-	-	-
	55 (34)	-4.73	3.40	-3.77	2.33	-	-	-	-
	70 (43.5)	-4.50	3.40	-3.37	1.97	-5.27	3.90	-4.00	2.47

Strain Response – Light Truck Test

Load Case:		LC-1 Strain (με)				LC-2 Strain (με)			
Section		**Section 1**		**Section 2**		**Section 1**		**Section 2**	
Test	**Speed (km/h (mph))**	**KM9**	**KM10**	**KM9**	**KM10**	**KM9**	**KM10**	**KM9**	**KM10**
AM	**8 (5)**	3.87	-3.87	4.57	-3.77	-	-9.90	3.97	-3.03
	40 (25)	3.40	-3.70	4.70	-3.30	-	-	-	-
	55 (34)	3.70	-3.60	5.10	-3.53	-	-	-	-
	70 (43.5)	3.37	-3.30	4.93	-3.37	-	-	2.63	-2.03
PM	**8 (5)**	-5.17	3.93	-5.70	3.00	-12.00	-	-5.57	3.67
	40 (25)	-5.47	4.17	-5.40	3.30	-	-	-	-
	55 (34)	-5.53	4.43	-5.97	3.60	-	-	-	-
	70 (43.5)	-5.23	4.40	-6.03	3.23	-	-	-5.70	3.33
		KM11	**KM12**	**KM11**	**KM12**	**KM11**	**KM12**	**KM11**	**KM12**
AM	**8 (5)**	2.97	-2.77	4.07	-2.60	2.40	-2.50	3.50	-2.13
	40 (25)	2.60	-2.07	3.97	-2.33	-	-	-	-
	55 (34)	2.87	-2.67	4.20	-2.43	-	-	-	-
	70 (43.5)	2.37	-2.03	3.97	-2.20	1.53	-1.53	2.53	-1.37
PM	**8 (5)**	-5.67	5.03	-6.37	3.20	-6.65	5.85	-7.10	4.07
	40 (25)	-5.67	5.87	-6.37	3.53	-6.65	-	-7.10	-
	55 (34)	-5.40	5.33	-6.53	3.53	-	-	-	-
	70 (43.5)	-5.33	5.70	-6.30	3.43	-5.63	5.03	-5.77	3.47
		KM13	**KM14**	**KM13**	**KM14**	**KM13**	**KM14**	**KM13**	**KM14**
AM	**8 (5)**	3.73	-3.13	4.50	-2.97	5.10	-2.50	3.77	-2.13
	40 (25)	3.13	-2.63	4.10	-2.57	-	-	-	-
	55 (34)	2.87	-3.20	4.37	-2.47	-	-	-	-
	70 (43.5)	3.03	-2.43	4.30	-2.40	2.10	-1.53	2.27	-1.53
PM	**8 (5)**	-5.33	5.20	-5.13	2.93	-16.00	5.80	-5.43	3.23
	40 (25)	-5.27	5.23	-5.23	3.33	-	-	-	-
	55 (34)	-5.13	5.07	-5.77	3.53	-	-	-	-
	70 (43.5)	-5.20	5.43	-5.03	3.23	-5.57	4.93	-5.10	2.93
		KM15	**KM16**	**KM15**	**KM16**	**KM15**	**KM16**	**KM15**	**KM16**
AM	**8 (5)**	4.70	-4.57	9.43	-5.37	4.10	-4.05	10.43	-5.60
	40 (25)	4.43	-4.30	9.23	-5.00	-	-	-	-
	55 (34)	4.73	-3.90	8.83	-4.83	-	-	-	-
	70 (43.5)	4.07	-3.73	7.97	-4.53	2.57	-2.70	8.13	-4.17
PM	**8 (5)**	-6.57	6.57	-7.30	3.57	-6.85	6.80	-6.37	3.60
	40 (25)	-6.00	6.27	-6.60	3.43	-	-	-	-
	55 (34)	-5.50	6.30	-6.20	3.27	-	-	-	-
	70 (43.5)	-5.57	6.20	-6.10	3.17	-5.47	6.47	-5.57	3.37

Strain Response – Light Truck Test

Load Case:		LC-1 Strain (με)				LC-2 Strain (με)			
Section		Section 1		Section 2		Section 1		Section 2	
Test	Speed (km/h (mph))	KM17	KM18	KM17	KM18	KM17	KM18	KM17	KM18
AM	8 (5)	5.17	-4.17	6.20	-4.03	4.10	-3.30	5.73	-3.63
	40 (25)	4.83	-3.67	6.30	-3.77	-	-	-	-
	55 (34)	4.70	-3.47	5.90	-3.43	-	-	-	-
	70 (43.5)	4.33	-3.23	5.50	-3.40	2.50	-	4.43	-
PM	8 (5)	-7.40	6.77	-7.33	4.10	-8.50	7.55	-7.40	4.47
	40 (25)	-7.03	6.27	-6.37	4.00	-	-	-	-
	55 (34)	-6.33	6.47	-5.97	3.30	-	-	-	-
	70 (43.5)	-6.27	6.30	-6.10	3.73	-7.00	-	-6.20	-

Appendix D Supplemental Fall 2010 Truck Testing Data

Deflection Response – Heavy Truck Load

Deflection (mm):		S1LV1	S2LV1	S1LV2	S2LV2	S1LV3	S2LV3	S1LV4	S2LV4	S1LV5	S2LV5
Speed (km/h)		**Upward**									
AM 1	**8**	0.0032	0.0311	0.0020	0.0008	0.0023	0.0154	0.0046	0.0157	0.0042	0.0121
	40	0.0021	0.0316	0.0012	0.0011	0.0009	0.0173	0.0042	0.0187	0.0045	0.0136
		Downward									
	8	-0.2069	-0.2679	-0.1485	-0.1207	-0.2177	-0.2847	-0.1332	-0.2228	-0.0575	-0.1302
	40	-0.1955	-0.2684	-0.1452	-0.1243	-0.2262	-0.2759	-0.1312	-0.2117	-0.0531	-0.1201
Speed (km/h)		**Upward**									
AM 2	**8**	0.0015	0.0276	0.0007	0.0009	0.0010	0.0130	0.0027	0.0126	0.0028	0.0084
	40	0.0014	0.0201	0.0007	0.0016	0.0006	0.0130	0.0019	0.0124	0.0017	0.0083
	70	0.0029	0.0166	0.0007	0.0008	0.0017	0.0113	0.0016	0.0100	0.0008	0.0073
		Downward									
	8	-0.1814	-0.2188	-0.1257	-0.0979	-0.1819	-0.2322	-0.1155	-0.1963	-0.0552	-0.1259
	40	-0.1490	-0.2079	-0.0937	-0.0998	-0.1316	-0.2134	-0.0937	-0.1663	-0.0422	-0.1002
	70	-0.1173	-0.2110	-0.0654	-0.0867	-0.0923	-0.1763	-0.0792	-0.1381	-0.0363	-0.0820
Speed (km/h)		**Upward**									
PM	**8**	0.0008	0.0025	0.0008	0.0006	0.0009	0.0016	0.0008	0.0008	0.0008	0.0010
	40	0.0008	0.0023	0.0006	0.0008	0.0008	0.0019	0.0008	0.0011	0.0010	0.0011
	70	0.0008	0.0005	0.0007	0.0008	0.0008	0.0012	0.0007	0.0016	0.0006	0.0042
		Downward									
	8	-0.0387	-0.0582	-0.0433	-0.0320	-0.0439	-0.0591	-0.0678	-0.0908	-0.0354	-0.0666
	40	-0.0370	-0.0586	-0.0379	-0.0328	-0.0426	-0.0585	-0.0656	-0.0858	-0.0318	-0.0679
	70	-0.0393	-0.0701	-0.0436	-0.0390	-0.0461	-0.0594	-0.0647	-0.0747	-0.0295	-0.0433

Deflection (mil):		S1LV1	S2LV1	S1LV2	S2LV2	S1LV3	S2LV3	S1LV4	S2LV4	S1LV5	S2LV5
Speed (mph)		Upward									
AM 1	5	0.126	1.224	0.079	0.031	0.091	0.606	0.181	0.618	0.165	0.476
	25	0.083	1.244	0.047	0.043	0.035	0.681	0.165	0.736	0.177	0.535
		Downward									
	5	-8.146	-10.547	-5.846	-4.752	-8.571	-11.209	-5.244	-8.772	-2.264	-5.126
	25	-7.697	-10.567	-5.717	-4.894	-8.906	-10.862	-5.165	-8.335	-2.091	-4.728
Speed (mph)		Upward									
AM 2	5	0.059	1.087	0.028	0.035	0.039	0.512	0.106	0.496	0.110	0.331
	25	0.055	0.791	0.028	0.063	0.024	0.512	0.075	0.488	0.067	0.327
	43.5	0.114	0.654	0.028	0.031	0.067	0.445	0.063	0.394	0.031	0.287
		Downward									
	5	-7.142	-8.614	-4.949	-3.854	-7.161	-9.142	-4.547	-7.728	-2.173	-4.957
	25	-5.866	-8.185	-3.689	-3.929	-5.181	-8.402	-3.689	-6.547	-1.661	-3.945
	43.5	-4.618	-8.307	-2.575	-3.413	-3.634	-6.941	-3.118	-5.437	-1.429	-3.228
Speed (mph)		Upward									
PM	5	0.031	0.098	0.031	0.024	0.035	0.063	0.031	0.031	0.031	0.039
	25	0.031	0.091	0.024	0.031	0.031	0.075	0.031	0.043	0.039	0.043
	43.5	0.031	0.020	0.028	0.031	0.031	0.047	0.028	0.063	0.024	0.165
		Downward									
	5	-1.524	-2.291	-1.705	-1.260	-1.728	-2.327	-2.669	-3.575	-1.394	-2.622
	25	-1.457	-2.307	-1.492	-1.291	-1.677	-2.303	-2.583	-3.378	-1.252	-2.673
	43.5	-1.547	-2.760	-1.717	-1.535	-1.815	-2.339	-2.547	-2.941	-1.161	-1.705

Strain Response – Heavy Truck Test

Load Case:		LC-1 Strain (με)				LC-2 Strain (με)			
Section		Section 1		Section 2		Section 1		Section 2	
Test	Speed (km/h (mph))	KM1	KM2	KM1	KM2	KM1	KM2	KM1	KM2
AM 1	8 (5)	5.88	-5.15	7.00	-4.17	-7.70	7.43	-8.53	5.00
	40 (25)	5.23	-4.70	6.40	-3.67	-7.63	7.17	-7.87	4.63
AM 2	70 (43.5)	3.83	-3.33	5.47	-2.93	-7.30	6.93	-8.23	4.40
PM	8 (5)	2.73	-2.47	3.17	-2.03	-8.60	8.27	-8.30	4.83
	40 (25)	2.70	-2.13	3.40	-2.10	-8.13	8.17	-8.13	4.80
	70 (43.5)	2.60	-2.23	3.57	-1.90	-7.83	7.93	-8.83	4.93
		KM3	KM4	KM3	KM4	KM3	KM4	KM3	KM4
AM 1	8 (5)	5.00	-4.73	8.27	-4.73	-7.83	8.85	-8.80	4.53
	40 (25)	4.47	-4.20	7.93	-4.33	-7.47	8.90	-9.33	4.93
AM 2	70 (43.5)	3.27	-2.93	5.23	-2.83	-7.57	8.90	-8.23	4.53
PM	8 (5)	2.20	-2.07	2.97	-1.80	-9.67	10.47	-9.37	5.30
	40 (25)	1.93	-1.93	3.10	-1.77	-9.30	10.03	-10.23	5.60
	70 (43.5)	2.10	-1.83	3.13	-1.67	-9.33	10.33	-8.87	4.97
		KM5	KM6	KM5	KM6	KM5	KM6	KM5	KM6
AM 1	8 (5)	4.90	-4.50	8.13	-4.83	-7.93	8.58	-6.87	4.40
	40 (25)	4.37	-4.03	7.33	-4.23	-7.50	8.13	-6.33	4.83
AM 2	70 (43.5)	3.23	-2.67	5.80	-3.47	-7.57	8.43	-5.63	4.77
PM	8 (5)	2.57	-2.03	4.03	-2.17	-9.07	9.03	-8.00	5.07
	40 (25)	2.23	-1.87	3.60	-1.63	-8.23	8.07	-8.40	5.70
	70 (43.5)	2.17	-1.63	4.03	-1.80	-8.20	8.80	-6.43	5.27
		KM7	KM8	KM7	KM8	KM7	KM8	KM7	KM8
AM 1	8 (5)	4.95	-3.78	2.77	-1.87	-5.33	3.78	-1.83	1.00
	40 (25)	4.30	-3.30	2.37	-1.53	-5.50	3.90	-1.87	1.00
AM 2	70 (43.5)	2.97	-2.10	1.80	-0.97	-5.63	4.47	-1.93	1.00
PM	8 (5)	2.17	-1.60	1.27	-0.93	-7.53	5.67	-2.17	1.57
	40 (25)	2.07	-1.70	1.17	-0.77	-7.27	5.67	-2.40	1.60
	70 (43.5)	1.80	-1.53	1.23	-0.70	-7.30	5.97	-2.07	1.33
		KM9	KM10	KM9	KM10	KM9	KM10	KM9	KM10
AM 1	8 (5)	3.80	-3.50	2.33	-1.87	-4.58	5.77	-2.10	1.13
	40 (25)	3.30	-3.97	2.03	-1.53	-3.97	2.43	-1.77	0.93
AM 2	70 (43.5)	2.10	-1.90	1.27	-1.10	-3.33	2.80	-1.47	0.90
PM	8 (5)	1.70	-2.47	0.73	-1.07	-5.33	3.70	-1.23	1.57
	40 (25)	1.47	-1.83	0.77	-0.90	-5.43	4.20	-1.23	1.30
	70 (43.5)	1.13	-1.10	0.53	-0.67	-4.30	3.70	-1.03	1.03

Strain Response – Heavy Truck Test

Load Case:		LC-1 Strain (με)				LC-2 Strain (με)			
Section		Section 1		Section 2		Section 1		Section 2	
Test	Speed (km/h (mph))	KM11	KM12	KM11	KM12	KM11	KM12	KM11	KM12
AM 1	8 (5)	3.43	-2.93	2.40	-1.50	-4.85	4.08	-2.60	1.33
	40 (25)	2.83	-2.57	2.00	-1.23	-5.10	4.40	-2.17	1.17
AM 2	70 (43.5)	1.80	-1.83	1.53	-0.80	-4.27	4.13	-1.93	1.23
PM	8 (5)	1.67	-1.50	1.17	-0.87	-6.33	5.97	-3.07	1.83
	40 (25)	1.43	-1.27	1.10	-0.73	-6.77	6.40	-3.10	1.77
	70 (43.5)	1.27	-0.97	1.00	-0.63	-5.90	5.67	-2.20	1.17
		KM13	KM14	KM13	KM14	KM13	KM14	KM13	KM14
AM 1	8 (5)	4.58	-3.65	2.67	-1.40	-4.63	4.08	-2.00	1.23
	40 (25)	3.90	-3.07	2.13	-1.17	-4.97	3.83	-1.73	1.13
AM 2	70 (43.5)	2.70	-1.53	1.47	-1.00	-4.03	3.67	-1.67	1.17
PM	8 (5)	2.17	-1.33	1.40	-0.83	-5.77	5.13	-2.50	1.60
	40 (25)	2.13	-1.27	1.13	-0.70	-5.13	4.47	-2.40	1.63
	70 (43.5)	1.53	-1.00	0.87	-0.63	-4.87	4.23	-1.77	1.27
		KM15	KM16	KM15	KM16	KM15	KM16	KM15	KM16
AM 1	8 (5)	6.25	-5.78	13.43	-6.70	-6.23	6.45	-7.50	3.67
	40 (25)	6.17	-5.87	13.70	-6.47	-6.33	6.23	-7.43	3.87
AM 2	70 (43.5)	4.30	-4.13	11.53	-5.43	-5.90	6.30	-7.10	3.47
PM	8 (5)	2.87	-2.57	6.63	-3.10	-6.70	8.17	-7.90	4.17
	40 (25)	2.93	-2.50	6.57	-3.23	-5.87	6.87	-8.40	4.13
	70 (43.5)	2.43	-2.23	6.13	-2.97	-6.50	7.50	-8.27	4.13
		KM17	KM18	KM17	KM18	KM17	KM18	KM17	KM18
AM 1	8 (5)	6.50	-5.03	8.70	-5.17	-7.63	6.78	-7.87	4.57
	40 (25)	6.23	-4.50	9.00	-5.27	-7.40	6.60	-6.73	4.27
AM 2	70 (43.5)	4.13	-3.07	6.33	-3.73	-6.97	6.37	-7.07	4.90
PM	8 (5)	2.47	-1.87	3.53	-1.97	-9.57	8.80	-8.13	5.37
	40 (25)	2.27	-1.83	3.33	-2.17	-9.20	7.97	-7.50	4.70
	70 (43.5)	2.27	-	3.13	-	-8.83	-	-7.93	-

Strain Response – Light Truck Test

Load Case:		LC-1 Strain (με)				LC-2 Strain (με)			
Section		Section 1		Section 2		Section 1		Section 2	
Test	Speed (km/h (mph))	KM1	KM2	KM1	KM2	KM1	KM2	KM1	KM2
AM 1	8 (5)	5.05	-4.50	6.03	-3.63	-7.10	6.63	-7.75	4.53
	40 (25)	4.67	-4.23	5.73	-3.30	-6.77	6.33	-6.97	4.13
AM 2	70 (43.5)	3.53	-2.97	4.47	-2.83	-6.03	5.90	-7.37	4.20
PM	8 (5)	2.60	-2.23	2.70	-1.77	-7.93	7.77	-7.10	4.13
	40 (25)	2.40	-2.07	2.83	-1.87	-7.07	7.17	-7.63	4.60
	70 (43.5)	2.43	-2.03	2.93	-1.67	-6.53	7.00	-7.00	4.17
		KM3	KM4	KM3	KM4	KM3	KM4	KM3	KM4
AM 1	8 (5)	4.30	-4.00	7.00	-3.78	-7.40	7.78	-8.33	4.30
	40 (25)	3.73	-3.63	6.37	-3.63	-7.60	7.87	-7.57	4.00
AM 2	70 (43.5)	2.60	-2.47	4.53	-2.50	-6.70	7.63	-7.57	4.23
PM	8 (5)	1.93	-1.70	2.47	-1.50	-9.23	9.47	-7.60	4.67
	40 (25)	1.73	-1.53	2.67	-1.47	-8.97	9.27	-8.47	4.97
	70 (43.5)	2.00	-1.57	2.80	-1.50	-7.57	8.80	-7.97	4.43
		KM5	KM6	KM5	KM6	KM5	KM6	KM5	KM6
AM 1	8 (5)	4.40	-4.20	7.65	-4.50	-7.78	7.55	-6.60	4.03
	40 (25)	3.97	-3.87	6.93	-4.13	-7.80	7.70	-6.47	3.83
AM 2	70 (43.5)	2.73	-2.67	5.20	-2.97	-6.70	7.20	-6.07	4.30
PM	8 (5)	2.37	-1.70	3.43	-1.87	-8.23	8.10	-7.17	4.33
	40 (25)	1.93	-1.73	3.43	-1.73	-7.97	7.63	-7.50	4.97
	70 (43.5)	2.40	-1.53	3.43	-1.67	-7.03	7.63	-7.07	4.63
		KM7	KM8	KM7	KM8	KM7	KM8	KM7	KM8
AM 1	8 (5)	4.13	-3.33	2.40	-1.70	-4.95	3.45	-1.68	0.98
	40 (25)	3.80	-2.93	2.13	-1.30	-5.00	3.27	-1.83	1.13
AM 2	70 (43.5)	2.50	-1.73	1.60	-1.00	-4.90	3.57	-1.60	1.07
PM	8 (5)	1.93	-1.60	1.03	-0.80	-6.73	5.17	-2.17	1.57
	40 (25)	1.80	-1.40	0.97	-0.70	-6.63	4.93	-1.90	1.33
	70 (43.5)	1.93	-1.37	0.90	-0.70	-6.20	4.67	-1.83	1.27
		KM9	KM10	KM9	KM10	KM9	KM10	KM9	KM10
AM 1	8 (5)	4.03	-3.27	2.45	-1.98	-5.28	5.30	-2.60	1.48
	40 (25)	3.43	-3.27	2.20	-1.63	-4.13	3.47	-2.40	1.40
AM 2	70 (43.5)	2.20	-3.37	1.27	-1.07	-4.17	2.50	-1.87	1.33
PM	8 (5)	1.87	-2.07	0.83	-0.93	-6.17	4.93	-1.43	1.80
	40 (25)	1.60	-1.87	0.77	-1.00	-5.47	4.17	-1.13	1.63
	70 (43.5)	1.63	-1.80	0.53	-0.77	-4.40	3.53	-1.37	1.33

Strain Response – Light Truck Test

Load Case:		LC-1 Strain (με)				LC-2 Strain (με)			
Section		Section 1		Section 2		Section 1		Section 2	
Test	Speed (km/h (mph))	KM11	KM12	KM11	KM12	KM11	KM12	KM11	KM12
AM 1	8 (5)	3.28	-2.88	2.15	-1.38	-5.73	5.15	-2.93	1.73
	40 (25)	2.67	-2.50	1.97	-1.23	-4.97	4.23	-3.03	1.53
AM 2	70 (43.5)	1.73	-1.57	1.43	-0.77	-4.73	4.37	-2.33	1.47
PM	8 (5)	1.50	-1.47	1.07	-0.80	-7.40	7.13	-3.30	2.13
	40 (25)	1.47	-1.23	1.00	-0.77	-7.27	7.10	-2.90	1.87
	70 (43.5)	1.43	-1.27	1.07	-0.80	-5.87	5.73	-2.60	1.63
		KM13	KM14	KM13	KM14	KM13	KM14	KM13	KM14
AM 1	8 (5)	5.08	-3.88	2.78	-1.53	-5.10	4.95	-2.63	1.50
	40 (25)	4.00	-3.13	2.70	-1.37	-4.60	4.23	-2.63	1.63
AM 2	70 (43.5)	2.53	-1.73	1.57	-0.97	-4.40	4.00	-2.10	1.17
PM	8 (5)	2.50	-1.33	1.33	-0.83	-6.70	5.83	-2.73	1.73
	40 (25)	1.90	-1.23	1.30	-0.67	-6.33	5.57	-2.53	1.73
	70 (43.5)	1.83	-1.03	1.03	-0.57	-5.10	4.53	-2.37	1.33
		KM15	KM16	KM15	KM16	KM15	KM16	KM15	KM16
AM 1	8 (5)	5.65	-5.65	12.20	-6.10	-5.78	6.03	-7.20	3.43
	40 (25)	5.43	-5.07	11.67	-5.73	-5.93	5.87	-5.57	3.13
AM 2	70 (43.5)	3.80	-3.87	10.23	-5.00	-4.83	5.37	-6.03	3.17
PM	8 (5)	2.57	-2.40	5.67	-2.90	-6.17	7.33	-5.87	3.53
	40 (25)	2.63	-2.43	6.07	-2.97	-5.93	6.77	-6.63	3.70
	70 (43.5)	2.27	-2.03	5.37	-2.70	-5.53	6.80	-6.13	3.50
		KM17	KM18	KM17	KM18	KM17	KM18	KM17	KM18
AM 1	8 (5)	5.58	-4.28	7.25	-4.23	-6.73	6.18	-7.73	4.23
	40 (25)	5.03	-4.00	7.17	-3.87	-7.70	6.23	-6.70	3.93
AM 2	70 (43.5)	3.47	-2.63	5.40	-3.43	-6.47	5.97	-6.57	3.93
PM	8 (5)	2.40	-1.73	2.77	-1.67	-8.83	7.80	-6.53	4.40
	40 (25)	2.30	-1.60	2.87	-1.67	-8.10	7.17	-6.50	4.40
	70 (43.5)	2.10	-	2.73	-	-8.23	-	-7.07	-

Appendix ESupplemental Fall 2011 Truck Testing Data

Deflection

Deflection Response - Dual-Axle

Section:		**1**	**2**	**1**	**2**	**1**	**2**	**1**	**2**	**1**	**2**
Speed (km/h):		**Upward (mm)**									
AM	**8**	0.0036	0.0108	0.0014	0.0059	0.0045	0.0151	0.0041	0.0162	0.0030	0.0211
	40	0.0019	0.0076	0.0007	0.0009	0.0014	0.0123	0.0030	0.0158	0.0019	0.0108
	88.5	0.0030	0.0153	0.0010	0.0022	0.0032	0.0140	0.0021	0.0156	0.0010	0.0106
		Downward (mm)									
	8	-0.1516	-0.2340	-0.1089	-0.1476	-0.1344	-0.2372	-0.0961	-0.1795	-0.0564	-0.1136
	40	-0.1424	-0.2256	-0.0926	-0.1529	-0.1112	-0.2415	-0.0837	-0.1729	-0.0317	-0.1042
	88.5	-0.1184	-0.2350	-0.0745	-0.1356	-0.0807	-0.2206	-0.0713	-0.1505	-0.0456	-0.0928
Speed (km/h):		**Upward (mm)**									
PM	**8**	0.0026	0.0080	0.0007	0.0051	0.0025	0.0095	0.0014	0.0082	0.0011	0.0079
	40	0.0023	0.0074	0.0008	0.0009	0.0025	0.0097	0.0013	0.0086	0.0010	0.0052
	88.5	0.0020	0.0059	0.0006	0.0017	0.0031	0.0074	0.0018	0.0070	0.0009	0.0043
		Downward (mm)									
	8	-0.0827	-0.1608	-0.0583	-0.0966	-0.0644	-0.1512	-0.0713	-0.1221	-0.0414	-0.0803
	40	-0.0875	-0.1531	-0.0541	-0.0923	-0.0646	-0.1485	-0.0716	-0.1222	-0.0394	-0.0811
	88.5	-0.1048	-0.1319	-0.0676	-0.0708	-0.0741	-0.1015	-0.0666	-0.0719	-0.0316	-0.0461

Section:		1	2	1	2	1	2	1	2	1	2
Speed (mph):		Upward (mil)									
AM	5	0.142	0.425	0.055	0.232	0.177	0.594	0.161	0.638	0.118	0.831
	25	0.075	0.299	0.028	0.035	0.055	0.484	0.118	0.622	0.075	0.425
	55	0.118	0.602	0.039	0.087	0.126	0.551	0.083	0.614	0.039	0.417
		Downward (mil)									
	5	-5.969	-9.213	-4.287	-5.811	-5.291	-9.339	-3.783	-7.067	-2.220	-4.472
	25	-5.606	-8.882	-3.646	-6.020	-4.378	-9.508	-3.295	-6.807	-1.248	-4.102
	55	-4.661	-9.252	-2.933	-5.339	-3.177	-8.685	-2.807	-5.925	-1.795	-3.654
Speed (mph):		Upward (mil)									
PM	5	0.102	0.315	0.028	0.201	0.098	0.374	0.055	0.323	0.043	0.311
	25	0.091	0.291	0.031	0.035	0.098	0.382	0.051	0.339	0.039	0.205
	55	0.079	0.232	0.024	0.067	0.122	0.291	0.071	0.276	0.035	0.169
		Downward (mil)									
	5	-3.256	-6.331	-2.295	-3.803	-2.535	-5.953	-2.807	-4.807	-1.630	-3.161
	25	-3.445	-6.028	-2.130	-3.634	-2.543	-5.846	-2.819	-4.811	-1.551	-3.193
	55	-4.126	-5.193	-2.661	-2.787	-2.917	-3.996	-2.622	-2.831	-1.244	-1.815

Deflection Response - Single-Axle

Sensor:		**LVDT 1**		**LVDT 2**		**LVDT 3**		**LVDT 4**		**LVDT 5**	
Section:		**1**	**2**	**1**	**2**	**1**	**2**	**1**	**2**	**1**	**2**
Speed (km/h):		**Upward (mm)**									
AM	**8**	0.0026	0.0089	0.0019	0.0024	0.0024	0.0088	0.0023	0.0093	0.0026	0.0083
	40	0.0019	0.0110	0.0008	0.0032	0.0013	0.0095	0.0018	0.0100	0.0019	0.0105
	88.5	0.0013	0.0080	0.0006	0.0021	0.0016	0.0088	0.0015	0.0084	0.0014	0.0052
	-	**Downward (mm)**									
	8	-0.1004	-0.1597	-0.0686	-0.0889	-0.0954	-0.1689	-0.0665	-0.1334	-0.0340	-0.0765
	40	-0.0926	-0.1407	-0.0535	-0.0885	-0.0744	-0.1733	-0.0542	-0.1342	-0.0304	-0.0765
	88.5	-0.0783	-0.1670	-0.0417	-0.0859	-0.0659	-0.1418	-0.0539	-0.1081	-0.0299	-0.0620
Speed (km/h):		**Upward (mm)**									
PM	**8**	0.0015	0.0086	0.0005	0.0006	0.0014	0.0051	0.0008	0.0042	0.0008	0.0029
	40	0.0021	0.0074	0.0007	0.0027	0.0019	0.0069	0.0008	0.0052	0.0008	0.0055
	88.5	0.0019	0.0065	0.0006	0.0006	0.0019	0.0063	0.0011	0.0058	0.0007	0.0031
	-	**Downward (mm)**									
	8	-0.0470	-0.0966	-0.0258	-0.0476	-0.0342	-0.0958	-0.0446	-0.0927	-0.0284	-0.0625
	40	-0.0575	-0.1054	-0.0281	-0.0526	-0.0399	-0.1068	-0.0452	-0.0913	-0.0247	-0.0552
	88.5	-0.0693	-0.1265	-0.0334	-0.0561	-0.0534	-0.1000	-0.0496	-0.0857	-0.0236	-0.0527

Sensor:		LVDT 1		LVDT 2		LVDT 3		LVDT 4		LVDT 5	
Section:		1	2	1	2	1	2	1	2	1	2
Speed (mph):		Upward (mil)									
AM	5	0.102	0.350	0.075	0.094	0.094	0.346	0.091	0.366	0.102	0.327
	25	0.075	0.433	0.031	0.126	0.051	0.374	0.071	0.394	0.075	0.413
	55	0.051	0.315	0.024	0.083	0.063	0.346	0.059	0.331	0.055	0.205
		Downward (mil)									
	5	-3.953	-6.287	-2.701	-3.500	-3.756	-6.650	-2.618	-5.252	-1.339	-3.012
	25	-3.646	-5.539	-2.106	-3.484	-2.929	-6.823	-2.134	-5.283	-1.197	-3.012
	55	-3.083	-6.575	-1.642	-3.382	-2.594	-5.583	-2.122	-4.256	-1.177	-2.441
Speed (mph):		Upward (mil)									
PM	5	0.059	0.339	0.020	0.024	0.055	0.201	0.031	0.165	0.031	0.114
	25	0.083	0.291	0.028	0.106	0.075	0.272	0.031	0.205	0.031	0.217
	55	0.075	0.256	0.024	0.024	0.075	0.248	0.043	0.228	0.028	0.122
		Downward (mil)									
	5	-1.850	-3.803	-1.016	-1.874	-1.346	-3.772	-1.756	-3.650	-1.118	-2.461
	25	-2.264	-4.150	-1.106	-2.071	-1.571	-4.205	-1.780	-3.594	-0.972	-2.173
	55	-2.728	-4.980	-1.315	-2.209	-2.102	-3.937	-1.953	-3.374	-0.929	-2.075

Strain

Strain Response - Dual-Axle

Load Case:		LC-1 Strain (με)				LC-2 Strain (με)			
Section:		Section 1		Section 2		Section 1		Section 2	
Test	Speed (km/h (mph))	KM1	KM2	KM1	KM2	KM1	KM2	KM1	KM2
AM	8 (5)	4.47	-3.70	6.07	-3.73	-6.43	6.77	-6.20	4.50
	40 (25)	3.70	-3.13	6.00	-3.70	-5.73	5.67	-6.00	4.13
	88.5 (55)	3.43	-2.90	4.80	-2.87	-5.83	6.30	-6.40	4.43
PM	8 (5)	3.17	-3.07	4.80	-3.08	-6.00	5.47	-6.15	4.10
	40 (25)	3.10	-2.90	4.73	-2.87	-5.97	5.33	-6.93	4.17
	88.5 (55)	3.03	-2.73	3.00	-1.83	-5.20	5.13	-4.03	2.70
		KM3	KM4	KM3	KM4	KM3	KM4	KM3	KM4
AM	8 (5)	4.53	-3.77	7.80	-4.40	-6.10	6.97	-6.43	4.10
	40 (25)	3.63	-3.10	7.77	-4.33	-6.50	7.30	-5.67	3.57
	88.5 (55)	3.87	-3.13	6.57	-3.57	-5.43	6.73	-5.60	3.33
PM	8 (5)	3.30	-3.03	5.55	-3.50	-6.60	6.00	-6.50	3.70
	40 (25)	2.97	-2.70	5.80	-3.33	-6.27	6.07	-6.27	3.73
	88.5 (55)	3.07	-2.77	3.70	-2.13	-5.63	5.47	-3.87	2.27
		KM5	KM6	KM5	KM6	KM5	KM6	KM5	KM6
AM	8 (5)	4.40	-3.70	6.07	-4.27	-5.93	6.60	-5.90	3.97
	40 (25)	3.23	-2.87	5.80	-3.80	-6.10	6.50	-6.10	4.07
	88.5 (55)	3.63	-2.97	5.40	-3.77	-4.77	5.67	-5.17	3.33
PM	8 (5)	3.07	-2.93	4.88	-3.60	-5.73	5.20	-5.60	3.35
	40 (25)	3.13	-2.87	5.07	-3.23	-5.27	5.20	-6.07	4.07
	88.5 (55)	2.90	-2.77	3.30	-2.27	-4.87	4.87	-3.17	2.27
		KM7	KM8	KM7	KM8	KM7	KM8	KM7	KM8
AM	8 (5)	4.23	-3.30	2.80	-1.83	-3.97	3.07	-1.30	0.97
	40 (25)	3.50	-2.47	2.57	-1.50	-4.00	2.90	-1.17	0.83
	88.5 (55)	3.63	-2.70	2.23	-1.23	-3.77	2.87	-1.17	0.80
PM	8 (5)	3.13	-2.47	2.00	-1.38	-4.60	3.37	-1.50	1.08
	40 (25)	2.90	-2.30	2.07	-1.27	-4.27	3.03	-1.30	1.07
	88.5 (55)	2.97	-2.17	1.23	-0.90	-4.00	2.83	-0.93	0.60
		KM9	KM10	KM9	KM10	KM9	KM10	KM9	KM10
AM	8 (5)	4.27	0.00	1.17	0.00	-5.33	NA	-2.20	NA
	40 (25)	3.03	0.00	1.30	-1.30	-4.43	NA	-1.53	1.40
	88.5 (55)	3.47	0.00	1.03	-1.10	-5.03	NA	-1.73	1.63
PM	8 (5)	2.63	0.00	1.15	-1.43	-4.10	NA	-1.55	1.60
	40 (25)	2.23	0.00	1.00	-1.20	-3.67	NA	-1.50	1.60
	88.5 (55)	2.00	0.00	0.67	-0.63	-2.90	NA	-0.93	0.83

Load Case:		LC-1 Strain (με)				LC-2 Strain (με)			
Section:		Section 1		Section 2		Section 1		Section 2	
Test	Speed (km/h (mph))	KM11	KM12	KM11	KM12	KM11	KM12	KM11	KM12
AM	8 (5)	3.60	-3.00	2.40	-1.53	-5.50	5.53	-2.60	1.77
	40 (25)	2.77	-2.30	2.20	-1.37	-5.70	6.00	-2.20	1.40
	88.5 (55)	2.83	-2.57	1.77	-1.07	-5.33	5.63	-2.20	1.33
PM	8 (5)	2.43	-2.30	1.73	-1.18	-4.77	4.50	-2.38	1.70
	40 (25)	2.07	-2.03	1.67	-1.17	-4.77	4.80	-2.40	1.63
	88.5 (55)	2.03	-1.83	1.03	-0.67	-3.73	3.60	-1.43	0.93
		KM13	KM14	KM13	KM14	KM13	KM14	KM13	KM14
AM	8 (5)	3.57	-3.13	2.40	-1.43	-5.83	5.43	-2.40	1.53
	40 (25)	2.87	-2.13	2.07	-1.27	-5.77	5.43	-2.17	1.23
	88.5 (55)	2.80	-2.17	1.90	-1.23	-5.10	5.00	-1.70	1.17
PM	8 (5)	2.10	-2.13	1.90	-1.23	-4.83	4.07	-2.03	1.35
	40 (25)	1.70	-1.87	1.80	-1.00	-5.07	4.07	-2.20	1.50
	88.5 (55)	1.87	-1.53	1.20	-0.67	-3.60	3.00	-1.07	0.77
		KM15	KM16	KM15	KM16	KM15	KM16	KM15	KM16
AM	8 (5)	4.83	-4.37	9.83	-5.37	-5.67	5.80	-7.57	3.83
	40 (25)	4.37	-3.83	9.60	-5.17	-5.53	5.80	-6.57	3.33
	88.5 (55)	3.63	-3.37	9.43	-5.13	-4.37	5.20	-6.17	3.50
PM	8 (5)	3.63	-3.30	8.20	-4.40	-4.83	4.60	-6.13	3.10
	40 (25)	3.67	-3.30	8.13	-4.20	-4.80	4.73	-6.00	3.20
	88.5 (55)	3.37	-2.97	5.20	-2.70	-4.17	4.17	-3.93	2.07
		KM17	KM18	KM17	KM18	KM17	KM18	KM17	KM18
AM	8 (5)	5.13	-4.03	6.63	-4.83	-6.27	5.67	-4.20	3.80
	40 (25)	4.53	-3.37	6.70	-4.87	-6.27	5.60	-3.87	3.23
	88.5 (55)	4.00	-2.87	6.13	-4.17	-5.60	5.33	-4.10	3.47
PM	8 (5)	3.77	-2.80	5.00	-3.45	-5.87	4.83	-4.73	3.65
	40 (25)	3.43	-2.60	5.13	-3.67	-5.97	4.90	-4.30	3.73
	88.5 (55)	3.60	-2.60	3.47	-2.40	-4.77	4.03	-2.87	2.07

Strain Response - Single-Axle

Load Case:		LC-1 Strain (με)				LC-2 Strain (με)			
Section:		Section 1		Section 2		Section 1		Section 2	
Test	Speed (km/h (mph))	KM1	KM2	KM1	KM2	KM1	KM2	KM1	KM2
AM	8 (5)	`	-3.00	4.37	-2.77	-5.17	5.33	-5.60	3.50
	40 (25)	2.75	-2.58	4.38	-2.75	-4.63	4.50	-5.08	3.08
	88.5 (55)	2.37	-2.00	4.20	-2.53	-4.87	4.63	-5.57	3.43
PM	8 (5)	2.53	-2.40	3.40	-2.17	-5.07	4.93	-5.40	3.60
	40 (25)	2.47	-2.40	3.20	-2.03	-5.40	5.10	-6.30	3.70
	88.5 (55)	2.13	-1.90	3.67	-2.00	-4.80	4.60	-5.43	3.63
		KM3	KM4	KM3	KM4	KM3	KM4	KM3	KM4
AM	8 (5)	3.10	-2.77	5.30	-2.90	-5.57	5.97	-6.13	3.63
	40 (25)	2.73	-2.40	5.18	-2.98	-5.55	5.83	-5.38	3.15
	88.5 (55)	2.47	-2.03	4.67	-2.67	-5.67	6.10	-5.10	2.50
PM	8 (5)	2.33	-2.13	3.73	-1.97	-6.13	6.10	-5.63	3.57
	40 (25)	2.10	-1.97	3.97	-2.17	-6.07	6.00	-6.03	3.33
	88.5 (55)	2.10	-1.93	3.87	-2.13	-5.47	5.97	-5.13	2.97
		KM5	KM6	KM5	KM6	KM5	KM6	KM5	KM6
AM	8 (5)	2.93	-2.73	4.30	-2.97	-5.23	5.43	-4.73	3.13
	40 (25)	2.50	-2.35	3.85	-2.70	-4.78	4.88	-5.28	3.25
	88.5 (55)	2.40	-2.00	3.90	-2.83	-4.73	5.50	-4.47	2.97
PM	8 (5)	2.20	-2.10	3.67	-2.33	-5.23	5.07	-5.43	3.30
	40 (25)	2.23	-2.07	3.50	-2.40	-4.83	4.83	-4.93	3.27
	88.5 (55)	2.07	-2.10	3.50	-2.53	-5.07	5.27	-4.13	3.03
		KM7	KM8	KM7	KM8	KM7	KM8	KM7	KM8
AM	8 (5)	2.97	-2.37	1.83	-1.27	-3.87	2.87	-1.40	1.00
	40 (25)	2.50	-2.00	1.80	-1.13	-4.15	3.18	-1.35	0.85
	88.5 (55)	2.23	-1.83	1.67	-0.90	-3.83	3.07	-1.17	0.67
PM	8 (5)	2.23	-1.87	1.43	-1.07	-4.33	3.20	-1.63	1.13
	40 (25)	1.97	-1.53	1.43	-0.93	-4.30	3.13	-1.47	0.83
	88.5 (55)	2.20	-1.60	1.43	-0.80	-4.40	3.30	-1.37	0.87
		KM9	KM10	KM9	KM10	KM9	KM10	KM9	KM10
AM	8 (5)	3.27	0.00	1.00	0.00	-3.80	0.00	-1.43	0.00
	40 (25)	2.45	0.00	1.05	-1.10	-3.30	0.00	-1.13	0.95
	88.5 (55)	2.30	0.00	0.90	-1.03	-2.97	0.00	-1.10	0.93
PM	8 (5)	2.47	0.00	0.90	-1.10	-4.07	0.00	-1.60	1.33
	40 (25)	1.73	0.00	0.90	-0.90	-3.30	0.00	-0.97	1.07
	88.5 (55)	1.67	0.00	0.80	-0.87	-2.37	0.00	-1.17	1.03

Load Case:		LC-1 Strain (με)				LC-2 Strain (με)			
Section:		Section 1		Section 2		Section 1		Section 2	
Test	Speed (km/h (mph))	KM11	KM12	KM11	KM12	KM11	KM12	KM11	KM12
AM	8 (5)	2.40	-2.07	1.53	-1.17	-4.33	3.77	-2.43	1.43
	40 (25)	2.00	-1.75	1.55	-0.93	-4.38	3.83	-1.95	1.28
	88.5 (55)	1.67	-1.50	1.40	-0.80	-4.23	4.07	-1.43	0.93
PM	8 (5)	1.87	-1.83	1.20	-0.90	-5.07	4.77	-2.40	1.53
	40 (25)	1.43	-1.43	1.10	-0.73	-4.07	3.90	-2.00	1.17
	88.5 (55)	1.43	-1.30	1.13	-0.80	-3.53	3.33	-1.83	1.00
		KM13	KM14	KM13	KM14	KM13	KM14	KM13	KM14
AM	8 (5)	2.47	-2.03	1.80	-1.17	-4.30	3.87	-1.53	0.97
	40 (25)	2.20	-1.68	1.55	-0.93	-3.63	3.28	-1.50	1.23
	88.5 (55)	1.97	-1.47	1.43	-1.03	-3.57	3.70	-1.37	1.00
PM	8 (5)	1.13	-1.77	1.43	-0.93	-5.60	4.30	-1.93	1.23
	40 (25)	1.60	-1.40	1.17	-0.87	-3.47	3.10	-1.63	1.13
	88.5 (55)	1.63	-1.17	1.17	-0.83	-3.10	3.03	-1.20	1.00
		KM15	KM16	KM15	KM16	KM15	KM16	KM15	KM16
AM	8 (5)	3.60	-3.40	7.53	-4.30	-4.33	4.07	-5.27	2.87
	40 (25)	3.05	-2.70	8.15	-4.55	-3.75	3.73	-4.48	2.23
	88.5 (55)	3.03	-3.07	6.97	-3.73	-3.80	4.10	-4.60	2.40
PM	8 (5)	2.57	-2.47	6.47	-3.33	-4.53	4.43	-4.37	2.73
	40 (25)	2.57	-2.37	7.00	-3.53	-4.20	4.00	-4.50	2.37
	88.5 (55)	2.77	-2.47	6.27	-3.30	-4.17	4.20	-4.17	2.07
		KM17	KM18	KM17	KM18	KM17	KM18	KM17	KM18
AM	8 (5)	3.63	-2.80	4.90	-3.60	-5.17	4.53	-4.67	3.40
	40 (25)	3.10	-2.30	5.00	-3.63	-5.05	4.60	-3.85	3.03
	88.5 (55)	2.90	-2.30	4.73	-3.27	-4.27	4.13	-3.17	2.93
PM	8 (5)	2.43	-1.93	3.63	-2.10	-5.60	4.73	-3.93	3.70
	40 (25)	2.23	-1.73	3.80	-2.77	-5.30	4.93	-4.10	3.50
	88.5 (55)	2.60	-1.87	3.40	-2.70	-4.70	4.47	-3.03	2.83

ORITE • 141 Stocker Center • Athens, Ohio 45701-2979 • 740-593-2476
Fax: 740-593-0625 • orite@ohio.edu • http://www.ohio.edu/orite/